

# **A NEW SYNTHETIC APPROACH FOR PREPARATION OF EFAVIRENZ**

**THESIS**

***Submitted***

*in the partial fulfillment of the requirements for  
the award of the degree of*

**DOCTOR OF PHILOSOPHY (Ph.D.)**

**in**

**FACULTY OF SCIENCE**

**By**

**SRAVANTHI CHADA**

[215208412]

Under the guidance of

Prof. Paul Watts

**NELSON MANDELA METROPOLITAN UNIVERSITY**

**PORT ELIZABETH, SOUTH AFRICA 6001**

**APRIL 2017**

## ABSTRACT OF THE THESIS

### A NEW SYNTHETIC APPROACH FOR THE SYNTHESIS OF EFAVIRENZ

Efavirenz, a drug that is still inaccessible to millions of people worldwide, is potent non-nucleoside reverse transcriptase inhibitor (NNRTI), is one of the preferred agents used in combination therapy for first-line treatment of the human immunodeficiency virus (HIV). NNRTIs attach to and block an HIV enzyme called reverse transcriptase, by blocking reverse transcriptase; NNRTIs prevent HIV from multiplying and can reduce the amount of HIV in the body. Efavirenz can't cure HIV/AIDS, but taken in combination with other HIV medicines (called an HIV regimen) every day helps people with HIV live longer healthier lives. Efavirenz also reduces the risk of HIV transmission and can be used by children who are suffering from HIV/AIDS. All the above therapeutic uses of efavirenz prompted us to identify the novel and hopefully cost efficient synthetic methodology for the preparation of efavirenz.

In this thesis a new synthetic method for asymmetric synthesis of efavirenz is described. This route started from commercially available starting materials and it is first established in traditional batch chemistry and further the parameters transferred to a semi continuous flow protocol for optimization.

The thesis is consists of five chapters:

**Chapter I, section A** deals with the introductory aspects of HIV/AIDS and efavirenz– their history, classifications, synthesis, dosage forms. **Section B** deals with the introduction to flow chemistry and literature review for the preparation of efavirenz.

**Chapter II, section A** summarizes the traditional batch chemistry results and discussion for the preparation of efavirenz and **section B** explains the results and discussion of semi-continuous flow protocol for the preparation of efavirenz. The results of semi-continuous flow protocol are explained in graphical form and model validations by using statistical methods. All the intermediates synthesized by semi-continuous flow protocol gave comparatively better yield than batch chemistry.

**Chapter III**, describes traditional batch experimental procedures for the preparation of efavirenz along with the analytical data. All the compounds synthesized in this chapter were evaluated by  $^1\text{H}$ -NMR,  $^{13}\text{C}$ -NMR,  $^{19}\text{F}$ -NMR, IR spectroscopy and elemental analysis.

**Chapter IV** describes the semi-continuous flow protocol for the preparation of efavirenz **8** along with the analytical data. All the compounds synthesized in this chapter were evaluated by  $^1\text{H}$ -NMR,  $^{13}\text{C}$ -NMR,  $^{19}\text{F}$ -NMR, FT-IR spectroscopy and elemental analysis. The compounds prepared in this chapter gave well to excellent yields.

**Chapter V**, the conclusion and future scope for the preparation of efavirenz are described.

*WITH BLESSINGS OF  
LORD SAIRAM.....*

*Dedicated to my beloved  
Family*

## **ACKNOWLEDGEMENTS**

I express my sincere gratitude to my research supervisor Prof. Paul Watts, Prof. of Chemistry, Nelson Mandela Metropolitan University, Port Elizabeth, South Africa, who gave me the opportunity to work in such a nice lab with him. His endless support, kindness, and generosity made me feel at home, his knowledge and vast experience has inspired me at every stage of my tenure and helped me to grow as a chemist, as well as a good researcher.

I sincerely acknowledge my thanks to Mr. C Bosma for statistical analysis consultation

My special thanks to NMMU InnoVenton: Institute of Chemical Technology research team and staff

My sincere and respectful regards to all the Faculty members, Dept. of Chemistry, Nelson Mandela Metropolitan University Port Elizabeth, South Africa for their kind support.

I would like to express sincere thanks, South African National Research Foundation for Doctoral bursary and Nelson Mandela Metropolitan University postgraduate bursary for the financial support.

I express my due respect to my teachers at my high school level for their inspirational teachings on all aspects of science and life in my early educational level. I would also like to greatly acknowledge my teachers in Bachelors, Dr. Agaiah, Dr. Ampati Srinivas, Dr. Martha Srinivas, Dr. Veerreddy Prabaker Reddy My due respect and thanks to all my teachers in masters especially, Prof. M. Sarangapani, Prof. J. Venkateswar Rao for their interesting lectures.

I thank all my Flow chemistry lab colleagues specially Faith Akwi, Dr. Mafu Chigondo Fidelis and Carla Venter for their enormous support, valuable suggestions, and encouragement during my Doctoral studies.

I specially thank all my friends Alivelu Samala, Anusha Macharla, Soumya Manala, Praveena, Vasuda Bakshi, Ragini, Anitha, Haritha Thegala, Mahender Sunkapaka and Rajesh.

I express my deepest thanks to my brother CVN Reddy and my Brother-in-law Ashok Reddy for their moral and emotional support.

My parents, my mother Ramani & father Sudharshan Reddy have been a constant source of support – emotional, moral and of course financial – during my postgraduate years, and this thesis would certainly not have existed without them.

I thank all my family members Shamala - Malla Reddy, Anitha-Srinivas Reddy, and Indira-Vinod Reddy.

I express my heartfelt thanks to my husband Dr. Devender Mandala for his affectionate encouragement, Knowledge sharing, professional and personal support from time to time. Your love always is my motivation to go forward. I admire my daughter Sai Akshara Reddy for her love that relieved, refreshed and rejuvenated me to continue to take the task ahead with full strength.

## DECLARATION

I Sravanthi Chada hereby declare that the work described in this thesis, entitled “**A New synthetic approach for synthesis of efavirenz**” which is being submitted by me in partial fulfillment for the award of **Doctor of Philosophy** (Ph.D.) in the Dept. of Chemistry of the Nelson Mandela Metropolitan University, is my original work and to the best of my knowledge the work was not submitted by any other person. The result of investigations carried out by me under the Guidance of **Prof. Paul Watts**, Prof. of Chemistry, Nelson Mandela Metropolitan University, Port Elizabeth, South Africa.

The work is original and has not been submitted for any Degree/Diploma of this or any other university.

Place:

Date:

Signature:

Name of the Candidate: **Sravanthi Chada**

s215208412

## Table of Contents

ABSTRACT OF THE THESIS .....	i
ACKNOWLEDGEMENTS .....	v
DECLARATION.....	vii
ABBREVIATIONS .....	xv
CHAPTER 1 SECTION A.....	1
INTRODUCTION TO HIV AIDS DRUGS.....	1
1A.1. Global epidemiology of HIV/AIDS .....	2
1A.2. Global response to HIV/AIDS .....	3
1A.3. HIV in South Africa .....	3
1A.4. HIV/AIDS statistics province wise in South Africa.....	4
1A.5. About the virus.....	5
1A.6. HIV structure.....	5
1A.7. HIV replication .....	7
1A.8. Classification of HIV.....	11
1A.9. Types of HIV .....	11
1A.10. Drugs for HIV/AIDS.....	13
1A.11. Types of antiretroviral drugs .....	14
1A.12. Drug combinations.....	26
1A.12.1. Advantages of combination therapy .....	28



1A.12.2. General combinations.....	28
1A.13. WHO guidelines for treatment .....	29
1A.14. Introduction to efavirenz .....	29
1A.14.1. History .....	30
1A.14. 2. Effectiveness .....	31
1A.14.3. Adverse drug reactions.....	34
CHAPTER 1 SECTION B.....	35
INTRODUCTION TO FLOW CHEMISTRY & LITRATURE REVIEW .....	35
1B.1. Definition- flow chemistry.....	36
1B.2. Background .....	36
1B.3. Types of flow systems .....	40
1B.4. Flow reactors: structure and design.....	41
1B.5. Advantages of the flow techniques .....	43
1B.6. Synthesis of APIs by using flow technology.....	45
1B.6.1. Synthesis of 2-chloro-3-amino-4-picoline (CAPIC) .....	45
1B.6.2. Synthesis of meclinertant .....	46
1B.7. Literature review of Efavirenz .....	49
1B.8. Aim .....	61
CHAPTER 2 SECTION A.....	62
TRADITIONAL BATCH CHEMISTRY RESULTS AND DISCUSSION .....	62

2A.1. Preparation of starting materials .....	64
2A.1.1. Preparation of cyclopropylacetylene 53 .....	64
2A.1.2. Preparation of 4-cyclopropyl-1,1,1-trifluoro-but-3-yn-2-one 29 .....	65
2A.1.3. Preparation of <i>N</i> -piperidine trifluoro acetic acid 67 .....	66
2A1.4. Preparation of (1 <i>R</i> ,2 <i>S</i> )- <i>N</i> -pyrrolidinylnorephedrine 60 .....	67
2A.2. Batch Synthesis of efavirenz 8 .....	67
2A.2.1. Step-1 .....	67
2A.2.2. Step-2 .....	70
2A.2.3. Step-3 .....	74
2A.2.4. Step-4 .....	77
2A.3. Summary of batch synthesis .....	79
CHAPTER 2 SECTION B .....	80
SEMI CONTINUOUS FLOW PROTOCOL RESULTS AND DISCUSSION .....	80
2B.1. Step-1 .....	82
2B.1.1. Effect of residence time on conversion of 68 .....	84
2B.1.2. Effect of concentration of di- <i>tert</i> -butyl dicarbamate at different residence times on conversion of 68 .....	85
2B.1.3. Effect of temperature at different residence times on conversion of 68 .....	88
2B.1.4. Comparison between the synthesis of 26 in batch and microreactors .....	90
2B.2. Step 2 .....	91

2B.2.1. Effect of temperature on conversion of 26.....	92
2B.2.2. Effect of concentration of piperidine trifluoroaceticacid 67 on conversion of 26.....	94
2B.2.3. Effect of residence time on conversion of 26.....	96
2B.2.4. Experimental design for residence times.....	98
2B.2.5. Experimental results.....	98
2B.2.6. Central composite design and observations.....	99
2B.2.7. Effect of residence time on conversion of 26.....	100
2B.3. Step-3.....	103
2B.3.1. Effect of residence time on conversion of 27.....	104
2B.3.2. Effect of temperature on conversion of 27.....	106
2B.3.3. Effect of concentration of cyclopropyl acetylene 53 on conversion of 27 .	108
2B.3.4. Effect of concentration of <i>n</i> -butyllithium on conversion of 27.....	109
2B.4. Step-4.....	111
2B.4.1. Effect of residence time on conversion of 56.....	112
2B.4.2. Effect of temperature on conversion 56.....	114
2.B.4.3. Effect of concentration of diethyl carbonate on conversion of 56 .....	115
2B.5. Conclusion of flow study .....	117
Chapter 3 .....	118
TRADITIONAL BATCH CHEMISTRY EXPERIMENTAL PROCEDURES.....	118

3. General experimental section .....	119
3.1. Experimental procedures .....	120
3.1.1. Preparation of 4-cyclopropylactylide 53 .....	120
3.1.2. Preparation of 4-cyclopropyl-1, 1, 1-trifluoro-but-3-yn-2-one 29.....	122
3.1.3. Preparation of <i>N</i> -piperidine trifluoro acetic acid 67 .....	123
3.1.4. Preparation of (1 <i>R</i> ,2 <i>S</i> )- <i>N</i> -pyrrolidinylnorephedrine 60.....	124
3.1.5. Preparation of <i>tert</i> -butyl-4-chloro phenyl carbamate 26.....	125
3.1.6. Preparation of <i>tert</i> -butyl-4-chloro-2-(2, 2, 2-trifluoroacetyl) phenyl carbamate 27.....	127
3.1.7. Preparation of <i>tert</i> -butyl-4-chloro-2-(4-cyclo propyl-1,1-trifluoro-2-hydroxy but- 3-yn-2-yl) phenyl carbamate 56 .....	129
3.1.8. Preparation of 6-chloro-2-(4-cyclopropylethynyl)-4-(trifluoromethyl)-1 <i>H</i> - benzo[ <i>d</i> ][1,3] oxazin-2-(4 <i>H</i> )-one 8 .....	132
CHAPTER 4 .....	134
4.1. Flow experimental procedures .....	135
4.1.1. Preparation of <i>tert</i> -butyl-4-chloro phenyl carbamate 26 .....	135
4.1.1.1. Effect of residence time on conversion of 68 .....	136
4.1.1.2. Effect of concentration of di- <i>tert</i> -butyl dicarbamate on conversion of 68 .	138
4.1.1.3. Effect of temperature on conversion of 68 .....	139
4.1.2. Preparation of <i>tert</i> -butyl-4-chloro-2-(2, 2, 2-trifluoroacetyl) phenyl carbamate 27 .....	140

4.1.2.1. Effect of residence time on conversion of 26 .....	145
4.1.2.2. Effect of concentration of <i>n</i> -butyllithium on conversion of 26 .....	146
4.1.2.3. Effect of concentration of trifluoro acetylating agent on conversion of 26 .....	147
4.1.2.4. Investigating the effect of temperature on conversion of 26 .....	148
4.1.2.5. Optimization of residence times by central composite design .....	149
4.1.2.6. Model derivation .....	150
4.1.3. Preparation of <i>tert</i> -butyl-4-chloro-2-(4-cyclo propyl-1, 1-trifluoro-2-hydroxybut-3-yn-2-yl) phenyl carbamate 56 .....	153
4.1.3.1. Effect of residence time on conversion of 27 .....	156
4.1.3.2. Effect of Concentration of <i>n</i> -butyllithium on conversion of 27 .....	157
4.1.3.3. Investigating the effect of concentration of cyclopropyl acetylene .....	157
4.1.3.4. Investigating the effect of temperature .....	158
4.1.4. Preparation of 6-chloro-2-(4-cyclopropylethynyl)-4-(trifluoromethyl)-1H-benzo[d][1,3] oxazin-2-(4H)-one 8 .....	159
4.1.4.1. Investigating the effect of residence time .....	162
4.1.4.2. Investigating the effect of temperature .....	163
4.1.4.3. Investigating the effect of concentration .....	163
CHAPTER 5 .....	165
CONCLUSION .....	165
CHAPPTER 6 .....	169

REFERENCES.....	169
CHAPTER 7 .....	182
APPENDIX .....	182

## ABBREVIATIONS

$^{13}\text{C}$ -	Carbon -13 Nuclear magnetic resonance
NMR	spectroscopy
$^{19}\text{F}$ -NMR	Fluorine-19 nuclear magnetic resonance
	spectroscopy
$^1\text{H}$ -NMR	Proton nuclear magnetic resonance spectroscopy
3D	Three dimensional
3TC	Lamivudine
$\text{Ac}_2\text{O}$	Acetic anhydride
ACN	Acetonitrile
AIDS	Acquired immune deficiency syndrome
ART	Antiretroviral therapy
ARV's	Antiretroviral drugs
Boc	<i>Tert</i> -Butyl carbamate
brs	Broad singlet
cART	Combination antiretroviral therapy
CCD	Central composite design
CD4	Cluster of differentiation
$\text{CDCl}_3$	Chloroform-d
d	Doublet
$\text{D}_2\text{O}$	Deuterium oxide
d4T	Stavudine
DBU	1,8-Diazabicyclo[5.4.0]undec-7-ene

DCM	Dichloromethane
ddl	Didanosine
DMF	Dimethyl formamide
DMSO-d <sub>6</sub>	Dimethyl sulfoxide-d <sub>6</sub>
DNA	Deoxyribonucleic acid
equiv	Equivalent
Et <sub>3</sub> N	Triethylamine
EtOAc	Ethyl acetate
EtOH	Ethanol
FDA	Food and Drug Administration
FT-IR	Fourier transform infrared spectroscopy
g	Gram
GC	Gas chromatography
Gp	Glycoprotein
h	Hour(s)
HCl	Hydrochloric acid
HIV	Human immunodeficiency virus
HPLC	High-performance liquid chromatography
HRMS	High-Resolution Mass Spectroscopy
Hz	Hertz
<i>J</i>	Coupling constant in Hertz
LTF	Little things factory
M	Molarity



m	Multiplet
M.P	Melting point
MeOH	Methanol
mg	Milligram
MHz	Mega Hertz
mL	Milliliter
mL/min	Millilitre per minute
mm	Millimeter
mmol	Millimoles
mRNA	Messenger ribonucleic acid
NNRTI's	Non-nucleoside reverse transcriptase inhibitors
NRTI's	Nucleoside reverse transcriptase inhibitors
PEG	Polyethylene glycol
PFA	Perfluoro alkoxy alkanes
PI	Protease inhibitors
PTA	Piperidine trifluoroacetic acid
PTFE	Polytetrafluoroethylene
RNA	Ribonucleic acid
RT	Room temperature
s	Singlet
t	Triplet
TFA	Trifluoroacetic acid
THF	Tetrahydrofuran

TLC	Thin layer chromatography
TMEDA	Tetramethylethylenediamine
UNAIDS	Joint United Nations Programme on HIV/AIDS
USA	United States of America
WHO	World Health Organization
ZDV	Zidovudine
$\alpha$	Alpha
$\beta$	Beta
$\mu\text{g}$	Microgram

# **CHAPTER 1**

## **SECTION A**

# **INTRODUCTION TO HIV AIDS DRUGS**

### 1A.1. Global epidemiology of HIV/AIDS

HIV/AIDS represents a major crisis that is increasingly affecting the population across the development sectors in sub-Saharan Africa and AIDS continues to be one of the biggest challenges faced by South Africa today.

The first case of the acquired immune deficiency syndrome (AIDS) was reported in 1981 in the USA. Within a short period of time, the spread of the human immunodeficiency virus (HIV) and AIDS had reached a pandemic form.<sup>[1]</sup> Now HIV has become one of the world's leading infectious killers, claiming more than 25 million lives over the past three decades.<sup>[2]</sup> Based on a recent UNAIDS World AIDS day report, there are 68 million people living with AIDS across the globe. AIDS had become one of the leading causes of death among adults in sub-Saharan Africa. An estimated 68% of all people living with HIV resided in sub-Saharan Africa.<sup>[3]</sup> The top ten most affected countries are listed in Table 1, which shows the percentage of the population affected.

**Table 1: HIV prevalence rate**

Rank	Country	Percentage%
1	Swaziland	27.73
2	Botswana	25.16
3	Lesotho	23.39
4	South Africa	18.92
5	Zimbabwe	16.74
6	Namibia	15.97
7	Zambia	12.37
8	Mozambique	10.58
9	Malawi	10.04
10	Uganda	7.25

### **1A.2. Global response to HIV/AIDS**

Zidovudine (ZDV) was the first antiretroviral drug for the treatment of HIV-infected patients introduced in 1986. A few years later, other nucleoside reverse transcriptase inhibitor (NRTIs) drugs such as didanosine (ddI), lamivudine (3TC) and stavudine (d4T) were introduced. These days, new classes of drugs such as protease inhibitors (PI) and non-nucleoside reverse transcriptase inhibitors (NNRTI) are available in order to prevent the emergence of resistance and to strengthen the immune function. Now, standard antiretroviral therapy (ART) consists of the combination of at least three antiretroviral (ARV) drugs.<sup>[4,5]</sup> The ART has provided relief to HIV-infected individuals by reducing the likelihood of opportunistic infection rather than curing the disease. During the last few years, a global effort had been made to scale up the antiretroviral drugs to enable that all the patients receive treatment.

### **1A.3. HIV in South Africa**

Sub-Saharan Africa is the worst affected area of the world for HIV-AIDS in terms of the number of individuals suffering from the condition. HIV-AIDS in South Africa, in particular, is a prominent health concern. Many factors contribute to the spread of HIV-AIDS. These include poverty, inequality, social instability, high levels of sexually transmitted infections, the low status of women, sexual violence, high mobility, limited access to medical care and a history of poor leadership. The hardship for those infected and their families begins long before people die. Suspected infection causes many people to delay or even refuse to be tested, fear and despair often follow diagnosis, due to poor quality counselling and lack of support, limited access to clinics, waiting lists for ARV treatment programs and

many people become seriously ill before accessing treatment, loss of income when the breadwinner becomes ill and burden upon family members.

#### **1A.4. HIV/AIDS statistics province wise in South Africa**

Province wise the HIV/AIDS prevalence rate in South Africa are KwaZulu-Natal (25.8% HIV positive), Mpumalanga (23.1% HIV positive), Free State (18.5% HIV-positive), North West (17.7% HIV-positive), Gauteng (15.2% HIV positive), Eastern Cape (15.2% HIV positive), Limpopo (13.7% HIV positive), Northern Cape (9.2% HIV positive) while only 5.3% of the population was HIV-positive in the Western Cape. These statistics demonstrate that there is a direct correlation between HIV/AIDS prevalence and black population size. HIV-AIDS statistics in 2015 are described in Table 2.

**Table 2: HIV -AIDS statistics in South Africa (2015)**

Number of people living with HIV	6,800,000
Adults aged 15 to 49 prevalence rate	18.9%
Adults aged 15 and up living with HIV	6,500,000
Women aged 15 and up living with HIV	3,900,000
Children aged 0 to 14 living with HIV	340,000
Deaths due to AIDS	140,000
Orphans due to AIDS aged 0 to 17	2,300,000

### **1A.5. About the virus**

HIV stands for human immunodeficiency virus. HIV is a virus spread through certain body fluids that attack the body's immune system, specifically the CD4 cells, often called T cells. Over time, HIV can destroy so many of these cells that the body can't fight off infections and disease. These special cells help the immune system fight off infections. Untreated, HIV reduces the number of CD4 cells in the body. This damage to the immune system makes it harder and harder for the body to fight off infections and other diseases.

### **1A.6. HIV structure**

HIV is a round, ball-shaped virus (Figure 1 and 2). It has two single strands of RNA for its genome. The RNA is used to carry the genetic information that is passed on when new HIV particles are produced. This is different than a normal cell, which uses DNA to carry its genetic information.

The outermost layer of the HIV particle is the envelope (Figure 1). The envelope takes part of the host cell's membrane as the virus leaves to make a membrane for itself. The envelope also has some proteins in it that help the virus invade the next host cell. One protein, gp120, helps the virus to attach to the CD4 receptor on the host cell. The other protein, gp41, helps the virus fuse with the cell membrane and enter the cell. The gp stands for glycoprotein, which is a protein with a carbohydrate attached while number 41 or 120 tells how big the protein is.

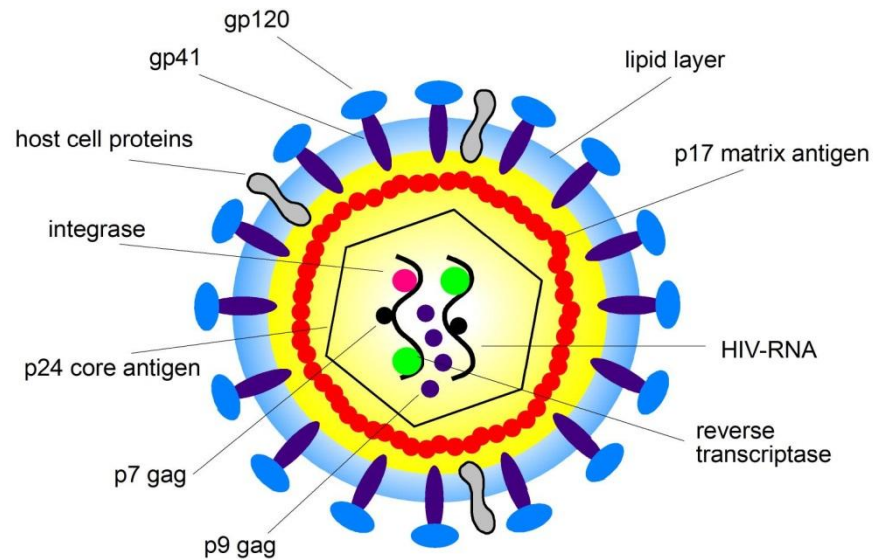


**Figure 1:** Structure of HIV [6]

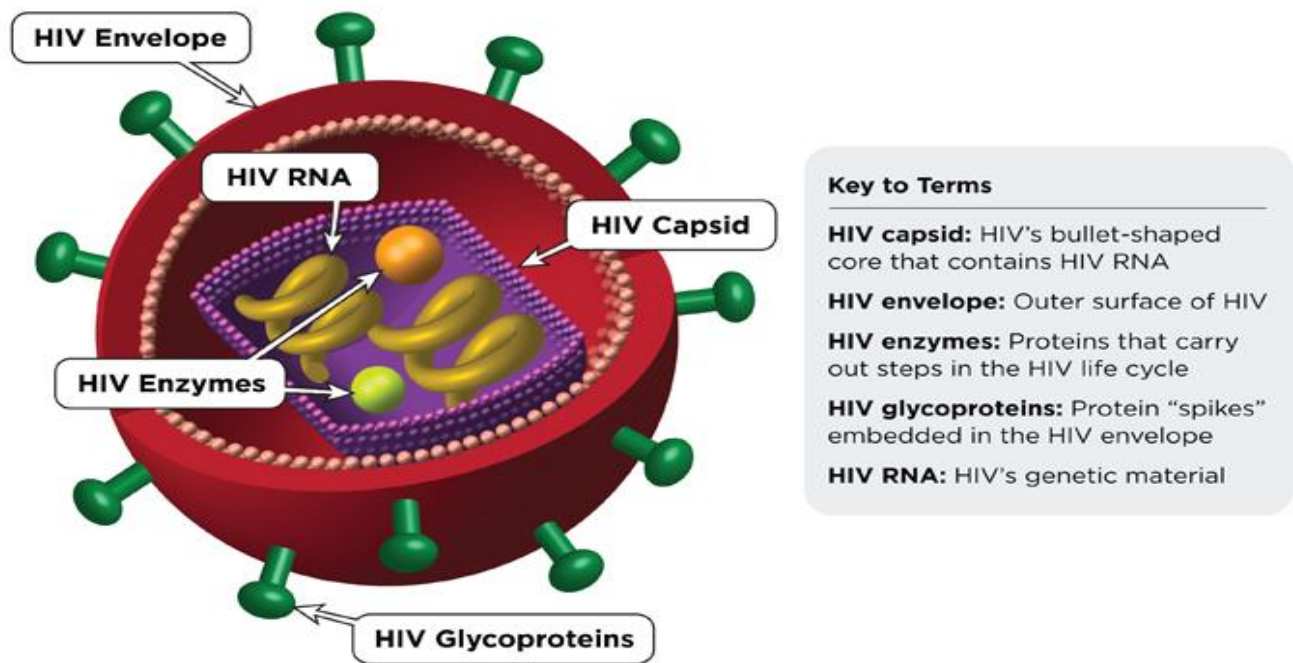


**Figure 2:** 3D structure of HIV virus [7]



Inside the envelope is the viral matrix. The p17 in the matrix (p stands for protein) helps hold the envelope proteins gp120 and gp41 to the rest of the virus. Inside the matrix is the viral core, made up of p24. The core houses the viral genome, as well as enzymes that the virus will need to replicate in the host cell.

### 1A.7. HIV replication

HIV gradually destroys the immune system by attacking and killing CD4 cells. CD4 cells are a type of white blood cell that plays a major role in protecting the body from infection. HIV uses the machinery of the CD4 cells to multiply (Figure 3) (make copies of itself) and spread throughout the body. This process, which includes seven steps or stages, is called the HIV life cycle. HIV medicines protect the immune system by blocking HIV at different stages of the HIV life cycle.

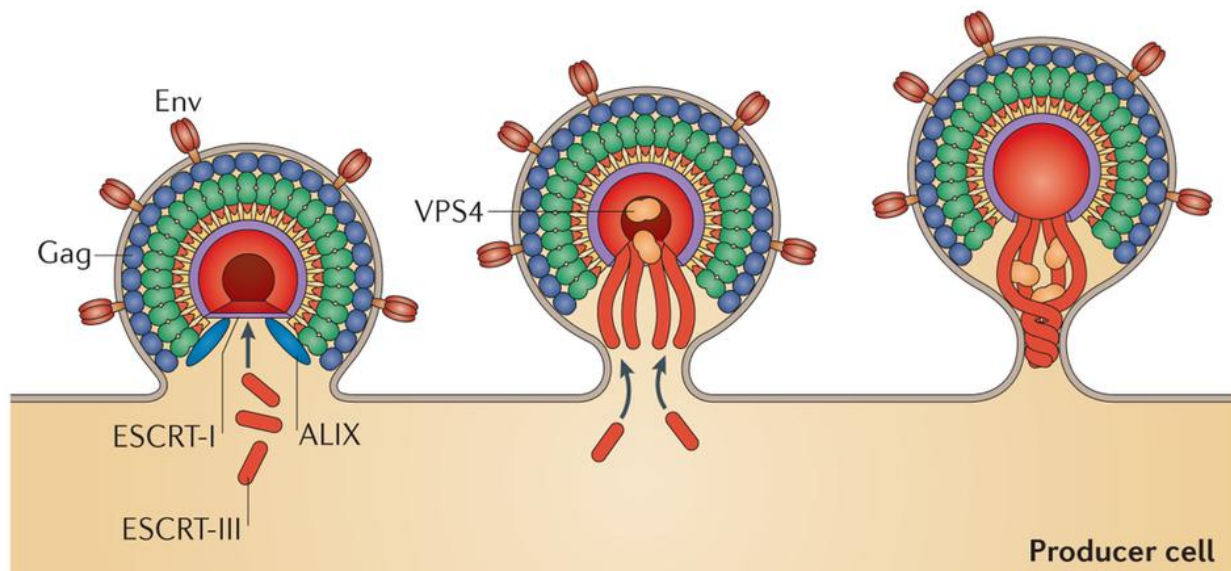


**Figure 3:** Formation of new HIV viral particle <sup>[8]</sup>

Like all viruses, HIV isn't considered a living entity because it requires a host cell in order to replicate. When HIV enters a cell, one of the first things it needs to do is reverse transcription of its RNA genome. Normally, biology tells us that DNA is converted to RNA

in a process called transcription. However, HIV does this backwards and converts RNA to DNA. This is where the name *retrovirus* comes from - *retro* means backwards. HIV uses one of the enzymes it brings with it in its matrix, called reverse transcriptase, to do this function.

After the DNA has been made, the next step in the virus' life cycle is integration. The newly made DNA is inserted into the host cell's own genome. This means that even if HIV is not actively making new virus particles, its genetic information is being copied every time the infected cell replicates. This is one of the reasons why it is so difficult to get rid of an HIV infection; the virus can hide in these so-called reservoirs when the environment is not good for making new viruses. Once the environment has improved, it can reactivate and make more viruses and so on.

Once the HIV DNA has integrated into the host cell's DNA, the virus can start to replicate. For this, HIV uses the host cell's replication machinery to turn its DNA into viral RNA. The viral RNA is then translated into protein. All of the proteins that the virus needs will be made at this stage, including the envelope, matrix, core proteins, as well as the reverse transcriptase enzyme. These proteins, along with the RNA, pack together to form new viral particles that will be released to start the infectious process all over again.

The seven stages of the HIV life cycle (Figure 4) are binding, fusion, reverse transcription, integration, replication, assembly and budding.

**Binding and fusion:** HIV begins its life cycle when it binds to a CD4 receptor and one of two co-receptors on the surface of a CD4+ T-lymphocyte. The virus then fuses with the host cell. After fusion, the virus releases RNA, its genetic material, into the host cell.

**Reverse Transcription:** An HIV enzyme called reverse transcriptase converts the single-stranded HIV RNA to double-stranded HIV DNA.

**Integration:** The newly formed HIV DNA enters the host cell's nucleus, where an HIV enzyme called integrase "hides" the HIV DNA within the host cell's own DNA. The integrated HIV DNA is called a provirus. The provirus may remain inactive for several years, producing few or no new copies of HIV.

**Replication:** When the host cell receives a signal to become active, the provirus uses a host enzyme called RNA polymerase to create copies of the HIV genomic material, as well as shorter strands of RNA called messenger RNA (mRNA). The mRNA is used as a blueprint to make long chains of HIV proteins.

**Assembly:** An HIV enzyme called protease cuts the long chains of HIV proteins into smaller individual proteins. As the smaller HIV proteins come together with copies of HIV's RNA genetic material, a new virus particle is assembled.

**Budding:** The newly assembled virus pushes out "buds" from the host cell. During budding, the new virus steals part of the cell's outer envelope. This envelope, which acts as a covering, is studded with protein/sugar combinations called HIV glycoproteins. These HIV glycoproteins are necessary for the virus to bind CD4 and co-receptors. The new copies of HIV can now move on to infect other cells.

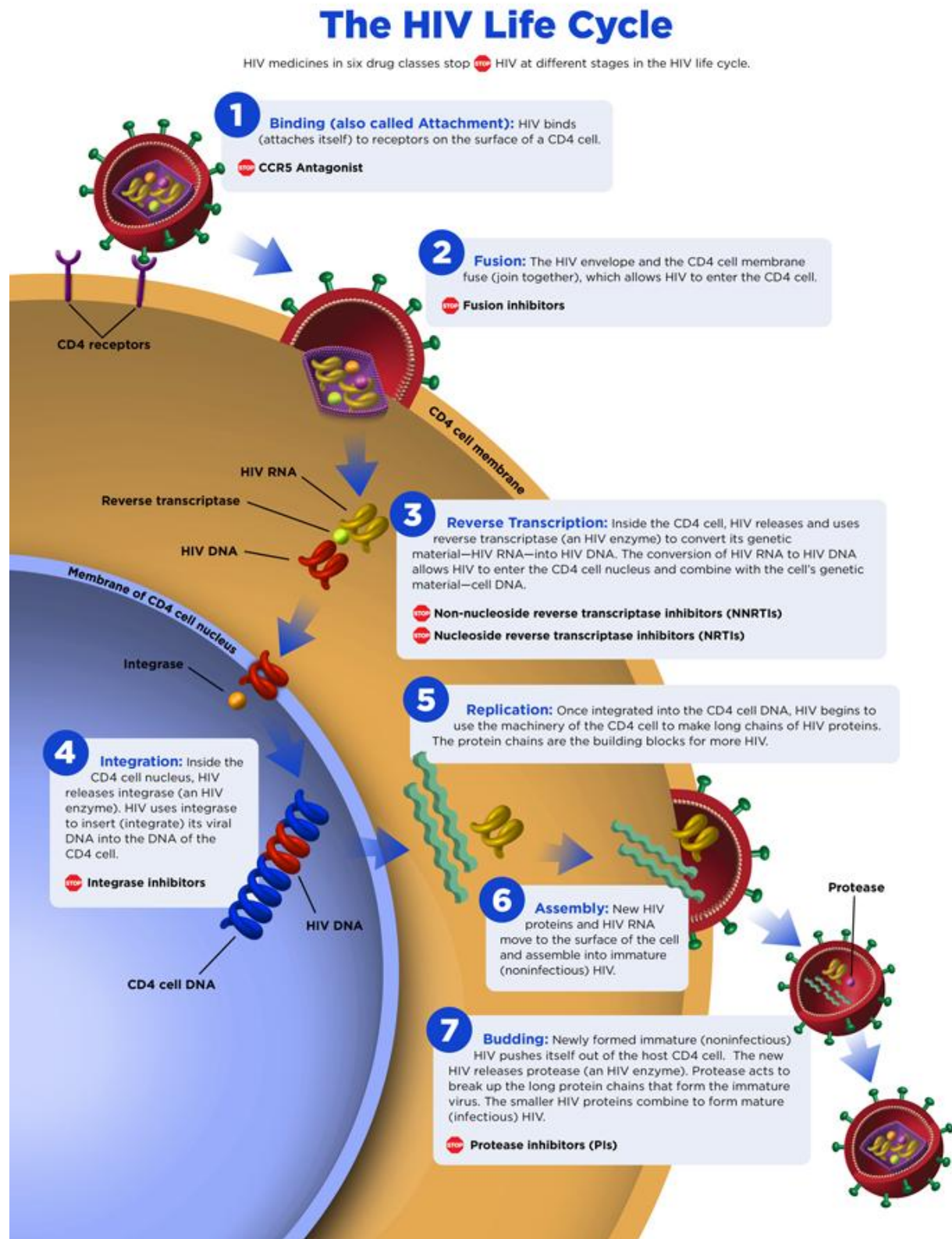


Figure 4: HIV life cycle<sup>[9]</sup>

### 1A.8. Classification of HIV

HIV is a member of the genus *lentivirus*,<sup>[10]</sup> part of the family *retroviridae*.<sup>[11]</sup> *Lentiviruses* have many morphologies and biological properties in common. Many species are infected by *lentiviruses*, which are characteristically responsible for long-duration illnesses with a long incubation period.<sup>[12]</sup> *Lentiviruses* are transmitted as single-stranded, positive-sense, enveloped RNA viruses. Upon entry into the target cell, the viral RNA genome is converted (reverse transcribed) into double-stranded DNA by a virally encoded reverse transcriptase that is transported along with the viral genome in the virus particle. The resulting viral DNA is then imported into the cell nucleus and integrated into the cellular DNA by a virally encoded integrase and host co-factors.<sup>[13]</sup> Once integrated, the virus may become latent, allowing the virus and its host cell to avoid detection by the immune system. Alternatively, the virus may be transcribed, producing new RNA genomes and viral proteins that are packaged and released from the cell as new virus particles that begin the replication cycle anew.

### 1A.9. Types of HIV

Each time HIV replicates (by infecting a new cell), small changes or mutations may occur. This means there are many different forms of HIV, included within the body of a single person living with HIV. Two types of HIV have been characterized: HIV-1 and HIV-2. HIV-1 is the virus that was initially discovered and termed both LAV and HTLV-III. HIV type 1 and HIV type 2 are two distinct viruses. Worldwide, the predominant virus is HIV-1, and generally when people talk about HIV without specifying the type of virus they are generally referring to HIV-1. The relatively uncommon HIV-2 virus is concentrated in West Africa, but has been seen in other countries. It is less infectious and progresses slower

than HIV-1. While commonly used antiretroviral drugs are active against HIV-2, optimum treatment is poorly understood. <sup>[14]</sup>

### HIV Types and Strains

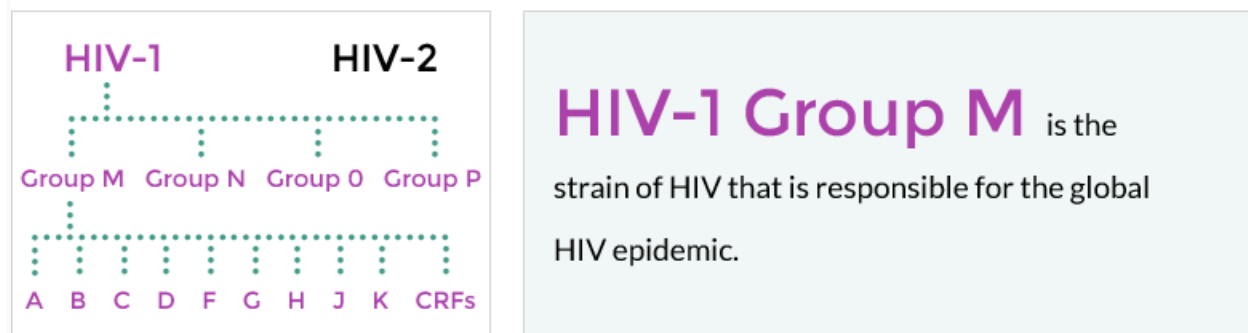


**Figure 5:** Subtypes of HIV <sup>[15]</sup>

The strains of HIV-1 can be classified into four groups (Figure 5). The most important group, M, is the 'major' group and is responsible for the majority of the global HIV epidemic. The other three groups are N, O and P. They are quite uncommon and only occur in Cameroon, Gabon and Equatorial Guinea.

### Subtypes within HIV-1 group M

Within group M there are known to be at least nine genetically distinct subtypes of HIV-1.

These are termed subtypes A, B, C, D, F, G, H, J and K.

Additionally, different subtypes can combine genetic material to form a hybrid virus, known as a 'circulating recombinant form' (CRFs), of which quite a few have been identified. <sup>[16]</sup> The dominant HIV subtype in the Americas, Western Europe and Australasia is subtype B. As a result, the great majority of HIV clinical research has been conducted in populations where subtype B predominates. However, this subtype represents only 12% of global HIV infections. In contrast, less research is available for

subtype C, although just under half of all people living with HIV have subtype C. It is very common in the high prevalence countries of Southern Africa, as well as in the horn of Africa and India. The greatest diversity of subtypes is found in Cameroon and the Democratic Republic of Congo; the region where the HIV-1 epidemic originated. However, these geographical patterns in the distribution of subtypes are changing over time, due to migration and the mixing of populations.

### **1A.10. Drugs for HIV/AIDS**

The drugs used to treat HIV are called antiretroviral drugs and referred to as ARVs. Combination antiretroviral therapy (cART) is referred to as ‘highly active ART’ (HAART). Combination therapy helps prevent drug resistance. ARVs reduce the viral load, the amount of virus in your bloodstream, but are not a cure. A blood test measures the viral load.

Antiretroviral drugs are used for:

ART (Antiretroviral Therapy)

PMTCT (Prevention of Mother To Child Transmission)

PEP (Post Exposure Prophylaxis)

PrEP (Pre Exposure Prophylaxis)

HAART (Highly Active Antiretroviral Therapy)

### **1A.11. Types of antiretroviral drugs**

There are six main antiretroviral drug classes currently used to construct first-line treatment regimens:

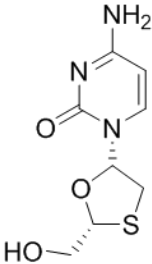
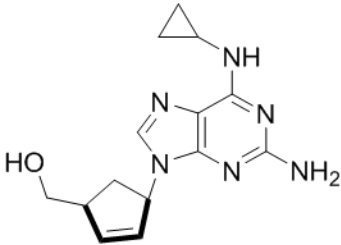
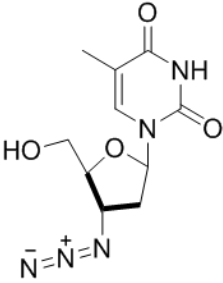
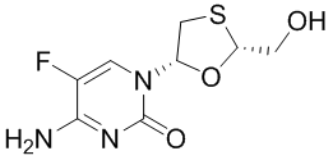
- (i) NRTI's (nucleoside reverse transcriptase inhibitors)
- (ii) NtRTI's (nucleotide reverse transcriptase inhibitors)
- (iii) NNRTI's (non-nucleoside reverse transcriptase inhibitors)
- (iv) PI's (protease inhibitors)
- (v) Fusion and entry inhibitors
- (vi) Integrase inhibitors

#### **(i) Nucleoside reverse transcriptase inhibitors (NRTI's)**

Discovery and development of nucleoside reverse-transcriptase inhibitors (NRTI's) began in the 1980s. The first NRTI was Zidovudine (AZT) which was synthesized by Horwitz at the Michigan Cancer Foundation in 1964. It was approved by the U.S. Food and Drug Administration (FDA) in 1987. The 3'hydroxyl group in the deoxyribose ring of thymidine is replaced by an azido group, which gives Zidovudine <sup>[16]</sup>. Further, NRTI's were developed by modifications on purine and pyrimidine bases. Table 3 describes the NRTI's structure, brand names and their dosage.



**Table 3: Some of the approved NRTI's drugs and their dosage**

Drug Name	Structure	Brand Name	Dosage
Lamivudine (3TC)	 <p style="text-align: center;"><b>1</b></p>	Epivir	300 mg once daily
Abacavir	 <p style="text-align: center;"><b>2</b></p>	Ziagen	300 mg BID
Zidovudine (AZT)	 <p style="text-align: center;"><b>3</b></p>	Retrovir	300BID
Emtricitabine	 <p style="text-align: center;"><b>4</b></p>	Emtriva	200 mg oral capsule once daily

### **Mechanism of action**

NRTI's works by selectively inhibiting HIV's reverse transcriptase, the enzyme that the virus uses to make a DNA copy of its RNA. Reverse transcription is necessary for the production of HIV's double-stranded DNA, which would be subsequently integrated into the genetic material of the infected cell.

Cellular enzymes convert NRTI's into the effective 5'-triphosphate form. NRTI's activated in the cell by the addition of three phosphate groups to their deoxyribose moiety, to form NRTI triphosphates. This phosphorylation step is carried out by cellular kinase enzymes. Studies have shown that the termination of HIV's forming DNA chains is the specific factor in the inhibitory effect.

### **Adverse reactions**

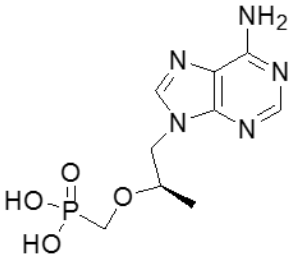
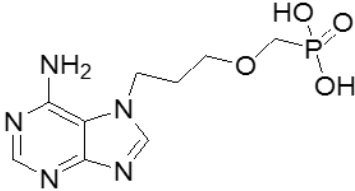
The NRTI's can interfere with mitochondrial DNA synthesis and lead to high levels of lactate and lactic acidosis, liver steatosis, peripheral neuropathy, myopathy and lipodystrophy. <sup>[17]</sup> Current first line NRTI's such as lamivudine/emtricitabine, tenofovir and abacavir are less likely to cause mitochondrial dysfunction. <sup>[18,19]</sup>

### **(ii) Nucleotide reverse transcriptase inhibitors NtRTI's**

Nucleoside analogs are converted into nucleotide analogs in the human body by dephosphorylation and act through the same mechanism of action. Tenofovir is a 'prodrug' activated by the enzymes in the human body, allowing a low dose of tenofovir to reach the site of desired activity. It is approved in the USA for the treatment of both HIV and hepatitis B. Adefovir is not approved by the FDA for treatment of HIV due to toxicity

issues, but a lower dose is approved for the treatment of hepatitis B. Table 4 describes some of the approved NtRTI's drug structures, brand names and their dosage.

**Table 4: Some of the approved NtRTI's drugs and their dosage**

Drug Name	Structure	Brand Name	Dosage
Tenofovir	 <p style="text-align: center;"><b>5</b></p>	Viread	300 mg once daily
Adefovir.	 <p style="text-align: center;"><b>6</b></p>	Preveon	10 mg once daily

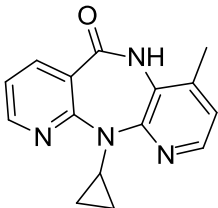
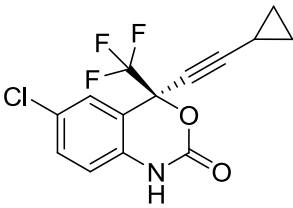
### Adverse drug reactions

Tenofovir mainly causes acute renal insufficiency, nausea, vomiting, diarrhea, abdominal discomfort, gastrointestinal symptoms and these are worse in lactose intolerant patients (Tenofovir formulated by lactose). Adefovir more common side effects are dark urine, general tiredness and weakness, light-colored stools, nausea and vomiting, upper right abdomen or stomach pain, yellow eyes and skin.

**(iii) Non nucleotide reverse transcriptase inhibitors NNRTI's**

Non-nucleoside reverse-transcriptase inhibitors (NNRTI's) are antiretroviral drugs used in the treatment of human immunodeficiency virus (HIV). NNRTIs inhibit reverse transcriptase (RT), an enzyme that controls the replication of the genetic material of HIV. RT is one of the most popular targets in the field of antiretroviral drug development <sup>[16]</sup>. Discovery and development of NNRTI's began in the late 1980s. <sup>[20]</sup> Table 5 described some approved NNRTI's drugs structure, dosage and brand names.

**Table 5: Some of the approved NNRTI's drugs and their dosage**

Drug Name	Structure	Brand Name	Dosage
Nevirapine	 <p style="text-align: center;"><b>7</b></p>	Viramune	200 mg BID or 400 mg once daily
Efavirenz	 <p style="text-align: center;"><b>8</b></p>	Sustiva	600 mg once daily, at or before bedtime

## Mechanism of action

The NNRTI's class of antiretroviral drugs are small hydrophobic chemical compounds that have a high affinity for a hydrophobic binding pocket located near the active site of the HIV reverse transcriptase enzyme. The binding causes the conformational change in the three-dimensional structure of the enzyme. This affects the catalytic activity of the enzyme and blocks the HIV-1 replication by inhibiting the polymerase active site (Figure 6). The global conformational change additionally destabilizes the enzyme on its nucleic acid template and reduces its ability to bind nucleotides.<sup>[21]</sup> The transcription of the viral RNA is inhibited and therefore the replication rate of the virus reduces.<sup>[22]</sup>

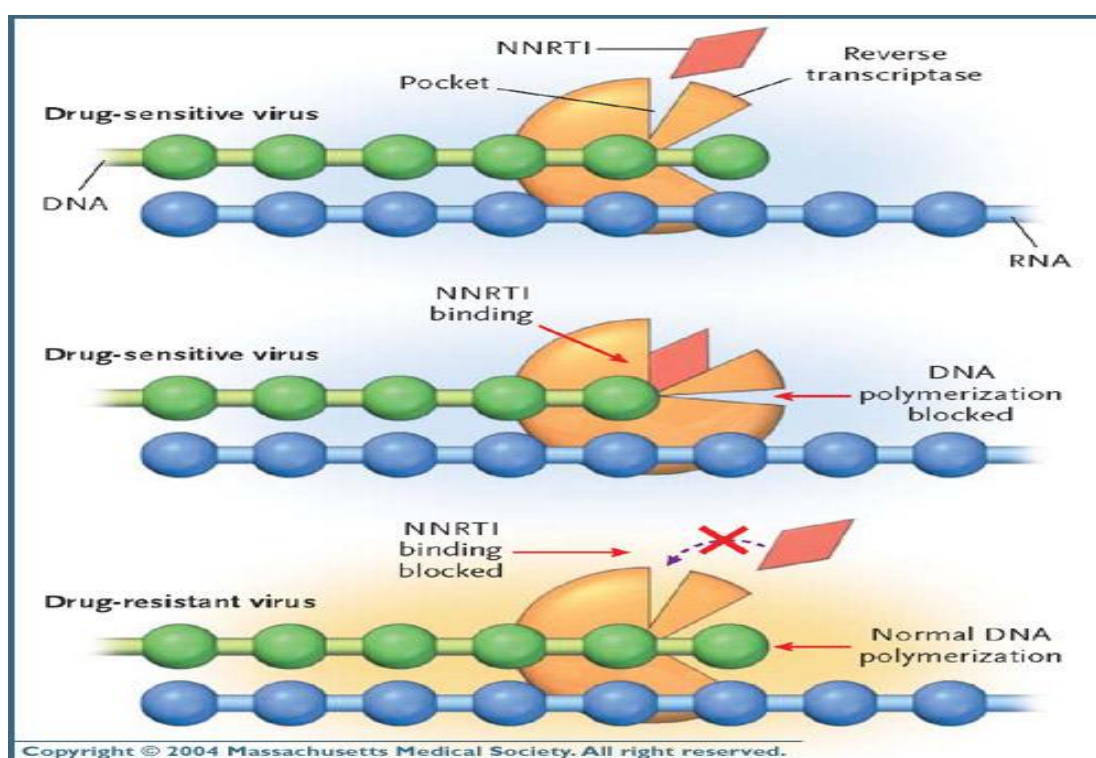


**Figure 6:** Mechanism of action of NNRTI's <sup>[23]</sup>

### **Adverse effects**

NNRTIs are generally safe and well tolerated. The main reason for discontinuation of efavirenz is neuro-psychiatric effects including suicidal tendencies. Nevirapine can cause severe hepatotoxicity, especially in women with high CD4 counts.<sup>[24]</sup>

#### **(iv) Protease Inhibitors (PI's)**

They are highly effective against HIV and since the 1990s, have been a key component of anti-retroviral therapies for HIV/AIDS.<sup>[25,26]</sup> Table 6 described the approved PI's structure, brand names and dosage.

**Table 6: Some of the approved PI's drugs and their dosage**

Drug Name	Structure	Brand Name	Dosage
Atazanavir	<p>Chemical structure of Atazanavir (9) is shown. It features a central core with a pyridine ring, a benzyl group, and a hydroxyl group. The structure is labeled with the number 9.</p>	Reyataz	400 mg once daily
Darunavir	<p>Chemical structure of Darunavir (10) is shown. It features a central core with a sulfonamide group, a hydroxyl group, and a tetrahydrofuran ring. The structure is labeled with the number 10.</p>	Prezista	800 mg once daily
Fosamprenavir	<p>Chemical structure of Fosamprenavir (11) is shown. It features a central core with a sulfonamide group, a hydroxyl group, and a tetrahydrofuran ring. The structure is labeled with the number 11.</p> <p>R = H; Amprenavir R = H<sub>2</sub>PO<sub>3</sub>; Fosamprenavir</p>	Telzir / Lexiva	1400 mg BID

### Mechanism of action

HIV protease inhibitors are peptide-like chemicals that competitively inhibit the action of the virus aspartyl protease. These drugs prevent proteolytic cleavage of HIV Gag and polyproteins that include essential structural and enzymatic components of the virus

(Figure 7). This prevents the conversion of HIV particles into their mature infectious form.

[27]

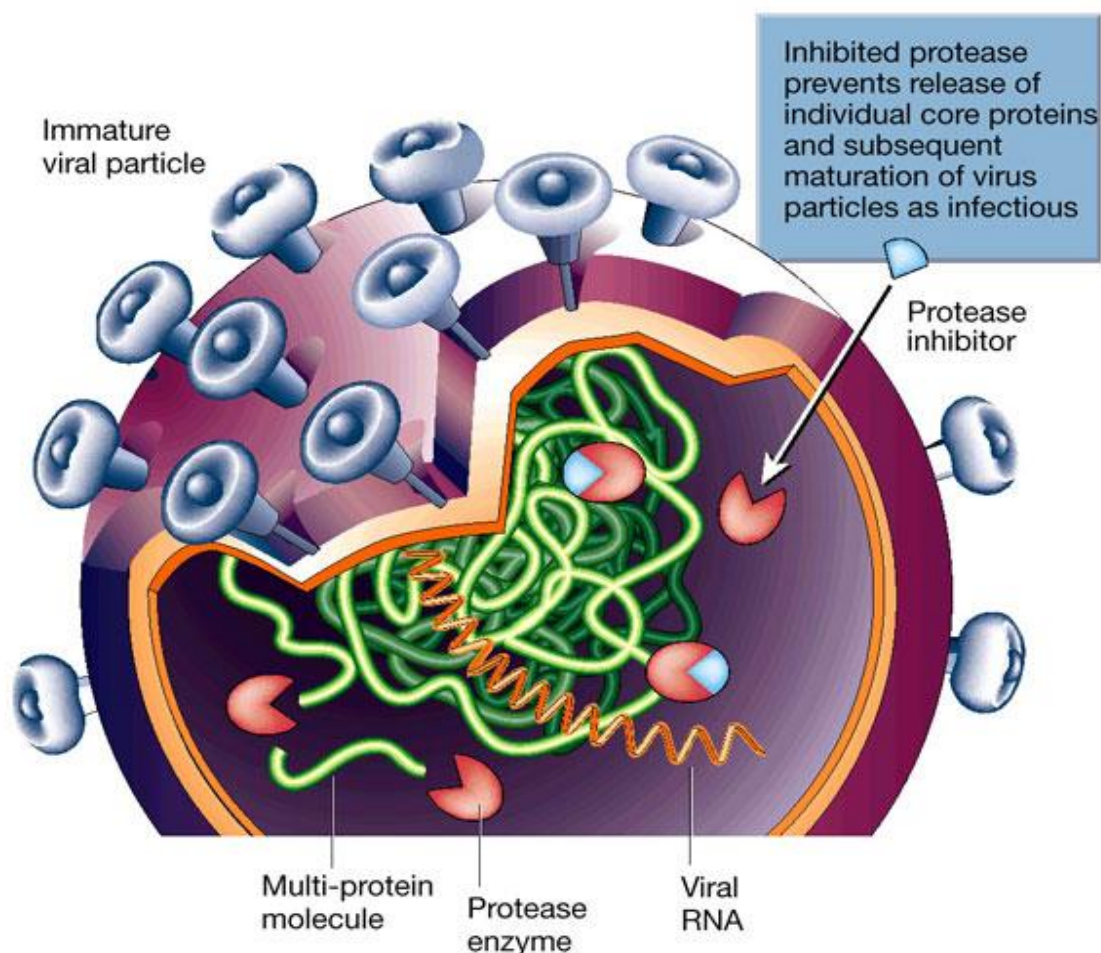


**Figure 7:** Mechanism of action of protease inhibitors [28]

### Adverse effects

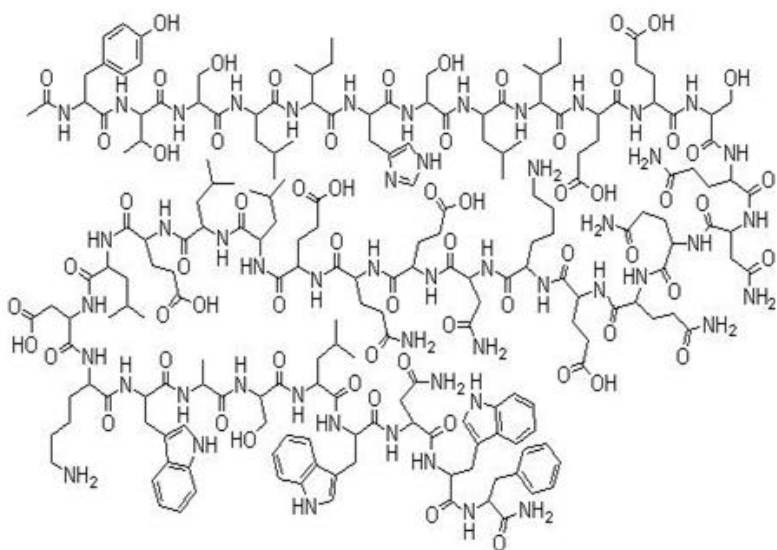
Protease inhibitors (PIs) are often given with ritonavir, a strong inhibitor of cytochrome P450 enzymes, leading to numerous drug-drug interactions. They are also associated with lipodystrophy (peripherals fat loss), elevated triglycerides and elevated risk of heart attack indirect hyperbilirubinemia, hyperglycemia, hyperlipidemia and skin rash.[29]



**(v) Fusion and entry inhibitors**

There is a single licensed fusion inhibitor enfuvirtide, (T-20), developed by Roche and Trimeris. Since T-20 is a protein that would be destroyed by acids in the stomach, it must be administered by injection.<sup>[30-33]</sup> Table 7 described FI's drug structure, brand name and its dosage.

**Table 7: Approved FI's drug and the dosage**

Drug Name	Structure	Brand Name	Dosa ge
Enfuvirtide	 <p style="text-align: center;">12</p>	Fuzeon	90 mg twice a day

### **Mechanism of action**

In order to enter a host cell, HIV must bind to two separate receptors on the cell's surface. First, the gp120 glycoprotein on HIV's envelope binds to the CD4 receptor, which is present on various types of immune cells including CD4 T-cells. When this is accomplished, gp120 must then bind to a second co-receptor. HIV-1 can use two chemokine co-receptors, CCR5 or CXCR4. Once HIV has attached to both CD4 and a co-receptor, its envelope can fuse with the host cell membrane and release viral components into the cell. After HIV's gp120 envelope glycoprotein attaches to a CD4 receptor and a co-receptor on the cell, a different glycoprotein, called gp41, is exposed. The glycoproteins then undergo shape changes that bring the virus and the cell closer together, allowing them to fuse, bind to the gp41 glycoprotein and prevents the shape changes that enable virus-cell fusion.

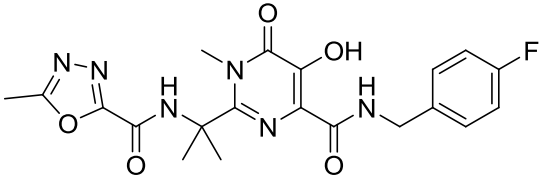
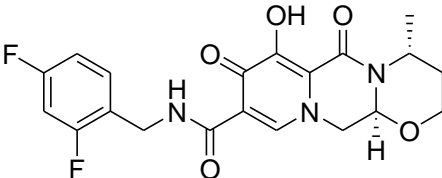
### **Adverse drug reactions**

More common side effects include injection site reactions; erythema, cysts, and nodules at injection sites, neutropenia, the possible increased frequency of pneumonia.

### **(vi) Integrase inhibitors**

Integrase inhibitors, also known as integrase strand transfer inhibitors (INSTIs), are a class of antiretroviral drug designed to block the action of the integrase enzyme. The first integrase inhibitor raltegravir was approved by the FDA on October 12, 2007. Some of the approved INSTI's drugs and their dosage described in Table 8.

**Table 8: Some of the approved INSTI's drugs and their dosage**

Drug Name	Structure	Brand Name	Dosage
Raltegravir	 <p style="text-align: center;"><b>13</b></p>	Isentress	400 mg BID
Dolutegravir	 <p style="text-align: center;"><b>14</b></p>	Tivicay	50 mg once daily or 50 mg BID

**Mechanism of action**

Integrase inhibitors, also known as integrase strand transfer inhibitors (INSTIs), are a class of antiretroviral drug designed to block the action of integrase, a viral enzyme that inserts the viral genome into the DNA of the host cell. The mechanism of action of Integrase inhibitors is explained in Figure 8, since integration is a vital step in retroviral replication, blocking it can halt further spread of the virus. Integrase inhibitors were initially developed for the treatment of HIV infection, but they could be applied to other retroviruses.

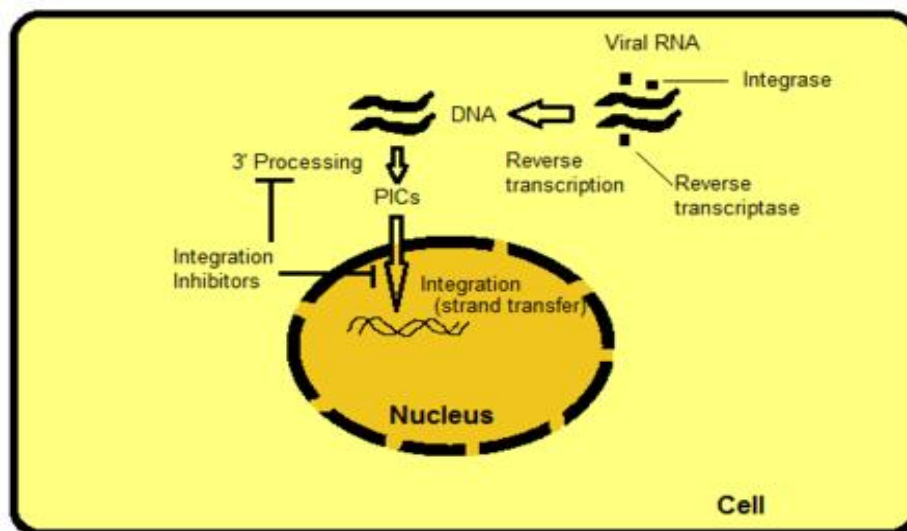


**Figure 8:** Mechanism of action of Integrase inhibitor <sup>[34]</sup>

### Adverse effects

Integrase inhibitors (INSTIs) are among the best tolerated of the antiretroviral with excellent short and medium term outcomes. Given their relatively new development, there is less long term safety data available. They are associated with an increase in creatinine kinase levels and rarely myopathy.

### 1A.12. Drug combinations

Combinations of antiretrovirals create multiple obstacles to HIV replication to keep the number of offspring low and reduce the possibility of a superior mutation. If a mutation that conveys resistance to one of the drugs being taken arises, the other drugs continue to suppress reproduction of that mutation. With rare exceptions, no individual antiretroviral drug has been demonstrated to suppress an HIV infection for long; these agents must be taken in combinations in order to have a lasting effect. As a result, the standard of care is to use combinations of antiretroviral drugs. Combinations usually consist of three drugs

from at least two different classes described above.<sup>[35]</sup> This three drug combination is commonly known as a triple cocktail.<sup>[36]</sup> Combinations of antiretrovirals are subject to positive and negative synergies, which limit the number of useful combinations. In recent years, drug companies have worked together to combine these complex regimens into simpler formulas, termed fixed-dose combinations.<sup>[37]</sup> Commercial fixed dosage combinations are described in Table 9 while Table 10 explains drug combinations in special cases.

**Table 9: Commercial fixed-drug combinations**

Combination	Trade name
Zidovudine + lamivudine	Combivir
Zidovudine + abacavir	Epzicom
Zidovudine + lamivudine + abacavir	Trizivir
Tenofovir + emtricitabine	Truvada
Tenofovir + emtricitabine + efavirenz	Atripla
Stavudine + lamivudine + nevirapine	Triomune
Lopinavir + ritonavir	Kaletra
Rilpivirine + tenofovir/ emtricitabine	Complern
Elvitegravir + cobicistat + tenofovir + emtricitabine	Stribild

**Table 10: Drug combinations in special case**

Target population	Preferred options
Pregnant women	AZT+3TC+EFV
HIV+TB	AZT or TDF +3TC or FTC +EFV
HIV+HBV	TDF+3TC or FTC+EFV or NVP

**1A.12.1. Advantages of combination therapy**

i) Synergism: The interaction or cooperation of two or more substances to produce a combined effect greater than the sum of their separate effects.

ii) Reduced toxicity.

iii) Prevent resistance.

**1A.12.2. General combinations**

i) 2 NRTI + 1 NNRTI

ii) 1 NRTI + 1 NtRTI + 1 NNRTI

iii) 2 NRTI + boosted PI

iv) 1 NRTI + 1 NtRTI + boosted PI

v) 3 NRTI (One must be Abacavir)

**1A.13. WHO guidelines for treatment**

As per WHO guidelines for HIV/AIDS, first line treatment should consist of at least two nucleoside reverse transcriptase inhibitors and one protease inhibitor or efavirenz, and the second line treatment should consist of a boosted protease inhibitor and two nucleoside reverse transcriptase inhibitors. Some of the first and second line drugs listed in Table 11.

**Table11: First and second line HIV/AIDS drugs**

First line drugs	Second line drugs
AZT+d4T+3TC	ABC+TDF+AZT
NVP+EFV	NFV+IND

**1A.14. Introduction to efavirenz**

Efavirenz (EFV, brand names Sustiva, Stocrin, Efavir) (Figure 9) is a non-nucleoside reverse transcriptase inhibitor (NNRTI) and is used as part of a highly active antiretroviral therapy(HAART) for the treatment of a human immunodeficiency virus (HIV) type 1.

For HIV infections that have not previously been treated, the United States Department of Health and Human Services Panel on antiretroviral guidelines currently recommends the use of efavirenz in combination with tenofovir/emtricitabine (Truvada) as one of the preferred NNRTI in the adults and adolescents. Efavirenz is also used in combination with other antiretroviral agents as part of an expanded post exposure prophylaxis regimen in order to reduce the risk of HIV infection in people exposed to a significant risk (e.g. needle stick injuries, certain types of unprotected sex *etc.*). The usual adult dose is 600 mg once

a day. It is usually taken on an empty stomach at bedtime to reduce neurological and psychiatric adverse effects.



**Figure 9:** Efavirenz drug image

#### **1A.14.1. History**

Efavirenz was approved by the FDA on September 21 1998, as the 14th approved antiretroviral drug and the European license was granted in May 1999. Efavirenz, formerly known by the codename DMP 266, was developed by Du Pont Pharma.

Efavirenz is marketed by Bristol-Myers Squibb under the trade name *Sustiva* in the United States, United Kingdom, Ireland, France, Germany, Italy and Spain. The trade name *Stocrin* is used by Merck Sharp & Dohme, who market the drug in other European countries, Australia, Brazil, Latin America, South Africa and other regions. Generic versions are manufactured in India as *Efavir* (made by Cipla), *Estiva* (Genixpharma), *Viranz* (Aurobindo) and *Effervan* (Ranbaxy).

Efavirenz chemically known as (4*S*)-6-chloro-4-(cyclopropylethynyl)-1,4-dihydro-4-(trifluoromethyl)-2*H*-3,1-benzoxazin-2-one, is a highly potent non-nucleoside reverse transcriptase inhibitor (NNRTI). A number of compounds are effective in the treatment of



the human immunodeficiency virus (HIV) which is the retrovirus that causes progressive destruction of the human immune system. Effective treatment through inhibition of HIV reverse transcriptase is known for non-nucleoside based inhibitors. Benzoxazinones have been found to be useful non-nucleoside based inhibitors of HIV reverse transcriptase, efficient synthetic processes for its production needs to be developed. Even though many prior art processes report the method for the preparation of efavirenz, each process has some limitations with respect to yield, purity, plant feasibility etc. Hence in view of the commercial importance of efavirenz, there remains need for an improved process.

#### **1A.14. 2. Effectiveness**

Efavirenz is a powerful anti-HIV drug, taken in combination with other antiretroviral drugs. It has been proven to reduce HIV-1 viral load to below 400 copies/mL within six months in 60 to 80% of people who have not previously taken any HIV treatments. Efavirenz is not active against HIV-2.

Efavirenz's potency was demonstrated in clinical studies, in which efavirenz was found to be superior to indinavir (*Crixivan*),<sup>[38]</sup> when either drug was combined with AZT (zidovudine, *Retrovir*) and 3TC (lamivudine, *Epivir*). After three years, more patients taking efavirenz maintained viral suppression, even in patients with viral loads above 300,000 copies/mL before treatment began. Researchers have estimated that the average time to virological failure on efavirenz, AZT and 3TC is six years, based on long-term follow-up of this study.<sup>[39]</sup>

Efavirenz-based treatment is also effective in patients starting therapy with CD4 cell counts below 100 cells/mm<sup>3</sup>.<sup>[40]</sup> However, its efficacy has not been assessed in patients

starting with CD4 cell counts below 50 cells/mm<sup>3</sup> or after failure of protease inhibitor-containing regimens.

A large-scale, comparative study called ACTG 384, was completed in 2002. It found that efavirenz, AZT and 3TC was the preferred first-line therapy in terms of antiviral efficacy and toxicity after 144 weeks of follow-up.<sup>[41,42]</sup> In addition, two observational studies have suggested that people taking efavirenz are more likely to achieve and sustain undetectable viral load than those taking a protease inhibitor.<sup>[43,44]</sup> Similarly, a retrospective study based in San Francisco has shown that first-line anti-HIV drug regimens containing efavirenz give better survival outcomes than any other combinations available prior to 2002.<sup>[45]</sup> Another randomized study, which compared efavirenz with d4T (stavudine, *Zerit*) and ritonavir (*Norvir*) boosted amprenavir (*Agenerase*) when taken in combination with AZT and 3TC, has also favored efavirenz as first-line treatment.<sup>[46]</sup> Similarly, efavirenz is more likely to suppress viral load than the protease inhibitor nelfinavir (*Viracept*) when combined with d4T and ddI (didanosine, *Videx*), although the two drugs have similar immunological outcomes.<sup>[47]</sup>

There is some dispute about the comparative efficacy of the non-nucleoside reverse transcriptase inhibitors efavirenz and nevirapine (*Viramune*). The randomized 2NN study showed that nevirapine was not inferior to efavirenz, although the participants taking efavirenz experienced fewer side-effects.<sup>[48]</sup> The quality of life was also similar in patients taking nevirapine and efavirenz.<sup>[49]</sup> Despite this, based on several large cohort studies that have found efavirenz to be superior to nevirapine in terms of efficacy and rebound rates, United States treatment guidelines recommend efavirenz as the preferred NNRTI in first-line treatment.<sup>[50,-52]</sup> British guidelines do not endorse efavirenz as the superior

NNRTI and suggest that drug choices should be individualized, however this clearly makes treatment more complicated.

There is a growing body of research indicating that switching to efavirenz from a protease inhibitor is an effective strategy. For example, one large randomized study found that the likelihood of adhering to the drug regimen and maintaining viral suppression after one year was greater among people who substituted efavirenz for a protease inhibitor than those who continued on protease inhibitor therapy.<sup>[53]</sup> Results from a Swiss HIV Cohort also indicate that people who switch from a protease inhibitor to efavirenz are more likely to maintain virological control one year after switching, although a recent study has suggested that this may be due to better adherence associated with a regimen that is easier to take.<sup>[54,55]</sup>

Further information on this came from results of ACTG 5142.<sup>[56]</sup> This is a multicentre open-label randomized 96-week study of 753 treatment-naïve patients with viral load over 2000 copies/mL and any CD4 count. At the start of the study, the median viral load was approximately 100,000 copies/mL and the median CD4 cell count was 182 cells/mm<sup>3</sup>, suggesting that the study population had relatively advanced HIV disease, and was starting treatment somewhat later than current guidelines recommend.

Patients received one of three regimens: efavirenz + 2 NRTIs, *Kaletra* (LPV/r) + 2 NRTIs, or an NRTI-sparing combination of efavirenz and *Kaletra*. The NRTI options were 3TC or FTC combined with stavudine (d4T), TDF, or zidovudine (ZDV). By intent-to-treat analysis, 89% of the participants receiving efavirenz-based triple therapy had viral loads below 50 copies/mL after 96 weeks, as compared with 77% receiving *Kaletra*-based triple therapy.

The researchers were unclear why fewer participants on *Kaletra*-based triple therapy achieved viral loads below 50 copies/mL at week 96, compared with those on efavirenz-based triple therapy, since they found that the time to treatment-limiting toxicity was similar for all, and the proportion of grade 3 or 4 clinical adverse events was similar in each, at around 20%.

There is evidence to suggest that efavirenz penetrates the cerebrospinal fluid that surrounds the brain and the spinal cord and that it may be effective against HIV in the brain. One small study found that efavirenz-containing drug combinations reduced the amount of HIV in the cerebrospinal fluid to below 400 copies/mL over 26 weeks.<sup>[57]</sup> There is also evidence that a combination containing efavirenz can reduce HIV in the lymph tissue to very low levels.<sup>[58]</sup>

HIV-positive African Americans taking efavirenz are less likely to experience immunological failure than Caucasians, which may be due to a high prevalence of a genetic variant that slows down clearance of the drug.<sup>[59,60]</sup> This variant also means that patients stopping efavirenz treatment who have this variant are at risk of developing efavirenz resistance for an extended period, while drug levels fall.<sup>[61]</sup>

### **1A.14.3. Adverse drug reactions**

Dizziness, trouble sleeping, drowsiness, unusual dreams and trouble concentrating may frequently occur. These side effects may begin 1-2 days after starting this medication and usually go away after 2-4 weeks. They are also reduced by taking efavirenz on an empty stomach at bedtime. Alcohol and street drugs while taking efavirenz may worsen these side effects.

# **CHAPTER 1**

## **SECTION B**

### **INTRODUCTION TO FLOW CHEMISTRY & LITERATURE REVIEW**

### 1B.1. Definition- flow chemistry

Flow chemistry, sometimes referred to as microchemistry or continuous flow chemistry is the process of performing chemical reactions in a tube or pipe. Reactive components are pumped together at a mixing junction and flowed down a temperature controlled pipe or tube<sup>[62]</sup>(Figure 10).

In other words, pumps move fluid into a tube, and where tubes join one another, the fluids contact each other where they mix and subsequently if these fluids are reactive, a reaction takes place.<sup>[63]</sup>

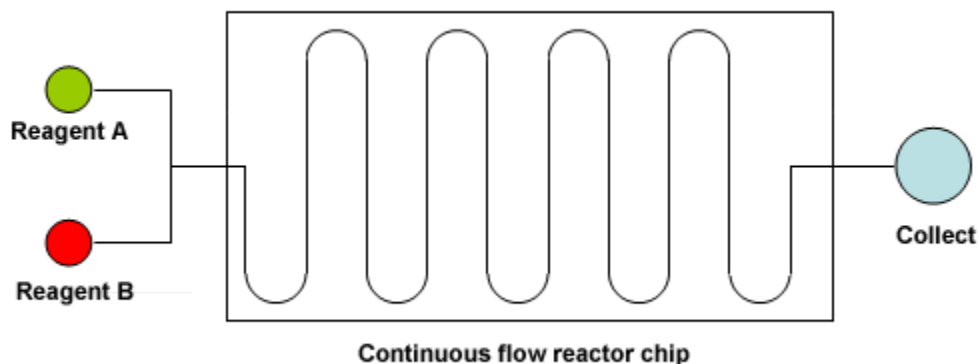


**Figure 10:** Flow reactor general set up

### 1B.2. Background

Organic synthesis has traditionally been performed in batch, which means in round bottomed flasks, test tubes, or closed vessels; recently, continuous flow methodologies in microreactors (Figure 11) have gained much attention from synthetic organic chemists.<sup>[64, 65]</sup> Until a few years ago, continuous flow processes were a prerogative of the petrochemical and bulk chemicals industries, where dedicated continuous plants exist and proved most economical; recently, application of these systems for the preparation

of fine chemicals, such as natural products <sup>[66]</sup> or Active Pharmaceutical Ingredients (APIs) has become very popular, especially in academia. Although many pharmaceutical industries still rely on multipurpose batch or semi batch reactors, recently some of the pharmaceutical companies started using the flow chemistry technology as a result of this evolution is the increasing number of reactions successfully performed with this technique and reported in the literature.<sup>[67]</sup>

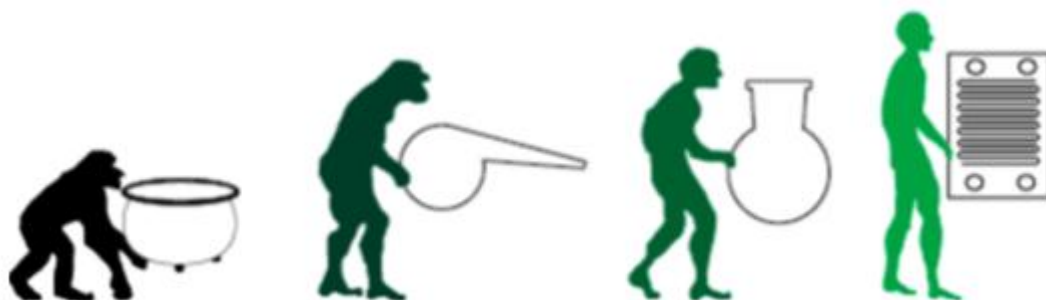


**Figure 11:** Evolution of organic reactor <sup>[65]</sup>

Continuous flow reactors have been used by chemical engineers for over a century. Only recently have scaled-down versions become available to the synthetic organic chemist.<sup>[68]</sup> Several simple synthetic chemicals produced in large volumes, such as ethylene dichloride and methanol, are manufactured by highly efficient continuous or semi-continuous flow processes.<sup>[69]</sup> However, continuous processing is still very limited. Things have started to change; laboratory-scale flow reactors, which are commonly referred to as microreactors <sup>[70-72]</sup>, a small-diameter device in which the reaction takes place under rigorously controlled conditions in a confined space. Academic labs are publishing continuous synthetic routes for drugs and major corporations have announced production and or processes for production of drugs and drug intermediates by continuous

processing.<sup>[73-74]</sup> In addition to providing a new way to run reactions and synthesize a very broad variety of specialty chemicals, including highly functionalized and chiral compounds, the technology of microreactors is well-suited for combinatorial, high throughput, rapid screening of catalysts.<sup>[75]</sup> The great peculiarity of a flow system is very efficient heat and mass transfer, that allows speeding the reaction rate up so that productivity is generally greatly improved with respect to the batch system.<sup>[76]</sup> Advantageously, the flow reactor configuration can also be readily customized to meet the specific demands of the reaction and the continuous processing requirements. The construction of the reactor is often modular being assembled from several specialized yet easily integrated components such as heating and cooling zones, micro-mixers, residence tubing coils, separators and analysis units. This workflow not only allows for facile automation and continuous operation of such processes but also enables the chemist to perform more potentially hazardous and otherwise forbidden transformations in a safer and more reliable fashion.<sup>[77-82]</sup>

Not only is heat transfer favored, but also the heat exchange can be precisely monitored: due to the small dimensions, it is very easy to apply and remove a heating (or cooling) source, thus permitting very precise temperature control along the microreactor and avoiding uncontrolled hazardous exothermic processes. In general, reaction parameters such as temperature, pressure and flow rate, are more easily set up and monitored with respect to a batch process, resulting in a more reliable and reproducible process.<sup>[83]</sup> Due to the small volume required per experiment, flow processes can be used to perform fast screening of the reaction conditions, and then, with the optimized conditions in hand, the reaction can be scaled up. Scaling up a chemical reaction often represents a challenging



process since many problems may arise (e.g., runaway reactions, inefficient mixing, or byproduct formation). In principle, the reaction scale up in microreactors is easier than in batch; three different approaches can be used to produce a large amount of compound: the easiest one is to run the process longer (scaling-out). Alternatively, multi reactors in parallel (numbering up) can be used, or the process can be performed on larger continuous reactors (scaling-up).<sup>[83]</sup>

Economic analysis of continuous processes has shown large savings (up to 30%) over equivalent batch-based processes.<sup>[84]</sup>

Researchers from the Novartis-MIT Center for Continuous Manufacturing in Cambridge (USA) reported on the preparation of aliskiren hemifumarate<sup>[85]</sup> in that they described that the batch process requires a processing time of 300 h and 21 unit operations vs the 48 h and 13 unit operations in the flow process. Those figures result in the automated flow process having a lower, environmental factor and a reduced footprint. The just mentioned example clearly testifies for the great potentialities of the flow systems. Continuous flow synthetic methodologies can also be easily combined with other enabling technologies leading to improved efficiency.<sup>[86]</sup>

Given all of these advantages, it is not surprising that continuous processing is emerging as one of the techniques that can significantly impact the synthesis of APIs (or APIs intermediates). Recently, the safe manufacturing of organic intermediates and APIs under continuous flow conditions has been examined in a review by Kappe and coworkers.<sup>[87]</sup> As pointed out by the authors, some synthetic steps that were not permitted for safety reasons (e.g., use of potentially toxic or explosive intermediates, reactions run under high pressures, or above the boiling point of the solvent) can now be performed under flow

conditions with minimum risk. For these reasons flow chemistry can be seen as a novel technology that opens the way for new synthetic routes of valuable molecules.

### **1B.3. Types of flow systems**

The continuous flow systems reported so far in the literature can be generally divided into four types, as suggested by Kobayashi and co-workers (Figure 12).<sup>[88]</sup> In type I, all of the reagents flow through the reactor, and at the end the product is collected. In type II, one of the reactants is supported onto a solid and confined into the reactor; the substrate is passed through the reactor, and if the reaction goes to completion, the reaction mixture will contain the desired product only; in effect the supported system assists in product purification. Both types I and II do not require the use of any catalyst during the reaction. In type III, a homogeneous catalyst is employed; the catalyst flows through the reactor together with the reactants, so at the end, a separation step of the product from the catalyst (and possible byproducts) is required. In type IV, the catalyst resides inside the reactor, while the reagents pass by, of course, an immobilization step of the catalyst onto a solid support is required, but, in principle, no separation of the product from the catalyst is needed. In addition, through this methodology the catalyst could be easily recycled.

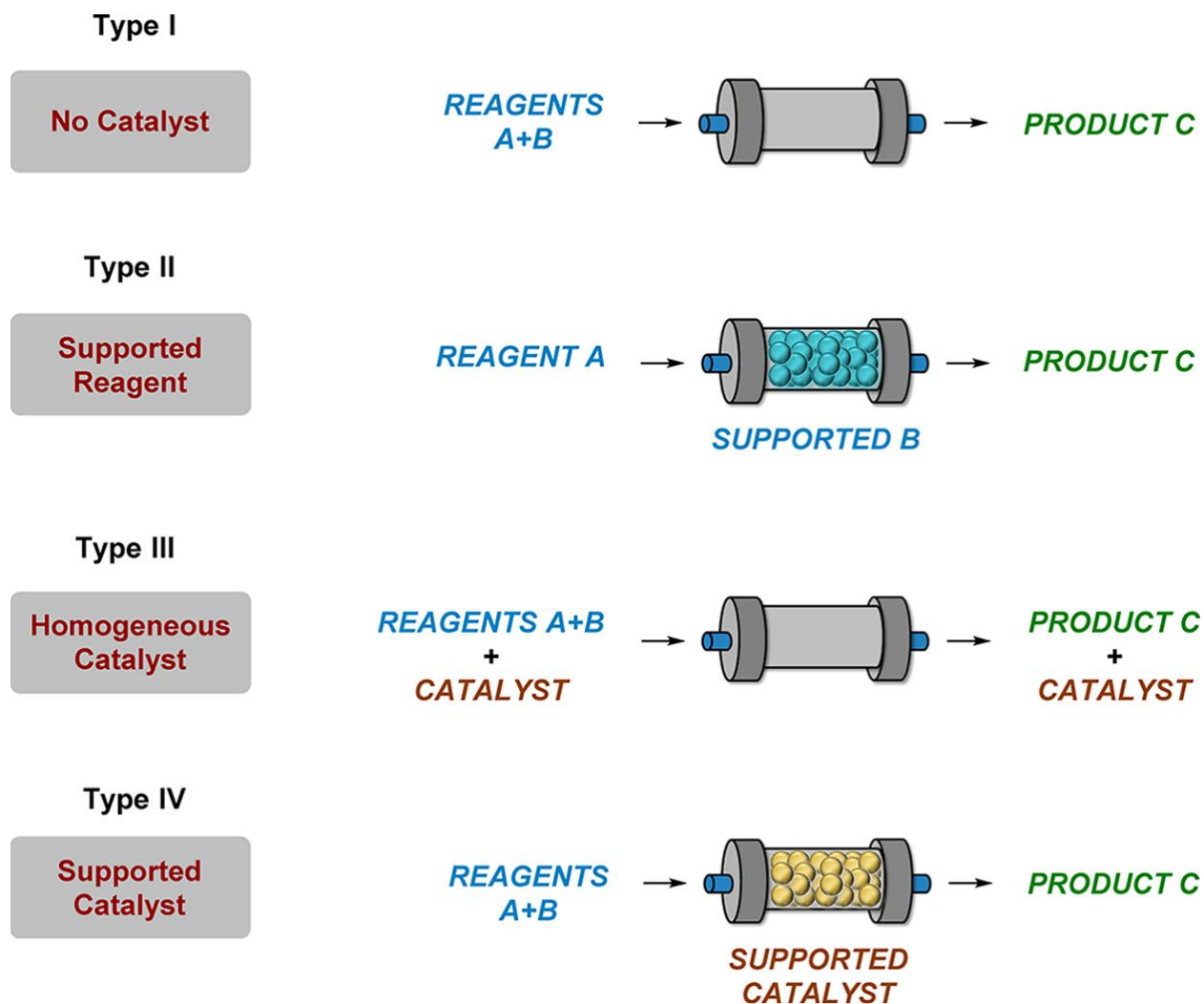


**Figure 12:** Types of continuous flow systems<sup>[88]</sup>

#### 1B.4. Flow reactors: structure and design

In flow chemistry, a chemical reaction is performed in a continuously flowing stream in a network of interconnecting channels: where they join one another, the fluids come into contact and the reaction takes place. Flow reactors are generally composed of the following basic components: one or more fluid control devices which load/pump the solutions of different reactants to the reactor section, the reactor, that usually can be heated or cooled, in which reactions can occur under a precise control of temperature and pressure and suitable reservoirs to collect the resulting mixture (Figure 13).

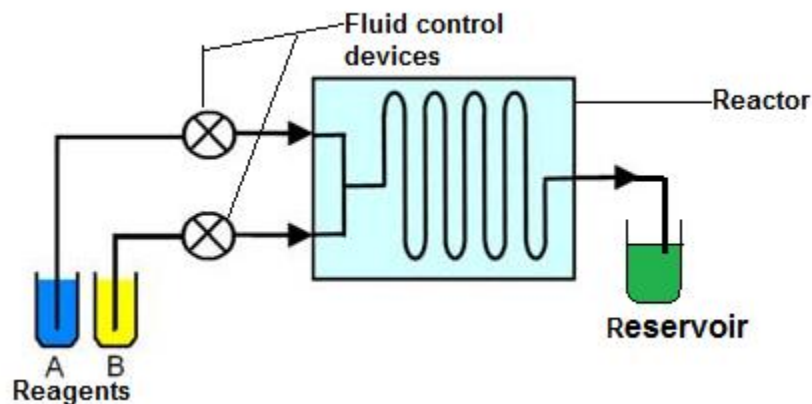


**Figure 13:** General scheme for a Flow Reactor

Laboratory scale flow reactors can generally be divided into two broad classes on the basis of channels size and volume: micro- and meso flow reactors. In general, but the distinction is not so sharp and well defined, micro flow reactors present channel having a diameter from 10 to 1000  $\mu\text{m}$ , whereas meso flow reactors are characterized by larger channels with diameter up to 10,000  $\mu\text{m}$  (1 cm).

A range of materials, including glass, silicon, stainless steel, metals, and polymers have been used for the construction of flow microreactors, some of them are shown in Figure 14.

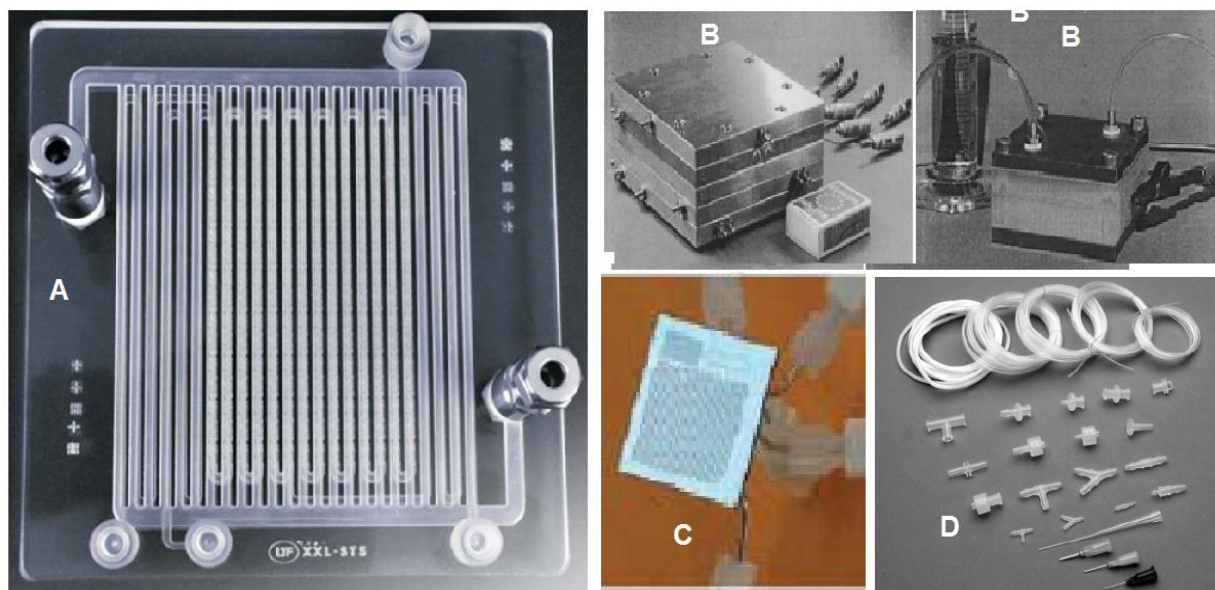


**Figure 14:** A) Glass reactor B) stainless steel reactor C) silicon reactor D) polymer reactor (PTFE tubing)<sup>[90]</sup>

### 1B.5. Advantages of the flow techniques

The main advantages associated with the flow processes performed in microreactors are described below:

#### a) Small dimensions of the channels

In the classical batch reactors (round bottom flasks), the heat control and mass distribution is generally achieved by the use of hot plate with mechanical stirring. In most cases however, non-homogeneous temperatures and mixing are obtained with the formation, in connection with reactor geometry, of concentration gradients and hot spots that can lead to poor yields and low reaction selectivity.

On the other hand, microreactors assure a rapid and efficient mixing of reagents because of the continuous and controlled addition of small volumes of reagents, reducing up to

milliseconds the time required to obtain a homogeneous solution, avoiding the formation of hot spots.<sup>[89]</sup>

**b) Pressure control: superheating effects**

In batch chemistry, the highest reaction temperature that can be obtained depends on the boiling point of the solvent being used. In flow reactors, working under pressure control, permits to perform reactions at a temperature higher than the solvent boiling point. Clearly it is possible to do batch chemistry under pressure, using autoclaves for example, but this requires the use of highly complex and specialized equipment; flow equipment enables much easier implementation of such conditions.

**c) Accessibility of exothermic reactions**

Microreactors are commonly used for exothermic and potentially explosive reactions as, for example, nitration of aromatic compounds. In fact this reaction is a classical dangerous exothermic process with a high industrial impact that has benefited from continuous reactors. Ducry and Roberge<sup>[85]</sup> reported a study on autocatalytic nitration of phenol in the presence of  $\text{HNO}_3$  in acetic acid and water as solvents. The microreactor technology is an efficient tool for kilogram scale syntheses in continuous mode and is particularly effective for hazardous reactions that do not allow scale-up in conventional reactors.

**d) Reaction time and higher selectivity yield**

Small channel size, accurate pressure control and superheating effects lead to less reaction time and higher selectivity towards the product.

**e) Continuous nature of the process**

To the continuous nature of the flow chemistry technique are associated some benefits which include,

- Easy scale-up
- Possible use of solid supported reagents or scavenger in-line
- Continuous sequential steps
- Reaction conditions independently varied during the experiment facilitating the optimization process.

## **1B.6. Synthesis of APIs by using flow technology**

### **1B.6.1. Synthesis of 2-chloro-3-amino-4-picoline (CAPIC)**

McQuade and Gupton <sup>[91]</sup> in 2013 reported the synthesis of 2-chloro-3-amino-4-picoline (CAPIC) **17** (Scheme 1), which is a strategic building block for the preparation of nevirapine **7**.

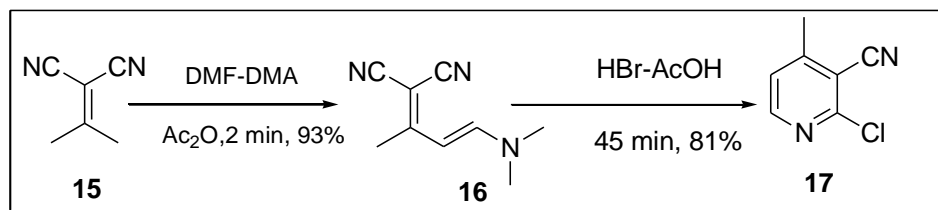
Nevirapine **7** was the first commercially available non-nucleoside reverse transcriptase inhibitor (NNRTI), and has remained an important medicine in the management of human immunodeficiency virus (HIV). Nevirapine combined with lamivudine (3TC) and azidothymidine (AZT) or tenofovir (TDF) is one of the preferred first-line combination drug therapies recommended by the World Health Organization (WHO).

The investigation for the synthesis of CAPIC **17** started from optimizing the enamine formation, which is a key step for the synthesis of CAPIC **17**. Initial batch studies revealed that the reaction occurred rapidly (1 h) in toluene heated to 45 °C to produce **15** in 94% yield, but the product precipitated and these conditions were rejected to avoid reactor clogging. Based on literature precedent and their own screening, the authors discovered that DCM was the best solvent for the preparation. They initially investigated the effect of temperature and concentration, as a result of their findings 93% yield was obtained at 95 °C, at 1.0 M conc, and with a residence time of just 2 min. In comparison, batch method

with similar concentration conditions in toluene were only complete after 1 h reaction time with 94% yield.

Then they proceeded to develop an integrated continuous process by coupling the enamine step with the Knoevenagel condensation (Scheme 1). To achieve this, the authors included two columns: a packed-bed of  $\text{Al}_2\text{O}_3$  to catalyze the first reaction and a packed bed of 3 Å molecular sieves to absorb water before the addition of DMF-DMA (Scheme 1). Assuming that the Knoevenagel condensation occurred primarily in the  $\text{Al}_2\text{O}_3$  column, they only varied the temperature of the  $\text{Al}_2\text{O}_3$  column. As a result the compound **16** yielded 91%.

After the successful combination of the Knoevenagel/enamine steps, the resulting enamine **16** solution was treated with HBr in AcOH for 45 min (55 °C) to afford the desired nicotinonitrile **17**, which crystallized out of solution in 81% overall yield.



**Scheme 1:** Synthesis of 2-chloro-3-amino-4-picoline (CAPIC) by McQuade<sup>[91]</sup> *et.al*

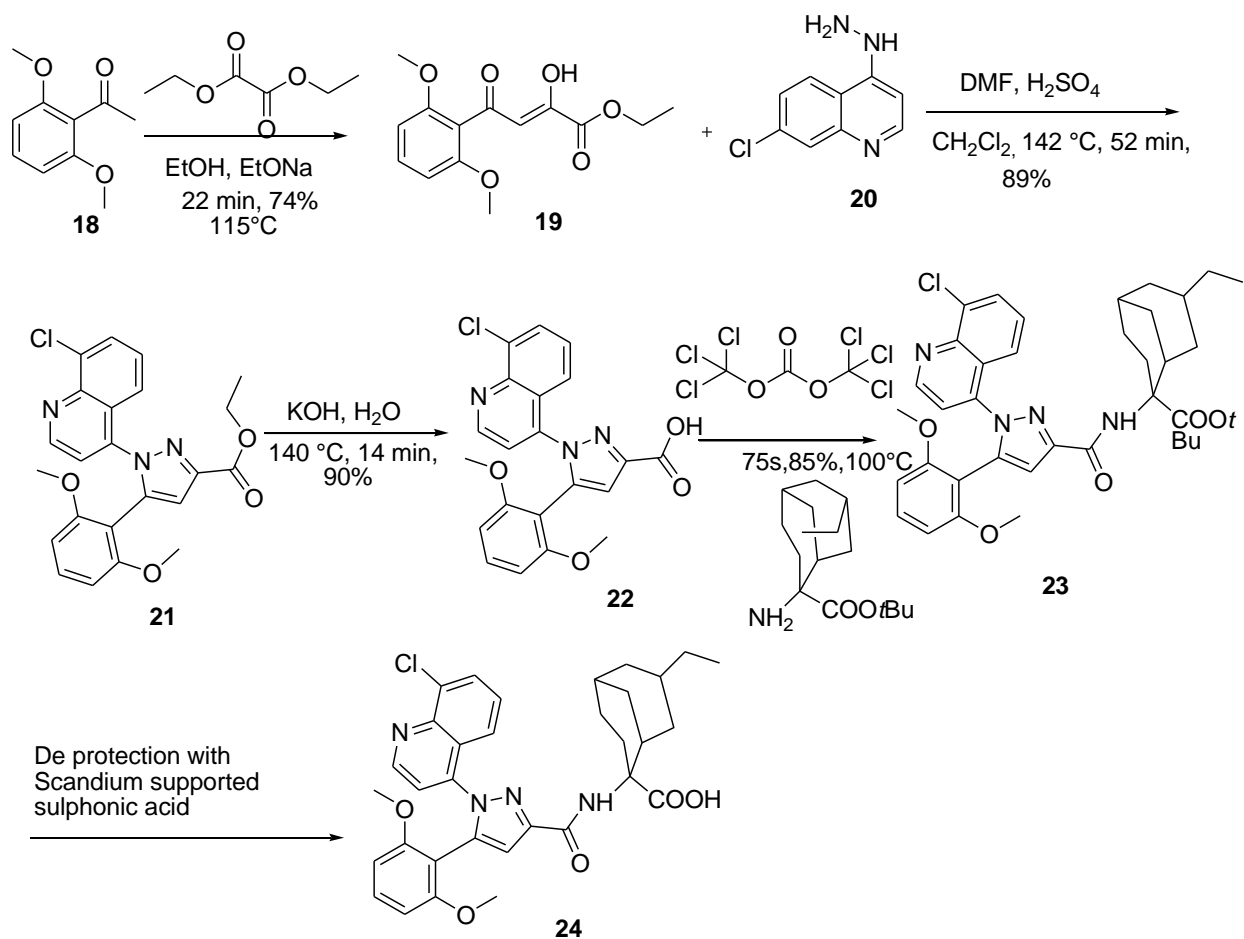
### 1B.6.2. Synthesis of meclintertant

Although batch processes remain the most used procedure for running chemical reactions, the use of machine-assisted flow methodologies enables an improved efficiency and high throughput. A direct comparison between the conventional batch preparation and flow multistep synthesis of selective neurotensine probe SR48692 (Meclintertant) was reported by Ley and co-workers<sup>[92]</sup> in 2013 (Scheme 2). In this case study, the authors investigated whether flow technology could accelerate a multistep



synthesis (*i.e.*, higher yields and/or lower reaction times) and overcome many synthetic issues (*i.e.*, solid precipitation or accumulation of byproducts). The initial Claisen condensation between ketone **18** and ethyl glyoxalate in the presence of sodium ethoxide as base and ethanol as solvent in batch is run at room temperature and the product **19** is obtained in 60% yield after 3 h stirring. Superheating (115 °C) (heat above solvent boiling point) the reaction in flow provided a faster alternative: with a residence time of just 22 min giving the corresponding product **19** in 74% yield. Subsequently the reaction between **19** and commercially available hydrazine **20** was performed in DMF in the presence of concentrated H<sub>2</sub>SO<sub>4</sub>. After 52 min of residence time at 140 °C, in a 52 mL PFA reactor coil, the crude mixture was treated with an aqueous Na<sub>2</sub>CO<sub>3</sub> solution and then inline extracted through a semipermeable membrane with CH<sub>2</sub>Cl<sub>2</sub>. After crystallization, pyrazole ester **21** was isolated in 89% yield. The corresponding reaction in batch was conducted in DMF under microwave irradiation at 140 °C for 2 h, giving product **21** in a lower yield (70%). The subsequent hydrolysis was performed combining a THF solution of ester **21** and 3 M aqueous KOH at 140 °C with a residence time of 14 min. The product precipitated, and was isolated by filtration in 90% yield. In this case, the corresponding batch hydrolysis afforded product **22** with the same yield (90%); however, a longer reaction time (1.5 h) was needed. The final amide formation was performed by reacting acid **22** and protected amino alcohol with triphosgene. An inline Flow-IR spectrometer was used to monitor the formation of phosgene without exposing the operator to the toxic gas during analysis. As soon as acyl chloride was formed it was reacted with protected amino alcohol. The amide formation took place into a 14 mL stainless steel reactor coil at 100 °C with a residence time of 75 s. Amide **23** was isolated

in 85% yield after quenching with  $\text{NH}_4\text{Cl}$  and extraction with ethyl acetate. For obvious safety concerns, avoiding the handling of phosgene and the isolation of the highly reactive acyl chloride intermediate represents a remarkable improvement with respect to the batch procedure. Finally, meclinetant **24** was obtained after deprotection of ester **23** by using a polymer-supported sulfonic acid. The last synthetic step was conducted in batch on a small scale; however, it could be easily transferred to flow mode by using a column packed with commercially available polymer-supported sulfonic acid.



**Scheme 2:** Synthesis of meclinetant by Ley<sup>[92]</sup> *et.al*

The wide range of applications and advantages of flow chemistry motivated us to synthesize our title drug using flow chemistry technology, after establishing our methodology using traditional batch chemistry.

### 1B.7. Literature review of Efavirenz

Efavirenz **8** is chemically described as (S)-6-chloro-(cyclopropylethynyl)-1,4-dihydro-4-(trifluoromethyl)-2H-3,1-benzoxazin-2-one. Efavirenz **8** has a stereogenic quaternary carbon center bearing a trifluoromethyl group with the (S) configuration (Figure 15).

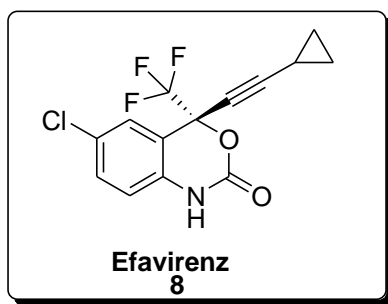
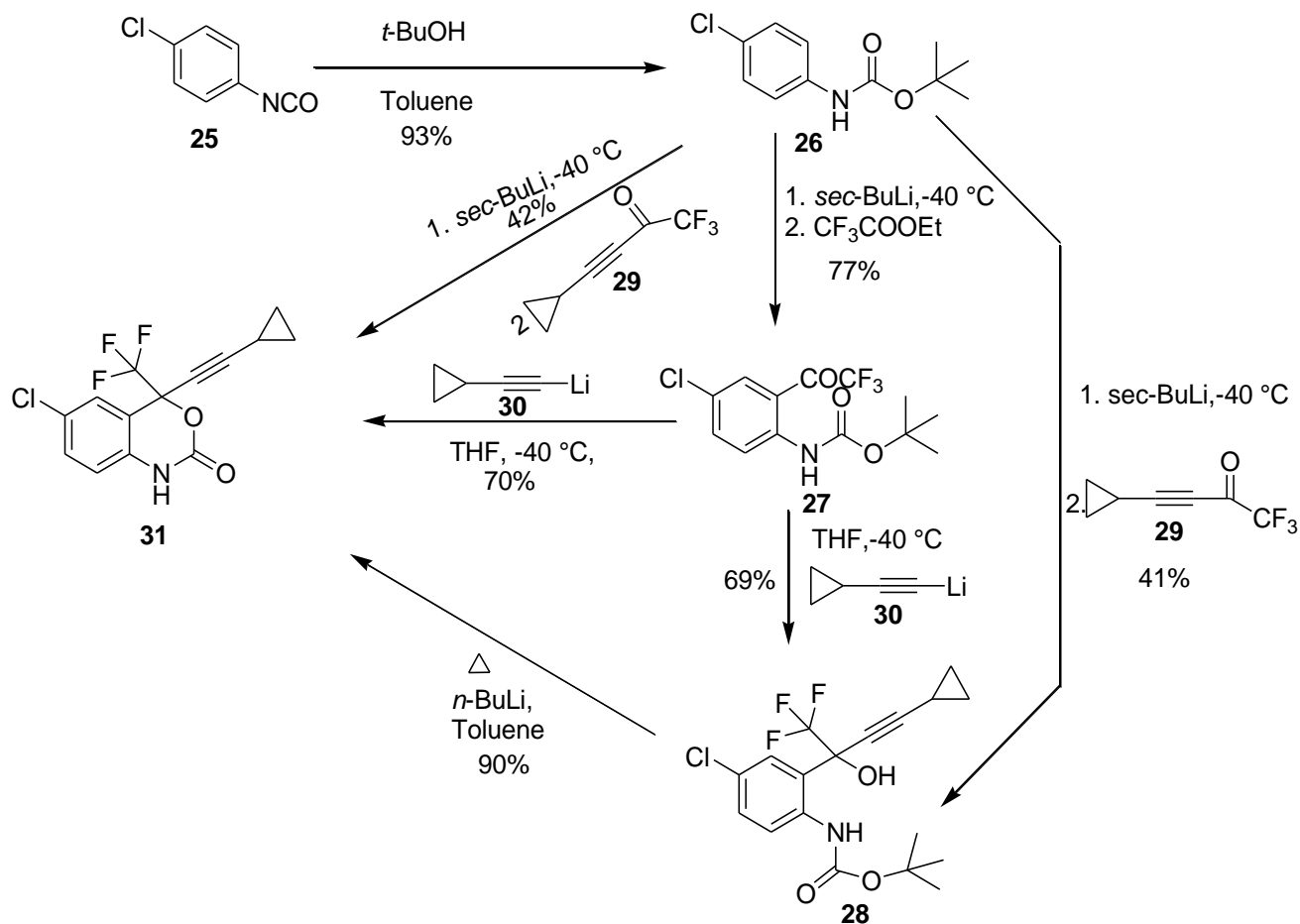


**Figure 15:** Structure of efavirenz

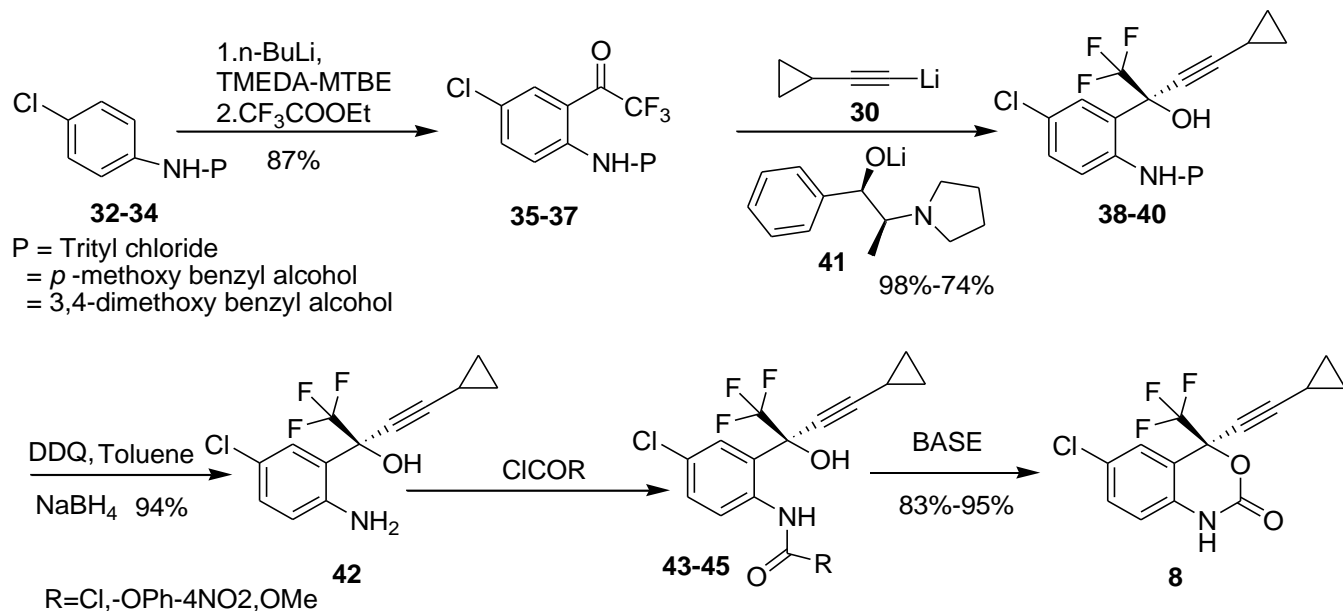
**1B.7.1.** Radesca *et.al.*<sup>[93]</sup> synthesized efavirenz **31** (Scheme 3) from commercially available and inexpensive 4-chlorophenyl isocyanate **25**. The isocyanate reacted with *t*-BuOH in toluene under reflux temperature to give *N*-protected chloroaniline **26** which on reaction with *sec*-BuLi at -40 °C, followed by addition of trifluoroacetate to form trifluoromethyl ketone **27**. This tri fluoroketone compound reacts with cyclopropylacetylide **30** in THF at -40 °C and cyclized to get the efavirenz **31** as a racemic compound. Which is purified by (-)-camphanic acid treatment to the diastereomerically pure (>99.7%) crystalline pure product. Alternatively the compound **31** also prepared in two other ways as shown in Scheme below. One is conversion of compound **26** to compound **31** by using compound **29**. Other one from compound **27** to compound **31** by using compound **30**.



**Scheme 3:** Synthesis of efavirenz **31** by Radesca *et.al*

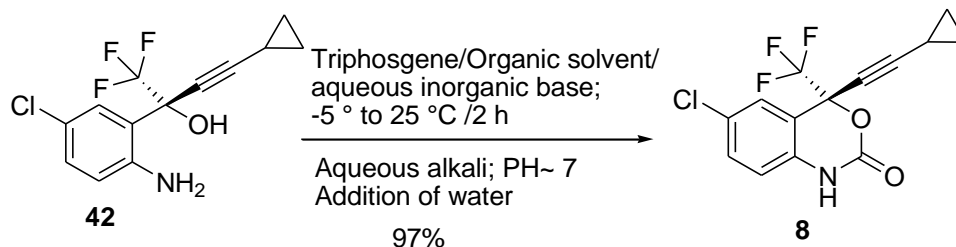
**1B.7.2.** Pierce *et.al.*<sup>[94]</sup> explained a practical asymmetric synthesis of efavirenz **8** in seven steps. The synthesis provides analytically pure product in an overall yield of 62%, starting from commercially available compounds **32-34**. Directed ortho metalation of **32-34** with 2 equivalents of *n*-butyllithium or *n*-hexyllithium generated the corresponding dianion, which was quenched with ethyl trifluoroacetate to afford ketoamide **35-37**. Then again protection of amine with *p*-methoxy benzyl and reacts with (1*R*,2*S*)-*N*-pyrrolidinylnorephedrine **41** and 2 equivalents of lithium-cyclopropyl acetylide **30** followed by cyclization to get efavirenz **8** (Scheme 4). The author explained the enantioselectivity of the compound highly depends on the *N*-protecting group. Excellent enantioselectivities were obtained

the *p*-methoxybenzyl-protected keto aniline (98%) and 3,4-dimethoxybenzyl protected keto aniline (99%), and useful results were obtained with the trityl-protecting group (90%).



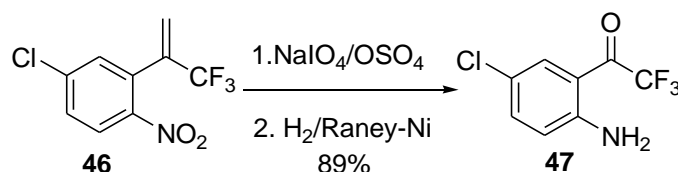
**Scheme 4:** Synthesis route for efavirenz **8** by Pierce *et.al*

**1B.7.3.** Gurjar *et.al.*<sup>[95]</sup> reported a novel process for the preparation of efavirenz **8** (Scheme 5) by a process comprising reaction of 5-chloro- $\alpha$ -(cyclopropylethynyl)-2-amino- $\alpha$ -(trifluoromethyl)benzene **42** with triphosgene in organic solvents like acetonitrile, acetone or 1,2-dimethoxyethane, in the presence of a base like sodium/potassium bicarbonates. After completion of the reaction, the reaction was neutralized with an aqueous alkali carbonate or bicarbonate solution if required. Water was then added to the reaction mixture and the product separating out was filtered and dried. The product **8** was obtained in quantitative yield (97%) with high purity.



**Scheme 5:** Synthesis of efavirenz **8** by Gurjar *et.al*

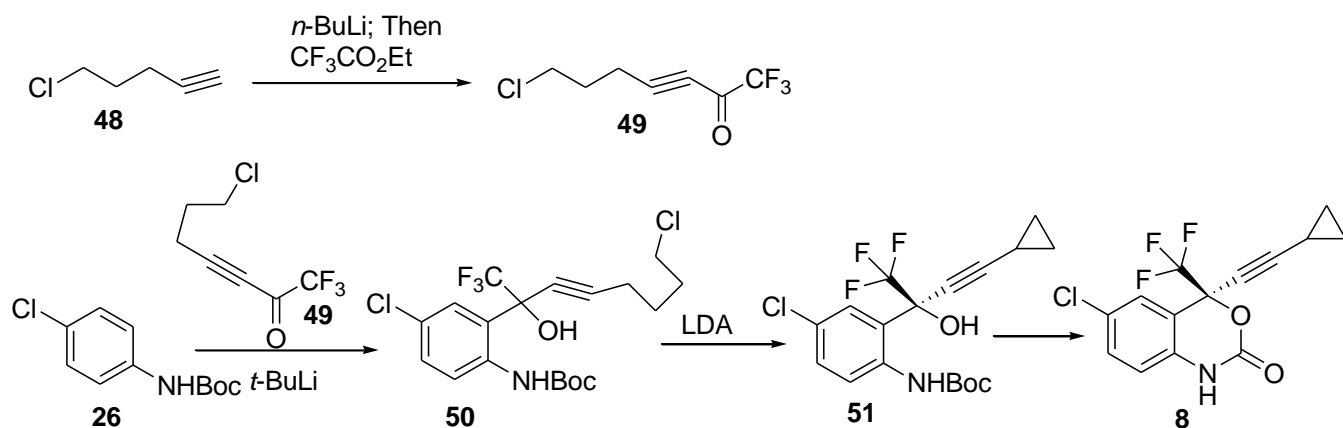
**1.B.7.4.** Jiang *et.al.*<sup>[96]</sup> reported the preparation of the trifluoro ketone (Scheme 6), which is an important intermediate for the synthesis of efavirenz **8** via  $\alpha$ -trifluoromethylstyrene derivative. The trifluoroketone has been synthesized from the reaction between *n*-butyllithium and an *N*-protected aniline with ethyl trifluoroacetate at low temperature. This process suffers from high cost and strict reaction conditions. The  $\alpha$ -trifluoromethylstyrene **46** was easily converted into tri fluoroketone **47** in high yield simply by oxidation of the ethynyl bond using  $\text{NaIO}_4$  and catalytic  $\text{OsO}_4$  (0.01 equivalents) in *tert*-BuOH/ $\text{H}_2\text{O}$  (4:1), followed by hydrogenation over Raney Ni in ethanol.



**Scheme 6:** Synthesis of compound **47** by Jiang *et.al*

**1B.7.5.** Nicolaou *et.al.*<sup>[97]</sup> explained the use of anilines and their derivatives as versatile starting materials for chemical synthesis and offer rapid access to novel heterocycles like efavirenz **8**. 5-Chloropentyne **48** was converted to tri fluoroketone **49** in high yields via its lithium anion with *n*-butyllithium in toluene (-10 °C) and quenching with trifluoromethyl acetate. A one-pot procedure from 4-chloro *N*-Boc aniline **26** involving sequential addition

of *t*-BuLi (2.2 equiv), trifluoro ketone **49** (0.9 equiv), LDA (6.0 equiv), and heating in toluene at reflux proved successful, furnishing efavirenz **8** via compound **51** (Scheme 7) in 38% overall yield.

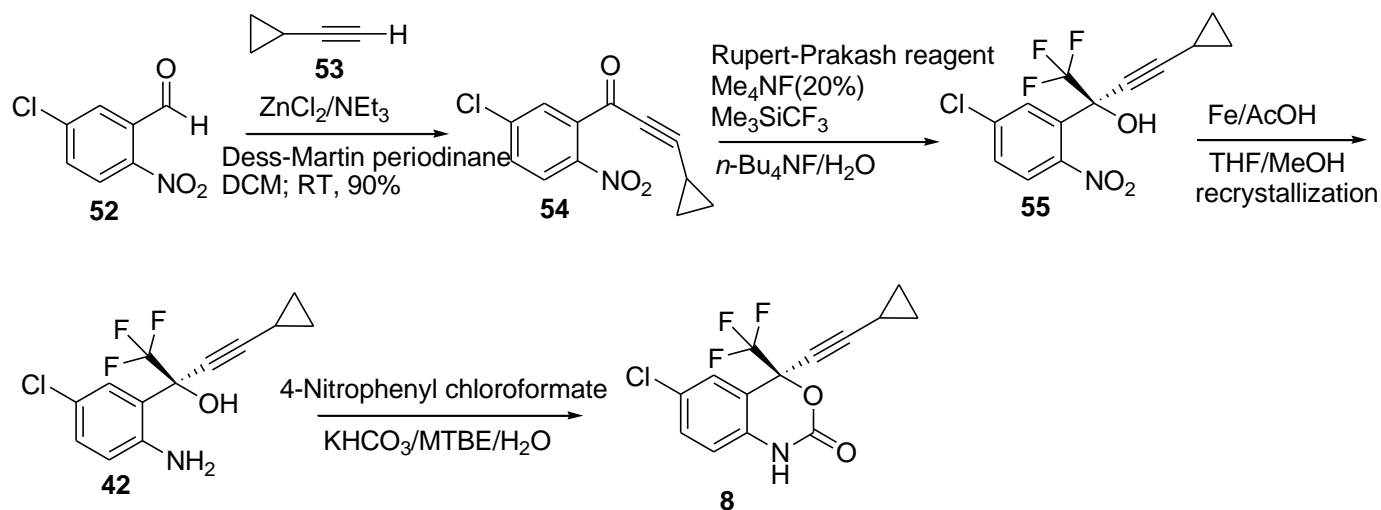


**Scheme 7:** Synthesis route for efavirenz **8** by Nicolaou *et.al*

**1B.7.6.** Shibata *et.al.*<sup>[98]</sup> reported the enantioselective trifluoromethylation of an alkynyl ketone **54** by using the Rupert-Prakash reagent. This is the first method of the synthesis of efavirenz **8** by using a direct trifluoromethylation approach (Scheme 8). For the synthesis of efavirenz **8**, the authors choose 5-chloro-2-nitrobenzaldehyde **52** as starting material. The compound 5-chloro-2-nitrobenzaldehyde reacted with cyclopropylacetylide **53** in the presence of  $\text{ZnCl}_2$ , TEA, and then reduction using Dess-Martin periodinane in DCM provided cyclopropyl intermediate compound **54**. On reaction with the Rupert-Prakash reagent and catalytic amount of  $\text{Me}_4\text{NF}$  with  $\text{Me}_3\text{SiCF}_3$  in toluene/DCM (2:1) to give (*S*)-2-(5-chloro-2-nitrophenyl)-4-cyclopropyl-1,1,1-trifluorobut-3-yn-2-ol **55**. The nitro group reduction was successfully achieved by iron in the presence of AcOH in THF/MeOH solvent (2:1) to furnish the corresponding amino alcohol **42**, the enantiopurity of the amino

alcohol was easily increased from 50-94% ee by a single recrystallization (hexane/DCM).

Treatment of amino alcohol with 4-nitrophenyl chloroformate under basic condition afforded efavirenz **8** in 94%.



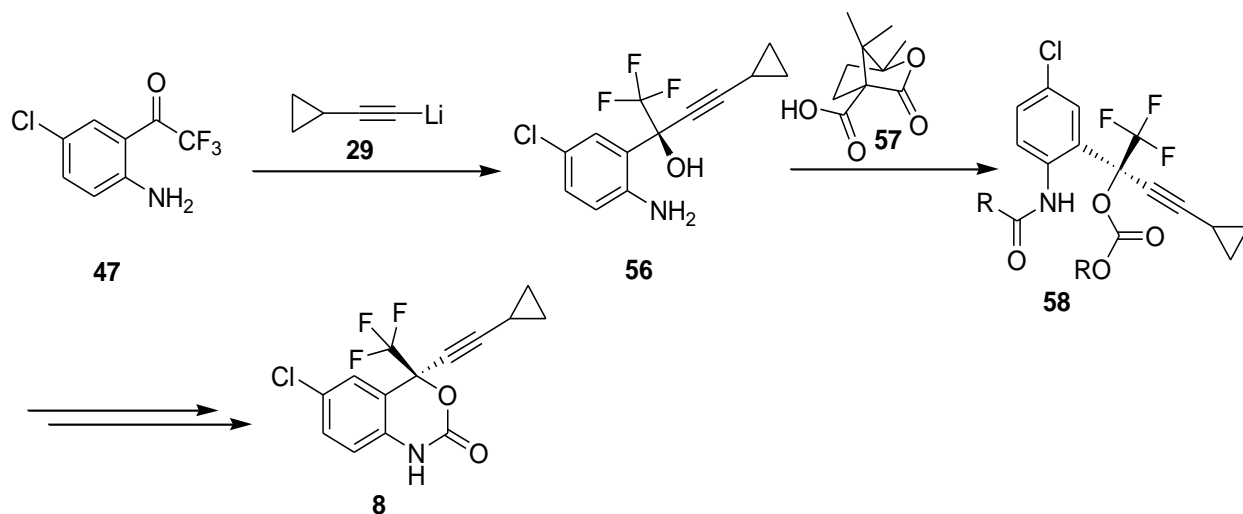
**Scheme 8:** Synthesis route for efavirenz **8** by Shibata *et.al*

**1B.7.7.** Chen *et.al.*<sup>[99]</sup> described a method for the preparation of efavirenz **8** (Scheme 9).

The author described a novel chiral acylating agents such as (-)-camphanic acid, (-)-camphanoyl chloride, or (*R*)-2-chloro-2-oxo-1-phenethyl pivalate. The stereoselectivity of the cyclopropylacetylide reaction may be controlled by introduction of an appropriate chiral carbonyl auxiliary group on the aniline nitrogen.

The Scheme started with keto aniline **47** and followed by alkylation in the presence of compound **29**, which gives compound **56**. And which undergoes acetylation in the presence of (-)-camphanic acid to get compound **58** and finally cyclisation to get compound **8**.

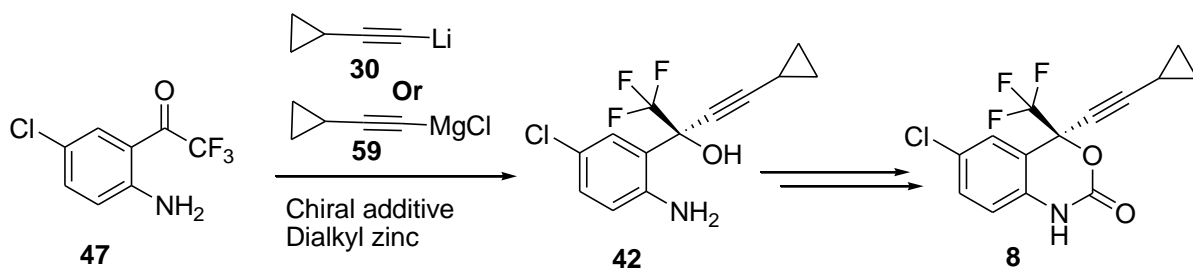




Wherein R = alkyl or aryl or substituted alkyl or aryl etc..

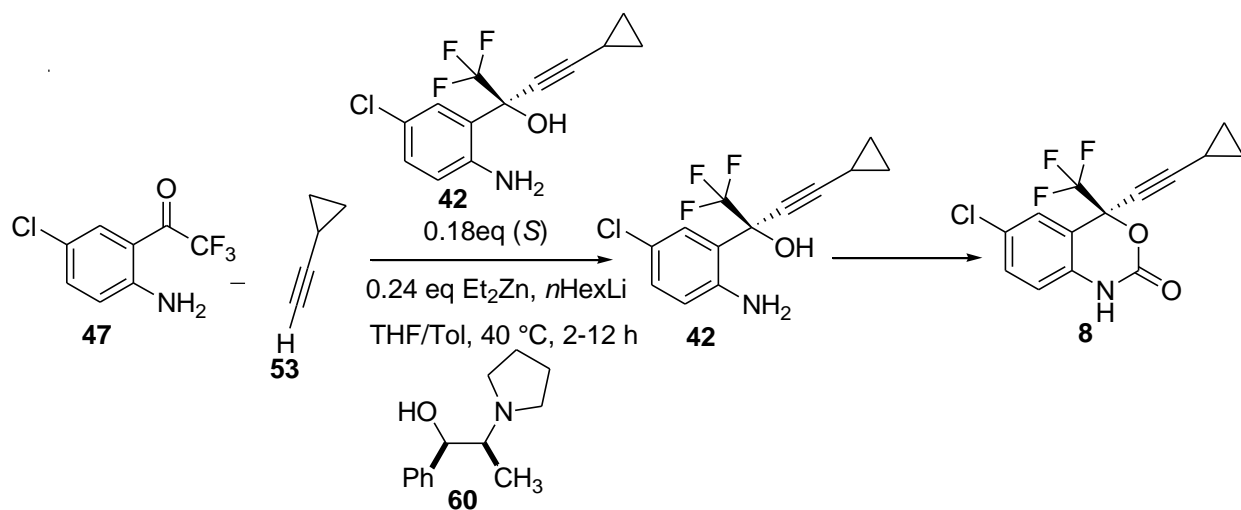
**Scheme 9:** Synthesis route for efavirenz **8** by Chen *et.al*

**1B.7.8.** Bollu *et.al.*<sup>[100]</sup> reported a process for the preparation of chiral organometallic complexes used in the synthesis of efavirenz **8**. Firstly the nucleophile **47** is treated with a chiral additive and dialkyl zinc to form a chiral complex, which then reacts with the starting material **47** to get compound **42** and finally which is converted to compound **8**. It is an efficient method for the preparation of organometallic complexes used for cyclization of amino alcohols with high enantioselectivity and high product yields. The chiral additive is selected from diols, amino alcohols, ethylene diamines, quinines, camphor sulfonamides, prolines and derivatives (Scheme 10).



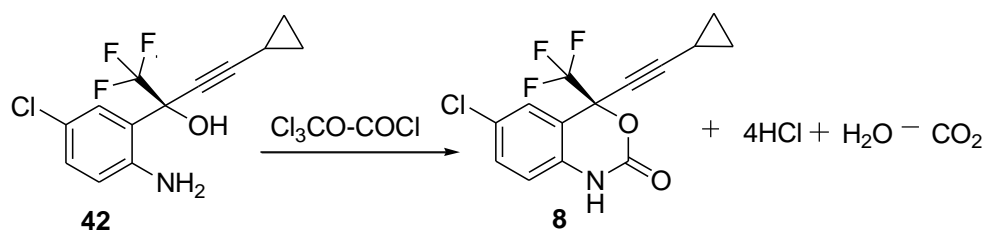
**Scheme 10:** Synthesis of efavirenz **8** by Bollu *et.al*

**1B.7.9.** Carreira *et.al.*<sup>[101]</sup> reported the catalytic use of the enantioselective isomer as intermediate (S)-amino alcohol **42** at the outset of reaction. The catalytic reaction benefits from the presence of product as an auto catalyst, resulting in a more atom-economical route to efavirenz **8** in 79% yield and 99.6% ee. Beyond the economic relevance, this process showcases the first example that employs autocatalysis in the synthesis of a pharmaceutical agent which may be conducted on large scale. This reaction started from compound **47**, which upon reaction with compound **53** in the presence of compound **42** as auto catalytic agent and finally cyclisation in the presence of di ethyl carbonate to get final compound **8**. (Scheme 11).

**Scheme 11:** Synthesis route for efavirenz **8** by Carreira *et.al*

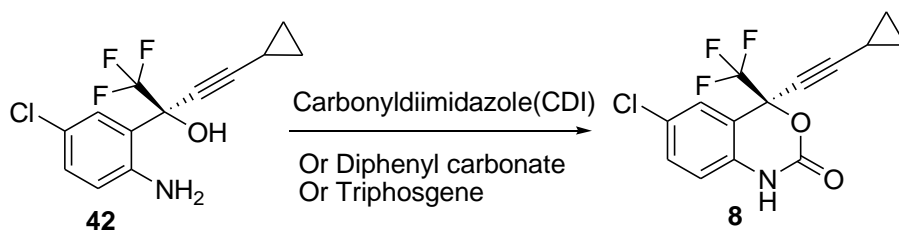
**1B.7.10.** Leganza *et.al.*<sup>[102]</sup> have reported the preparation of efavirenz **8** by the reaction of an amino alcohol **42** with diphosgene in an organic solvent or in a biphasic medium comprised of an organic solvent and water. The ratio between the organic solvent and the water phase can range between 0.3:1 to 1:0.3. This reaction can be performed in an organic solvent such as, for example, hexane, heptane and diethyl ether, diisopropyl

ether, tetrahydrofuran, dioxane or a mixture of such solvents. Preferably the reaction was performed in the presence of a weak base in an amount sufficient to neutralize the reaction mixture (Scheme 12).



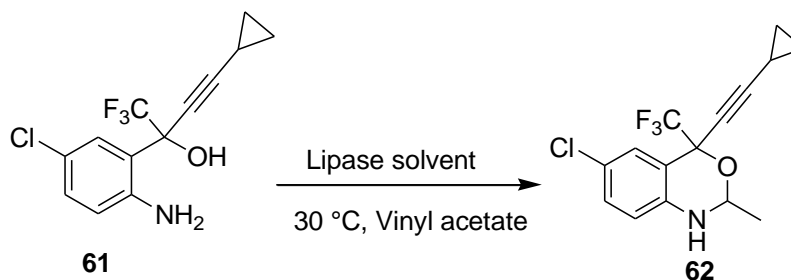
**Scheme 12:** Synthesis of efavirenz **8** by Leganza *et.al*

**1B.7.11.** Pal *et. al.*<sup>[103]</sup> demonstrated a process for the cyclization of the optically pure (S)-2-(2-amino-5-chlorophenyl)-4-cyclopropyl-1,1,1-trifluoro-3-butyn-2-ol (amino alcohol) **42** using CDI, diphenyl carbonate or triphosgene to give optically pure efavirenz **8**. The major advantage of the improved process is high yield and low cost. The reaction is carried out in presence of aprotic solvent like THF (Scheme 13).



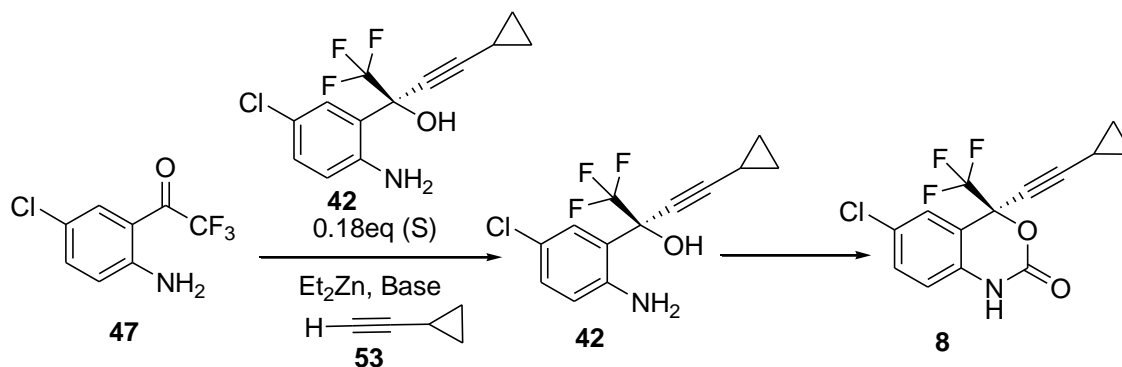
**Scheme 13:** Synthesis of efavirenz **8** by Pal *et.al*

**1B.7.12.** Husain *et.al.*<sup>[104]</sup> during attempted biocatalytic resolution of (R/S)-5-chloro- $\alpha$ -(cyclopropyl ethynyl)-2-amino- $\alpha$ -trifluoromethyl benzene methanol **61** using lipase B, an unexpected efavirenz analogue **62** was formed (Scheme 14).



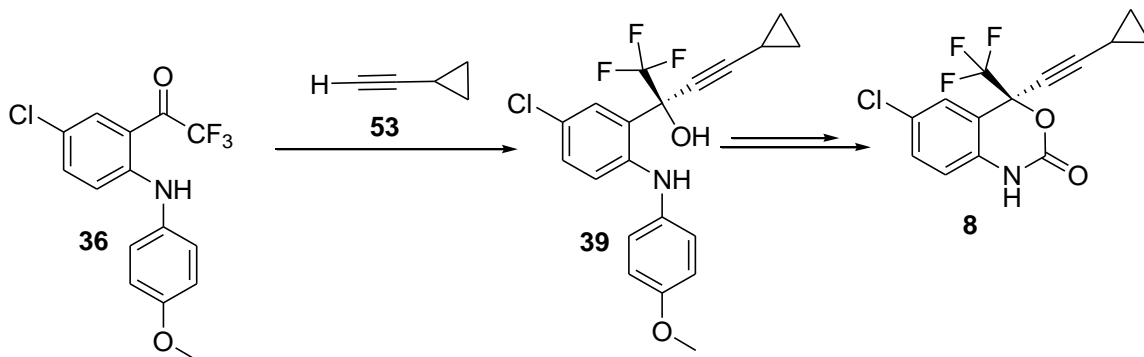
**Scheme 14:** Synthesis route for efavirenz analogue **62** by Husain *et.al*

**1B.7.13.** Erick *et.al.*<sup>[105]</sup> described an asymmetric autocatalytic synthesis of efavirenz **8** (Scheme 15), for the enantioselective addition of compound **53** to compound **47** to get compound **42**. In this reaction compound **42** acted as catalyst (auto catalyst) in catalytic amounts to get enantiomerically pure efavirenz **8**.



**Scheme 15:** Synthesis of efavirenz **8** by Erick *et.al*

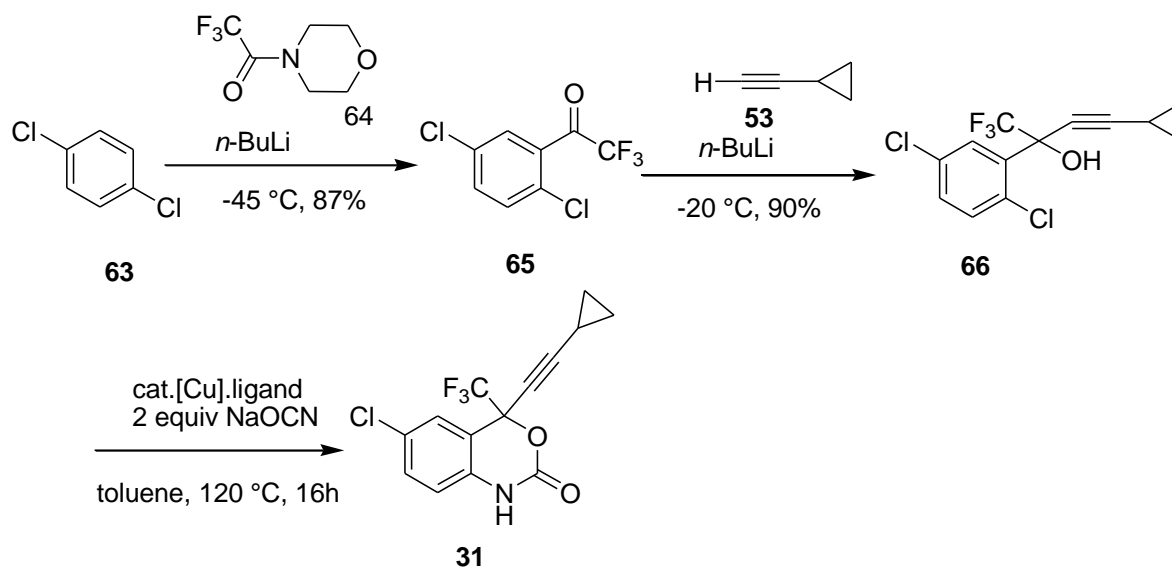
**1B.7.14.** Corley *et.al.*<sup>[106]</sup> explained the use of an ephedrine alkoxide to mediate enantioselective addition of an acetylide to a prochiral ketone and the synthesis of efavirenz **8** (Scheme 16).



**Scheme 16:** Synthesis route for efavirenz **8** Corley *et.al*

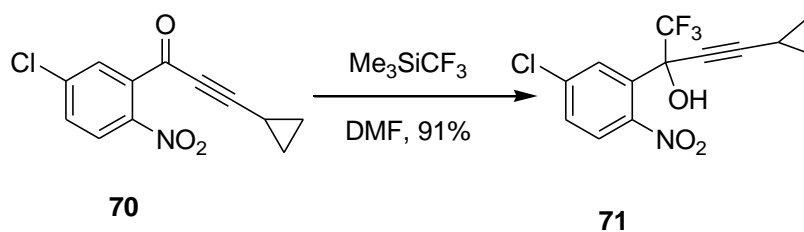
#### 1B.7.15. Literature review for the synthesis of efavirenz by flow chemistry

Seeberger *et.al.*<sup>[107]</sup> reported a semi-continuous flow synthesis of efavirenz **31** with an overall yield of 45% from 1,4 dichlorobenzene **63** as described in Lonza's patent.<sup>[108]</sup> In this synthesis, they used dichlorobenzene **63** as starting material. Further this material **63** was trifluoroacetylated to compound **65** with 87% yield by morpholine trifluoroacetic acid **64**. At the end of this trifluoroacetylation reaction, the morpholine byproduct was removed by using a silica column. The compound **65** upon alkylation with compound **53** at -20°C afforded compound **66** in 90%. The final step of cyclization was done by using a copper catalyst, through copper-catalyzed carbamate formation to get a racemic mixture of efavirenz **31** from compound **66** as shown in Scheme 17. No attempt was made in the paper towards the chiral purification of the compound.



**Scheme 17:** Synthesis of efavirenz **31** by Seeberger *et.al*

**1B.7.16.** Shibata *et.al.*<sup>[108]</sup> reported a trifluoromethylation reaction in flow by using Rupert Prakash reagent (Scheme 18). Previously this reaction was reported in traditional batch chemistry by the same author. This flow process was started from compound **70** which was trifluoro acetylated by Rupert-Prakash reagent to get compound **71** in 91% yield. The yield was improved when compared to the batch process (66%) and this compound **71** claimed as an intermediate for the synthesis of efavirenz **31**.



**Scheme 18:** Trifluoromethylation by Shibata *et.al*

**1B.8. Aim**

The aim of this study is to develop an efficient synthetic route for the preparation of optically pure efavirenz in traditional batch chemistry as well as in flow chemistry. Previously Seeberger *et.al.*<sup>[107]</sup> reported a semi-continuous flow synthesis of *rac*-efavirenz with an overall yield of 45%. Although the *R* isomer is biologically not active, by considering this we aimed to synthesize optically pure efavirenz with improved yields in most economical way, in order to facilitate methodology that would enable local manufacture of such drugs within Africa.

.

# **CHAPTER 2**

## **SECTION A**

# **SYNTHESIS OF EFAVIRENZ- TRADITIONAL BATCH CHEMISTRY RESULTS AND DISCUSSION**

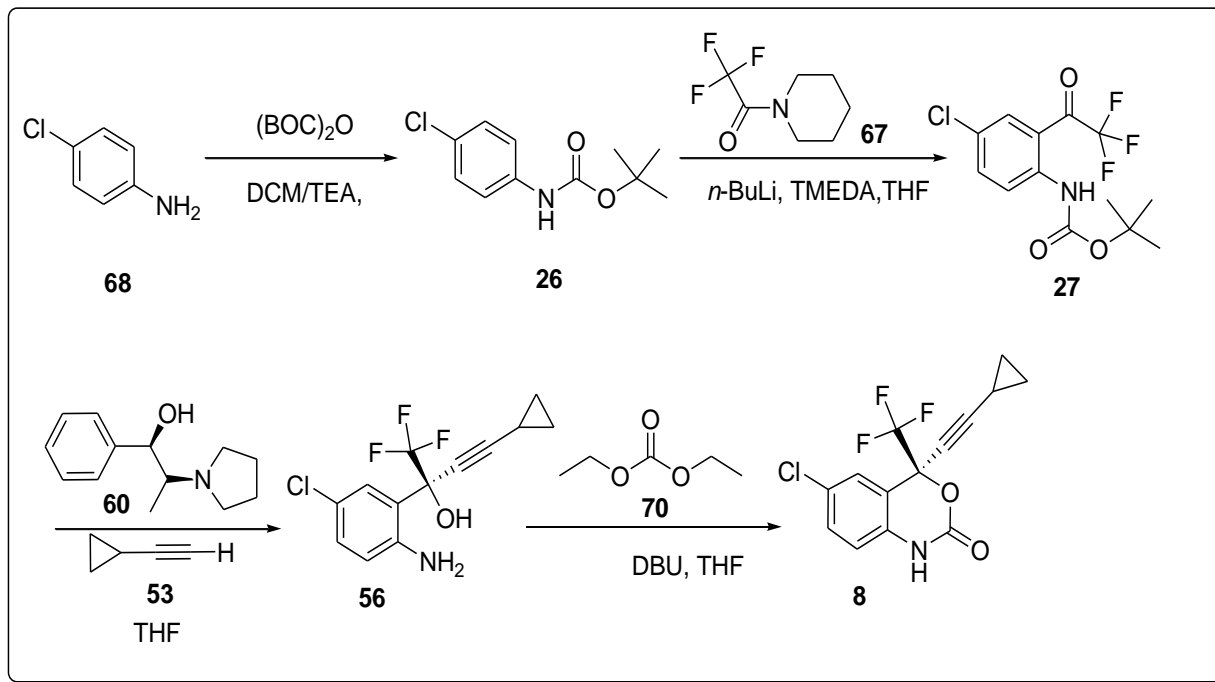


## 2A. Traditional batch chemistry

Efavirenz **8** is a potent, non-nucleoside, reverse transcriptase inhibitor of HIV-1 and has been used in combination with other antiretroviral drugs (lamivudine, emtricitabine and tenofovir *etc.*) for the treatment of HIV infection. Efavirenz **8** has a stereogenic quaternary carbon center bearing a trifluoromethyl group with the (*S*) configuration. Biological evaluation of optically active efavirenz **8** revealed that the (*R*) enantiomer exhibits virtually no activity. Therefore, establishment of the quaternary carbon center with the (*S*) configuration in an asymmetric manner is one of the main challenges for the synthesis of efavirenz **8**.

As described above the biological importance of efavirenz **8** is highly dependent on stereochemistry, which prompted us to design an efficient synthesis of stereochemically pure efavirenz **8** which is described in Scheme 19.

The Scheme proposed below is not fully similar to the any of the methods described in the literature review, although the intermediates are similar. The aim behind changing of the conditions and reagents is to make it more economical.



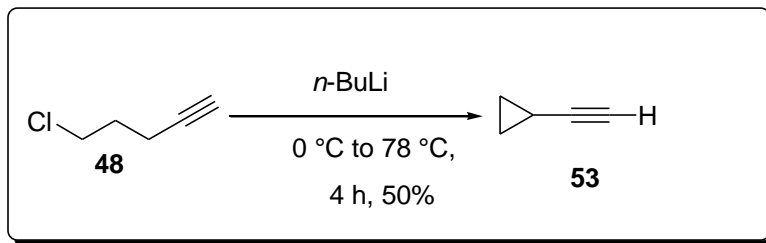
**Scheme 19:** Synthesis of efavirenz **8**

### 2A.1. Preparation of starting materials

The synthesis of efavirenz **8** proposed in Scheme 19 required the preparation of four materials which are not commercially available *i.e.* cyclopropyl acetylene **53**, cyclopropylethynyl trifluoromethyl ketone **29**, piperidine trifluoroacetic acid **67** and *N*-pyrrolidinyl-norephedrine **60**.

#### 2A.1.1. Preparation of cyclopropylacetylene **53**

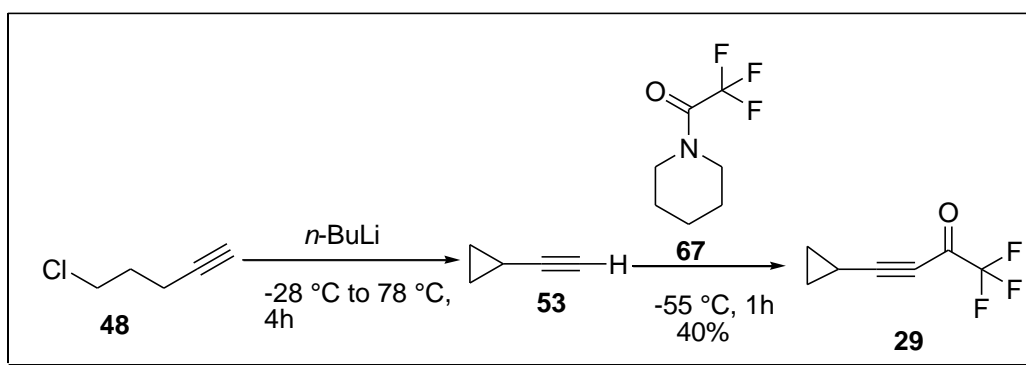
Firstly cyclopropylacetylene **53** was readily prepared by treating 5-chloro1-pentyne **48** with 2 equivalents of *n*-butyllithium in THF<sup>[110]</sup> as described in Scheme 20.



**Scheme 20:** Preparation of 4-cyclopropylacetylene **53**

To a round bottomed flask 5-chloro-1-pentyne **48** in cyclohexane was added and the temperature of the flask was maintained at 0 °C, to this *n*-butyllithium was added drop wise. During the addition of *n*-butyllithium a thick precipitate was formed, which was refluxed for 3 hours at 78 °C. After reaction completion the reaction mixture was cooled to -10 °C and quenched with saturated ammonium chloride. The layers were separated and the organic layer was washed with water and dried with Na<sub>2</sub>SO<sub>4</sub>. The crude product distilled to obtain pure compound **53** in 50% yield.

#### 2A.1.2. Preparation of 4-cyclopropyl-1,1,1-trifluoro-but-3-yn-2-one **29**

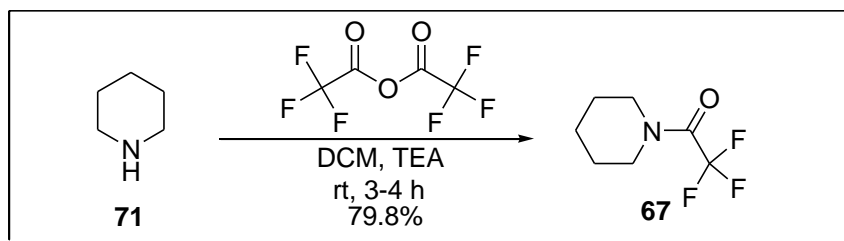


**Scheme 21:** Preparation of 4-cyclopropyl-1,1,1-trifluoro-but-3-yn-2-one **29**

Compound **29** was prepared as shown in Scheme 21. The *n*-butyllithium was added to the 5-chloro-1-pentyne **48** in cyclohexane at -20 °C. The reaction mixture kept at the

same temperature for 1 hour and then heated to reflux for 3 hours at 78 °C, at this time a sample was analyzed by GC which indicated the total disappearance of starting material **48**; then the reaction mixture was cooled to -55 °C and piperidine trifluoro acetic acid **67** was added. After completion of reaction, the reaction mixture was quenched with 2N HCl. The separated organic layer was washed with water and dried with Na<sub>2</sub>SO<sub>4</sub>. The crude product was evaporated *in vacuo* and distilled to yield the compound **29** in 40%.

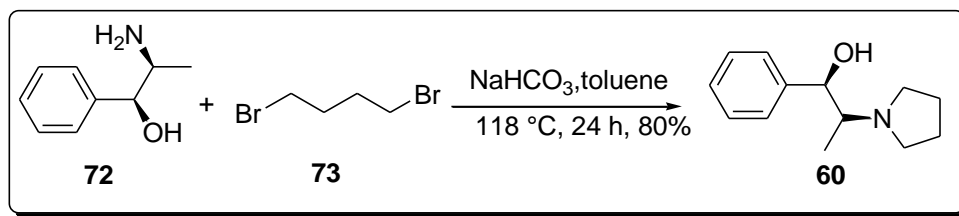
### 2A.1.3. Preparation of *N*-piperidine trifluoro acetic acid **67**



**Scheme 22:** Preparation of *N*-piperidine trifluoroacetic acid **67**

*N*-Piperidine trifluoroacetic acid **67** was prepared as described in Scheme 22. To the mixture of compound **71** in DCM and TEA in a round bottomed flask the trifluoroacetic anhydride was added and this resulting mixture stirred at room temperature for 3-4 hours and after completion of reaction the reaction mixture washed with water, sodium bicarbonate and dil HCl to remove unreacted starting material. The layers were separated and the organic layer evaporated *in vacuo* and the compound **67** obtained as yellow colored oil with 79.8% yield and this was used without any purification.

#### 2A1.4. Preparation of (1*R*,2*S*)-*N*-pyrrolidinylnorephedrine **60**

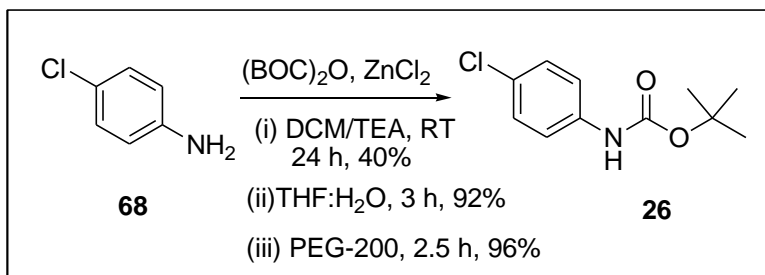


**Scheme 23:** Preparation of (1*R*,2*S*)-*N*-pyrrolidinylnorephedrine **60**

(1*R*,2*S*)-*N*-pyrrolidinylnorephedrine **60** would be required as a ligand for the asymmetric synthesis and has been reported in the literature.<sup>[80,81]</sup> The alkylation of (1*R*,2*S*)-norephedrine **72** with 1,4-dibromobutane **73** using  $\text{NaHCO}_3$  as base and toluene as solvent (Scheme 23).<sup>[112]</sup> The reaction mixture was refluxed for 24 hours at  $120^\circ\text{C}$ . After reaction completion, inorganic salts were filtered and the filtrate was washed with water to give the product **60** as a solution in toluene. This solution can be used directly in the chiral addition step or alternatively, the hydrochloride salt of **60** isolated by the addition of HCl in 2-propanol solution (0.275 mol) in 80% yield.

### 2A.2. Batch Synthesis of efavirenz **8**

#### 2A.2.1. Step-1



**Scheme 24:** Preparation of *tert*-butyl-4-chloro phenyl carbamate **26**

The synthesis of efavirenz **8** started from 4-chloroaniline **68** which is commercially available and inexpensive, which initially proceeds through the *N*-protection as the di-*tert*-butyl carbamate (Boc) group. Among the many protecting groups for 4-chloroaniline **68**, we choose the di-*tert*-butyl dicarbamate for the ease of its installment and removal, as well as its stability under metalation conditions.<sup>[113]</sup> Furthermore, the *tert*-butoxycarbonyl group (Boc) is easily cleaved under mild anhydrous acidic conditions.

The *tert*-butyl-4-chlorophenylcarbamate **26** was prepared from 4-chloroaniline **68** as shown in Scheme 24. The reaction of 4-chloroaniline **68** with di-*tert*-butyl dicarbamate afforded *tert*-butyl 4-chlorophenylcarbamate **26**. This reaction was optimized by using three different reaction conditions and solvents.

Firstly, with dichloromethane as solvent and triethylamine as mild base. Triethylamine activates the starting material towards the reaction, this reaction typically takes 24 h. After reaction completion the reaction mixture was poured into ice cold water, where *tert*-butyl 4-chlorophenylcarbamate **26** precipitated as white colored solid and the yield was 40%. Although the isolation process was simple, clearly the yield was not satisfactory.

We thereafter went ahead and investigated the effect of THF: water as the second solvent on the same reaction. No effort was made to investigate the optimum ratio of this solvent system. As such, a ratio of 1:1 THF: water was used. This was found to give considerably better yield of 92%. This reaction typically took just 3 hours under these conditions. The compound again precipitated as a white colored solid from water as described above.

Finally by a solvent free reaction <sup>[114]</sup> consisting of 4-chloroaniline **68** and Boc anhydride in the presence of a little amount of PEG-200 (1mL/g). PEG-200 facilitates the migration of a reactant from one phase to another phase where the reaction occurs, this reaction proceeds smoothly with higher conversion when compared to the first two reactions. PEG-200 was recovered by evaporating the aqueous layer after completion of the reaction, which could be used for several times without loss of activity; the recovered PEG-200 from the aqueous phase was used in a second reaction where the product yield (96%) was maintained the same as the first reaction. This reaction gave higher conversion than compared to the other two solvents *i.e.* 96%. The product was collected by filtration as a white colored solid and characterized by <sup>1</sup>H-NMR, <sup>13</sup>C-NMR, IR and elemental analysis. Figure 16 describes the effect of solvent on the reaction.

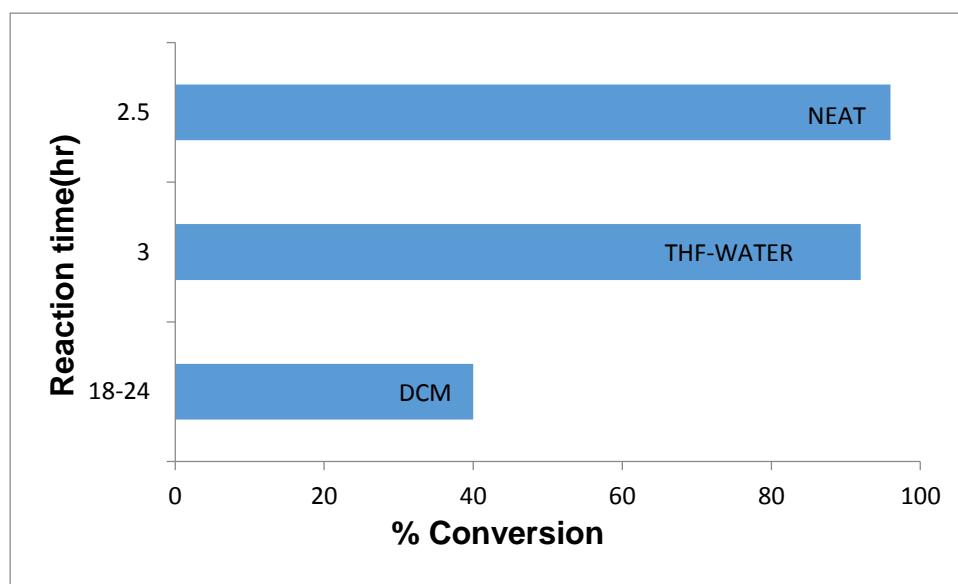
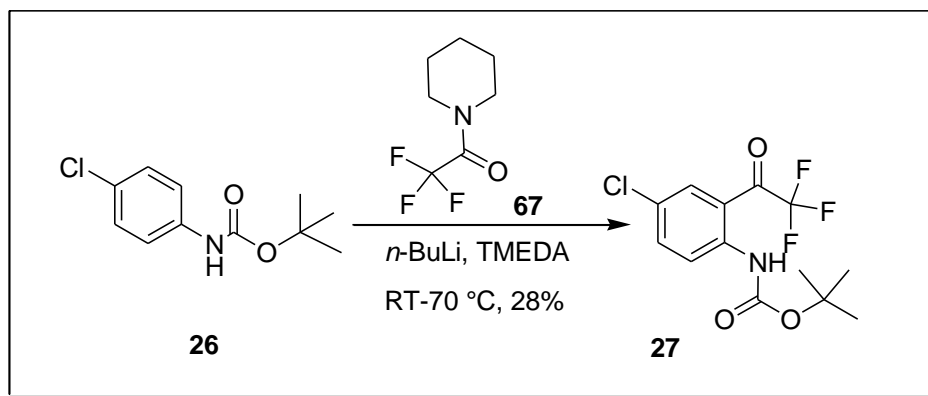


**Figure 16:** Effect of solvents on % conversion of the reaction

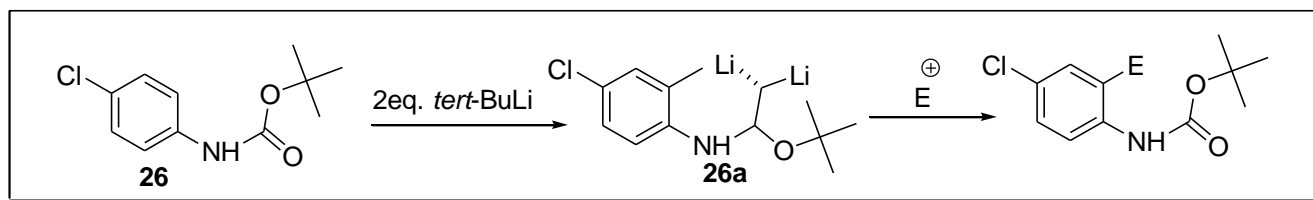
### 2A.2.2. Step-2

Having developed a method to synthesize Boc protected derivative **26** in high yield, our attention then turned to the trifluoroacetylation reaction (Scheme 25).



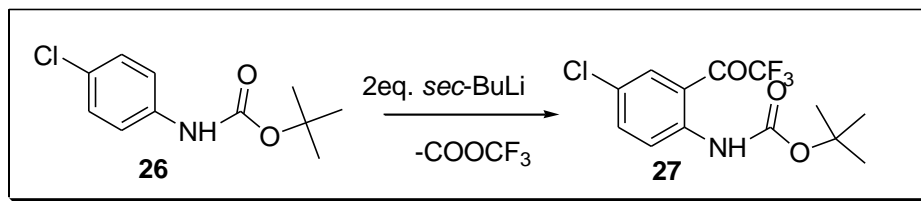
**Scheme 25:** Preparation of *tert*-butyl-4-chloro-2-(2,2,2-trifluoroacetyl) phenyl carbamate **27**

From the literature, *ortho* lithiation of *tert*-butyl 4-chlorophenylcarbamate **26** was reported only to occur with *tert*-butyllithium<sup>[115]</sup> and *sec*-butyllithium<sup>[116]</sup> as shown in Schemes 26 and 27.



**Scheme 26:** Lithiation in the presence of *tert*-butyllithium<sup>[115]</sup>





**Scheme 27:** Lithiation in the presence of *sec*-butyllithium to afford trifluoroketone derivative<sup>[116]</sup>

We envisioned that 4-chlorophenylcarbamate **26** could also be lithiated with excess *n*-butyllithium (e.g. 5 equivalents) (Scheme 25); a reagent safer and more suitable for use on a large scale compared with *sec*-butyllithium and *tert*-butyllithium. The scope of the metalation reaction has been expanded by the use of complexing agents such as tetramethylethylenediamine (TMEDA), which increases the rate of metalation, increase the stability of intermediate carbanion and thus extends the range of compounds which can be deprotonated. While the metalation reaction often provides the cheapest route to a lithium reagent, many cannot be made this way because the metalation process is too slow (*i.e.*, proton not sufficiently acidic), or not sufficiently selective. In these situations, the lithium/metal exchange reactions may provide the best route.<sup>[117-126]</sup>

After addition of *n*-butyllithium to 4-chlorophenylcarbamate **26** in THF, the reaction mixture turned from white to a yellow-orange suspension (Figure 17), this metalation was continued at -70 °C to room temperature for 1 hour and subsequently the liberated dianion was quenched at -55 °C with the trifluoro acetylating agent to afford *tert*-butyl 4-chloro-2-(2,2,2-trifluoroacetyl) phenylcarbamate **27**. We used the novel trifluoro acetylating agent *i.e.* piperidine trifluoroacetic acid **67**, as previously this reaction was

reported with ethyl trifluoroacetate. Ethyl trifluoroacetate reacts slowly, is highly moisture sensitive and often forms foul smelling by products.

After completion of the reaction, the reaction mixture turned to a brown colored solution (Figure 17) which was quenched with saturated ammonium chloride solution and extracted with ethyl acetate. The combined organic layers were washed with brine solution and evaporated under reduced pressure to get the crude compound as yellow solid. This crude compound was purified by column chromatography to afford *tert*-butyl 4-chloro-2-(2,2,2-trifluoroacetyl) phenylcarbamate **27** as light yellow colored solid in a modest 28% yield. We further tried to optimize the reaction towards the best yield but all the attempts in batch were not successful. However we were able to fully characterize the product by <sup>1</sup>H-NMR, <sup>13</sup>C-NMR, IR and elemental analysis.



4-chlorophenylcarbamate in THF.



Color of reaction mixture during dianion formation.



The color of the reaction mixture during quenching with trifluoro acetylating agent.

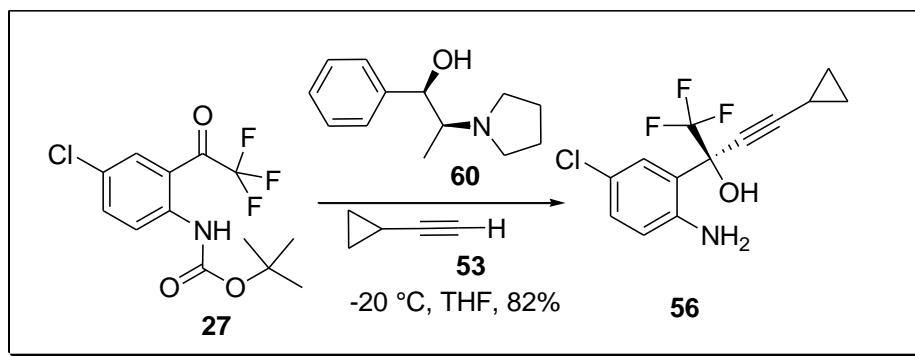


Colour change after completion of the reaction

**Figure 17:** Colour changes during lithiation reaction

### 2A.2.3. Step-3

Having developed a method to synthesize a synthetic standard of the ketone **27**, our attention then turned to the next step of the reaction (Scheme 28).

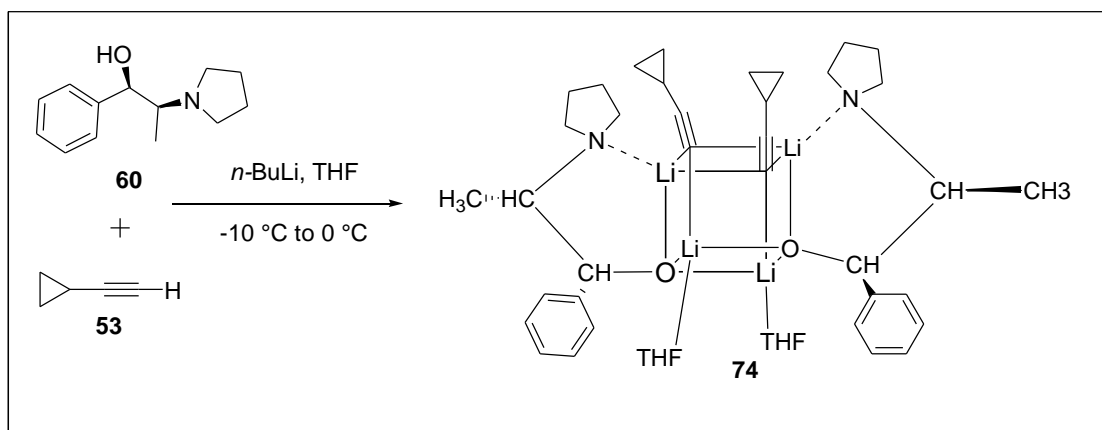


**Scheme 28:** Preparation of *tert*-butyl-4-chloro-2-(4-cyclo propyl-1,1-trifluoro-2-hydroxybut-3-yn-2-yl) phenyl carbamate **56**

(*S*)-2-(2-amino-5-chlorophenyl)-4-cyclopropyl-1,1,1-trifluoro-3-butyn-2-ol (amino alcohol) **56** (Scheme 28) was prepared by adding cyclopropyl acetylene **53** and (1*R*,2*S*) *N*-pyrrolidinylnorephedrine **60** to *tert*-butyl 4-chloro-2-(2,2,2-trifluoroacetyl) phenylcarbamate **27**. The mixture was cooled to -20 °C and to this solution *n*-butyllithium and compound **27** was added dropwise under nitrogen. The resulting orange colored solution was stirred for 1 hour at that temperature, then the reaction was quenched by the addition of 6N HCl. The mixture was warmed to ambient temperature, extracted with ethyl acetate and evaporated to get the product as fine yellow powder **56** in 82% yield, after purification by using flash column chromatography (10% ethyl acetate and hexane). (1*R*,2*S*) *N*-Pyrrolidinylnorephedrine **60** was used in this reaction as a chiral additive, which promotes enantioselective alkylation. The chiral additive forms a complex with the alkylating agent cyclopropyl acetylene **53** at lower temperatures which

blocks the undesired side attack of keto compound **27** to specifically yield compound **56**.

Experimentally, the chiral complex **69** was prepared by reaction of *n*-butyllithium with a mixture of (1*R*,2*S*)-*N*-pyrrolidinylnorephedrine **60** and cyclopropyl acetylene **53** at -10 °C to 0 °C (aggregate equilibration) in a THF (Scheme 29).



**Scheme 29:** Alkoxide-acetylide **74** complex formation

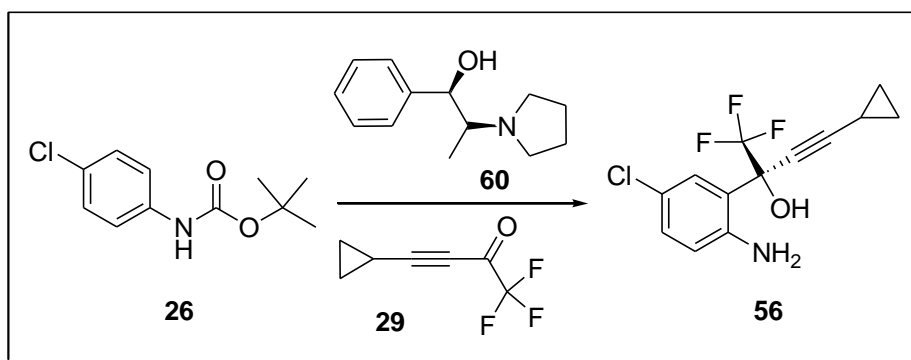
From the literature, many of the extensive lithium NMR studies prove that when 2:2 (1*R*,2*S*)-*N*-pyrrolidinylnorephedrine **60** and cyclopropyl acetylene **53** (alkoxide-acetylide) mixture generated at low temperatures exists as a complex which rapidly equilibrates as a single compound at -40 °C. This prevents the formation of the racemic mixture; finally the reaction is completed within minutes after addition of compound **27** to the chiral complex.

After completion of the reaction, the product was analyzed for chiral purity using Cyclobond I 2000 chiral column, methanol and water (80:20) as mobile phase. In this

the product peak as major (97.8% at 2.42 min) and other isomer (2.2% at 3.5 min) and it was compared with standard (99% purity at 2.42 min).

The product was purified by recrystallization with 10:1 heptane: toluene at 25 °C for 3h to afford the pure compound. After purification the compound **56** was again tested for chiral purity, which had now increased to 98.9%.

Alternatively, *tert*-butyl-4-chloro-2-(4-cyclopropyl-1,1-trifluoro-2-hydroxybut-3-yn-2-yl) phenyl carbamate **56** could also be prepared by using cyclopropylethynyl trifluoromethyl ketone **29** (Scheme 30).



**Scheme 30:** Preparation of *tert*-butyl-4-chloro-2-(4-cyclopropyl-1,1-trifluoro-2-hydroxybut-3-yn-2-yl) phenyl carbamate **56** by using cyclopropylethynyl trifluoromethyl ketone **29**.

The 4-chlorophenylcarbamate **26** was cooled to -55 °C and 5 equiv of *n*-butyllithium was added. The liberated dianion was quenched with cyclopropylethynyl trifluoromethyl ketone **29** to afford *tert*-butyl-4-chloro-2-(4-cyclopropyl-1,1-trifluoro-2-hydroxybut-3-yn-2-yl) phenyl carbamate **56** in 47% yield after purification by flash column chromatography eluting with 10% ethyl acetate and hexane.

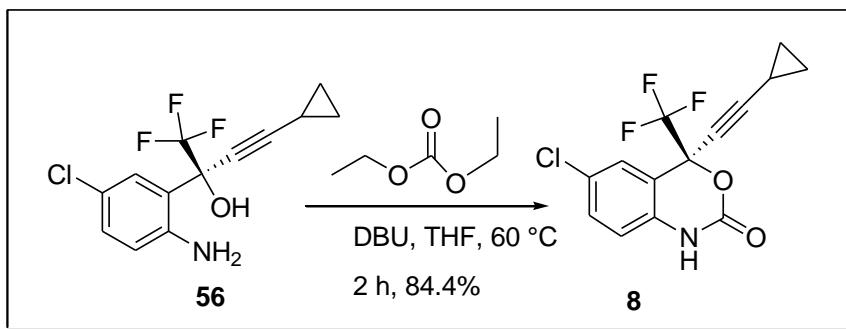
It is noteworthy to mention that we had to prepare cyclopropylethynyl trifluoromethyl ketone **29** ourselves, as it was not commercially available. Preparation of ketone **29** was described under preparation of starting materials (Scheme 21).

The chiral purity of the compound was tested by using HPLC. The chiral column (Cyclobond I 2000) used as stationary phase and methanol: water (80:20) used as mobile phase. The results obtained from the chromatogram were matched with the standard compound. The major peak observed at 2.49 min with 86.5% purity.

Although this method gave us good yield, compared to the other method but the chiral purity of the compound is less.

#### 2A.2.4. Step-4

Having developed a method to synthesize the key intermediate **56** in high yield, our attention then turned to the final cyclisation step of the reaction (Scheme 31).



**Scheme 31:** Preparation of 6-chloro-2-(4-cyclopropylethynyl)-4-(trifluoromethyl)-1*H*-benzo[d][1,3] oxazin-2-(4*H*)-one **8**

The optically pure (*S*)- 2-(2-amino-5-chlorophenyl)-4-cyclopropyl-1,1,1-trifluoro-3-butyn-2-ol (amino alcohol) **56** was reacted with carbonyl delivering agent (diethyl

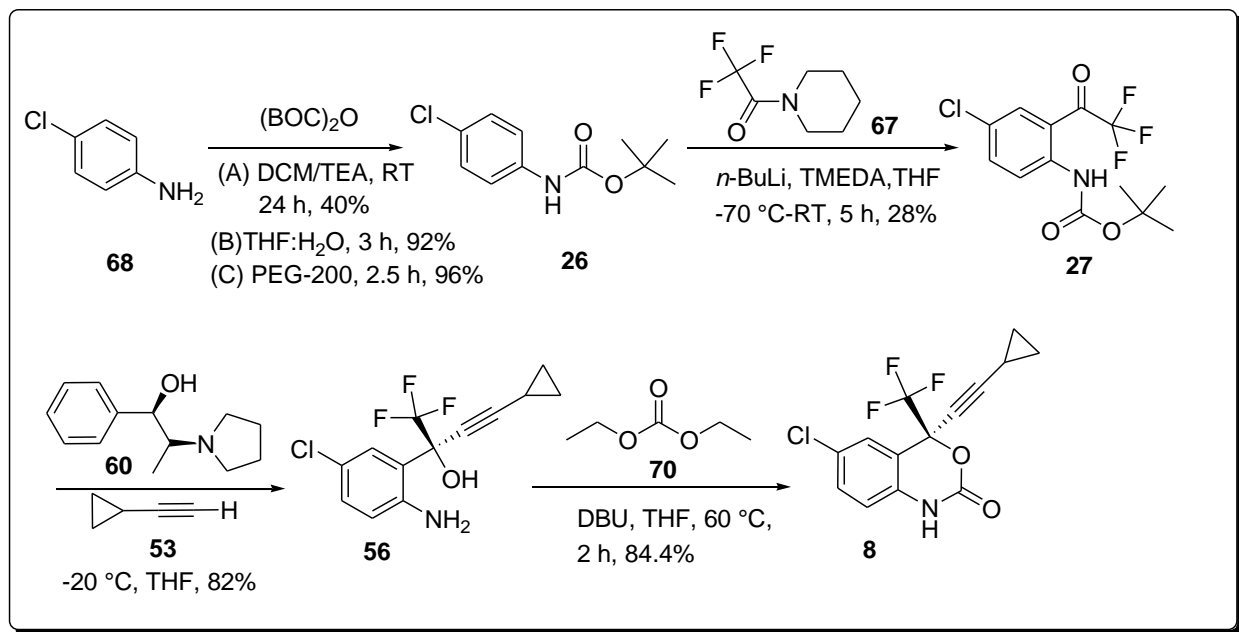
carbonate) in the presence of DBU at 60 °C in order to undergo cyclisation to give optically pure (-)-6-chloro-4-cyclopropylethynyl-4-trifluoromethyl-1,4-dihydro-2*H*-3,1-benzoxazin-2-one (efavirenz) **8** (Scheme 31). The compound was characterized by <sup>1</sup>H-NMR, <sup>13</sup>C-NMR, <sup>19</sup>F-NMR, IR and elemental analysis.

After recrystallization with 5% ethyl acetate in heptane the compound was tested for the chiral purity by using HPLC with Cyclobond I 2000 column. The chromatogram showed 99% purity at 2.51 min and it was matched with the standard compound chromatogram (2.51 min, 99% purity).



### 2A.3. Summary of batch synthesis

A novel four step synthetic method for the preparation of efavirenz **8**, with an overall yield of 51% was obtained. The method presently used for the synthesis of efavirenz **8** by Merck research laboratories consist of seven steps with an overall yield of 62% however the process described in this thesis gave us 51% overall yield in three less steps; hence overall we propose that this process is going to be more economical because of less reaction steps. The detailed yields conditions for each step was presented in Scheme 32 below. However we must clarify that this process was not optimized further in batch as the aim was to transfer to flow and fully optimize the process at that stage.



**Scheme 32:** Synthesis of efavirenz **8**

# **CHAPTER 2**

## **SECTION B**

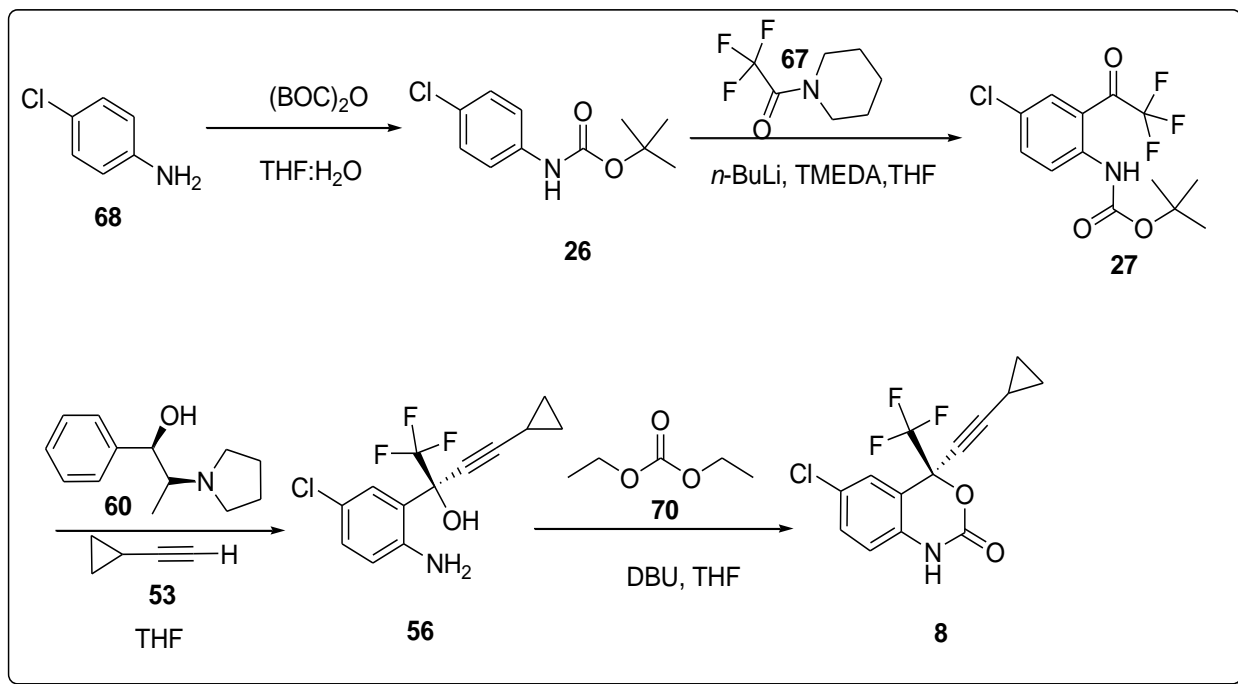
### **SEMI CONTINUOUS FLOW PROTOCOL RESULTS AND DISCUSSION**

## 2B. Semi continuous flow protocol

The inaccessibility of efavirenz **8**, a common drug used in combination therapy for AIDS, to millions of people worldwide, prompted us to develop an efficient process for its synthesis in classic batch chemistry as well as further optimizing all process parameters by incorporating a semi continuous flow protocol. The bench top synthesis has its limits (if conducted at larger scale), which include inefficient temperature and pressure controls as well as the inability to handle hazardous reagents safely. The application of continuous flow microreactors to reaction chemistries such as this one, could provide a potential practical solution that could be used to overcome some of these drawbacks and also to give new opportunities for efficient local drug manufacture.<sup>[130]</sup>

In continuous flow reactors, the reaction takes place in microcapillaries, which result in rapid mixing of reagents within seconds,<sup>[131-134]</sup> the temperature and pressure can be controlled fast and very accurately,<sup>[135-136]</sup> clean products are obtainable, safe handling of reagents and easy scale up of reaction processes is possible <sup>[137]</sup> and as such ultimately improving drug manufacturing.<sup>[138]</sup> Based on the advantages that continuous flow reactors present, we investigated the preparation of efavirenz **8** using a semi-continuous flow protocol in an attempt to meet the rising global needs for life-saving medicines.

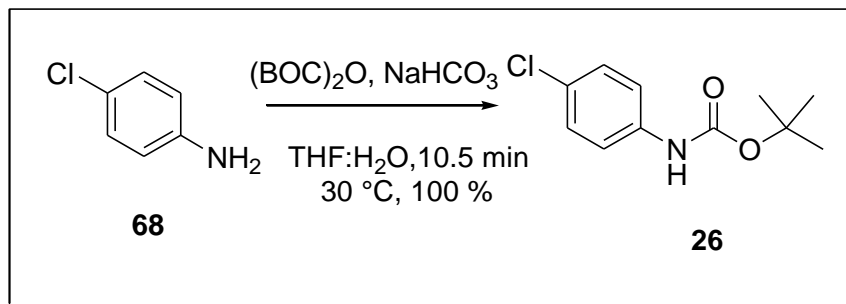
The synthetic route employed in our study involved the use of the inexpensive starting material 4-chloroaniline and proceeds through protection, trifluoroacetylation, nucleophilic addition and finally cyclization to yield optically pure efavirenz **8** (Scheme 33). The optical purity was tested by using HPLC in order to compare the results obtained in batch processing.



**Scheme 33:** Synthesis of efavirenz **8** by semi continuous flow protocol

### 2B.1. Step-1

Having developed the synthetic methodology in batch, our first investigation was to see if we could improve the Boc protection reaction by exploiting flow chemistry (Scheme 34).



**Scheme 34:** Preparation of *tert*-butyl-4-chloro phenyl carbamate **26**

Preparation of *tert*-butyl-4-chloro phenyl carbamate **26** (Scheme 34) in flow was done by using Chemyx Fusion syringe pumps and LTF microreactors. This reaction was first

established in traditional batch chemistry where the reaction parameters attained were transferred into flow chemistry technology for further investigation and optimization.

We started the preparation of efavirenz **8** from 4-chloroaniline **68**, which undergoes protection with di-*tert*-butyl dicarbamate in the presence of aqueous sodium bicarbonate as a base. This preliminary flow reaction was carried out as shown in Figure 18 below, these concentrations of compound **68** and Boc anhydride (0.78 M and 0.93 M respectively) were selected from batch studies and the reaction carried out at the room temperature. The reason behind the taking the concentrations from batch study was to compare the results of batch study to flow protocol results.

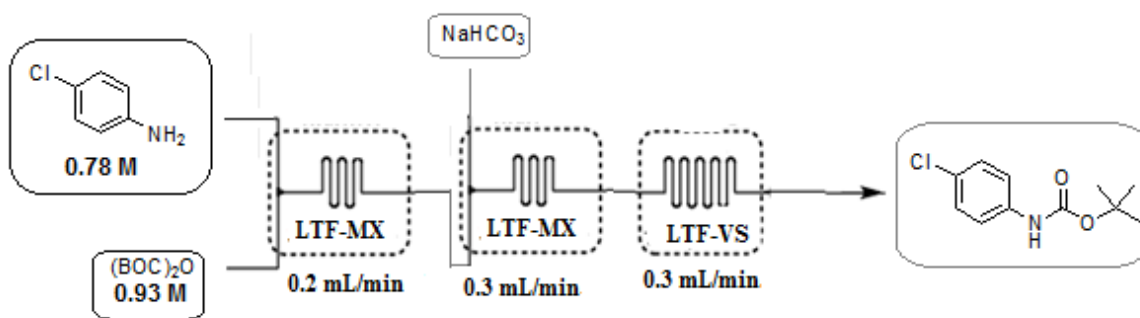


**Figure 18:** Schematic diagram for step-1 preliminary flow reaction

It needs to be emphasized that in batch we showed that the reaction worked well under solvent free conditions. Clearly this was not possible and we needed to use solvent as we cannot use solids in the flow reactors. We used THF and water as the solvent for this reaction as this was the best solvent system previously studied. THF and water was taken in 1:1 ratio. Water used in this reaction to make an aqueous sodium bicarbonate solution.

In this study, we investigated the effect of residence time, temperature and reagent concentration on the conversion of 4-chloroaniline **68**. The results of the study are represented here in graphical form.

### **2B.1.1. Effect of residence time on conversion of 68**

After preliminary conformation in the flow protocol the reaction was first investigated for the effect of residence time by keeping the concentration of the starting material **68** at 0.78 M and the Boc anhydride at 0.93 M (1.2 equiv) and the reaction was carried out at the room temperature. For completeness the reason we used this concentration, was that calculations showed that the batch reaction also correlated to a concentration of 0.78 M. We knew that the reagents were soluble under these conditions and furthermore by using identical concentrations enabled detailed comparison of batch and flow conditions. This study of residence time was conducted from 0.35 min to 21 min.

In this reaction it was found that as the residence time decreases, the conversion of **68** decreased. According to the flow chemistry, residence time is defined as the amount of time that the reaction mixture is in the microreactor. The relationship between the flow rate and residence time is best explained by the equation 1

$$R = \frac{V}{TF} \quad \text{(Equation 1)}$$

*where R=residence time, V= volume of the reactor, TF= total flow rate.*

From the reaction, residence time is directly proportional to the volume of reactor and inversely proportional to the total flow rate. From the graph (Figure 19) presented below, a decrease in the residence time shows that the conversion also decreased as expected.

The findings of this investigation are illustrated in Figure 19 below. Where the maximum conversion is observed at a residence time of 7 min (100%).

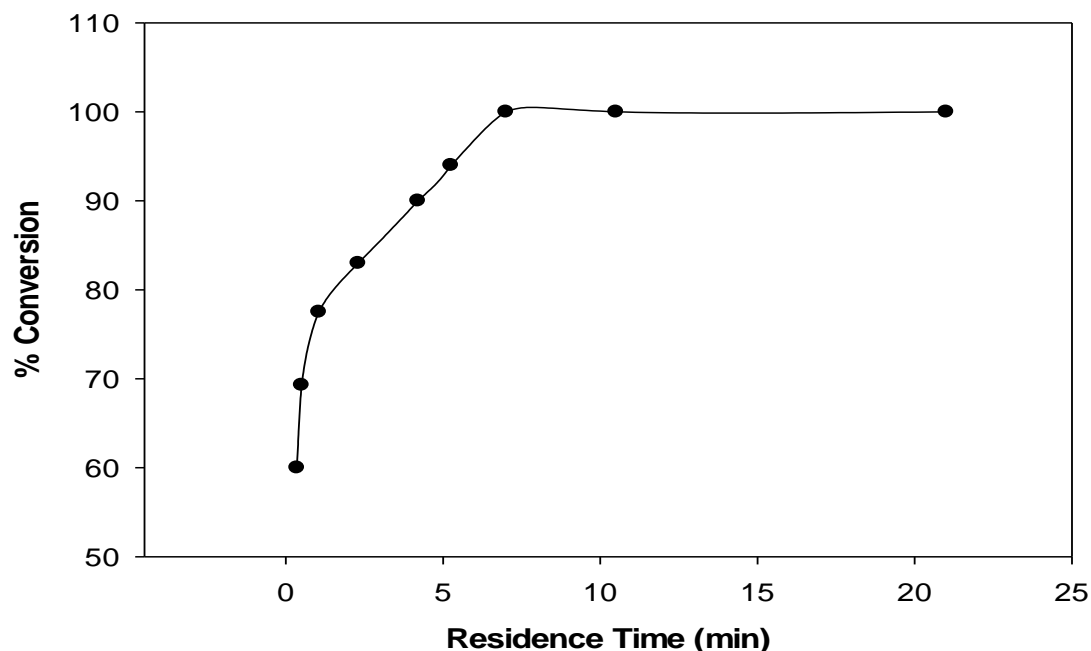


**Figure 19:** Effect of residence time on conversion of **68** at 0.78 M of **68**, 0.93 M of Boc anhydride and at room temperature.

The data in the graph shows that it is possible to use reaction times greater than 7 mins, however the goal is to use as little time as possible in order to gain maximum throughput from the reactor per unit time. As such if one transferred these conditions into an industrial scenario these would be the conditions used.

#### **2B.1.2. Effect of concentration of di-*tert*-butyl dicarbamate at different residence times on conversion of **68****

After the study of residence time we moved to see the effect of concentration of di-*tert*-butyl dicarbamate. Our initial objective was to minimize the concentration of di-*tert*-butyl

dicarbamate for the production of **26**. To achieve this, we started our investigation by changing the molar concentration of di-*tert*-butyl dicarbamate. The initial concentration was 0.93 M and we investigated the molar concentration from 0.93 M to 0.70 M at different residence times. This study was conducted at room temperature.

In earlier batch studies, 1.2 equiv (0.93 M) of di-*tert*-butyl dicarbamate to the starting material **68** was used, by considering this we started our flow study with 1.2 equiv for initial conformation and after attaining the results our aim was to decrease the concentration of di-*tert*-butyl dicarbamate to 1 equiv (0.78M) in try to make the process more 'green'.

The reaction was performed at different residence times of 5.25 min, 10.5 min and 21.5 min and concentration of di-*tert*-butyl dicarbamate 0.70 M, 0.78 M, 0.93 M by keeping the other reagents concentration constant (0.78 M of starting material **68**) in order to study the effect of concentration of di-*tert*-butyl dicarbamate and residence time on conversion of 4-chloroaniline **68**.

As the concentration decreases the conversion of 4-chloroaniline **68** decreased because of less availability of the reagent, which led to an insufficient ratio of the reactants in a microreactor. In the batch reaction of di-*tert*-butyl dicarbamate (0.93 M) and 4-chloroaniline **68** (0.78 M) a reaction conversion of 96% was attained, however, at similar reagent concentrations, 100% conversion was achieved in semi continuous flow protocol. We also found that even at a lower concentration of di-*tert*-butyl dicarbamate (0.78 M) the same conversion was sustained in the flow protocol.



At the lowest concentration of di-*tert*-butyl dicarbamate (0.70 M), it was observed that a higher residence time (21 min) was required to achieve a reaction conversion of 70%. This means that a lower concentration of di-*tert*-butyl dicarbamate can also be used for the reaction, however, a higher residence time may be required to achieve comparable reaction conversions. But clearly the yield would never go to 100% under these conditions, but we were interested to observe the effect.

The results of this study are shown below in Figure 20. It is seen that the maximum conversion is attained at 0.78 M concentration of di-*tert*-butyl dicarbamate for a residence time of 21 min.

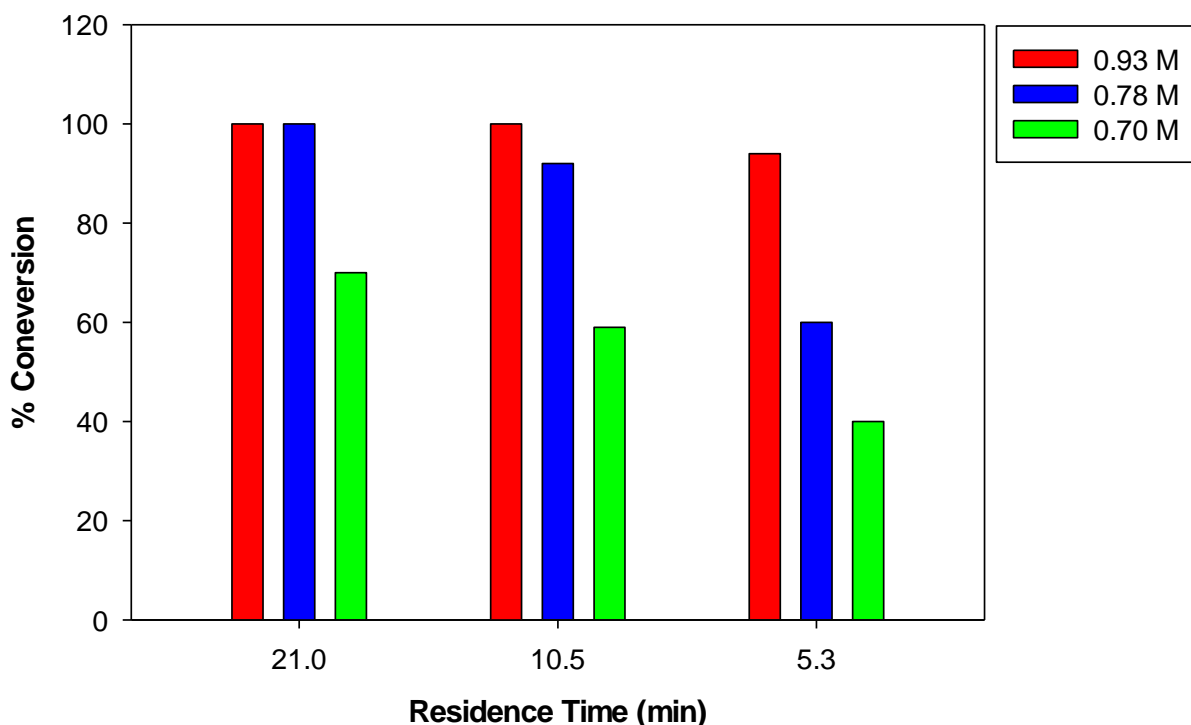


**Figure 20:** Effect of concentration of di-*tert*-butyl dicarbamate on conversion of **68** at different residence times, room temperature and the concentration of **68** was 0.78 M.

As the residence time decreases from 21 min to 5.25 min, the conversion of 4-chloroaniline **68** to **26** is seen to decrease with a decrease in the concentration of Boc anhydride. At a residence time of 10.5 min, for example, an increase in the concentration of Boc anhydride from 0.70 M to 0.93 M led to a 41% decrease in conversion of 4-chloroaniline **68** to desired product **26**.

From this, it can be stated that the best residence time of reaction reagents and concentration of Boc anhydride that provides an optimum conversion of 4-chloroaniline **68** (100%) is residence time 10.5 min and concentration of 0.78 M of all the reagents. As described above with this optimization of concentration of Boc anhydride we got optimum results for a stoichiometric ratio (1 equiv to starting material **68**).

#### **2B.1.3. Effect of temperature at different residence times on conversion of 68**

After getting the optimum results for residence time (7 min) and concentration (0.78 M of **68** and 0.78 M of Boc anhydride) at room temperature we moved forward to investigate the effect of temperature for the same reaction. As a third variable towards the optimization, a range of temperatures (30 °C to 120 °C) were investigated at different residence times (5.3 min, 10.5 min, 21.5 min) as detailed in Chapter 4. The above mentioned concentrations was kept constant throughout the reaction. Previous to this study the reaction carried out at room temperature.

As the temperature increases the conversion of 4-chloroaniline **68** decreased which was slightly surprising. However we observed that at higher temperatures blockage of channels were observed because the precipitation of solid compound in the microchannels of the reactor, which decreased the conversion of 4-chloroaniline **68**.

The findings of this study illustrated by graphical form in below (Figure 21)

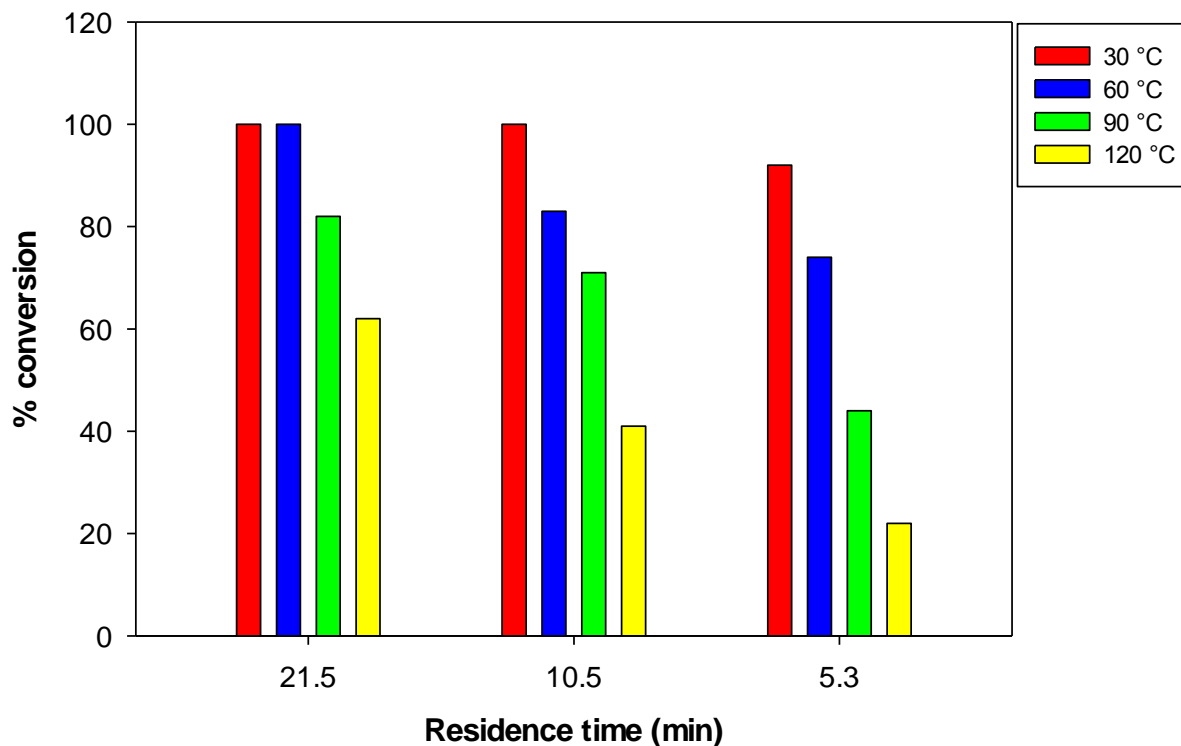


**Figure 21:** Effect of Temperature on the conversion of **68** at different residence times and at a concentration of 0.78M of compound **68** and Boc anhydride

As the residence time decreases from 21 min to 5.25 min, the conversion of 4-chloroaniline **68** to **26** is seen to decrease with an increase in the temperature.

At a temperature of 30 °C, a decrease in residence time from 21 min to 5.25 min led to an 8% decrease in conversion of 4-chloroaniline **68** to the desired product **26**, but as the temperature increases from 30 °C to 120°C the conversion difference is increased with the decrease of residence time. At 60 °C, a decrease in residence time from 21 min to

5.25 min, the conversion decreased to 26%, at 90 °C the conversion decreased to 38% and at 120 °C the conversion decreased to 40%.

From this, it can be stated that the best residence time of reaction reagents and temperature that provides an optimum conversion of 4-chloroaniline **68** (100%) is residence time of 10.5 min and temperature 30 °C at a concentration of 0.78M of compound **68** and Boc anhydride.

In this investigation of reaction reagent parameters *i.e.* residence time, concentration, temperature has a significant effect on the conversion of **68** to a desired product **26**. The summary of results of this study listed in below Table 12.

**Table12: Optimized conditions for step-1**

Residence time (min)	Concentration (M)	Temperature (°C)
10.5	0.78 M of Boc anhydride	30

#### 2B.1.4. Comparison between the synthesis of **26** in batch and microreactors

As explained earlier, this reaction was first established in traditional batch chemistry, further optimization of the reaction reagent parameters transferred into a continuous flow protocol.

In traditional batch chemistry this reaction took 3 hours (180 min) at room temperature and the conversion was 92%, but in the continuous flow microreactor the reaction taken place in comparatively less time *i.e.* 10.5 min at 30 °C and the conversion was 100%, at lower concentration of di-*tert*-butyl dicarbamate **73** (Batch 1.2equiv *i.e.* 0.93 M, Flow 1

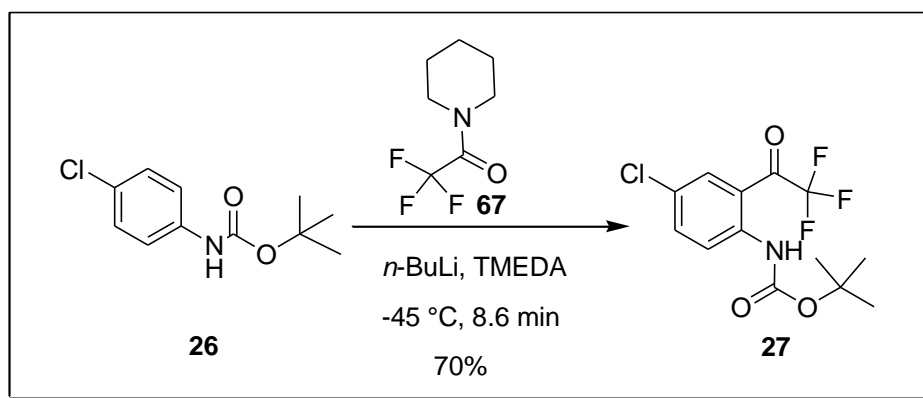
equiv, *i.e.* 0.78 M). The findings from the traditional batch process and a semi continuous flow protocol are presented below (Table 13).

**Table 13: Comparison between the synthesis of *tert*-butyl-4-chloro phenyl carbamate **26** in batch and microreactors**

Entry	Option	Temperature (°C)	Time (min)	Conc of <b>68</b> (M)	Concentration of di- <i>tert</i> -butyl dicarbamate (M)	%Conversion
1	Batch	Room temperature	180	0.78	0.93	92
2	Microreactor	30	10.5	0.78	0.78	100

## 2B.2. Step 2

Having developed a method for the continuous flow synthesis of the Boc protected derivative **26** in very high yield, our attention then turned to the trifluoroacetylation reaction in flow (Scheme 35).



**Scheme 35:** Preparation of *tert*-butyl-4-chloro-2-(2,2,2-trifluoroacetyl) phenyl carbamate **27**

This reaction was first established by using traditional batch chemistry; the parameters from batch chemistry were transferred into a continuous flow protocol for further investigation and optimization. The preliminary flow reaction was performed, as shown in Figure 22 below. The concentration of reagents was selected based on the preliminary batch study for easy comparability to the flow reaction.

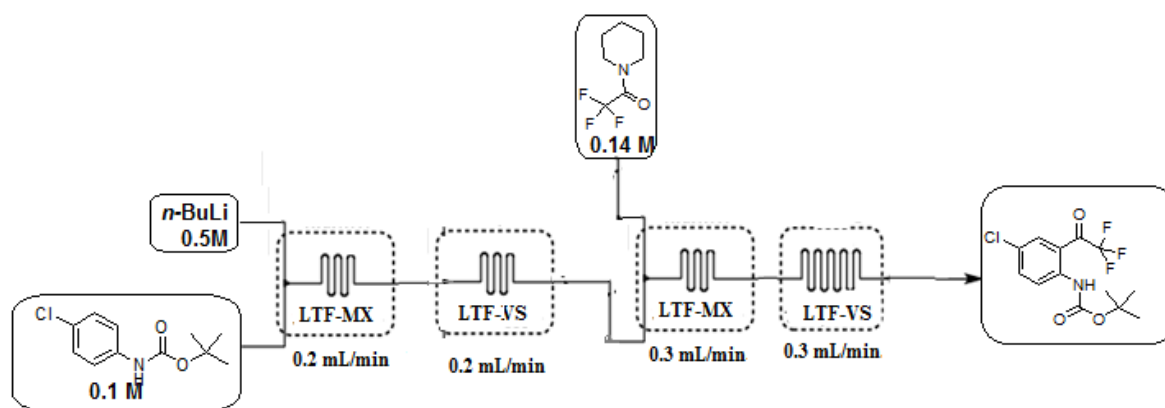


**Figure 22:** Schematic diagram for the step-2 preliminary flow reaction

After preliminary conformation of the reaction in microreactor the reaction further explored for effect of temperature, residence time and concentration on conversion of **26**.

### 2B.2.1. Effect of temperature on conversion of **26**

As a first trial towards the optimization for the preparation of **27**, the reaction investigated for the effect of temperature. In the batch reactor this reaction was performed at a temperature of -78 °C, maintaining low temperatures for a long time always need more attention and also literature revealing the most of the lithiation reactions in flow can work at higher temperatures than compared to batch.<sup>[107]</sup> These points made us interested towards the study of temperature. To achieve this, we started our investigation by varying the temperature of the reaction from -70 °C to 0°C.

This reaction was carried out at a concentration of 0.5 M of *n*-butyllithium, 0.1 M of compound **27**, 0.14 M of compound **67**. All these concentrations were taken based on batch results and the flow rate of the reaction was maintained at 0.3 mL/min (8.6 min) throughout study.

As the temperature increases the conversion of **26** decreased because of decomposition of *n*-butyllithium at higher temperatures in THF. The findings of this study are represented below in Figure 23 by graphical form, maximum conversion observed at -70 °C and 45 °C.

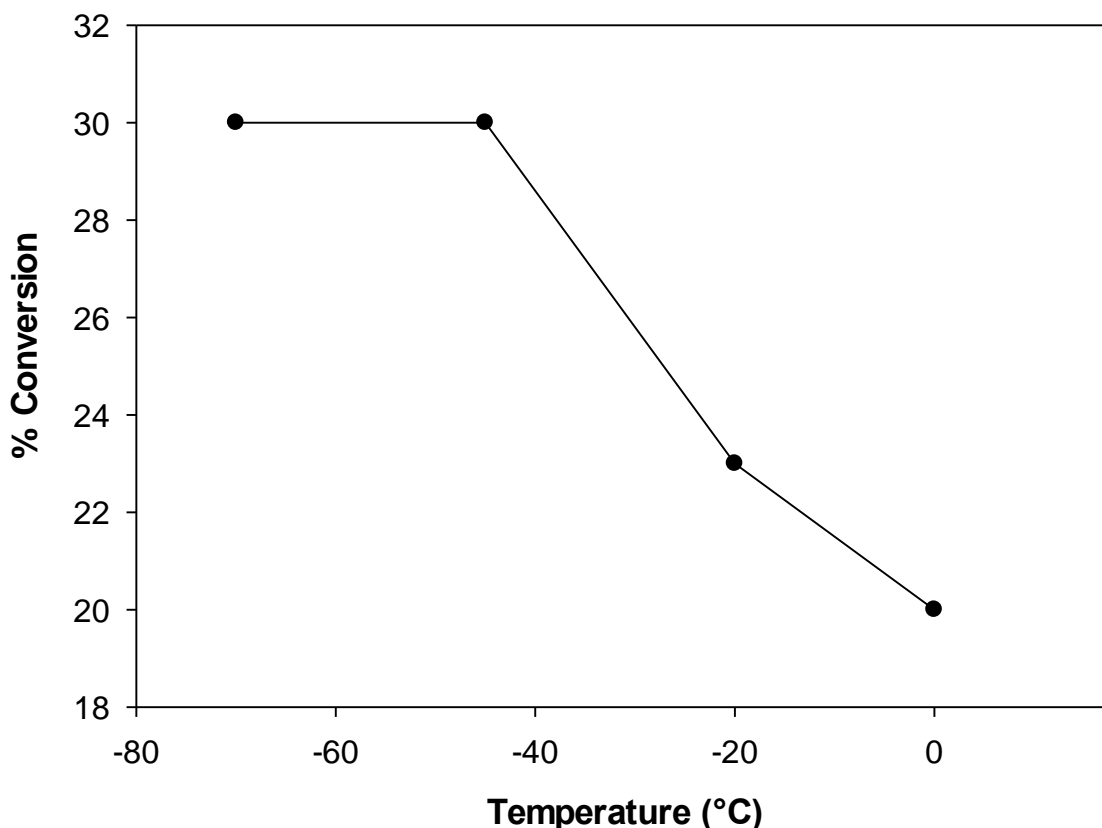


**Figure 23:** Effect of temperature on % conversion of **26** at 0.5 M of *n*-butyllithium, 0.1 M of compound **27**, 0.14 M of compound **67** and at a residence time of 8.6 min.

As can be seen from the graph the study performed for a temperature range of -70 °C to 0 °C, at -70 °C the conversion was 30% and it decreased with increases in temperature because of instability of generated carbanion or less formation of carbanion. The key step of this reaction is a generation of carbanion, which is more favored at low temperatures.

In batch chemistry, the generation of the carbanion occurred at -78 °C (28%) however on warming to -45° C the reaction was unsuccessful. In the case of semi continuous flow protocols the reaction proceeded at a higher temperature and comparatively more conversion (70%) attained because of equal distribution of temperature throughout the reactor; this is in agreement with the literature protocols described by Yoshida on butyl lithium based chemistry.

#### **2B.2.2. Effect of concentration of piperidine trifluoroacetic acid **67** on conversion of **26****

Towards the optimization of compound **27**, the other reaction parameter *i.e.* concentration of trifluoro acetylating agent **67** was investigated. The other two reagents concentrations kept constant at 0.25 M of *n*-butyllithium and 0.1 M of compound **26**, the residence time 8.6 min and the temperature at -45 °C. These concentrations, temperature and residence time were selected as a result of previous optimization studies. We started our investigation by varying the concentration of **67**. The initial concentration of compound **67** was 0.14 M, at this concentration we achieved 30% conversion. To improve the results the concentration of compound **67** was investigated.

The results of this study illustrated below in Figure 24 show that as the concentration increases the conversion of **26** increased to a certain level after that it is started to



decrease. Maximum conversion was observed at 0.2 M concentration of **67**, this suggests two equivalents to be optimal.

From the graph, the conversion of **27** is highly influenced by the concentration of **67**, at a concentration of 0.14 M the conversion is 30% further the conversion of **27** reached 70% as increase in concentration to 0.2 M but the same trend was not followed throughout the investigation after further increase from 0.2 M to 0.25 M the conversion decreased. The concentration is further increased from 0.25 M to 0.3 M to further confirm the effect.

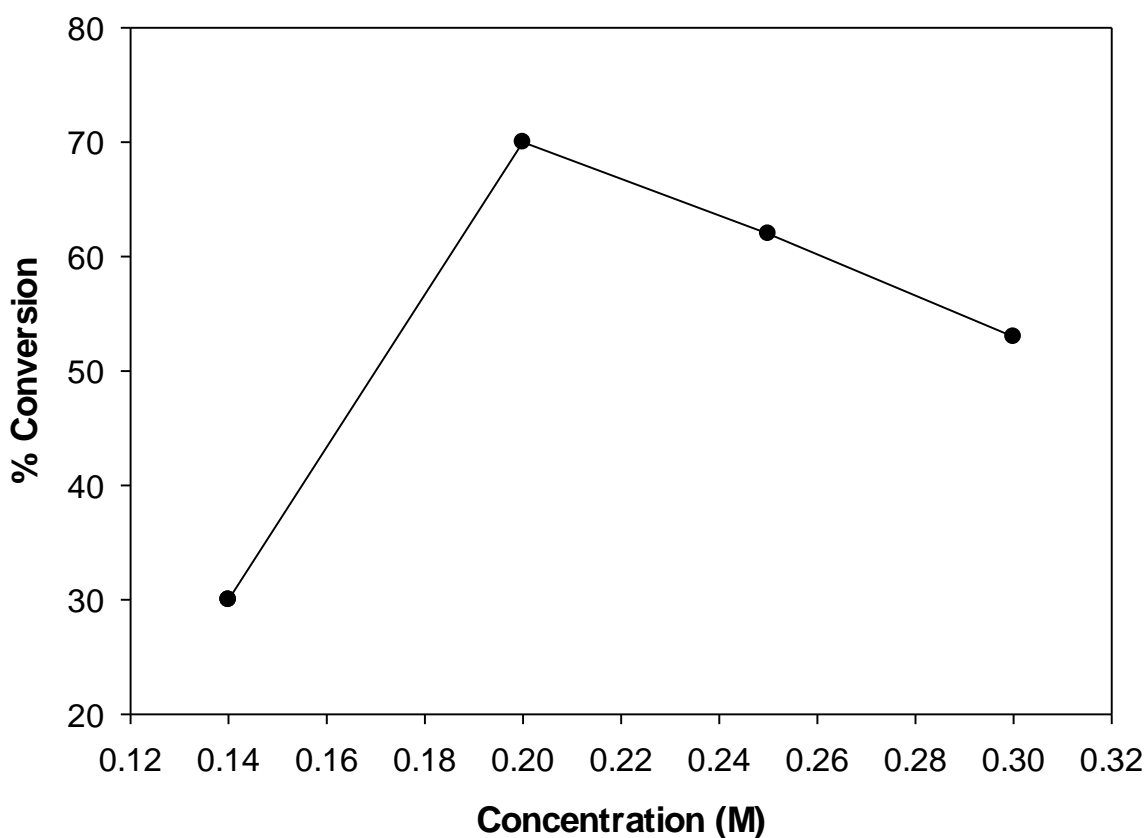


**Figure 24:** Effect of concentration of **67** on the conversion of **26** at 0.25 M of *n*-butyllithium, 0.1 M of compound **26** at -10 °C

The chemical possible reason for this inverted V graph, at higher concentrations of **67** the reaction between the newly formed compound **27** and compound **67** generates the other undesired compound, as a result of proposed Boc deprotection under the acidic conditions.<sup>[93]</sup>

### 2B.2.3. Effect of residence time on conversion of **26**

After attaining the optimum results for the concentration (0.25 M of *n*-butyllithium, 0.1 M of compound **26**, 0.2 M of compound **67**), temperature (-45 °C) we moved forward towards the optimization of compound **27**, the effect of residence time on conversion of **26** was investigated. The above mentioned concentrations and temperature were kept constant throughout the study. To achieve this, we started our investigation by varying the residence time from 4.3 min to 17.3 min as detailed in Chapter 4.

Effect of residence time on the conversion of **26** represented below in Figure 25 by graphical form, as the residence time decreases the conversion of **26** decreased. The shorter residence time led to insufficient contact of the reactants in a microreactor. This is explained by equation 1 above where it is shown that the residence time is inversely proportion to the flow rate. Maximum conversion observed at a residence time of 17.3 min and 8.6 min.

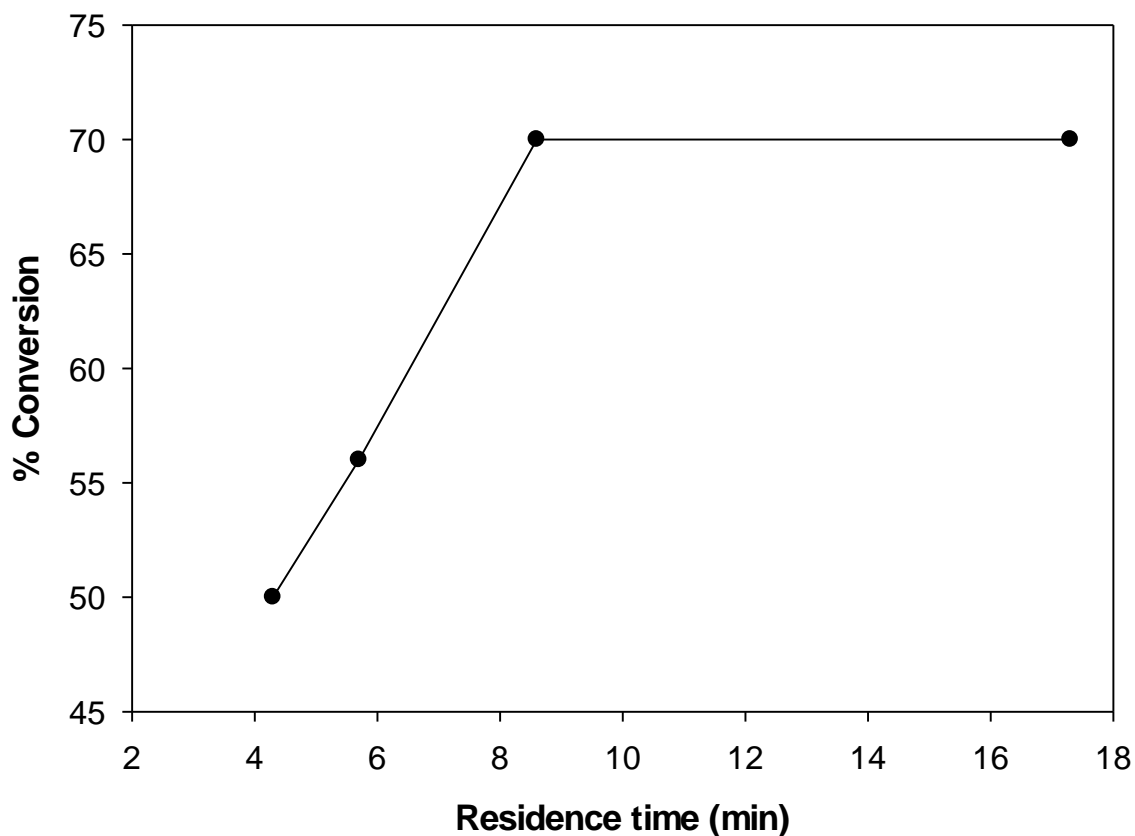


**Figure 25:** Effect of residence time on conversion of **27** at 0.25 M of *n*-butyllithium, 0.1 M compound **26**, 0.2 M compound **67** at -10 °C

This study started at a residence time of 17.3 min (as used previously), where we achieved 70% conversion and it continued until 8.6 min, after this the conversion slowly started to decrease because of decreased residence time. These residence times were investigated at a range of 17.3 min to 4.3 min and the conversion led to decrease from 70% to 50%.

By keeping the preliminary results in mind the reaction was further investigated for residence times by creating an experimental domain using central composite design.

#### 2B.2.4. Experimental design for residence times

#### 2B.2.5. Experimental results

The trifluoroacetylation reaction with piperidine trifluoroacetic acid in the presence of TMEDA was initially optimized in LTF microreactor plates using *n*-butyllithium a lithiating agent. After preliminary screening of the reaction an experimental domain was established in order to try to get a better understanding of this complex process. The developed experimental domain was further used to create the central composite design to execute the experiments in a well-developed fashion (Table 14). For this reaction all the reagents concentrations was kept constant (*n*-butyllithium at 0.25 M, compound **67** at 0.2 M and compound **26** at 0.1 M) and temperature was -45 °C

**Table14: Experimental domain for residence times (min) of step 2**

	<i>n</i> -Butyllithium (min)	Piperidine trifluoroacetic acid (min)	<i>N</i> -Boc aniline (min)
Minimum	52	260	86.6
Maximum	13	5.2	5.2

During the study, a total of 20 experiments were carried out from the central composite design. Before the actual study was resumed, the reactor system was tested for repeatability. Additionally, a systematic error was also analyzed on the gas chromatography to determine its repeatability.

### 2B.2.6. Central composite design and observations

The central composite design (CCD) was established from the experimental domain (Table 14) to optimize the residence time. The optimization process was carried out by varying residence time. The central composite design of the experiments and the observations are detailed below (Table 15).

**Table 15: Central composite design for trifluoro acetylation reaction**

Entry	<i>n</i> -Butyllithium (min)	Piperidine trifluoroacetic acid (min)	N-Boc aniline (min)	% Conversion
1	21.6	9.6	43	26
2	21.6	86	9.6	20
3	32.5	9.6	32.5	60
4	15.2	20	86	35
5	21.6	9.6	43.3	14
6	15.2	6.5	86	23
7	21.6	9.6	26	45
8	21.6	5.2	43.3	11
9	32.5	20	86	45
10	21.6	9.6	43.3	24
11	32.5	6.5	86	24
12	32.5	6.5	32.5	18
13	21.6	9.6	260	7.7
14	15.2	20	32.5	70

15	21.6	9.6	43.3	26
16	21.6	9.6	43.3	26.2
17	52	9.6	43.3	7.1
18	21.6	9.6	43.3	26
19	13	9.6	43.3	35
20	15.2	6.5	32.5	37

The reaction variable residence times were investigated for their statistical significant influence on the observed experimental data (Table 15). The study was carried out by using a logistic regression model (explained in Chapter 4). The outcome of the analysis will bring a better understanding of the residence times that have an effect towards the trifluoro acetylation reaction. Moreover, to deduce the optimum conditions that leads to the optimum conversion.

#### **2B.2.7. Effect of residence time on conversion of 26**

The effect of residence time on conversion has been investigated at three levels *i.e.* minimum, mid, maximum residence times of *n*-butyllithium and piperidine trifluoroacetic acid. The observed results are summarized below (Figure 26).

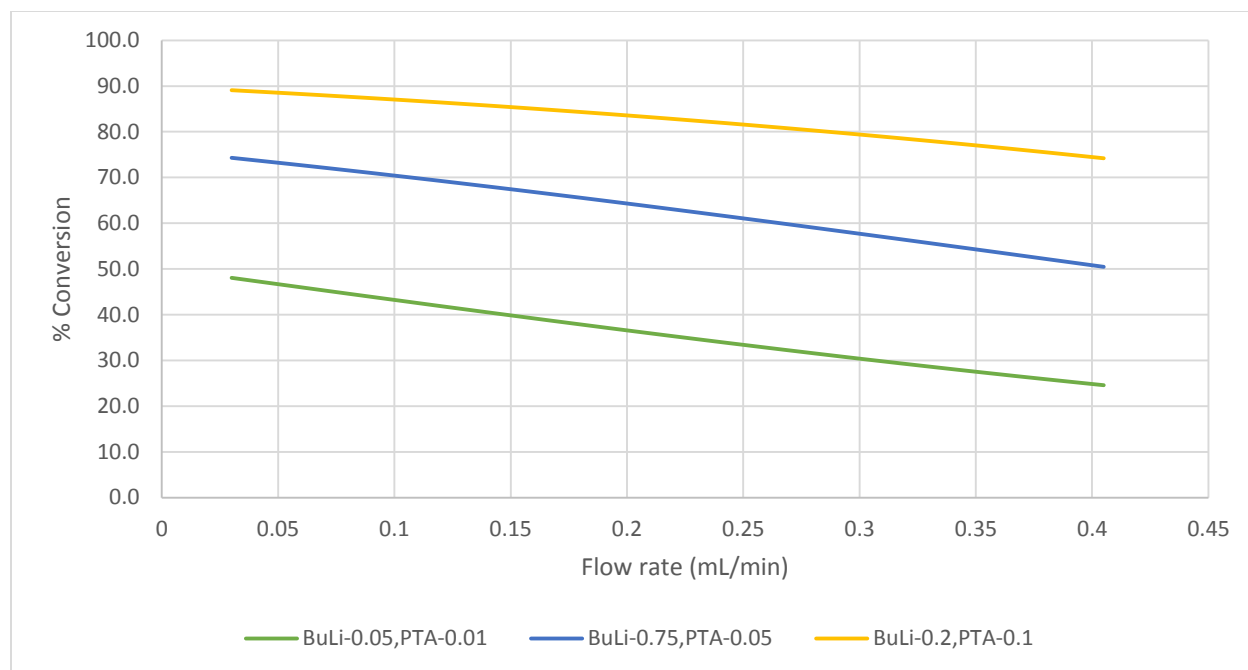


**Figure 26:** Effect of residence time on conversion of **26** at 0.25 M of *n*-butyllithium, 0.1 M of compound **26**, 0.2 M of compound **67** at -45 °C

From the graph above (Figure 26) as the residence time decreased the conversion of compound **26** decreased. As the residence time decreased, the time of contact of reaction reagents also decreased which is responsible for less conversion.

To achieve the best conversion in this step, we have screened the temperature, residence time, concentration and the optimum concentration of reaction reagents from the study are shown below Table 16. From the study, the optimum residence time of the reaction is 7.7 min and the temperature is -45 °C.

**Table 16: Optimum conditions for step-2**

Reagents	Concentration M
<i>n</i> -butyllithium	0.25
piperidine trifluoroacetic acid	0.2
compound <b>26</b>	0.1

By using a semi continuous flow microreactor the reaction takes place in less time, concentration and temperature, whereas in batch it requires several hours (3 hours) to complete the reaction.

The comparison between the synthesis of *tert*-butyl-4-chloro-2-(2,2,2-trifluoroacetyl) phenyl carbamate **27** in batch and microreactors are shown in Table 17. As compared to the batch in the flow process the reaction time is greatly decreased and the conversion is also increased.

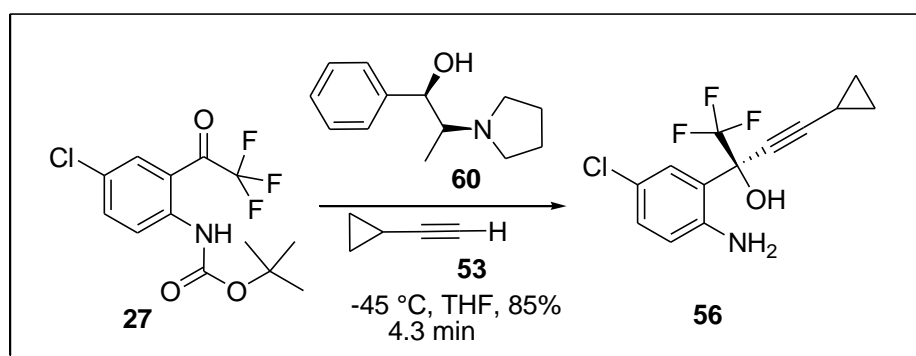
**Table 17: Comparison between the synthesis of compound 27 in batch and microreactors**

Entry	Reaction time (min)	Concentration (M)			Temperature (°C)	% Conversion
		<i>n</i> -BuLi	Pip. Trifluoroacetic acid	compound <b>26</b>		
<b>Batch</b>	180	0.5	0.14	0.1	-70	28
<b>Microreactor</b>	7.7	0.25	0.2	0.1	-45	70



### 2B.3. Step-3

After optimization of trifluoroacetylation reaction (step 2), we moved to the alkylation reaction (step 3) which is one of the important step in the synthesis of efavirenz **8** as this generates the chiral center of the molecule. In this reaction compound **27** converted to compound **56** in the presence of chiral axillary **60** by the addition of compound **53** (Scheme 36).



**Scheme 36:** Preparation of *tert*-butyl-4-chloro-2-(4-cyclo propyl-1,1-trifluoro-hydroxybut-3-yn-2-yl) phenyl carbamate **56**

By considering the batch conditions, the preliminary flow reaction was established as shown in Figure 27 below. The concentration of reagents was maintained the same as the batch study for better comparability and at this concentrations the compounds are highly soluble in the solvent.

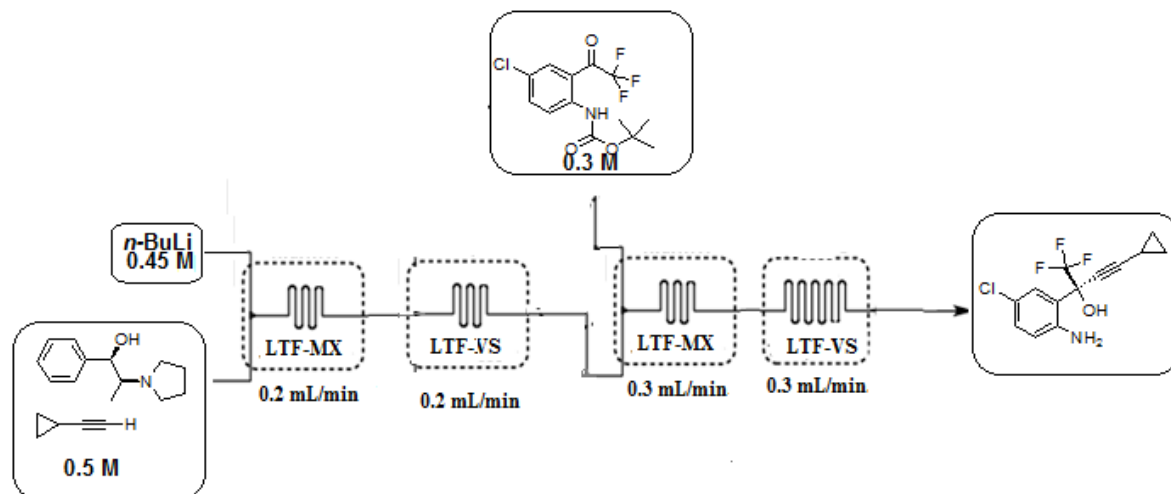


**Figure 27:** Schematic diagram for step-3 preliminary flow reaction

After reaction conformation in the flow reactor the reaction was further optimized by screening the reaction parameters *i.e.* residence time, concentration and temperature for a better conversion of **27**.

### 2B.3.1. Effect of residence time on conversion of **27**

As a first attempt towards the optimization investigation of residence time was chosen. For this investigation the concentration 0.45 M of *n*-butyllithium, 0.5 M of compound **53**, 0.35 M of compound **27** was taken as a result of previous optimization studies. The reaction temperature was maintained at -45 °C. The above mentioned concentrations were prepared by using THF.

Effect of residence time on the conversion of **27** represented below in Figure 28 by graphical form, as the residence time decreases the conversion of **27** decreased. The shorter residence time led to insufficient contact of the reactants in a microreactor. This is further explained by equation 1 above where it is shown that the residence time is

inversely proportion to the flow rate. The maximum conversion observed at a residence time of 8.6 min.

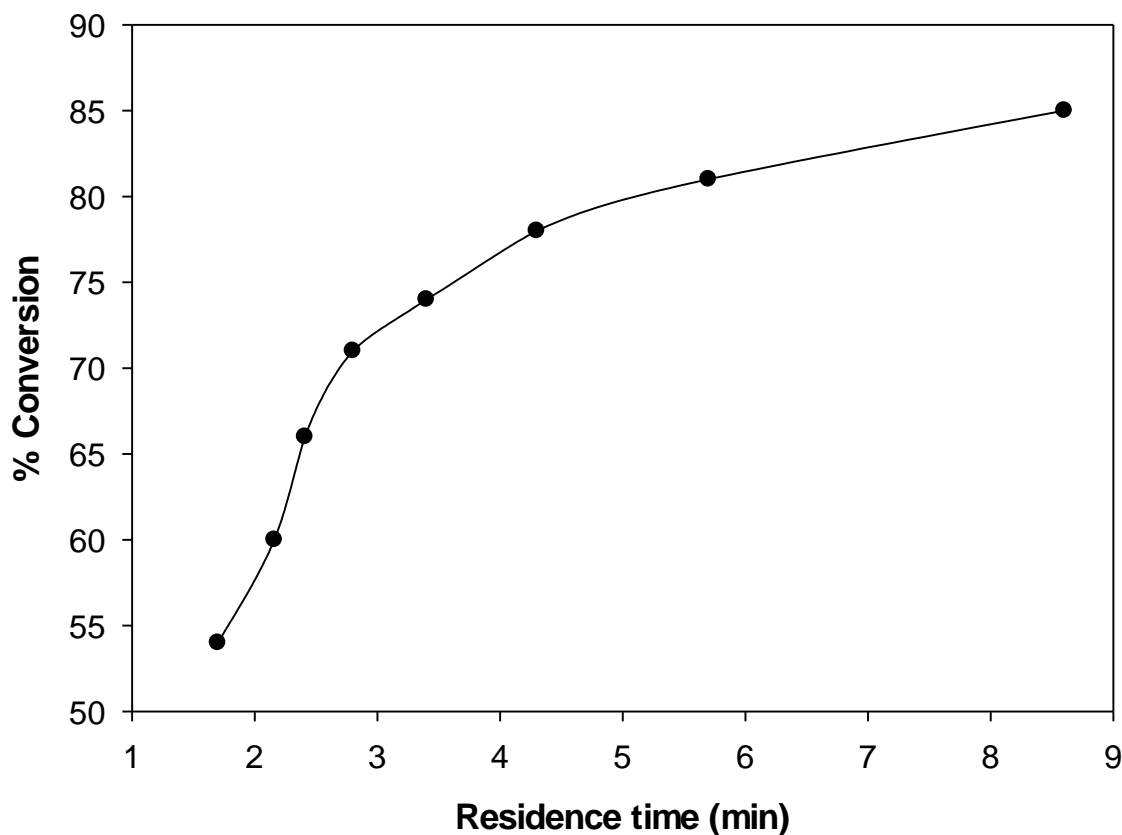


**Figure 28:** Effect of residence time on % conversion of **27** at 0.45 M of *n*-butyllithium, 0.5 M of compound **53**, 0.35 M of compound **27** at -45 °C

We started our investigation of residence time at 8.6 min, at this residence time the conversion is 85% and at 5.7 min 81% conversion and the same pattern continued throughout the investigation as decreasing residence time. We investigated residence time in a range of 8.6 min to 1.7 min and the conversion led to decrease from 85% to 54%

### 2B.3.2. Effect of temperature on conversion of **27**

Towards the optimization of the alkylation reaction, after residence time we focused on the effect of temperature on the % conversion of **27**. For the previous investigations we worked at -45 °C and we made this study to see how a temperature increase effects the reaction. The concentrations were kept constant throughout the study at 0.45 M of *n*-butyllithium, 0.5 M of compound **53**, 0.35 M of compound **27**. The residence time was 4.3 min.

Effect of temperature on the conversion of **27** represented below in Figure 29 by graphical form. As the temperature increases the conversion of **27** to a desired product **56** decreased because of decomposition of *n*-butyllithium, maximum conversion observed at -45 °C.

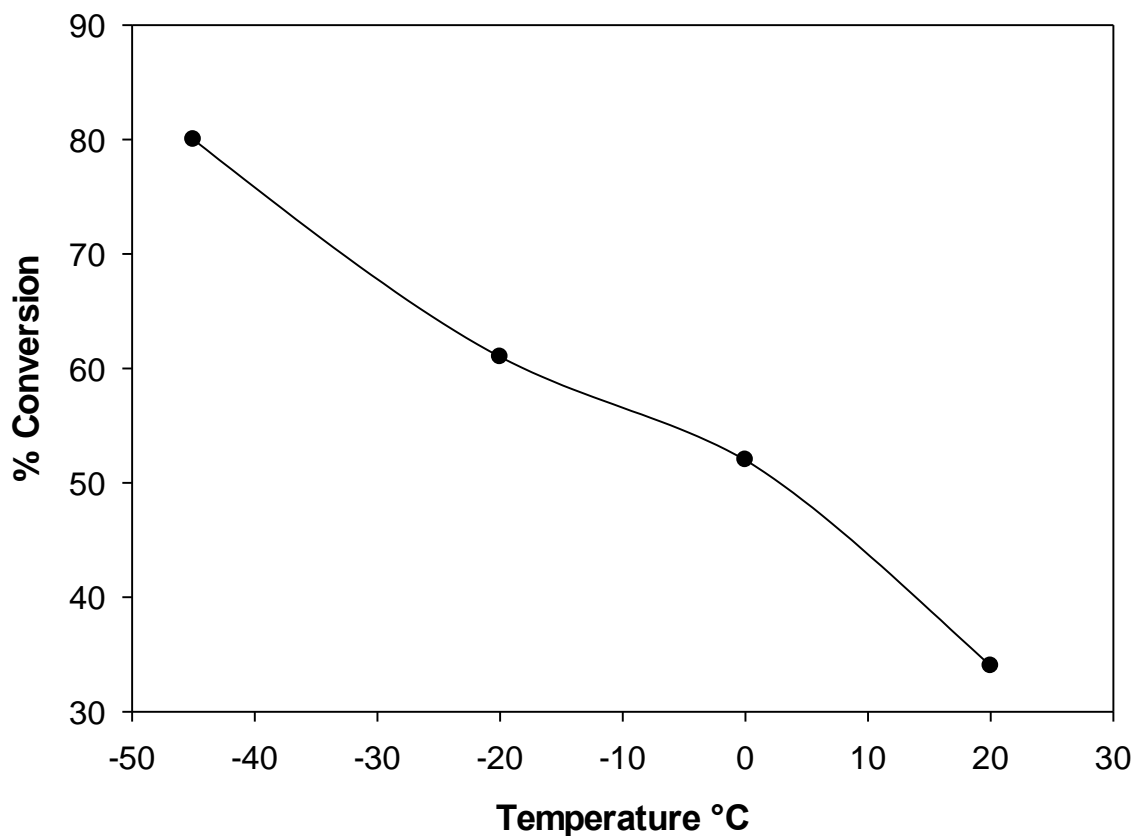


**Figure 29:** Effect of temperature on conversion of **27** 0.45 M of *n*-butyllithium, 0.5 M of compound **53**, 0.35 M of compound **27**

The study performed for a temperature range of -45 °C to 20 °C, at -45 °C the conversion is 80% and it decreased with increasing temperature because of the instability of In batch chemistry, the generation of the carbanion occurred at -55 °C and at higher temperatures there is no progress in the reaction but in the case of semi continuous flow protocol the reaction proceeded even at higher temperature and comparatively more conversion attained because of equal distribution of temperature throughout the reactor.

### 2B.3.3. Effect of concentration of cyclopropyl acetylene **53** on conversion of **27**

In order to get fine reaction conditions, the investigation was continued by focusing on the concentration of reaction reagents, in this the first attempt made to study the effect of cyclopropyl acetylene **53** concentration on conversion of **27**.

Before this study the concentration of compound **53** was 0.45 M. At this concentration we attained 85% conversion for a residence time of 4.8 min, after we focused to vary the concentration of compound **53** to see how it effect the rate of conversion by keeping the other reagents concentration at 0.45 M of *n*-butyllithium, 0.35 M of compound **27**. The temperature of the reaction was maintained constant at -45 °C.

The effect of concentration of cyclopropyl acetylene **53** on conversion is represented in the graph below (Figure 30). As the concentration increases, conversion of **27** is increased to a certain level after further increase shows no difference in conversion observed.

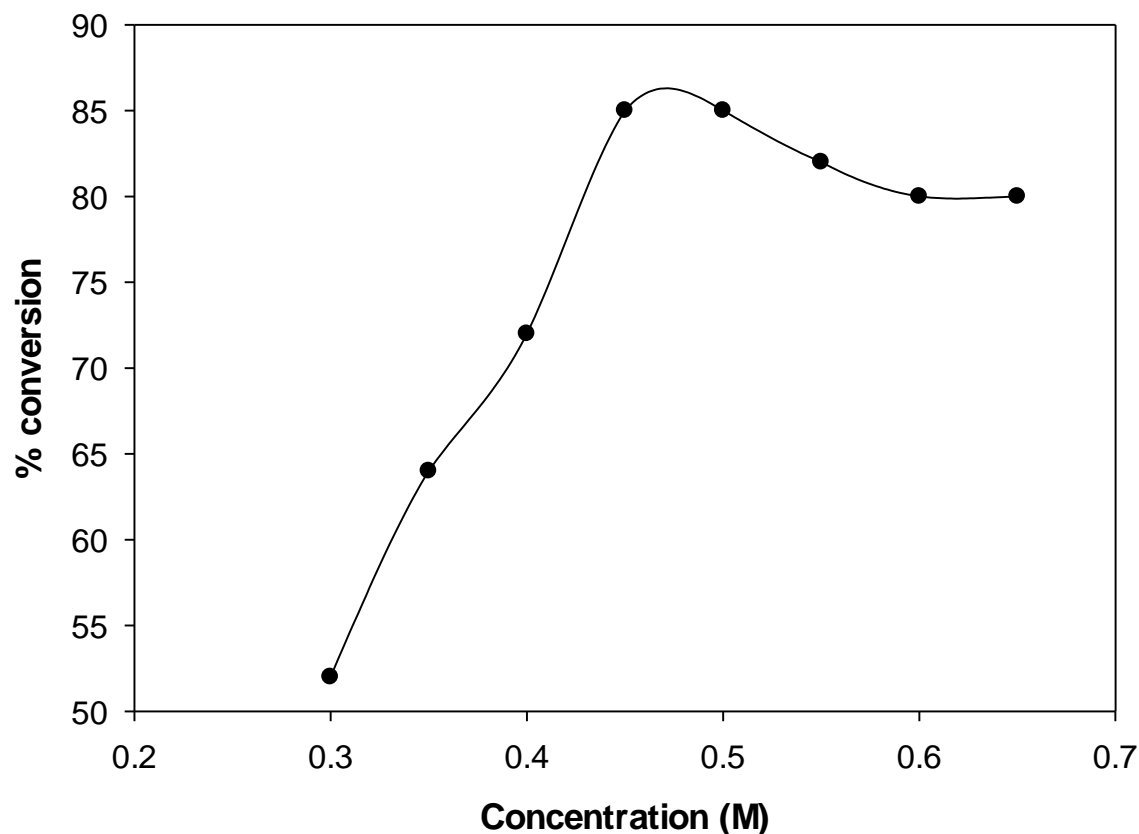


**Figure 30:** Effect of concentration of **53** on conversion of **56** at a concentration of 0.45 M of *n*-butyllithium, 0.35 M of compound **27**.

We started this study at a concentration of 0.3 M of cyclopropyl acetylene **53** at this the conversion is 52%, at 0.35 M concentration of cyclopropyl acetylene **53** the conversion increased by 12% and this pattern continued to a concentration of 0.45 M to 21%. After 0.45 M further increase in concentration of cyclopropyl acetylene **53** to significantly no effect on conversion.

#### **2B.3.4. Effect of concentration of *n*-butyllithium on conversion of **27****

As a second attempt in the investigation of concentration of the reagents towards the conversion of **27**, we choose to change the concentration of *n*-butyllithium. Before this

study, the concentration of *n*-butyllithium was maintained at 0.45 M. We focused to decrease the concentration of *n*-butyllithium, by considering the readily reactive nature with air and moisture, flammability of the *n*-butyllithium. The concentration of cyclopropyl acetylene was 0.45 M, compound **27** at 0.35 M and temperature -45 °C was maintained throughout the reaction.

As the concentration of *n*-butyllithium increases from 0.27M to 0.45M, conversion of **27** increased, which represented below in graphical form (Figure 31).

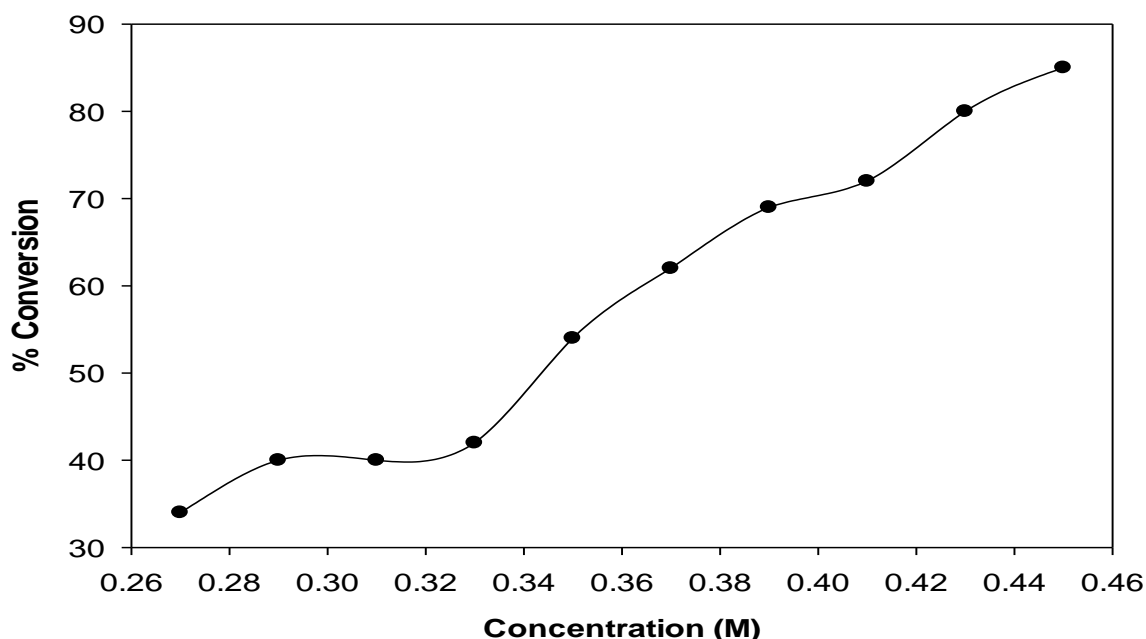


**Figure 31:** Effect of *n*-butyllithium concentration on conversion of **27** at a concentration of 0.45 M of compound **53**, 0.35 M of compound **27**.

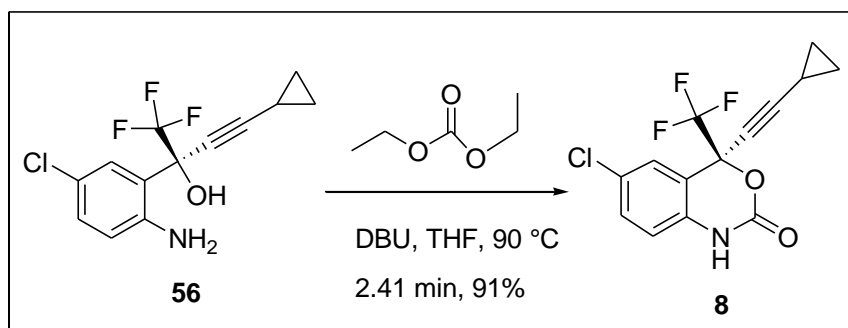
We started the study at 0.45 M of *n*-butyllithium at this point the conversion is 85% and at 0.43 M *n*-butyllithium the conversion is decreased by 2% and it's continued throughout the study as the decrease in concentration the conversion is decreased. This



concentration investigated for a range of 0.45 M to 0.27 M and the conversion led to decrease from 85% to 34%. Because *n*-butyllithium used in this reaction for the generation of the anion, which is a crucial step in this reaction so as the decrease of concentration of *n*- butyllithium, decreased the generation of anion and decreased the conversion of **27**.

#### 2B.4. Step-4

After attaining a well-developed flow method for the alkylation reaction (step 3) we moved onto the final step of the synthesis *i.e.* cyclisation reaction, to afford the desired product of our research programme



**Scheme 37:** Preparation of 6-chloro-2-(4-cyclopropylethynyl)-4-(trifluoromethyl)-1*H*-benzo[*d*][1,3] oxazin-2-(4*H*)-one **8**

The cyclisation reaction (Scheme 37) in flow was done as shown in Figure 32 below. Firstly this reaction was established in batch chemistry and then the same reactions conditions were applied for preliminary flow reaction, however under these conditions there is a clear possibility of reaction and the results can be easily compared with the batch study.

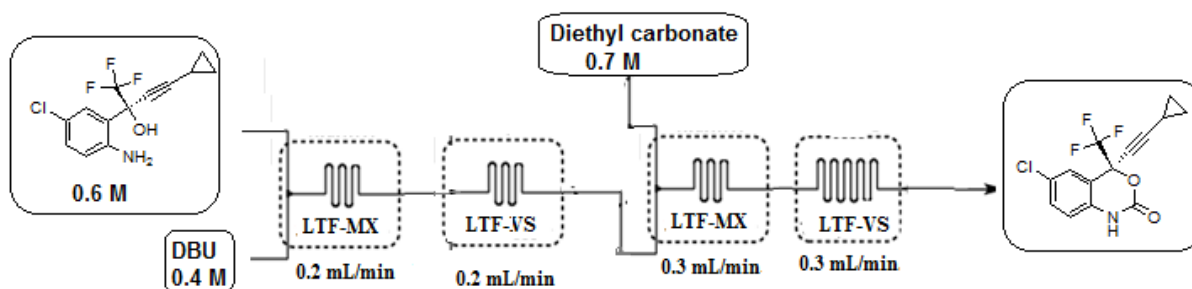


**Figure 32:** Schematic diagram for step-4 preliminary flow reaction

After preliminary conformation of the cyclization reaction in flow, we further investigated for the effect of residence time, temperature and concentration on the conversion of **56**.

#### 2B.4.1. Effect of residence time on conversion of **56**

Residence time investigation on conversion of **56** chosen as a first attempt in cyclisation reaction where the reagent concentrations was maintained at 0.60 M of compound **56**, 0.40 M of 1,8-diazabicyclo[5.4.0]undec-7-ene (DBU), 0.70 M of diethyl carbonate (DEC) and temperature was maintained at 90 °C. These concentrations were taken from the preliminary flow reaction.

As the residence time decreases the conversion of **56** decreased because of shorter residence time which led to insufficient contact of the reactants in a microreactor. This is explained by equation 1 below where it is shown that the residence time is inversely proportion to the flow rate.

Effect of residence time on the conversion of **56** represented below in Figure 33 by graphical form. Maximum conversion observed at a residence time of 17.3 min and it sustained until the residence time of 2.8 min (92%)

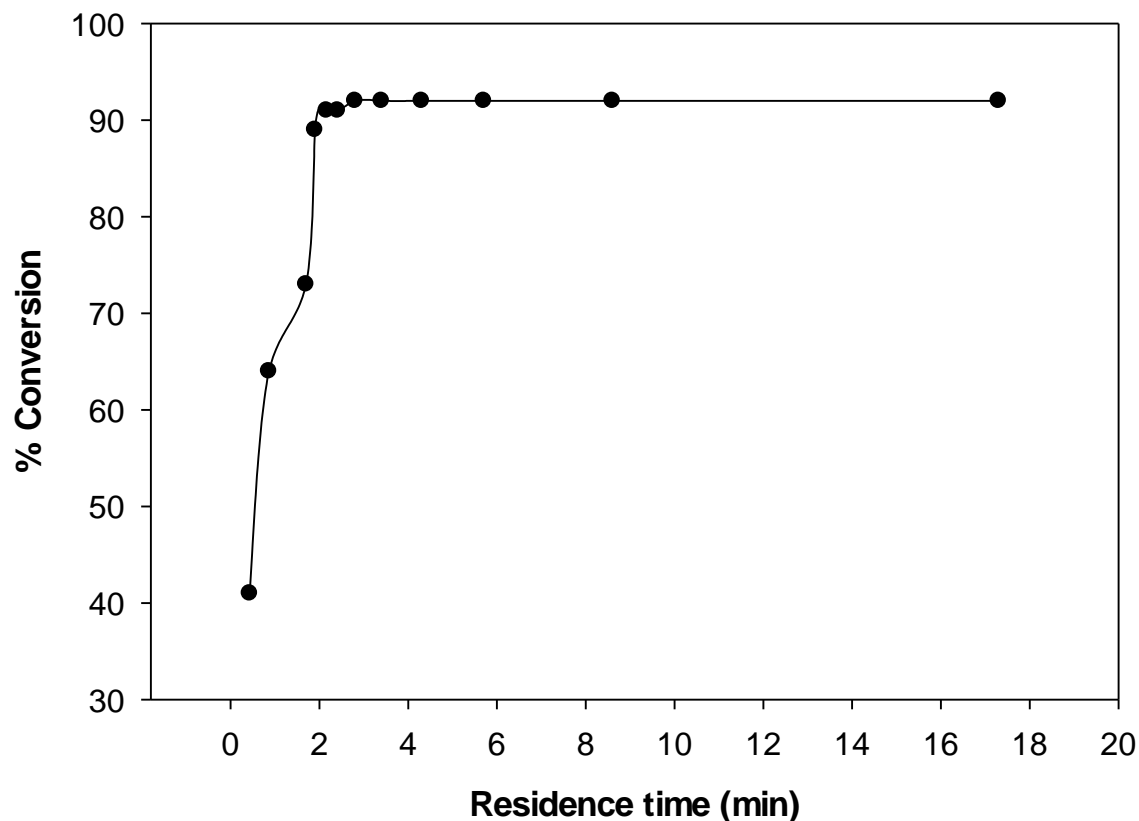


**Figure 33:** Effect of residence time on conversion of **56** at a concentrations of 0.60 M of **56**, 0.40 M of DBU, 0.70 M of DEC and temperature 90 °C.

This study was started at a residence time of 17.3 min and the conversion is 92%. The same conversion was continued until the residence time of 2.8 min. After this, the conversion started to decrease with decreasing residence time. From 2.41 min to 1.7 min the conversion decreased by the difference of 19% and it continued until the end of the study. The residence times were investigated at a range of 17.3 min to 0.43 min and the conversion led to decrease 92% to 41%.

#### 2B.4.2. Effect of temperature on conversion **56**

To achieve the optimized conditions for the reaction reagents, the other parameter temperature was investigated after residence time. Before this study the temperature was maintained at 90 °C. In this study we investigated the effect of temperature when increased and decreased from 90 °C on conversion of **56**. For this study the concentrations was maintained at 0.60 M of **56**, 0.40 M of DBU, 0.70 M of DEC with a residence time of 2.41 min. The findings of the study showed in graphical form below (Figure 34).As the temperature increases, conversion of **56** increased.

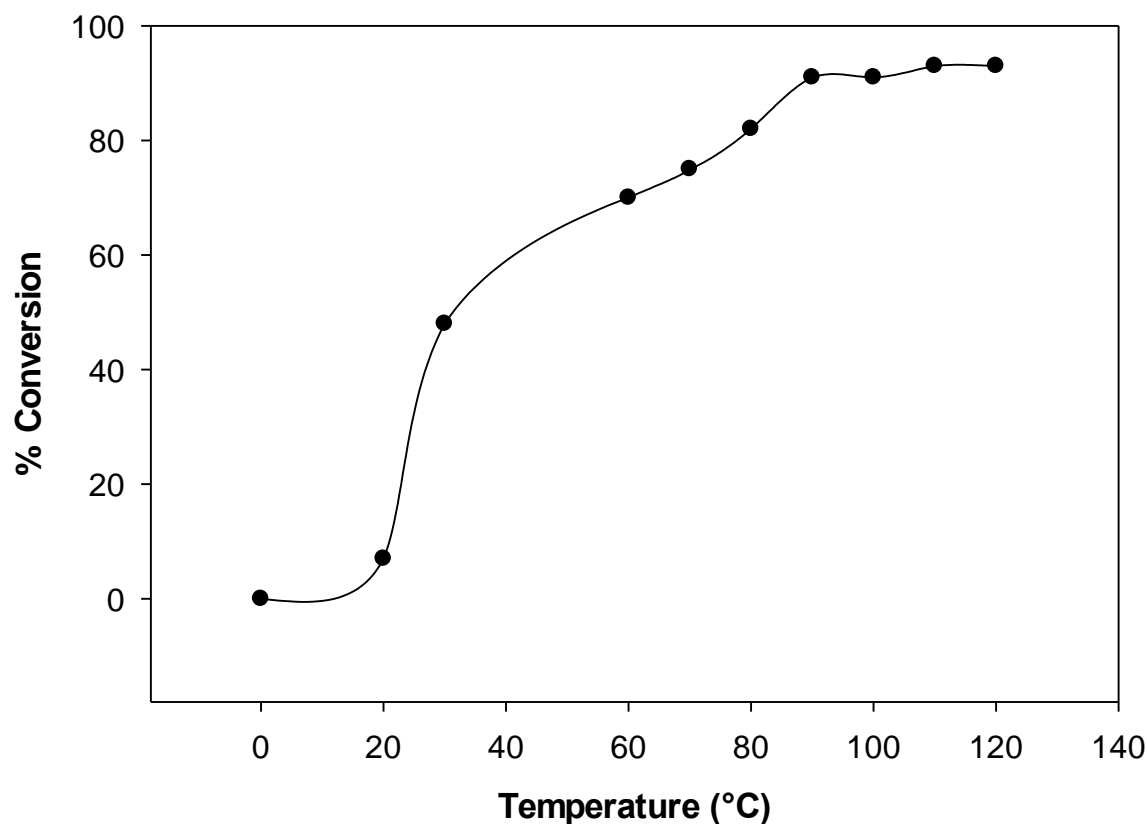


**Figure 34:** Effect of temperature on % conversion of **56** at a concentration of 0.60 M of compound **56**, 0.40 M of DBU, 0.70 M of DEC.

The study started at a temperature of 0 °C at this point the reaction did not proceed, the reaction started to work at 20 °C with 7% conversion and after that, the conversion increased to 48% and it continued until the end of the study. The investigation of temperature was done in a range of 0 °C to 120 °C and the conversion increased from 0 % to 93%.

#### **2.B.4.3. Effect of concentration of diethyl carbonate on conversion of 56**

As a final attempt towards the optimization of compound **8**, the last reaction reagent parameter *i.e.* concentration of DEC was investigated. Before this investigation the concentration was 0.70 M, during this study the concentrations investigated for a range of 0.40 M to 1 M. For this study the concentration of other reagents *i.e.* 0.60 M of compound **56**, 0.40 M of DBU kept constant and the temperature was maintained at 90 °C. The findings from the study described in graphical form below (Figure 35)

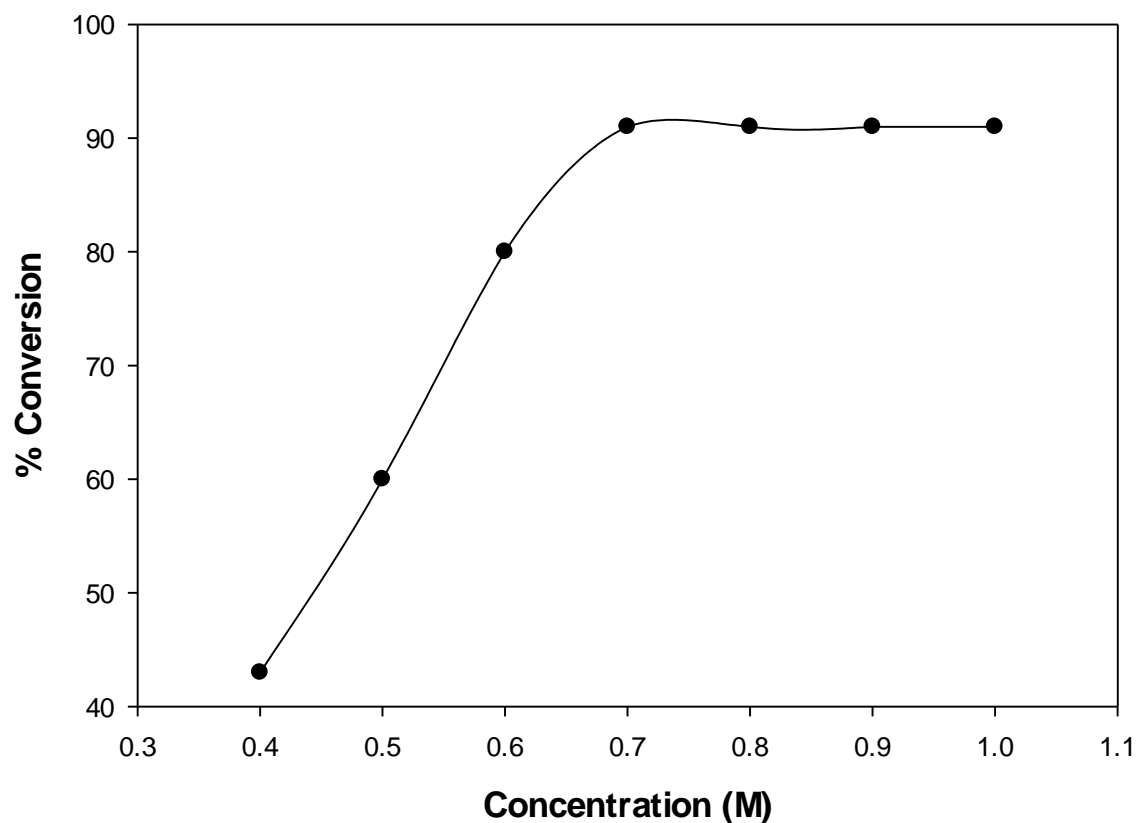
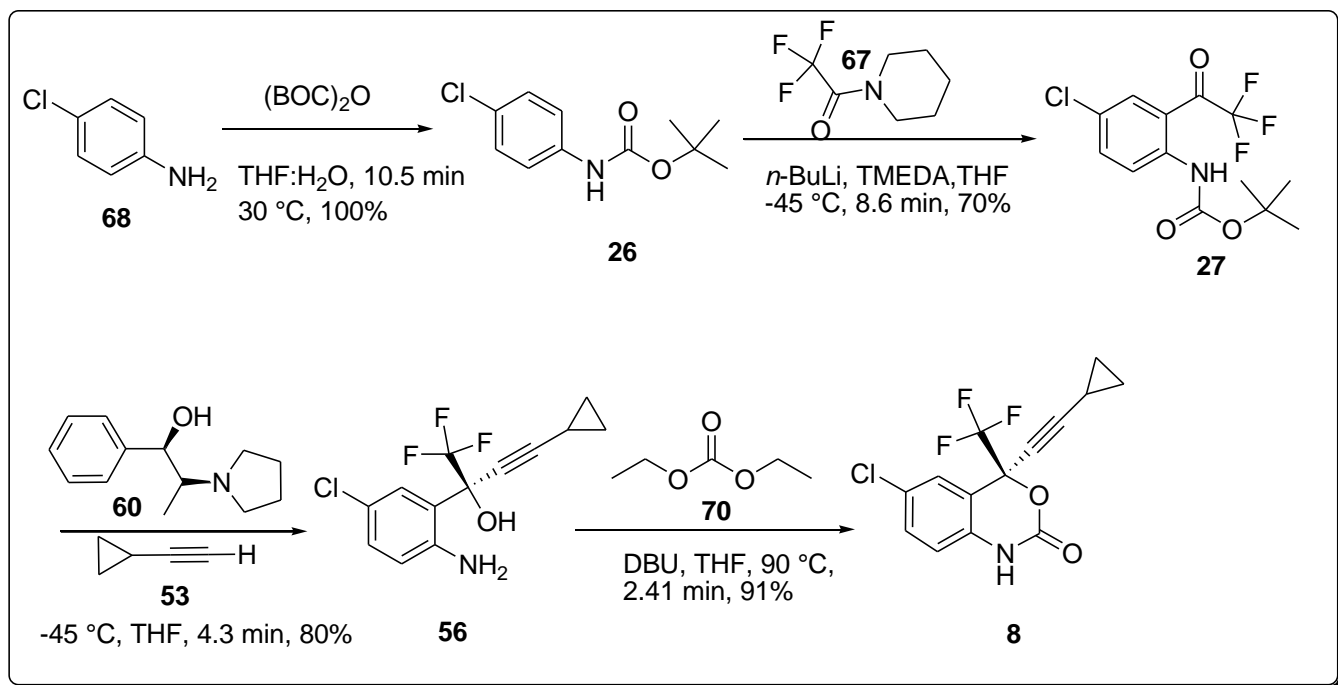


**Figure 35:** Effect of concentration of **70** on conversion of **56**

This reaction in traditional batch chemistry performed at a concentration of 0.70 M of compound **70**, the same concentration was used in flow protocol for preliminary confirmation. In the study of optimization the concentration of compound **70** investigated in a range of 1 M – 0.40 M, from 0.70 M to 1 M the conversion of compound **56** remain unchanged but when the concentration of **70** changed from 0.70 M to 0.40 M the conversion is drastically decreased as shown in above graph from 91% to 43%.

## 2B.5. Conclusion of flow study

The results from the flow study summarized below in Scheme 38. As a result of optimization of reaction reagents for every step, most of the yields were improved over the batch studies.



**Scheme 38:** Synthesis of efavirenz **8** in flow chemistry

# CHAPTER 3

## SYNTHESIS OF EFAVIRENZ- TRADITIONAL BATCH CHEMISTRY EXPERIMENTAL PROCEDURES



### 3. General experimental section

All the reagents (analytical grade) were purchased from Sigma Aldrich and were used without purification. Air and moisture sensitive reactions were carried out under an atmosphere of nitrogen in oven-dried glassware (reagent flasks) that was allowed to cool to room temperature under high vacuum. Tetrahydrofuran (THF) was dried by the published procedure,<sup>[146]</sup> stored over activated 4Å° molecular sieves and subjected to Karl-Fisher analysis. All the solvents used were anhydrous and the solvents removed by rotary evaporator. Brine solution refers to saturated sodium chloride solution. (1*R*,2*S*)-*N*-Pyrrolidinylnorephedrine,<sup>[147]</sup> cyclopropyl acetylene and<sup>[148]</sup> piperidine trifluoroacetic acid,<sup>[149]</sup> were prepared as shown in the literature. Reactions were monitored by thin-layer chromatography (TLC) and gas chromatography (GC).

TLC carried out on 0.25 mm E. Merck silica gel plates (60F-254) using UV light as a visualizing agent, and either ninhydrin, cerium sulfate, cerium ammonium molybdate or potassium permanganate staining solutions and heat as developing agents.

GC was carried out on Agilent 7820A instrument using a DB<sub>5</sub> column equipped with a flame ionization detector and ultra-high purity nitrogen carrier gas at a flow rate of 2.8mL/min. Oven temperature was maintained at 100 °C for 3 min and then ramped to 324 °C (hold time 5 min) at 35 °C/min with a total run time of 16.4 min.

Chiral HPLC was carried out using an Agilent 1220 Infinity LC instrument using Cyclobond I 2000 column equipped with diode array detector, flow rate 1 mL/min, mobile phase: methanol/DI water; 80:20, DAD, which gave optimum detection at 252 nm with a total runtime of 30 min

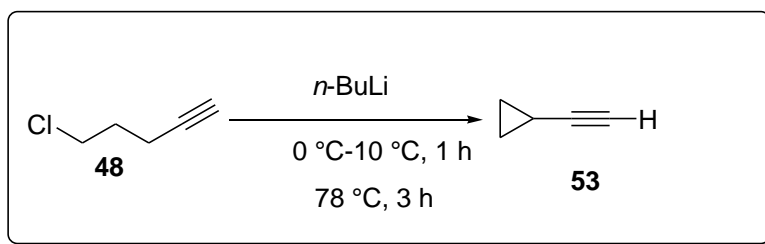
Nuclear magnetic resonance (NMR) spectra were recorded using Bruker spectrometer (Bruker Ultrashield™ 400 plus) which was operated at 400 MHz for proton and 100 MHz for carbon. Spectra were calibrated using the residual  $^1\text{H}$  chemical shift in  $\text{CDCl}_3$  (7.26ppm) or  $\text{DMSO } d_6$  (2.62ppm) which was used as the internal reference standards for  $^1\text{H}$  NMR and  $^{13}\text{C}$  NMR Spectroscopy. The chemical shift values for all spectra are given in parts per million (ppm). The following abbreviations were used to explain NMR data, s = singlet, d = doublet, t = triplet, q = quartet, m = multiplet.

The FTIR characteristic peaks were recorded on a Bruker Platinum Tensor 27 spectrophotometer with an ATR fitting. The analyses of samples were recorded in the range  $4000\text{--}400\text{ cm}^{-1}$  and the peaks are reported in wavenumbers ( $\text{cm}^{-1}$ ). The solid and liquid samples were analyzed without any modification.

Elemental analysis was performed using a CHNS analyzer (Rhodes University, chemistry department, Grahamstown) and the data reported in percentages.

### 3.1. Experimental procedures

#### 3.1.1. Preparation of 4-cyclopropylactylide **53**

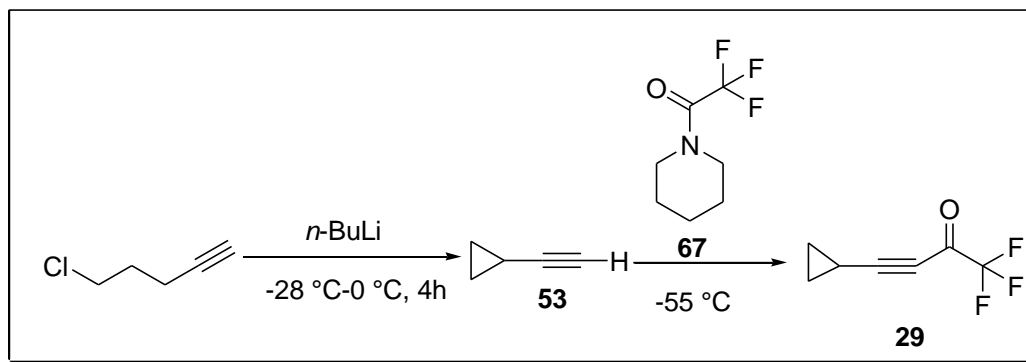


**Scheme 39:** Preparation of 4-cyclopropylactylide **53**<sup>[110]</sup>

A three-necked round-bottomed flask was equipped with a pressure-equalizing addition funnel and a reflux condenser that is fitted with a nitrogen inlet. The flask was charged with 5-chloro-1-pentyne (5 g, 49.01 mmol) and cyclohexane (50 mL), and the mixture cooled to -20 °C. To this reaction mixture, *n*-butyllithium (49 mL, 2.5 M in cyclohexane, 122.5 mmol) was added dropwise *via* the addition funnel over 1 hour maintaining the temperature at -20 °C. After the addition was completed the reaction mixture turned into a thick precipitate at this time the reaction mixture was heated to reflux (78 °C) and maintained at reflux for 3 hours. The completion of the reaction was monitored by TLC (20% ethyl acetate in hexane) and GC. After completion, the reaction was cooled to 0 °C to -10 °C and then quenched carefully by the dropwise addition of aqueous saturated ammonium chloride (35 mL). The aqueous layer was separated and the organic layer is fractionally distilled. The boiling range of 35-78 °C was collected. Which consists of 60-80% of cyclopropyl acetylene **53** (1.4 g, 50%); this fraction was distilled a second time and the boiling range of 52 -55 °C collected (Scheme 39). After the distillation, the obtained pure product was analyzed by NMR and IR spectroscopy, the resulting spectra correlating with reported standard compound spectra.

<sup>1</sup>H-NMR-(400MHz) in CDCl<sub>3</sub>: δ 0.69-0.80 (m, 4H); 1.21-1.27 (m, 1H); 1.76 (s, 1H). <sup>13</sup>C-NMR in CDCl<sub>3</sub> (100 MHz): 2.1, 4.0, 11.0, 70.2, 87.4. IR (cm<sup>-1</sup>) 1157, 2120, 2873, 3302, 3374.

### 3.1.2. Preparation of 4-cyclopropyl-1,1,1-trifluoro-but-3-yn-2-one **29**

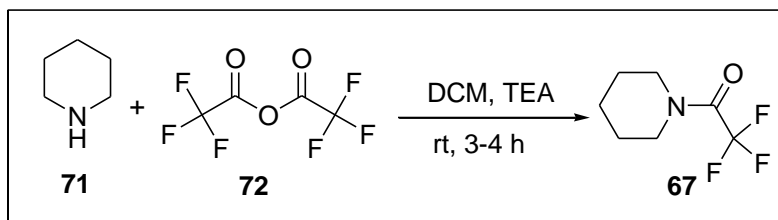


**Scheme 40:** Preparation of 4-cyclopropyl-1,1,1-trifluoro-but-3-yn-2-one **29**<sup>[92]</sup>

*n*-Butyllithium (49 mL, 2.5 M in cyclohexane) was slowly added *via* an addition funnel to 250 mL two-neck round-bottomed flask which was charged with 5-chloro-1-pentyne (5 g, 49.01 mmol) in THF (50 mL) at -28 °C, then the reaction mixture temperature was kept below 0 °C and stirred for 4 hours. After that the reaction mixture was cooled to -55 °C and piperidine trifluoroacetic acid (8.12 mL, 53.91 mmol) was added slowly. After 1 hour at same temperature, the reaction mixture was quenched with 2N HCl and the organic and aqueous layers were separated. After evaporation of the organic layer using a rotary evaporator the residue was washed with water (100 mL) and brine solution (100 mL) and extracted with ethyl acetate (3x100 mL). The combined organic layers were dried over anhydrous Na<sub>2</sub>SO<sub>4</sub> and the crude product was distilled *in vacuo*. After distillation, the product was obtained as a pale yellow oil **29** (2.76 g, 40%) (Scheme 40). This resulting compound was further subjected to analytical techniques (NMR and IR) that matched with the reported product.<sup>[92]</sup>

<sup>1</sup>H-NMR-(400MHz) in CDCl<sub>3</sub>: δ 1.20-1.25 (m, 4H); 1.55 (m, 1H). <sup>13</sup>C-NMR in CDCl<sub>3</sub> (100 MHz): 11.1, 68.2, 72.5, 114.3, 166.3. IR (cm<sup>-1</sup>) 2209, 1705, 1217, 1163, 1066, 920.

### 3.1.3. Preparation of *N*-piperidine trifluoroacetic acid **67**

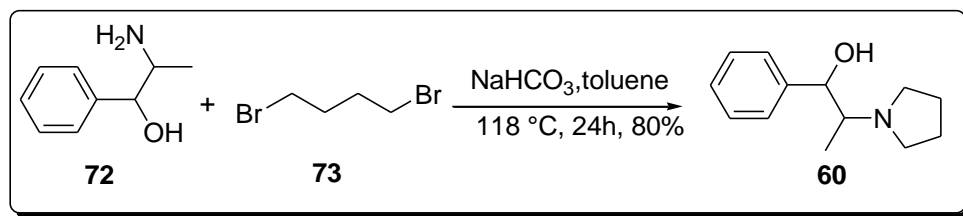


**Scheme 41:** Preparation of *N*-piperidine trifluoroacetic acid **67**

Piperidine (5.8 mL, 58.8 mmol) was added to a 250 mL two neck round-bottomed flask which is previously charged with a mixture of dichloromethane (45 mL) and triethylamine (12.2 mL, 88.2 mmol). To this mixture trifluoroacetic anhydride (11.5 mL, 81.8 mmol) was added, the resulting reaction mixture was stirred at room temperature for 3-4 hour and the completion of reaction was monitored by TLC (20% ethyl acetate in hexane) and GC. After completion of the reaction, the reaction mixture extracted with water, sodium bicarbonate and dil HCl. The organic layer separated and was dried *in vacuo*. The resulting pale yellow liquid **67** (8.5 g, 79.8%) (Scheme 41) subjected to NMR & IR spectroscopy.

$^1\text{H-NMR}$ -(400MHz) in  $\text{CDCl}_3$ :  $\delta$  1.57-1.63 (m, 6H); 3.47-3.54 (m, 4H).  $^{13}\text{C-NMR}$  in  $\text{CDCl}_3$  (100 MHz):  $\delta$  4.5, 26.7, 28.0, 44.5, 130.9, 132.1. IR ( $\text{cm}^{-1}$ ) 1184, 1286, 1465, 1682, 2863.

### 3.1.4. Preparation of (1*R*,2*S*)-*N*-pyrrolidinylnorephedrine **60**



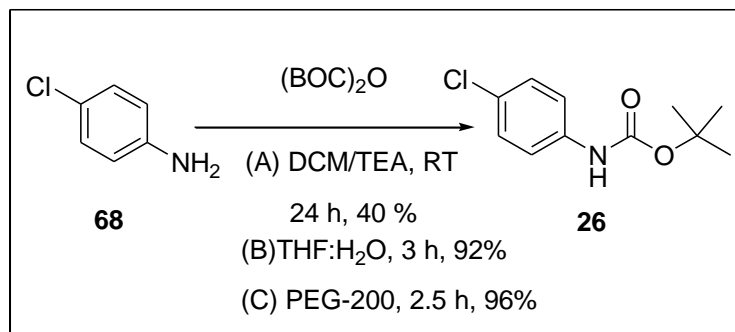
**Scheme 42:** Preparation of (1*R*,2*S*)-*N*-pyrrolidinylnorephedrine **60**<sup>[80,81]</sup>

A round-bottomed flask equipped with a mechanical stirrer, condenser with Dean-Stark trap and with a nitrogen inlet, was charged with toluene (20 mL), (1*R*,2*S*) norephedrine (5 g, 33 mmol), 1,4-dibromobutane (4.2 mL, 36.2 mmol) and Na<sub>2</sub>CO<sub>3</sub> (5.6 g, 68 mmol). The stirred heterogeneous reaction mixture was heated to reflux under a nitrogen atmosphere. Completion of reaction monitored by TLC and GC. After completion of the reaction the reaction mixture was cooled to ambient temperature, filtered through a sintered glass funnel to remove inorganic salts, and the cake was washed with toluene (3x10 mL). The combined filtrate washed with water (2x25 mL). The organic layer was separated and concentrated under reduced pressure. The toluene solution was cooled to 10-15 °C and hydrochloric acid (HCl) in 2-propanol (0.275 mol) was added slowly. During the acid addition, the product precipitates as its hydrochloride salt (5.4 g, 80%) (Scheme 42). The salt compound analyzed by <sup>1</sup>H-NMR & <sup>13</sup>C-NMR and IR for the structural conformation.

<sup>1</sup>H-NMR-(400MHz) in CDCl<sub>3</sub>: δ 1.14-1.27 (m, 3H); 2.08-2.29 (m, 4H); 3.04 (s, 2H); 3.31 (d, *J* = 6.24, 1H); 3.85 (d, *J* = 2.28, 1H); 4.15 (d, *J* = 4.56, 1H); 5.59 (d, *J* = 9.36, 1H); 7.42-7.20 (m, 5H); 11.85 (d, *J* = 2.28, 1H). <sup>13</sup>C-NMR-(100 MHz) in CDCl<sub>3</sub>: δ 14.5, 28.0,

56.3, 69.7, 72.7, 130.9, 132.1, 133.1. IR-(cm<sup>-1</sup>) 960, 1199, 1356, 1467, 1602, 2838, 2985, 3177.

### 3.1.5. Preparation of *tert*-butyl-4-chloro phenyl carbamate **26**<sup>[92]</sup>



#### Scheme 43: Preparation of *tert*-butyl-4-chloro phenyl carbamate **26**

Preparation of compound **26** was done by using three different methods, as presented below, to improve the reaction yield and reduce the reaction time.

##### 3.1.5.1. Method A

Triethylamine (7 mL, 78.74 mmol) was added to a solution of 4-chloroaniline **68** (5 g, 39.3 mmol) in dichloromethane (50 mL), and to this ZnCl<sub>2</sub> (5.35 g, 39.37 mmol) was added and stirred for 30 min at room temperature. Subsequently di-*tert*-butyl dicarbamate (9.13 mL, 43.3 mmol) was added dropwise to the above reaction mixture and stirred for 24 hours. The completion of the reaction was monitored by TLC (20% ethyl acetate in hexane) and GC. After completion of the reaction, the reaction mixture was poured into ice cold water and the product was precipitated as a lumpy cream-colored solid. Which is further extracted with ethyl acetate (3x50 mL), the combined organic layers were washed with water (25 mL), brine solution (25 mL) and dried over anhydrous Na<sub>2</sub>SO<sub>4</sub>. The

resulting organic layers evaporated by rotary to give product **26** as a white colored solid (3.56 g, 40%) (Scheme 43). This compound was analyzed by NMR, IR spectroscopy and elemental analysis.

<sup>1</sup>H-NMR (400 MHz) in CDCl<sub>3</sub>: δ 1.22 (s, 9H); 7.33 (d, *J* = 8.44, 2H); 7.69 (d, *J* = 8.40, 2H): 9.31 (s, 1H). <sup>13</sup>C-NMR in CDCl<sub>3</sub> (100 MHz): δ 27.6, 40.2, 81.0, 122.1, 127.1, 128.4, 138.8, 177.0. IR (cm<sup>-1</sup>): 1172, 1368, 1475, 1652, 2872, 2910, 3290. Anal.calcd for C<sub>11</sub>H<sub>14</sub>ClNO<sub>2</sub>: C 58.03, H 6.20, N 6.15, Found: C 58.08, H 6.16, N 6.11.

### 3.1.5.2. Method B

4-Chloroaniline **68** (5 g, 39.3 mmol) was added into a 100 mL round bottom flask charged with a 1:1 ratio of THF and water (50 ml) and stirred until the compound dissolved, to this di-*tert*-butyl dicarbamate (9.13 mL, 43.3 mmol) was added dropwise and stirred for 3 hours at room temperature. The completion of the reaction was monitored by TLC (20% ethyl acetate in hexane) and GC. After completion, the reaction mixture extracted with ethyl acetate (3x50 mL), washed with water (50 mL) and brine solution (50 mL). The resulting organic layer dried over anhydrous Na<sub>2</sub>SO<sub>4</sub> and evaporated under reduced pressure to get product as white colored solid (8.1 g, 92%) (Scheme 43) which was analytically compared with Method A results.

### 3.1.5.3. Method C

A mixture of 4-chloroaniline **68** (5 g, 39.3 mmol) and di-*tert*-butyl dicarbamate (9.13 mL, 43.3 mmol) in PEG-200 (5 mL, 7.8 mmol) was stirred at ambient temperature until TLC indicated the total disappearance of the aniline (2.5 hours). After completion, the reaction mixture was poured into ice cold water where the product precipitated as a cream colored

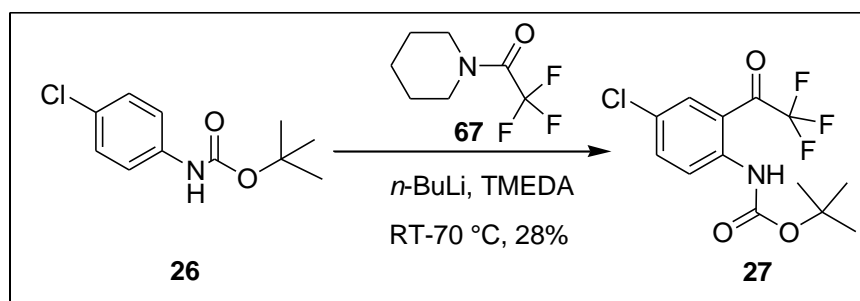


solid. Which was extracted into dry ether (3x25 mL) and the organic layer was dried over anhydrous Na<sub>2</sub>SO<sub>4</sub> and concentrated under reduced pressure to afford the compound **26** (8.54 g, 96%) as a white colored solid. The compound was subjected to analysis by NMR, IR spectroscopy and elemental analysis and compared with the reported product.<sup>[92]</sup>

*Analysis same as above*

### 3.1.6. Preparation of *tert*-butyl-4-chloro-2-(2, 2, 2-trifluoroacetyl) phenyl carbamate

**27**<sup>[92]</sup>



**Scheme 44:** Preparation of *tert*-butyl-4-chloro-2-(2, 2, 2-trifluoroacetyl) phenyl carbamate

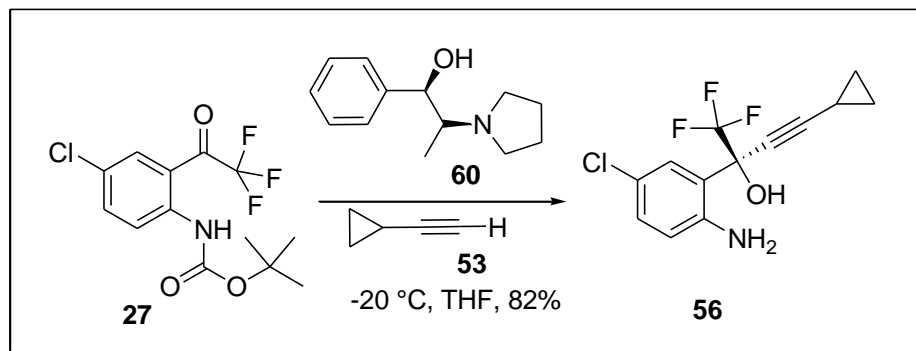
**27**

A 250 mL two neck round bottom flask equipped with mechanical stirrer and nitrogen inlet was charged with compound **26** (5 g, 23.6 mmol), THF (50 mL) and TMEDA (3.9 mL, 25.9 mmol). The resulting mixture stirred at ambient temperature until the total disappearance of solid. After that the temperature of reaction was brought down to -20 °C and then *n*-butyllithium (84.2 mL, 106 mmol) was added dropwise, the addition of *n*-butyllithium is an exothermic reaction so the temperature of the reaction was controlled by the rate of addition. After addition was completed, the reaction mixture was stirred at 0 °C-5 °C for 2 hours, the temperature of resulting mixture was again brought down to -15 °C, at this

temperature piperidine trifluoroacetic acid **67** (10.17 mL, 78.74 mmol) was added at once (addition of piperidine trifluoroacetic acid **67** at once, to avoid the formation of side products because of dimerization). The progress of the reaction was monitored by TLC (20% ethyl acetate in hexane) and GC. After completion of the reaction, the reaction mixture quenched with dropwise addition of previously cooled saturated ammonium chloride (25 mL), the organic layer was separated and washed with water (50 mL), brine solution (50 mL) and dried over anhydrous Na<sub>2</sub>SO<sub>4</sub>. The resulting organic layer evaporated by rotary evaporator to afford compound **27** (1.99 g, 28%); as yellow solid (Scheme 44). TLC and GC of the obtained product indicated the presence of 10% starting material. The crude product was purified by flash column chromatography by using 60-120 mesh silica gel. The pure product was eluted with ethyl acetate and hexane (1:9) as the mobile phase. The appropriate fractions were combined and the solvent evaporated *in vacuo* to give the product. The purified compound was confirmed by FT-IR, <sup>1</sup>H-NMR <sup>13</sup>C-NMR spectroscopy and elemental analysis.

<sup>1</sup>H-NMR-(400 MHz) in CDCl<sub>3</sub>: δ 1.38 (s, 9H); 7.67 (d, 1H); 7.93 (s, 1H); 8.91 (d, *J* = 9.24, 1H); 11.16 (brs, 1H). <sup>13</sup>C-NMR in CDCl<sub>3</sub> (100 MHz): δ 27.4, 81.0, 116.7, 122.7, 127.8, 131.0, 137.5, 142.5, 182.5. <sup>19</sup>FNMR in CDCl<sub>3</sub>: δ -69.45. IR (cm<sup>-1</sup>): 1093, 1247, 1411, 1636, 2972, 3374. Anal. calcd for C<sub>13</sub>H<sub>13</sub>ClF<sub>3</sub>NO<sub>3</sub> C, 48.24; H, 4.05; N, 4.33. Found: C, 48.15; H, 4.11; N, 4.36.

### 3.1.7. Preparation of *tert*-butyl-4-chloro-2-(4-cyclo propyl-1,1-trifluoro-2-hydroxy but-3-yn-2-yl) phenyl carbamate **56**



**Scheme 45:** Preparation of *tert*-butyl-4-chloro-2-(4-cyclo propyl-1,1-trifluoro-2-hydroxy but-3-yn-2-yl) phenyl carbamate **56** (Method A)

The *N*-pyrrolidinylnorephedrine **60** (7.3 g, 35.75 mmol) was added in a round bottomed flask (with nitrogen inlet) which is previously charged with dry degassed THF (50 mL). The resulting mixture was cooled to -25 °C. To this mixture, cyclopropyl acetylene **53** (3.55 mL, 35.78 mmol) and *n*-butyllithium (34.75 mL, 69.5 mmol) were added dropwise. After that, the reaction mixture temperature was raised to 0 °C and stirred for 30 min. Again the reaction mixture was cooled to -55 °C, at this temperature compound **27** (5 g, 16.25 mmol) in dry THF (25 mL) under nitrogen was added to the reaction mixture. After addition, the resulting orange colored solution was stirred for 1 hour at the same temperature. The reaction progress was monitored by TLC and GC, after completion the reaction was quenched with dropwise addition of 6N HCl and the final reaction mixture extracted with ethyl acetate (3x50 mL) and dried over anhydrous Na<sub>2</sub>SO<sub>4</sub>. The combined organic layers were evaporated to get the product as yellow color solid **56** (4.62 g, 84%) (Scheme 45). The chiral purity of the product was determined by using HPLC. A chiral

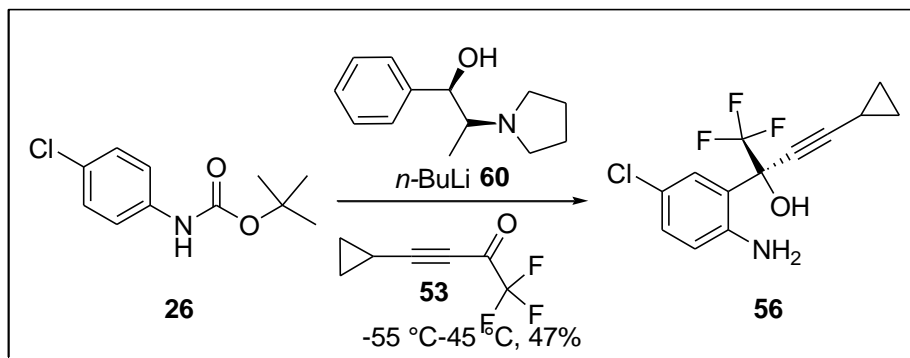
column Cyclobond I 2000 was used as stationary phase and the methanol: water (80:20) as the mobile phase, flow rate 1 mL/min, DAD, which gave optimum detection at 252 nm. The final product was confirmed by FT-IR,  $^1\text{H}$ -NMR and  $^{13}\text{C}$ -NMR and elemental analysis.

$^1\text{H}$ -NMR-(400 MHz) in  $\text{CDCl}_3$ :  $\delta$  0.74 (t,  $J$  = 3.36, 2H); 0.83 (t,  $J$  = 5.96, 2H); 1.21-1.55 (m, 1H) 4.17 (s, 1H); 7.25 (d,  $J$  = 8.92, 1H); 7.61 (s, 1H); 8.30 (d,  $J$  = 8.96, 1H); 9.41 (s, 1H).  $^{13}\text{C}$ -NMR in  $\text{CDCl}_3$  (100 MHz):  $\delta$  0.003, 9.1, 14.1, 27.1, 70.1, 75.2, 94.2, 120.5, 121.3, 125.0, 128.9, 130.9, 177.  $^{19}\text{F}$ NMR in  $\text{CDCl}_3$ :  $\delta$  -79.72 IR ( $\text{cm}^{-1}$ ) 1262, 1360, 1487, 2235, 2794, 3330, 3419. Anal.calcd for  $\text{C}_{13}\text{H}_{11}\text{ClF}_3\text{NO}$ ; C, 53.90; H, 3.83; N, 4.84; Found: C, 53.87; H, 3.89; N, 4.81.

Alternatively the reaction mixture was quenched by using saturated ammonium chloride and extracted with ethyl acetate, the combined organic layers were washed with brine solution and evaporated *in vacuo* to afford compound **51**. The chiral purity of the product was determined by using HPLC. A chiral column Cyclobond I 2000 was used as stationary phase and the methanol: water (80:20) as the mobile phase, flow rate 1 mL/min, DAD, which gave optimum detection at 252 nm. And finally product was confirmed by FT-IR,  $^1\text{H}$ -NMR,  $^{13}\text{C}$ -NMR and elemental analysis.

$^1\text{H}$ -NMR-(400 MHz) in  $\text{CDCl}_3$ :  $\delta$  0.74 (t,  $J$  = 3.36, 2H); 0.83 (t,  $J$  = 5.96, 2H); 1.14 (m, 9H); 1.21-1.55 (m, 1H); 4.17 (s, 1H); 7.25 (d,  $J$  = 8.92, 1H); 7.61 (s, 1H); 8.30 (d,  $J$  = 8.96, 1H); 9.41 (s, 1H).  $^{13}\text{C}$ -NMR in  $\text{CDCl}_3$  (100 MHz):  $\delta$  0.003, 9.2, 14.7, 27.9, 70.5, 77.9, 85.7, 122.6, 124.3, 124.8, 128.8, 130.7, 137.4, 177.5, .  $^{19}\text{F}$ NMR in  $\text{CDCl}_3$ :  $\delta$  -79.72 IR ( $\text{cm}^{-1}$ ) 1262, 1360, 1487, 2235, 2794, 3330, 3419. Anal.calcd for  $\text{C}_{13}\text{H}_{11}\text{ClF}_3\text{NO}$ ; C, 59.76; H, 5.83; N, 4.27; Found: C, 59.77; H, 5.84; N, 4.27.

### 3.1.7. 2. Method B (preparation of **56** by using **53** from **26**)<sup>[103]</sup>



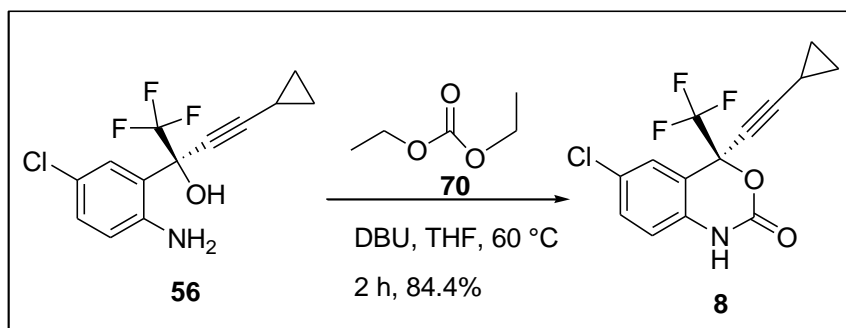
**Scheme 46:** Preparation of *tert*-butyl-4-chloro-2-(4-cyclopropyl-1,1-trifluoro-2-hydroxybut-3-yn-2-yl)phenyl carbamate **56** by using cyclopropylethynyl trifluoromethyl ketone **53**

*N*-Boc-4-Chloroaniline **26** (5 g, 21.27 mmol) was dissolved in THF (50 mL) and the resulting mixture was cooled to -55 °C and at this temperature *n*-butyllithium (42 mL, 106.3 mmol) was added slowly. The mixture was held at the same temperature for 1 hour. A mixture of compound **29** and **60** in dry THF (10 mL) was added to the above reaction and stirred for until completion of the reaction. The reaction progress was monitored by TLC and GC. After completion of the reaction, the reaction mixture quenched with dropwise addition of 6N HCl and the mixture was warmed to ambient temperature and extracted with MTBE. The combined organic layers dried over anhydrous Na<sub>2</sub>SO<sub>4</sub> evaporated *in vacuo*, to afforded compound as yellow color solid **56** (Scheme 46) (1.8 g, 47%). Analytically pure sample obtained by recrystallization with hexane. The chiral purity of the product was determined by using HPLC. A chiral column Cyclobond I 2000 was used as stationary phase and the methanol: water (80:20) as the mobile phase, flow rate

1 mL/min, DAD, which gave optimum detection at 252 nm. Finally the compound structure was confirmed by FT-IR,  $^1\text{H}$ -NMR,  $^{13}\text{C}$ -NMR and elemental analysis.

$^1\text{H}$ -NMR-(400 MHz) in  $\text{CDCl}_3$ :  $\delta$  0.74 (t,  $J$  = 3.36, 2H); 0.83 (t,  $J$  = 5.96, 2H); 1.21-1.55 (m, 1H) 4.17 (s, 1H); 7.25 (d,  $J$  = 8.92, 1H); 7.61 (s, 1H); 8.30 (d,  $J$  = 8.96, 1H); 9.41 (s, 1H).  $^{13}\text{C}$ -NMR in  $\text{CDCl}_3$  (100 MHz):  $\delta$  0.003, 9.1, 14.1, 27.1, 70.1, 75.2, 94.2, 120.5, 121.3, 125.0, 128.9, 130.9, 177.  $^{19}\text{F}$ NMR in  $\text{CDCl}_3$ :  $\delta$  -79.72 IR ( $\text{cm}^{-1}$ ) 1262, 1360, 1487, 2235, 2794, 3330, 3419. Anal. calcd for  $\text{C}_{13}\text{H}_{11}\text{ClF}_3\text{NO}$ ; C, 53.90; H, 3.83; N, 4.84; Found: C, 53.87; H, 3.89; N, 4.81

### 3.1.8. Preparation of 6-chloro-2-(4-cyclopropylethynyl)-4-(trifluoromethyl)-1*H*-benzo[*d*][1,3] oxazin-2-(4*H*)-one **8**



**Scheme 47:** Preparation of 6-chloro-2-(4-cyclopropylethynyl)-4-(trifluoromethyl)-1*H*-benzo[*d*][1,3] oxazin-2-(4*H*)-one **8**.

((*S*)-Amino alcohol **56** (5 g, 17.3 mmol) was added to a round bottomed flask which was previously charged with the THF (50 mL), to this DBU (5.67 mL, 11.42 mmol) was added at room temperature. To this above stirred mixture diethyl carbonate **70** (7.5 mL, 19.38 mmol) was added and the mixture was further stirred at 60 °C for 2 hours. The completion of the reaction was monitored by TLC and GC. After completion, the reaction mixture was

evaporated with rotary evaporator, diluted with water and extracted with ethyl acetate (3x50 mL). The combined organic layers were successively washed with aqueous hydrochloric acid, demineralized water and dried over anhydrous  $\text{Na}_2\text{SO}_4$ , concentrated in vacuo and purified on silica gel (60-120 mesh) column chromatography, the compound eluted with ethyl acetate and hexane (10:90) as mobile phase. Solvent evaporated to get the compound as white colored solid (5.8 g, 84.4%) (Scheme 47). The chiral purity of the product was determined by using HPLC. A chiral column Cyclobond I 2000 was used as stationary phase and the methanol: water (80:20) as the mobile phase, flow rate 1 mL/min, DAD, which gave optimum detection at 310 nm. Finally the structure of the compound was confirmed by FT-IR,  $^1\text{H}$ -NMR,  $^{13}\text{C}$ -NMR and elemental analysis.

$^1\text{H}$ -NMR-(400 MHz) in  $\text{CDCl}_3$ :  $\delta$  0.85-0.96 (m, 4H); 1.38-1.45 (m, 1H); 6.85 (d,  $J$  = 8.52, 1H); 7.39 (dd,  $J$  = 8.52, 2.2 1H); 7.5 (s, 1H); 9.1 (s, 1H).  $^{13}\text{C}$ -NMR in  $\text{CDCl}_3$  (100 MHz):  $\delta$  0.003, 9.4, 66.7, 77.9, 96.5, 116.8, 121.3, 124.1, 128.4, 133.8, 149.5,  $^{19}\text{F}$ NMR in  $\text{CDCl}_3$ :  $\delta$  -80.9. IR ( $\text{cm}^{-1}$ ) 1165, 1261, 1315, 1428, 1742, 2249, 3311. Anal.calcd for  $\text{C}_{14}\text{H}_9\text{ClF}_3\text{NO}_2$ ; C, 53.27; H, 2.87; N, 4.44; Found C, 53.21; H, 2.89; N, 4.49.

# CHAPTER 4

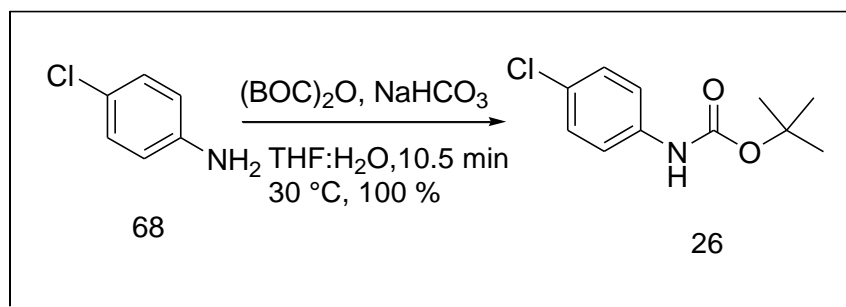
## FLOW CHEMISTRY EXPERIMENTAL PROCEDURES



## 4.1. Flow experimental procedures

### 4.1.1. Preparation of *tert*-butyl-4-chloro phenyl carbamate **26**

Preparation of *tert*-butyl-4-chloro phenyl carbamate **26** (Scheme 48) in flow was done by using microreactor setup shown in Figure 32. This microreactor setup was constructed by using Chemyx Fusion syringe pumps, 5 mL SGE glass syringes, and LTF reactor plates. Chemyx Fusion syringe pumps connected to four LTF microreactor plates *via* PTFE tubing, two of them are LTF-MX reactor plate which used for mixing the two reagents, another two are LTF-V reactor used for increasing the residence time.



**Scheme 48:** Preparation of *tert*-butyl-4-chloro phenyl carbamate **26**

#### Preparation of stock solutions:

**Stock solution A** was prepared by dissolving 4-chloroaniline **68** (5 g, 39.3 mmol) in THF (50 mL).

**Stock solution B** was prepared by dissolving di-*tert*-butyl dicarbamate (9.13 mL, 43.3 mmol) in THF (50 mL).

**Stock solution C** was prepared by dissolving sodium bicarbonate ((5 g, 78 mmol) in water (50 mL).

The stock solutions A, B and C were pumped into LTF microreactor plates using Chemyx Fusion syringe pumps and three 5 mL SGE glass syringes. These reactor plates were kept at a temperature of 30 °C and the samples collected at the end of the microreactor tubing were analyzed by using offline gas chromatography (GC). After completion, the reaction mixture extracted with ethyl acetate (3x50 mL), washed with water (50 mL) and brine solution (50 mL). The resulting organic layer dried over anhydrous Na<sub>2</sub>SO<sub>4</sub> and evaporated under reduced pressure and finally compound analyzed by FT-IR, <sup>1</sup>H-NMR <sup>13</sup>C-NMR spectroscopy and elemental analysis. Based on the results of GC the reaction further scrutinized towards the optimization by investigating the effect residence time, concentration and temperature on conversion of **68**.

#### 4.1.1.1. Effect of residence time on conversion of **68**

4-Chloroaniline **68** (5 g, 39.3 mmol), di-*tert*-butyl dicarbamate (9.13 mL, 43.3 mmol) were dissolved in anhydrous, degassed tetrahydrofuran to a concentration of 0.78 M each and sodium bicarbonate (5 g, 78 mmol) was dissolved in water to a concentration of 1.1 M. These reagent solutions were fed into microreactor as shown in Figure 33 at various residence times ranging from 0.35 min to 21 min into an LTF–MX reactor using three 5 mL SGE glass syringes, one syringe was filled with 4-chloroaniline **68**, another one with aq. sodium bicarbonate and the last one with di-*tert*-butyl dicarbamate. To increase the residence time of the reaction, a residence plate reactor was added to the set up (LTF–V reactor). A sample was thereafter collected and analyzed by offline GC.

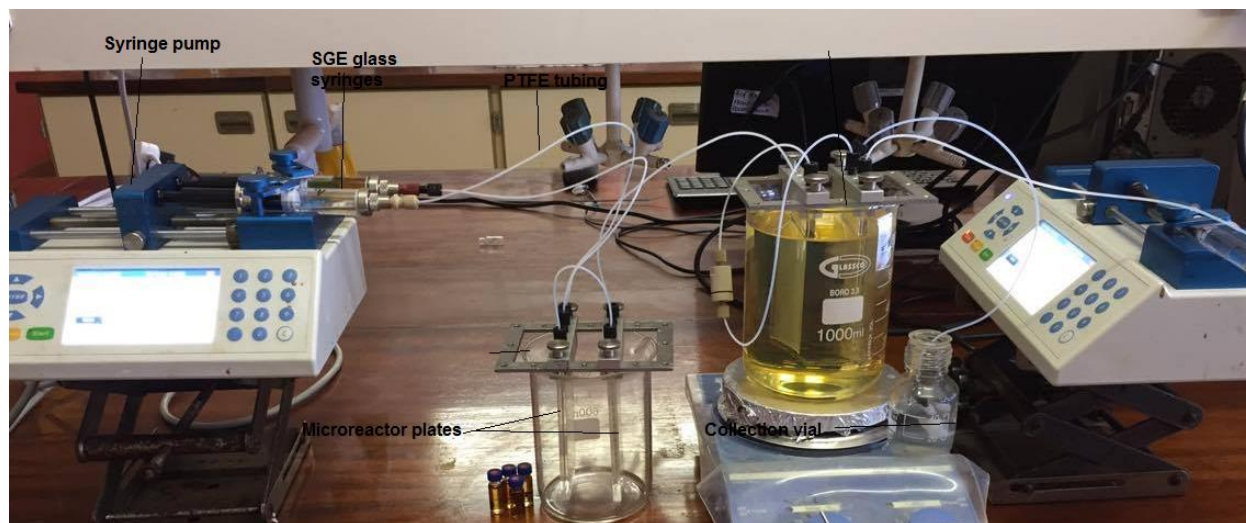


**Figure 36:** Step 1 microreactor set up

After collection of the sample, the reaction mixture washed with brine solution and dried over anhydrous  $\text{Na}_2\text{SO}_4$ . The resulting organic layer was evaporated under vacuum to afford white colored solid as product. Which used in step-2 without any purification and finally characterized by using  $^1\text{H-NMR}$ ,  $^{13}\text{C-NMR}$ , infrared spectroscopy and elemental analysis.

$^1\text{H-NMR}$  (400 MHz) in  $\text{CDCl}_3$ :  $\delta$  1.22 (s, 9H); 7.33 (d,  $J = 8.44$ , 2H); 7.69 (d,  $J = 8.40$ , 2H); 9.31 (s, 1H).  $^{13}\text{C-NMR}$  in  $\text{CDCl}_3$  (100 MHz):  $\delta$  27.6, 40.2, 81.0, 122.1, 127.1, 128.4, 138.8, 177.0. IR ( $\text{cm}^{-1}$ ): 1172, 1368, 1475, 1652, 2872, 2910, 3290. Anal.calcd for  $\text{C}_{11}\text{H}_{14}\text{ClNO}_2$ : C 58.03, H 6.20, N 6.15, Found: C 58.08, H 6.16, N 6.11.

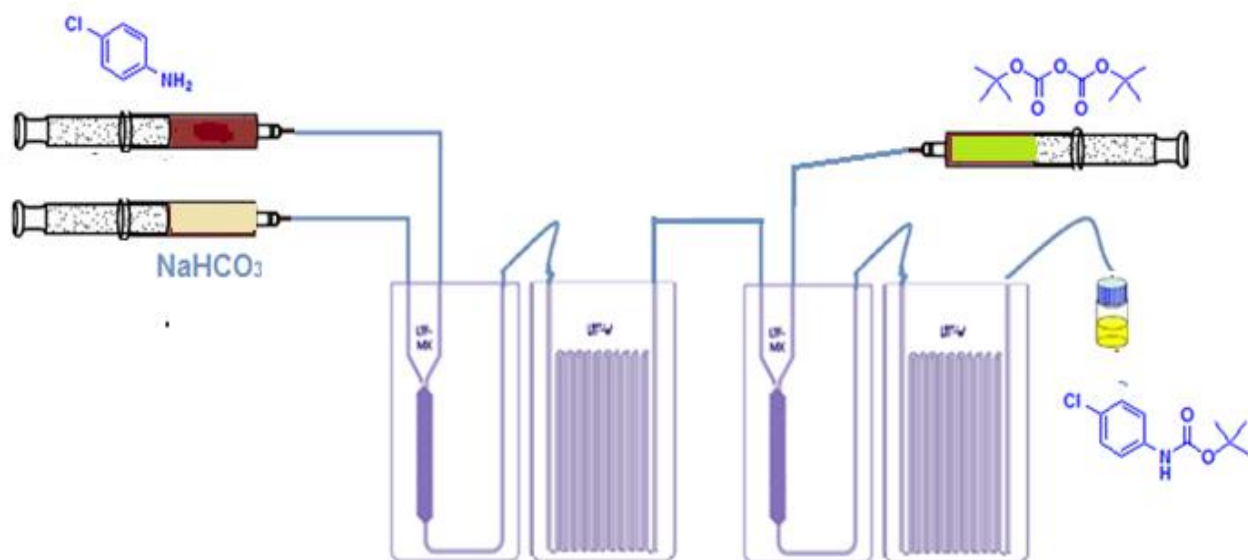


**Figure 37:** Step-1 microreactor set up block diagram

After looking the results of above study we further investigated the reaction by changing the concentration of di-*tert*-butyl dicarbamate as described below

#### 4.1.1.2. Effect of concentration of di-*tert*-butyl dicarbamate on conversion of **68**

4-Chloroaniline **68** (5 g, 39.3 mmol), was dissolved in anhydrous, degassed tetrahydrofuran to a concentration of 0.78 M, sodium bicarbonate was dissolved in water to a concentration of 1.1 M and di-*tert*-butyl dicarbamate (9.13 mL, 43.3 mmol) was also dissolved in anhydrous, degassed tetrahydrofuran to get a concentration ranging from 0.70 M -0.98 M. These reagent solutions were fed into microreactor as shown in Figure 33 at various concentrations ranging from 0.93 M to 0.70 M of di-*tert*-butyl dicarbamate into an LTF–MX reactor using 5 mL SGE glass syringe, at a constant residence time (10.5 min) and temperature. One syringe was filled with 4-chloroaniline **68** another one with aqs sodium bicarbonate, third syringe was with di-*tert*-butyl dicarbamate. To increase the residence time of the reaction, a residence plate reactor was added to the set up (LTF–V

reactor). All the microreactor plates were arranged as shown in Figure 32. A sample was thereafter collected at the end of the microreactor were analyzed by offline GC and the peak areas were used for calculating the % conversion of the product. After collection of the sample, the reaction mixture washed with brine solution and dried over anhydrous  $\text{Na}_2\text{SO}_4$ . The resulting organic layer was evaporated under vacuum to afford white colored solid as product which was directly used in step-2 without any purification and finally characterized by using  $^1\text{H}$ NMR,  $^{13}\text{C}$ NMR, infrared spectroscopy and elemental analysis.

*Analysis same as above.*

As moving forward we looked at the effect temperature on the reaction although in the batch we worked out this reaction at room temperature but we find an interest to see how the temperature of the reaction effect the conversion of **68**.

#### **4.1.1.3. Effect of temperature on conversion of 68**

4-Chloroaniline **68** (5 g, 39.3 mmol), di-*tert*-butyl dicarbamate (9.13 mL, 43.3 mmol) was dissolved in anhydrous, degassed tetrahydrofuran to a concentration of 0.78 M each and sodium bicarbonate was dissolved in water to a concentration of 1.1 M. These reagent solutions were fed into an into microreactor (Figure 32) using three 5 mL SGE glass syringes at various temperatures ranging from room temperature to 60 °C at constant residence time (10.5 min) and concentration, one syringe was filled with 4-chloroaniline **68** another one with aqs sodium bicarbonate and the third syringe was with di-*tert*-butyl dicarbamate. All these syringes connected to microreactor plates as shown in Figure 32, to increase the residence time of the reaction, a residence plate reactor was added to the

set up (LTF–V reactor). A sample was thereafter collected at the end of the microreactor were analyzed by offline GC and the peak areas were used for calculating the % conversion of the product. After collection of the sample, the reaction mixture washed with brine solution and dried over anhydrous Na<sub>2</sub>SO<sub>4</sub>. The resulting organic layer was evaporated under vacuum to afford white colored solid as product which was used in step 2 without any purification and finally characterized by using <sup>1</sup>HNMR, <sup>13</sup>CNMR, infrared spectroscopy and elemental analysis.

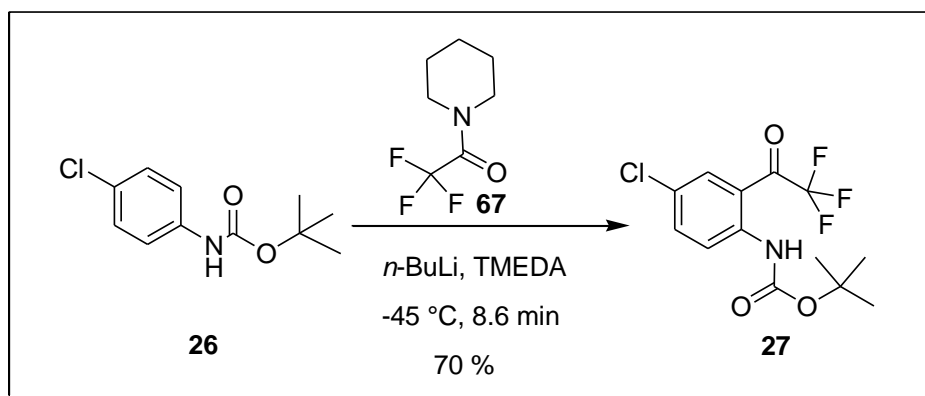
*Analysis same as above.*

After optimizing the conversion of 4-chloroaniline **68** by changing concentration, residence time and temperature of reaction reagents we moved forward to step 2 i.e. preparation and optimization of *tert*-butyl-4-chloro-2-(2,2,2-trifluoroacetyl)phenyl carbamate **27**.

#### **4.1.2. Preparation of *tert*-butyl-4-chloro-2-(2, 2, 2-trifluoroacetyl) phenyl carbamate **27****

Preparation of *tert*-butyl-4-chloro-2-(2, 2, 2-trifluoroacetyl) phenyl carbamate **27** in this thesis also called as trifluoro acetylation reaction. This reaction in flow (Scheme 49) was done by using microreactor setup shown below (Figure 34).The microreactor setup was built using MR-Q pump (Figure 36), Chemyx Fusion syringe pumps (Figure 37), PTFE tubing, LTF reactor plates (Figure 38) and quench columns. Quench columns were made using uniqsis glass column reactor with adjustable end fittings and which is filled with required amount of silica. Four LTF reactor plates (two LTF-MX reactor plate and two LTF-VS reactor plates) were used for this setup. These plates arranged in two beakers

each beaker one mixing plate one residence plate and they marked as beaker 1 and beaker 2 (Figure-34). MR-Q pump is used for pumping *n*-butyllithium, *tert*-butyl-4-chloro phenylcarbamate **26** and piperidine trifluoroacetic acid **67** in THF are pumped by using Chemyx Fusion syringe pumps. Two LTF-MX and two LTF-VS microreactor plates were used (Figure 38).



**Scheme 49:** Preparation of *tert*-butyl-4-chloro-2-(2, 2, 2-trifluoroacetyl) phenyl carbamate **27**

#### Preparation of stock solutions

**Stock solution A** was prepared by dissolving *tert*-butyl-4-chloro phenyl carbamate **26** (5 g, 23.6 mmol) in THF (50 mL).

**Stock solution B** was prepared by diluting 2.5 M of *n*-butyllithium (42.4 mL, 106.2 mmol) in dry degassed HPLC grade hexanes (50 mL).

**Stock solution C** was prepared by dissolving piperidine trifluoroacetic acid **67** (10.17 mL, 78.74 mmol) in THF (50 mL).

The stock solution A pumped into LTF microreactor plates with the help of MR-Q syringe pump, stock solution B also pumped into same reactor plate with the help of Chemyx Fusion syringe pump and SGE glass syringe. In this microreactor plate, *n*-butyllithium reacts with compound **26** and generates dianion (Scheme 49) which enters into LTF V microreactor plate, these two reactor plates kept at -75 °C and these plates are connected to another LTF MX microreactor plate where stock solution C enters into the plate with the help of other Chemyx Fusion syringe pump, the generated dianion in the first plate quenched with stock solution C. These reactor plates kept at a temperature of -45 °C at the end microreactor plate connected to a quench column. Quench column made with silica to bind the piperidine by product. The sample collected at the end of the quench column were analyzed by using offline gas chromatography (GC). After conformation of reaction progress, the reaction mixture quenched with saturated ammonium chloride. The organic layer extracted with ethyl acetate and evaporated in vacuo and the compound analyzed by FT-IR, <sup>1</sup>H-NMR <sup>13</sup>C-NMR spectroscopy and elemental analysis. Based on the results of GC the reaction further scrutinized towards the optimization by investigating the effect residence time, concentration and temperature on conversion of **26**.

<sup>1</sup>H-NMR-(400 MHz) in CDCl<sub>3</sub>: δ 1.38 (s, 9H); 7.67 (d, 1H); 7.93 (s, 1H); 8.91 (d, 1H); 11.16 (brs, 1H). <sup>13</sup>C-NMR in CDCl<sub>3</sub> (100 MHz): δ 27.4, 81.0, 116.7, 122.7, 127.8, 131.0, 137.5, 142.5, 182.5. <sup>19</sup>F-NMR in CDCl<sub>3</sub>: δ -69.45. IR (cm<sup>-1</sup>): 1093, 1247, 1411, 1636, 2972, 3374. Anal. calcd for C<sub>13</sub>H<sub>13</sub>ClF<sub>3</sub>NO<sub>3</sub> C, 48.24; H, 4.05; N, 4.33. Found: C, 48.15; H, 4.11; N, 4.36.



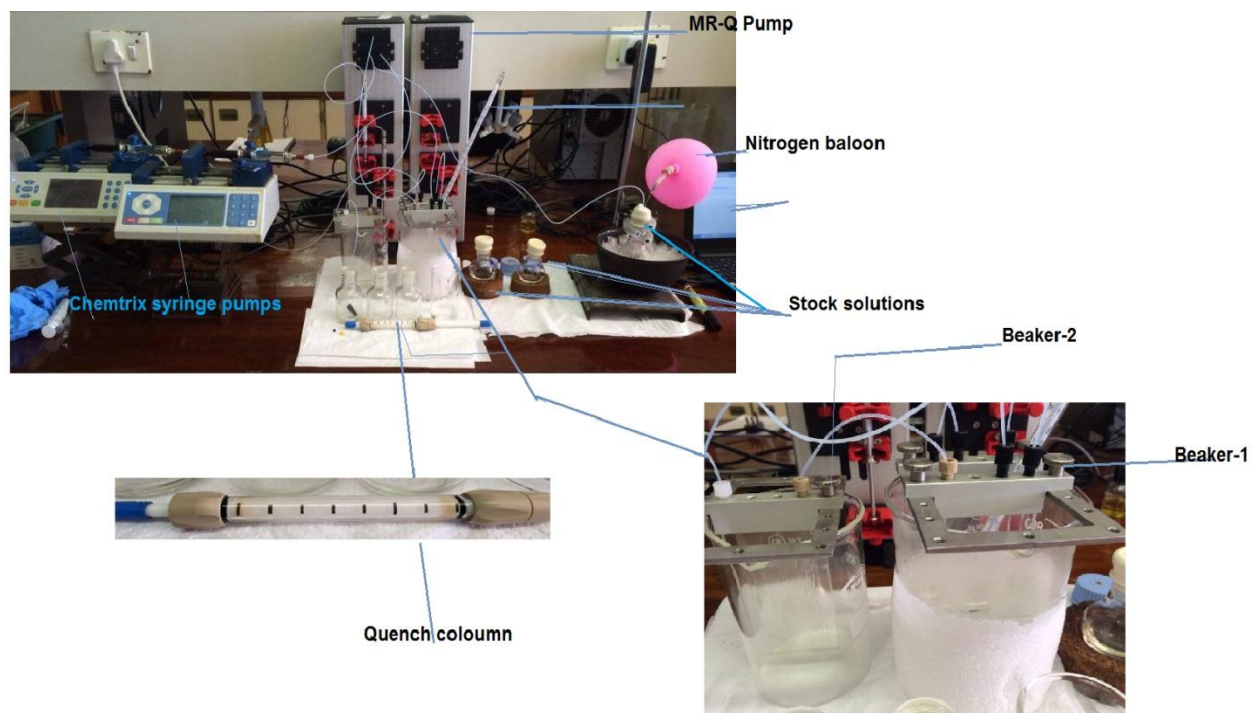


**Figure 38:** Tri-fluoro acetylation (step-2) microreactor set up

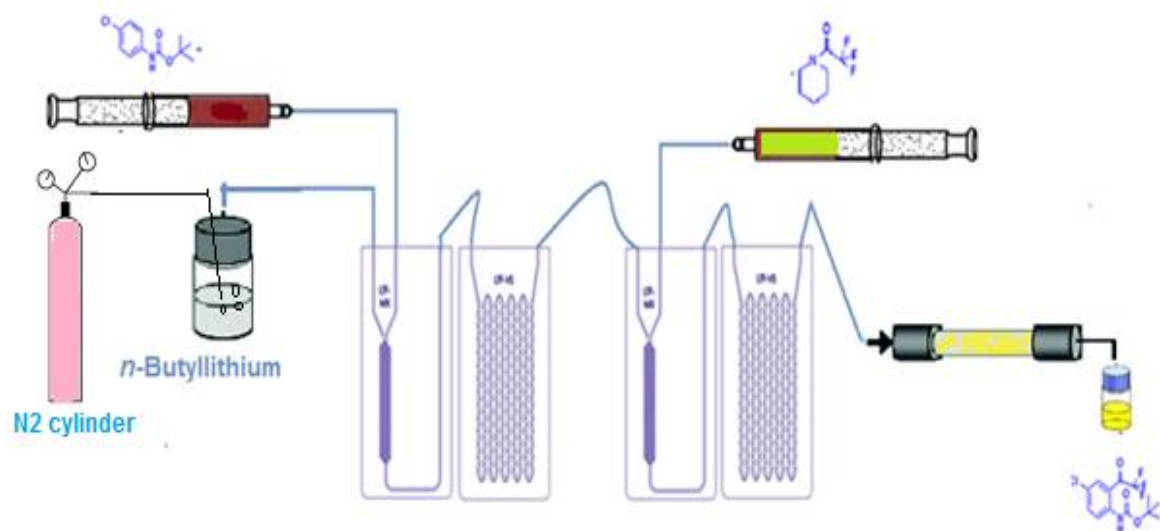


**Figure 39:** Tri-fluoro acetylation (Preparation of *tert*-butyl-4-chloro-2-(2,2,2-trifluoroacetyl) phenyl carbamate **27**) micro reactor set up block diagram.



**Figure 40:** MR-Q pump. It is a self-priming continuous flow pump ranging from 80 $\mu$ L/hour-3.5L/hour and works with PC software



**Figure 41:** Chemyx Fusion syringe pump.

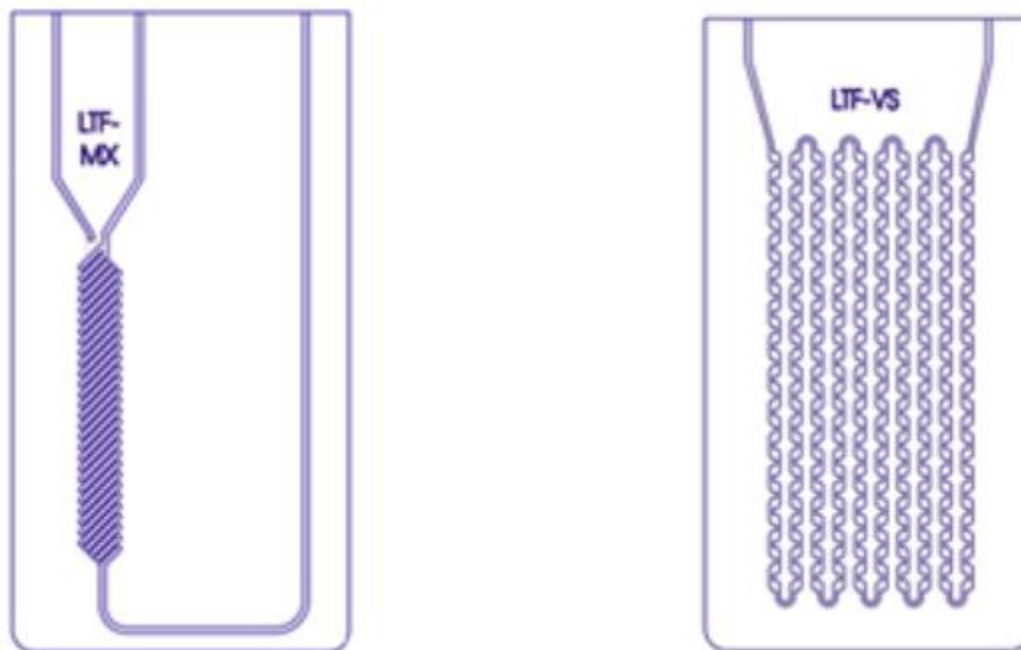


**Figure 42:** LTF MX mixer (left), for intensive mixing and LTF VS (right) for intensive mixing and residence time.

After the preliminary reaction, the reaction reagent parameters were further examined for a better conversion where residence time, concentration, temperature were investigated.

#### 4.1.2.1. Effect of residence time on conversion of **26**

The *tert*-butyl-4-chloro phenyl carbamate **26** (5 g, 23.6 mmol) was dissolved in anhydrous degassed THF to a concentration of 0.1 M and *n*-butyllithium (2.5 M in hexanes from Sigma-Aldrich) was diluted to a concentration of 0.25 M in dry degassed hexanes and the trifluoro acetylating agent, piperidine trifluoroacetic acid **67** (10.17 mL, 78.74 mmol) was dissolved to a concentration of 0.14 M in a dry degassed THF. All the reagent solutions kept under the atmosphere of dry nitrogen. The temperature of the first beaker maintained at -45 °C and second beaker at -10 °C using dry ice. The quench column and the reactor loops were first flushed with anhydrous degassed solvent THF. The reagents were

introduced into the reactor as shown in the block diagram (Figure 35) at different residence times ranging from 17.3 min - 4.3 min by keeping the concentration of reagents and temperature constant. The *tert*-butyl-4-chloro phenyl carbamate **26** and piperidine trifluoroacetic acid **67** were introduced into the reactor with the help of Chemyx Fusion syringe pumps and 10 mL SGE glass syringes, *n*-butyllithium fed into the reactor with the help of MR-Q syringe pump. Sample collected at the end of the microreactor were analyzed by offline GC and the % conversion was calculated by measuring peaks areas. The product obtained after evaporation of solvent subjected to the <sup>1</sup>HNMR, <sup>13</sup>CNMR, IR and elemental analysis.

*Analysis same as above*

#### 4.1.2.2. Effect of concentration of *n*-butyllithium on conversion of **26**

The *tert*-butyl-4-chloro phenyl carbamate **26** (5 g, 23.6 mmol) was dissolved in anhydrous degassed THF to a concentration of 0.1 M and *n*-butyllithium (2.5 M in hexanes from Sigma-Aldrich) was diluted to a concentrations from 0.5-0.25 M in dry degassed hexanes and the trifluoro acetylating agent, piperidine trifluoroacetic acid **67** (10.17 mL, 78.74 mmol) was dissolved to a concentration of 0.14 M in a dry degassed THF. All the reagent solutions kept under the atmosphere of dry nitrogen. The temperature of the first beaker maintained at -45 °C and second beaker at -10 °C using dry ice. The quench column and the reactor loops were first flushed with anhydrous degassed solvent THF. The reagents were introduced into the reactor as shown in the block diagram (Figure 35) at constant residence time (8.6 min), temperature (beaker 1 at -45 °C, beaker 2 at -10 °C) and by varying concentration of *n*-butyllithium from 0.5 M to 0.25 M. The *tert*-butyl-4-chloro phenyl carbamate **26** and piperidine trifluoroacetic acid **67** were introduced into the

reactor with the help of Chemyx Fusion syringe pumps and 10 mL SGE glass syringes, *n*-butyllithium fed into the reactor with the help of MR-Q syringe pump. A sample collected at the end of the microreactor were analyzed by offline GC and the % conversion was calculated by measuring peaks areas.

The product obtained after evaporation of solvent subjected to the  $^1\text{H}$ NMR,  $^{13}\text{C}$ NMR, IR and elemental analysis.

*Analysis same above*

#### 4.1.2.3. Effect of concentration of trifluoro acetylating agent on conversion of **26**

The *tert*-butyl-4-chloro phenyl carbamate **26** (5 g, 23.6 mmol) was dissolved in anhydrous degassed THF to a concentration of 0.1 M. *n*-butyllithium (2.5 M in hexanes from Sigma-Aldrich) was diluted to a concentration of 0.25 M in dry degassed hexanes and the trifluoro acetylating agent, piperidine trifluoroacetic acid **67** (10.17mL, 78.74 mmol) was dissolved to concentrations from 0.14-0.3 M in a dry degassed THF. All the reagent solutions kept under the atmosphere of dry nitrogen. The temperature of the first beaker maintained at -45 °C and second beaker at -10 °C using dry ice. The quench column and the reactor loops were first flushed with anhydrous degassed solvent. The reagents were introduced into the reactor as shown in the block diagram (figure 35) at constant residence time (8.6 min), temperature (beaker 1 at -45 °C, beaker 2 at -10 °C) and at different concentrations of piperidine trifluoroacetic acid **67** ranging from 0.14 M-0.3 M. The *tert*-butyl-4-chloro phenyl carbamate **26** and piperidine trifluoroacetic acid **67** were introduced into the reactor with the help of Chemyx Fusion syringe pumps and 10 mL SGE glass syringes, *n*-butyllithium fed into the reactor with the help of MR-Q syringe pump. A sample collected

at the end of the microreactor were analyzed by offline GC and the % conversion was calculated by measuring peak areas.

The product obtained after evaporation of solvent subjected to the  $^1\text{H}$ NMR,  $^{13}\text{C}$ NMR, IR and elemental analysis.

*Analysis same above*

#### 4.1.2.4. Investigating the effect of temperature on conversion of **26**

The *tert*-butyl-4-chloro phenyl carbamate **26** (5 g, 23.6 mmol) was dissolved in anhydrous degassed THF to a concentration of 0.1 M. *n*-butyllithium (2.5 M in hexanes from Sigma-Aldrich) was diluted to a concentration of 0.25 M in dry degassed hexanes and the trifluoro acetylating agent, piperidine trifluoroacetic acid **67** (10.17 mL, 78.74 mmol) was dissolved to a concentration of 0.14 M in a dry degassed THF. All the reagent solutions kept under the atmosphere of dry nitrogen. The temperature of the beakers maintained at lower temperatures by using dry ice. The quench column and the reactor loops were first flushed with anhydrous degassed solvent. The reagents were introduced into the reactor as shown in the block diagram (Figure 35) at constant residence time (8.6 min), concentration and at different temperatures ranging from room temperature to -70 °C. The *tert*-butyl-4-chloro phenyl carbamate **26** and piperidine trifluoroacetic acid **67** were introduced into the reactor with the help of Chemyx Fusion syringe pumps and 10 mL SGE glass syringes, *n*-butyllithium fed into the reactor with the help of MR-Q syringe pump. A sample collected at the end of the microreactor were analyzed by offline GC and the % conversion was calculated by measuring peaks areas.

The product obtained after evaporation of solvent subjected to the  $^1\text{H}$ NMR,  $^{13}\text{C}$ NMR, IR and elemental analysis.

*Analysis same above*

After a preliminary investigation of residence times, temperature and concentration of trifluoro acetylation reaction residence times further examined by central composite design at constant concentration and temperature for further optimization.

#### 4.1.2.5. Optimization of residence times by central composite design

The trifluoro acetylation reaction was optimized in microreactor setup showed in Figure 34, an experimental domain was established by using primary investigation results. The developed experimental domain was further used to create the central composite design to execute the experiments in a well-developed fashion (Table 18). For this reaction all the reagent concentrations was kept constant (0.25 M of *n*-butyllithium, 0.1 M of compound **26**, 0.2 M of **67**)

**Table 18: Experimental domain for residence times (min) step 2**

	<i>n</i> -Butyllithium (min)	Piperidine trifluoroacetic acid (min)	<i>N</i> -Boc aniline (min)
Minimum	52	260	86.6
Maximum	13	5.2	5.2

During the study, a total of 20 experiments were carried out from the central composite design including replications. The percentage of product conversion was investigated by GC by measuring the peak areas and finally, the data was analyzed by a statistical model.

#### 4.1.2.6. Model derivation

The observed experimental data of *tert*-butyl-4-chloro phenyl carbamate **26** conversion was fitted on the logistic regression model (Equation 2).

$$\hat{Y} = 100 / (1 + e^{b_0 + b_1 F_1 + b_2 F_2 + b_3 F_3 + b_4 F_1^2 + b_5 F_2^2 + b_6 F_3^2 + b_7 F_1 F_2 + b_8 F_1 F_3 + b_4 F_2 F_3 / F})$$

(Equation 2)

Where:  $\hat{Y}$  is the predicted conversion,  $F$  = Flow-rate and,  $i = 1, 2, 3, 4$  are the estimated regression coefficients.

The estimated regression coefficients from the analyzed experimental data are summarized below (Table 19). In this work, all estimated coefficients whose p-value is below 5%, will be assumed to be statistically significant. Therefore, the corresponding variables play a significant role in the conversion.



**Table 19: Estimated regression coefficients & associated statistics**

Co efficient	Term	b	Standard error	t-Test	p-Value
b0	Intercept	-1.06	1.023	-1.04	0.305
b1	<i>n</i> -butyllithium	18.28	8.637	2.117	0.041
b2	Boc anhydride	2.78	0.801	3.474	0.001
b3	Piperidine trifluoro acetic acid	35.19	17.769	1.98	0.055
b4	<i>n</i> -butyllithium* Piperidine trifluoro acetic acid	-414.7	149.043	-2.783	0.008

In order to obtain the final response surface model, all the insignificant terms (p-value > 0.05) must be eliminated from the predicted model. However, some of the observed estimated coefficients are not significant enough to define the model. After elimination of insignificant values (p-value > 0.05) final regression model is presented below (Equation 3).

$$=100/ 1+e^{b_0+b_1F_1+b_2F_2+b_3F_3+ b_4F_1F_3/F} \quad (\text{Equation 3})$$

From data presented in Table 19 above, the final model shows that residence time of *n*-butyllithium and piperidine trifluoroacetic acid has an antagonistic effect towards the conversion. This means a smaller decrease in the residence time, result to the significant decrease in the conversion.

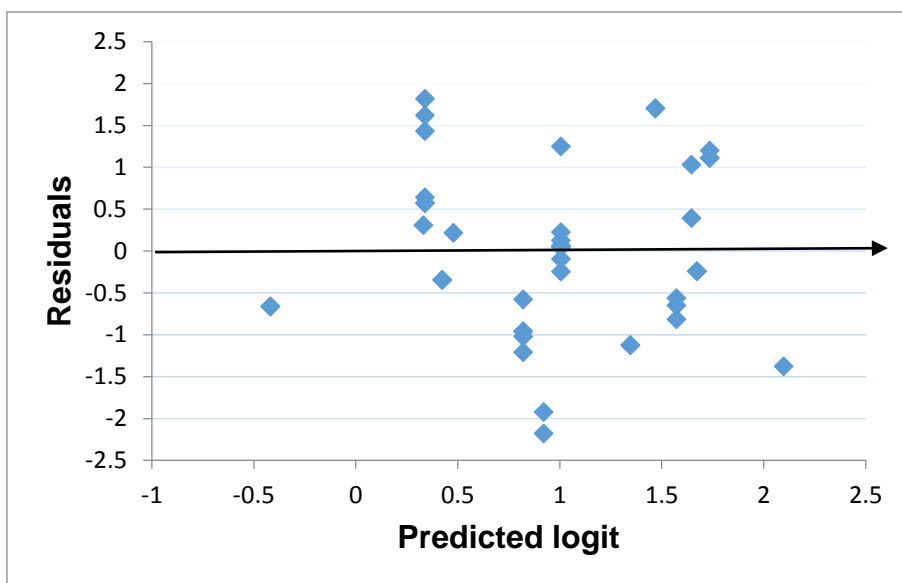
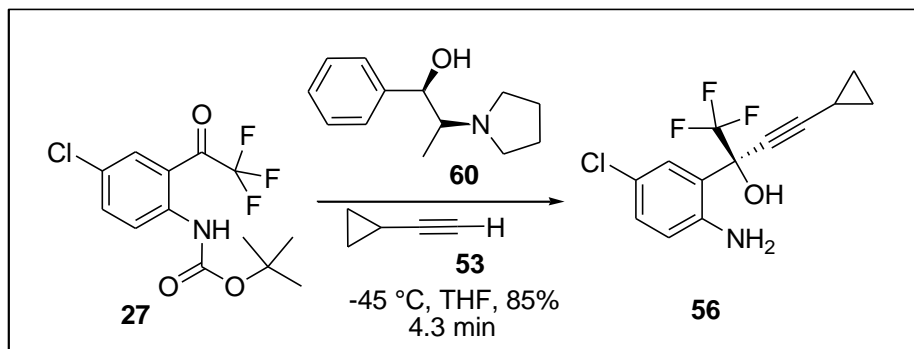


**Figure 43:** Outlier scattered plot for standard residuals and predicted logit

From the above graph, (Figure 39) the residuals are randomly distributed around the regression line (no observed heteroscedasticity). There is one outlier observed (-2.1).

### 4.1.3. Preparation of *tert*-butyl-4-chloro-2-(4-cyclopropyl-1,1-trifluoro-2-hydroxybut-3-yn-2-yl) phenyl carbamate **56**



**Scheme 50:** Preparation of *tert*-butyl-4-chloro-2-(4-cyclopropyl-1,1-trifluoro-2-hydroxybut-3-yn-2-yl) phenyl carbamate **56**.

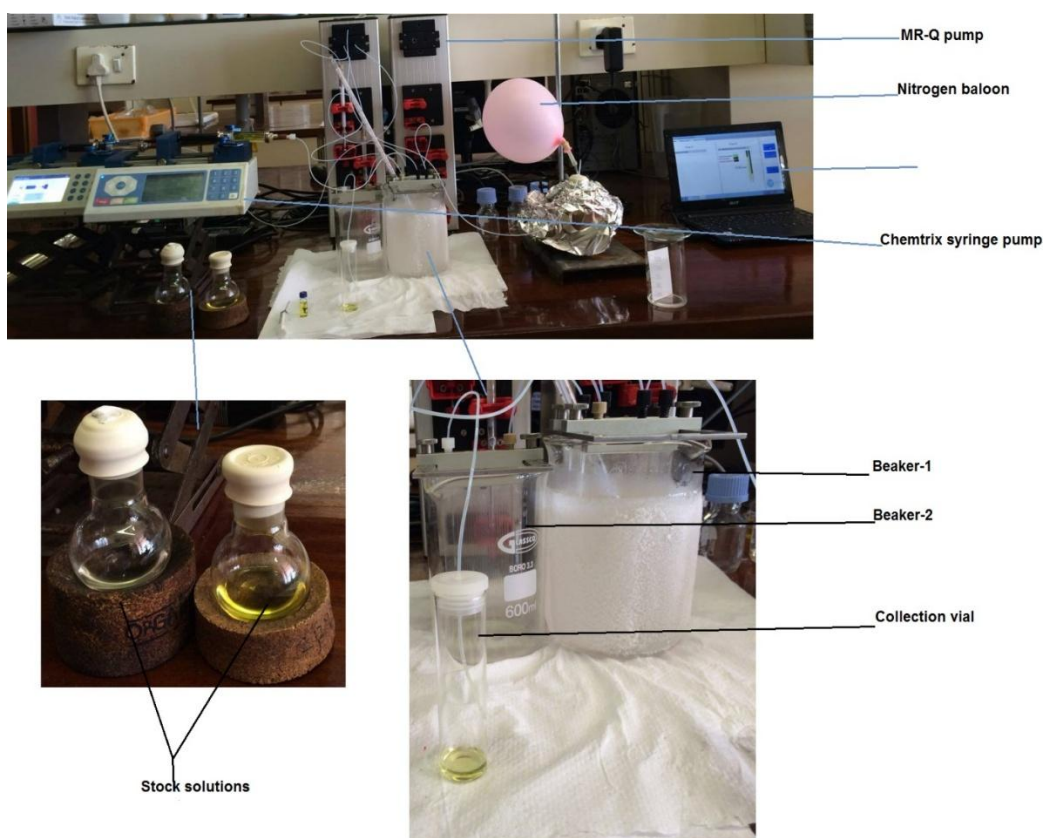


**Figure 44:** Alkylation reaction flow microreactor setup

In this thesis preparation of compound **56** generally known as alkylation reaction (Scheme 50) this reaction in flow was done by using microreactor setup shown below (Figure 40). The flow reactor setup was built using MR-Q pump, Chemyx Syringe Pumps, PTFE tubing, LTF reactor plates. Four LTF reactor plates (two LTF-MX reactor plate and two LTF-VS reactor plates) was used for this setup. These plates arranged in two beakers each beaker one mixing plate one residence plate and they marked as beaker 1 and beaker 2. MR-Q pump is used for pumping *n*-butyllithium, *N*-pyrrolidinylnorephedrine **60**, cyclopropyl acetylene **53** and *tert*-butyl-4-chloro-2-(2,2,2-trifluoroacetyl) phenyl carbamate **27** in THF were pumped using Chemyx Fusion syringe pump as shown in Figure 41.

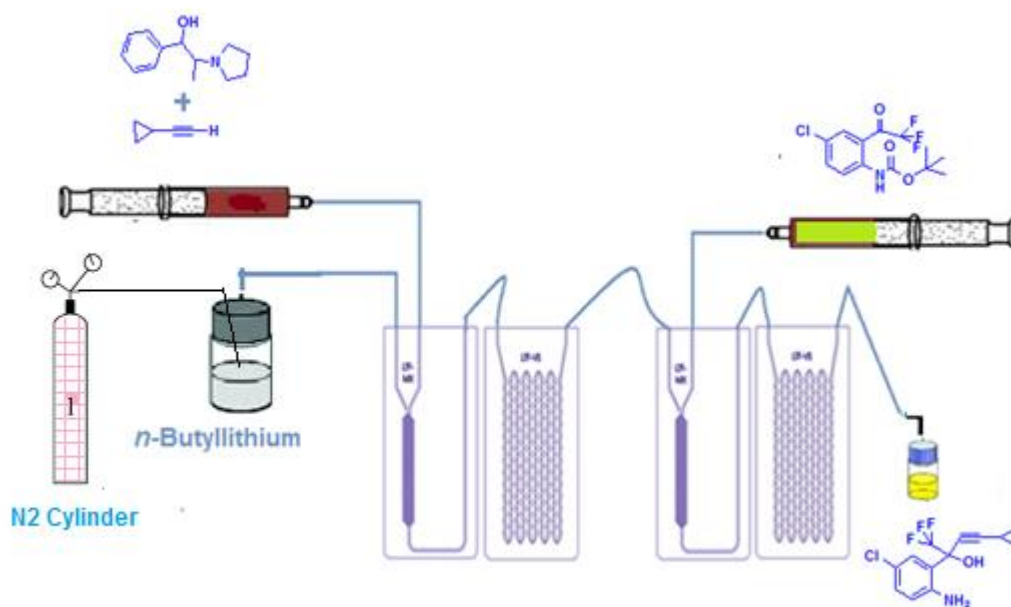


**Figure 45:** Alkylation reaction micro reactor set up block diagram

**Preparation of stock solutions**

**Stock solution A** was prepared by dissolving *N*-pyrrolidinylnorephedrine **60** (7.3 g, 35.75 mmol) and cyclopropyl acetylene **53** (3.35 mL, 35.78 mmol) in THF (50 mL).

**Stock solution B** was prepared by diluting 2.5 M of *n*-butyllithium (26 mL, 41.25mmol) in dry degassed HPLC grade hexanes (50 mL).

**Stock solution C** was prepared by dissolving *tert*-butyl-4-chloro-2-(2,2,2-trifluoroacetyl) phenyl carbamate **27** (5 g, 16.25 mmol) in THF (50 mL).

The stock solution B pumped into LTF microreactor plates with the help of MR-Q syringe pump, stock solution A also pumped into same reactor plate with the help of Chemyx Fusion syringe pump and SGE glass syringe. In this microreactor plate *n*-butyllithium reacts with compound **60** & **53** and generates complex **74** which enters into LTF V microreactor plate, these two reactor plates kept at -45 °C and these plates are connected to another LTF MX microreactor plate where stock solution C enters into the plate with the help of another Chemyx Fusion syringe pump, the generated complex **74** in first plate attacks onto the compound **27** to get compound **56** These reactor plates kept at a temperature of -45 °C at the end microreactor plate connected to a reservoir. The sample collected from the reservoir were analyzed by using offline Gas chromatography (GC) and the peak areas were used for calculating % conversion. After conformation from GC the reaction mixture extracted with ethyl acetate (3x50 mL) and dried over anhydrous Na<sub>2</sub>SO<sub>4</sub>. The combined organic layers were evaporated to get the product. The structure of the compound was confirmed by FT-IR, <sup>1</sup>H-NMR <sup>13</sup>C-NMR spectroscopy and elemental analysis. Based on the results of GC the reaction further scrutinized towards the

optimization by investigating the effect residence time, concentration and temperature on conversion.

$^1\text{H}$ -NMR-(400 MHz) in  $\text{CDCl}_3$ :  $\delta$  0.74 (t,  $J$  = 3.36, 2H); 0.83 (t,  $J$  = 5.96, 2H); 1.21-1.55 (m, 1H) 4.17 (s, 1H); 7.25 (d,  $J$  = 8.92, 1H); 7.61 (s, 1H); 8.30 (d,  $J$  = 8.96, 1H); 9.41 (s, 1H).  $^{13}\text{C}$ -NMR in  $\text{CDCl}_3$  (100 MHz):  $\delta$  0.03, 9.1, 14.1, 27.1, 70.1, 75.2, 94.2, 120.5, 121.3, 125.0, 128.9, 130.9, 177.  $^{19}\text{F}$ NMR in  $\text{CDCl}_3$ :  $\delta$  -79.72 IR ( $\text{cm}^{-1}$ ) 1262, 1360, 1487, 2235, 2794, 3330, 3419. Anal.calcd for  $\text{C}_{13}\text{H}_{11}\text{ClF}_3\text{NO}$ ; C, 53.90; H, 3.83; N, 4.84; Found: C, 53.87; H, 3.89; N, 4.81

#### 4.1.3.1. Effect of residence time on conversion of **27**

The *tert*-butyl-4-chloro-2-(2,2,2-trifluoroacetyl) phenyl carbamate **27** (5 g, 16.25 mmol) was dissolved in anhydrous degassed THF to a concentration of 0.35 M. *n*-Butyllithium (2.5 M in hexanes from Sigma-Aldrich) was diluted to a concentration of 0.45 M in dry degassed hexanes and *N*-pyrrolidinylnorephedrine **60** (7.3 g, 35.75 mmol), cyclopropyl acetylene **53** (3.55 mL, 35.78 mmol) were dissolved in THF to a concentration of 0.45 M. All the reagent solutions kept under the atmosphere of dry nitrogen. The temperature of the first beaker maintained at -45 °C and second beaker at -10 °C using dry ice. The reagents were introduced into the reactor as shown in the block diagram (Figure 41) at different residence times ranging from 8.6 min 1.7 min by keeping the concentration of reagents and temperature constant. A sample collected at the end of the microreactor were analyzed by offline GC and the % conversion was calculated by measuring peaks areas. The product obtained from the reaction analyzed by  $^1\text{H}$ NMR,  $^{13}\text{C}$ NMR, IR and elemental analysis.

*Analysis same as above*

Based the results of residence time investigation on conversion of **27** we further examined the reaction reagents concentration.

#### 4.1.3.2. Effect of Concentration of *n*-butyllithium on conversion of **27**

The *tert*-butyl-4-chloro-2-(2,2,2-trifluoroacetyl) phenyl carbamate **27** (5 g, 16.25 mmol) was dissolved in anhydrous degassed THF to a concentration of 0.35 M. *n*-Butyllithium (2.5 M in hexanes from Sigma-Aldrich) was diluted to a concentrations ranging from 0.25 M-0.45 M in dry degassed hexanes and *N*-pyrrolidinylnorephedrine **60** (7.3 g, 35.75 mmol), cyclopropyl acetylene **53** (3.55 mL, 35.78 mmol) were dissolved in THF to a concentration of 0.45 M. All the reagent solutions kept under the atmosphere of dry nitrogen. The temperature of first beaker maintained at -45 °C and second beaker at -10 °C using dry ice. The reagents were introduced into reactor as shown in block diagram (Figure 41) at constant residence time (4.3 min), temperature (beaker-1 at -45 °C, beaker-2 at -10 °C) and by varying concentration of *n*-butyllithium from 0.27 M to 0.45 M. A sample collected at the end of the microreactor were analyzed by offline GC and the % conversion was calculated by measuring peaks areas.

The product obtained from the reaction after purification subjected to <sup>1</sup>HNMR, <sup>13</sup>CNMR, IR and elemental analysis

*Analysis same as above*

#### 4.1.3.3. Investigating the effect of concentration of cyclopropyl acetylene

The *tert*-butyl-4-chloro-2-(2,2,2-trifluoroacetyl) phenyl carbamate **27** (5 g, 16.25 mmol) was dissolved in anhydrous degassed THF to a concentration of 0.35 M. *n*-Butyllithium

(2.5 M in hexanes from Sigma-Aldrich) was diluted to a concentration 0.45 M in dry degassed hexanes and *N*-pyrrolidinylnorephedrine **60** (7.3 g, 35.75 mmol), cyclopropyl acetylene **53** (3.55 mL, 35.78 mmol) were dissolved in THF to concentrations ranging from 0.5 M-0.65 M. All the reagent solutions kept under the atmosphere of dry nitrogen. The temperature of the first beaker maintained at -45 °C and second beaker at -10 °C using dry ice. The quench column and the reactor loops were first flushed with anhydrous degassed solvent. The reagents were introduced into the reactor as shown in the block diagram (Figure 41 ) at constant residence time (4.3 min), temperature (beaker-1 at -45 °C, beaker-2 at -10 °C) and at different concentrations of cyclopropyl acetylene **53** ranging from 0.5 M-0.65 M. A sample collected at the end of the microreactor were analyzed by offline GC and the % conversion was calculated by measuring peaks areas.

The product obtained from the reaction after purification subjected to <sup>1</sup>HNMR, <sup>13</sup>CNMR, IR and elemental analysis

*Analysis same as above*

After attaining the results of residence time and concentration investigation of reaction reagents we moved on to the investigation of reaction temperature for better conversion of **27**.

#### 4.1.3.4. Investigating the effect of temperature

The *tert*-butyl-4-chloro-2-(2,2,2-trifluoroacetyl) phenyl carbamate **27** (5 g, 16.25 mmol) was dissolved in anhydrous degassed THF to a concentration of 0.35M. *n*-Butyllithium (2.5 M in hexanes from Sigma-Aldrich) was diluted to a concentration of 0.45 M in dry degassed hexanes and *N*-pyrrolidinylnorephedrine **60** (7.3 g, 35.75 mmol), cyclopropyl



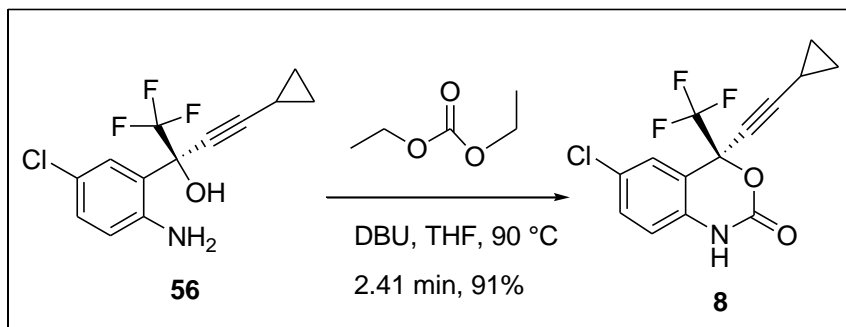
acetylene **53** (3.55 mL, 35.78 mmol) were dissolved in THF to a concentration of 0.5 M. All the reagent solutions kept under the atmosphere of dry nitrogen. The temperatures of the beakers maintained at lower temperatures by using dry ice. The reagents were introduced into the reactor as shown in the block diagram (Figure 41) at constant residence time (4.3 min), concentration and at different temperatures ranging from room temperature to -70 °C. A sample collected at the end of the microreactor were analyzed by offline GC and the % conversion was calculated by measuring peaks areas.

The product obtained from the reaction after purification subjected to <sup>1</sup>HNMR, <sup>13</sup>CNMR, IR and elemental analysis

*Analysis same as above*

#### **4.1.4. Preparation of 6-chloro-2-(4-cyclopropylethynyl)-4-(trifluoromethyl)-1H-benzo[d][1,3] oxazin-2-(4H)-one **8****

Preparation of compound **8** from compound **56** in this thesis often called as cyclisation reaction (Scheme 51). This reaction in flow was done by using microreactor setup shown in Figure 42. The set up were constructed by using two Chemyx Fusion syringe pumps, three SGE glass syringes, PTFE tubing and four LTF microreactors, these LTF microreactors arranged in two beakers each beaker accommodated with one mixing plate (LTF- MX microreactor) and one residence plate(LTF-MS microreactor). Chemyx Fusion syringe pumps connected to the LTF microreactors through PTFE tubing.



**Scheme 51:** Preparation of 6-chloro-2-(4-cyclopropylethynyl)-4-(trifluoromethyl)-1H-benzo[d][1,3] oxazin-2-(4H)-one **8**.

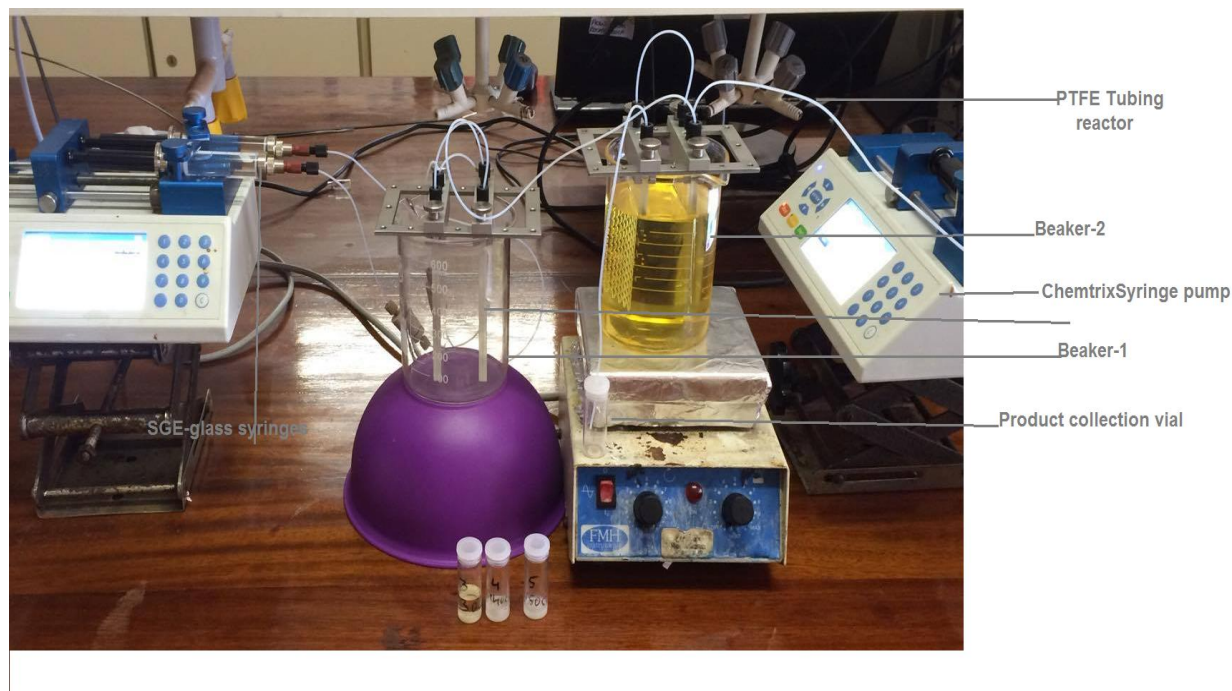


**Figure 46:** Microreactor set up for cyclisation reaction

### Preparation of stock solutions

**Stock solution A** was prepared by dissolving (*S*)-amino alcohol **56** (5 g, 17.3 mmol) in THF (50 mL).

**Stock solution B** was prepared by dissolving 1,8-diazabicyclo[5.4.0]undec-7-ene (5.67 mL, 11.42 mmol) in THF (50 mL).

**Stock solution C** was prepared by dissolving diethyl carbonate (7.5 mL, 19.38 mmol) in THF (50 mL).

The stock solution A & B pumped into LTF microreactor plates with the help of Chemyx Fusion syringe pump and SGE glass syringes where they get mixed well and enters into another set of microreactor plates, where stock solution C enters into the plate with the help of another Chemyx Fusion syringe pump. The cyclisation occurs in this microreactor plates. The second set of microreactor plates kept at a temperature of 60 °C. End of the microreactor connected to a back pressure regulator and to a reservoir. The sample collected from the reservoir were analyzed by using offline Gas chromatography (GC). The organic layers collected at the end of reactor washed with aqueous hydrochloric acid, demineralized water and dried over anhydrous Na<sub>2</sub>SO<sub>4</sub>, concentrated in vacuo and purified on silica gel (60-120 mesh) column chromatography, the compound eluted with ethyl acetate and hexane (10:90) as mobile phase. Solvent evaporated to get the compound as white colored solid. The structure of the compound was confirmed by FT-IR, <sup>1</sup>H-NMR, <sup>13</sup>C-NMR and elemental analysis. Based on the results of GC the reaction further examined towards the optimization by investigating the effect residence time, concentration and temperature on conversion.

<sup>1</sup>H-NMR-(400 MHz) in CDCl<sub>3</sub>: δ 0.85-0.96 (m, 4H); 1.38-1.45 (m, 1H); 6.85 (d, *J* = 8.52, 1H); 7.39 (dd, *J* = 8.52, 2.2 1H); 7.5 (s, 1H); 9.1 (s, 1H). <sup>13</sup>C-NMR in CDCl<sub>3</sub> (100 MHz): δ 0.003, 9.4, 66.7, 77.9, 96.5, 116.8, 121.3, 124.1, 128.4, 133.8, 149.5, <sup>19</sup>FNMR in CDCl<sub>3</sub>:

$\delta$  -80.9. IR (cm<sup>-1</sup>) 1165, 1261, 1315, 1428, 1742, 2249, 3311. Anal.calcd for C<sub>14</sub>H<sub>9</sub>ClF<sub>3</sub>NO<sub>2</sub>; C, 53.27; H, 2.87; N, 4.44; Found C, 53.21; H, 2.89; N, 4.49.

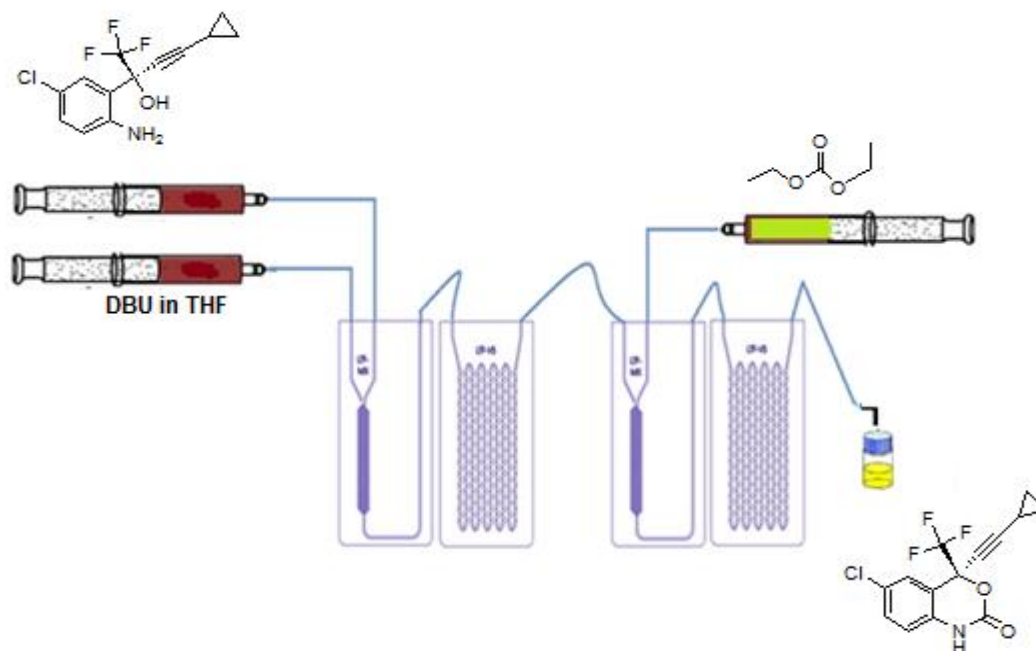


**Figure 47:** Microreactor set up block diagram for cyclisation reaction

#### 4.1.4.1. Investigating the effect of residence time

(*S*)-Amino alcohol **56** (5 g, 17.3 mmol) was dissolved in anhydrous THF to a concentration of 0.60 M, 1,8-diazabicyclo[5.4.0]undec-7-ene (5.67 mL, 11.42 mmol) was dissolved in anhydrous THF to a concentration of 0.40 M and diethyl carbonate (7.5 mL, 19.38 mmol) was dissolved in anhydrous THF to a concentration of 0.70 M. The temperatures of the first beaker maintained at room temperature and second beaker at 60 °C. The reagents were introduced into the reactor as shown in the block diagram (Figure 43) at various residence times ranging from 17.3 min – 0.43 min, at constant concentration and

temperature. A sample was collected at the end of the microreactor were analyzed by offline GC and the % conversion was calculated by measuring peaks areas.

The product obtained from the reaction analyzed by  $^1\text{H}$ NMR,  $^{13}\text{C}$ NMR, IR and elemental analysis.

*Analysis same as above*

#### **4.1.4.2. Investigating the effect of temperature**

(S)-Amino alcohol **56** (5 g, 17.3 mmol) was dissolved in anhydrous THF to a concentration of 0.60 M, 1,8-diazabicyclo[5.4.0]undec-7-ene (5.67 mL, 11.42 mmol) was dissolved in anhydrous THF to a concentration of 0.40 M and diethyl carbonate (7.5 mL, 19.38 mmol) was dissolved in anhydrous THF to a concentration of 0.70 M. The reagents were introduced into reactor as shown in block diagram (Figure 43) at constant residence time (2.4 min), concentration and at different temperatures of beaker 2 ranging from room temperature to 120 °C while keeping the beaker 1 temperature constant. A sample collected at the end of the microreactor were analyzed by offline GC and the % conversion was calculated by measuring peaks areas.

The product obtained from the reaction analyzed by  $^1\text{H}$ NMR,  $^{13}\text{C}$ NMR, IR and elemental analysis.

*Analysis same as above*

#### **4.1.4.3. Investigating the effect of concentration**

(S)-Amino alcohol **56** (5 g, 17.3 mmol) was dissolved in anhydrous THF to a concentration of 0.60 M, 1,8-diazabicyclo[5.4.0]undec-7-ene (5.67 mL, 11.42 mmol) was dissolved in

anhydrous THF to a concentration of 0.40 M and diethyl carbonate (7.5 mL, 19.38 mmol) was dissolved in anhydrous THF to get a concentrations ranging from 0.40 M – 1 M. The reagents were introduced into reactor as shown in block diagram (Figure 43) at constant residence time (2.4 min), temperature and at different concentrations ranging from 0.40 M – 1 M. A sample collected at the end of the microreactor were analyzed by offline GC and the % conversion was calculated by measuring peaks areas.

The product obtained from the reaction analyzed by  $^1\text{H}$ NMR,  $^{13}\text{C}$ NMR, IR and elemental analysis.

*Analysis same as above*

# CHAPTER 5

# CONCLUSION

The aim of present study was to develop an efficient synthesis route for the preparation of efavirenz **8**, used in the treatment of HIV/AIDS. This drug not only decreases the viral load but also decrease the chance of getting other infections associated with HIV/AIDS. Not only as a single drug, efavirenz **8** may also be used in combination with other antiretroviral drugs (HIV regimen) for better and greater effect.

Considering the above mentioned advantageous, lack of local manufacturing of the drug and high requirement and low availability of the drug in South Africa prompted us to design a suitable synthetic route for the preparation of efavirenz **8**.

In this thesis, we described the synthetic route for efavirenz **8** in traditional batch chemistry as well as semi continuous flow chemistry. Semi continuous flow chemistry is an enabling technique, which is shown to be most economical, safe, and facilitates easy upscaling.

In this thesis the preparation of efavirenz **8**, was started from commercially available starting material 4-chloroaniline **68** which undergoes amino group protection, trifluoro acetylation, the addition of cyclopropyl acetylene in the presence of chiral axillary and finally cyclization with diethyl carbonate to get the title compound. The same synthetic steps were followed from traditional batch chemistry and semi continuous flow chemistry and the results are compared.

To a great extent, this work has accomplished the aims and objectives of the study, where the flow process took approximately 10% time of the traditional batch process.

Improved safety, one of the major challenges that we faced in this work was *n*-butyllithium, was used as lithiating agent in two major steps of the synthesis, high flammability of the



reagent nature, when exposed to environment, gave us some safety issues during the synthesis in traditional batch process which were successfully overcome during semi continuous flow protocol. The traditional batch process was done by using traditional glassware like round bottomed flasks, beakers *etc.* The contents of this flask always have a chance to get exposed to the environment whereas flow process was done in closed microreactors and no chance for the environmental exposure so the artificial inert environment was quite easy to control in microreactors, which increase the safety of the reactions.

Improved yield, most of the reaction yields improved by the semi continuous flow protocol compared with traditional batch chemistry. Especially trifluoroacetylation reaction in batch gave us 28% yield where as in flow 70% was achieved. The uniform heat transfer, efficient mixing contributed for the high yield.

The highlights of this research work can be stated in terms of novelty, and the first semi continuous flow protocol for the synthesis of (-)-efavirenz **8** by using 4-chloroaniline **68** as starting material. The Seeberger approach for the synthesis of (+)-efavirenz by used 1,4-dichloro benzene.

In future, the synthetic methodology proven here can be developed into a process and incorporated into approaches to meet the rising needs for the antiretroviral drugs in South Africa.

Derivatives of efavirenz **8** can also be synthesized and evaluated for activity for an enhanced effect. And also a continuous flow protocol can also be established

However, our results clearly contributed towards the successful establishment of an efficient synthetic route for the preparation of efavirenz **8** in traditional batch chemistry and semi continuous flow protocol. As an additional benefit of the synthetic schemes demonstrated in this thesis, derivatives of efavirenz could also be synthesized and evaluated for a potential enhanced effect as future drugs.

# CHAPTER 6

# REFERENCES

1. World AIDS Day report: Joint United Nations Programme on HIV/AIDS 2011, <http://www.unaids.org>, (accessed April 2015).
2. HIV/AIDS fact sheet: World Health Organization, <http://www.who.int/mediacentre>, (accessed April 2015).
3. World AIDS Day Report: Joint United Nations Programme on HIV/AIDS, <http://www.unaids.org/en/media/unaids>, (accessed April 2015).
4. S. P. Wasti, P. Simkhada and E. Van Teijlingen, Antiretroviral treatment programmes in Nepal. Pro 2009.
5. <https://hivbook.com/tag/structure-of-hiv-1/>, (accessed June 2015).
6. H. Jin, K. Byung and W. Jeong, *Sensors*, 2015, **15**, 9915-9927.
7. HIV life cycle, <https://www.aids.gov/hiv-aids-basics/just-diagnosed-with-hiv-aids/hiv-in-your-body/hiv-lifecycle/>, (accessed June 2015).
8. Y.Campbell and RT.Gandhi, *Clinical Infectious Diseases*, 2011, **52**, 780-787.
9. National antiretroviral therapy guidelines: National Centre for AIDS & STD Control, [http://www.who.int/hiv/pub/guidelines/nepal\\_art.pdf](http://www.who.int/hiv/pub/guidelines/nepal_art.pdf), (accessed June 2015).
10. HIV/AIDS, <http://siteresources.worldbank.org>, (accessed May 2015).
11. Asia pacific Review Regional review of AIDS: Joint United Nations Programme on HIV/AIDS, [http://www.aidsdatahub.org/dmdocuments/Asia\\_Pacific\\_Regional\\_Review\\_2010.pdf](http://www.aidsdatahub.org/dmdocuments/Asia_Pacific_Regional_Review_2010.pdf), (accessed April 2015).
12. HIV/AIDS Antiretroviral therapy: World Health Organization, <http://www.who.int/hiv/topics/treatment/en/index.html>, (accessed June 2015).

13. J. Hemelaar, *Trends in Molecular Medicine.*, 2012, **18**, 182-192.
14. D. Dai, X. Long, B. Luo, A. Kulesza, J. Reichwagen and Y. Guo , PCT Int. Appl., WO2012097510, 2012.
15. W. Sneader and W. John *Drug prototypes and their exploitation.*, Wiley, United States 1996, 448–450.
16. J.B. Blaster, R. Douglas and B. John, *Principles and Practice of Infectious Diseases*, Elsevier, Churchill Livingstone, 2009.
17. A.A. Johnson, A. Ray, J. Hanes, Z. Suo, J.M. Colacino, K.S. Anderson and K.A. Johnson, *J Biol Chem.*, 2013, **276**,40847–40857.
18. G. Birkus, M.J. Hitchcock and T. Cihlar, *Antimicrob Agents Chemother.*, 2002,**46**, 716–723.
19. E. De Clercq, *Antiviral Research.*, 2005, **67**, 56–75.
20. O.J. Cruz and F.N. Uckun, *Journal of Antimicrobial Chemotherapy.*, 2006, **57**, 411–423.
21. A. Sosnik, D.A. Chiapetta and A.M. Carcabosa, *Journal of Controlled Release.*, 2009, **138**, 2–15.
22. HIV/AIDS in South Africa, <http://www.avert.org/professionals/hiv-around-world/sub-saharan-africa/south-africa>, (accessed June 2015).
23. I. Usach, V. Melis, and J. Esteban, *J Int AIDS Soc.*, 2013, **16**, 1–14.
24. Yanchunas J, *Antimicrobial Agent and Chemotherapy.*, 2005, **40**, 3825-3832.
25. Jump and E.T. Brower, *Chemical Biology & Drug Design.*, 2013, **71**, 298-305.

26. L.L. Brunton KL. Parker and J.S. Lazo, *The Pharmacological Basis of Therapeutics Goodman and Gilman's*, The McGraw-Hill Companies, China, 2006.
27. E.D. Clercq, *International Journal of Antimicrobial Agents.*, 2009, **33**, 307–320
28. J Acquir, *Immune Defic Syndr.*, 2007.
29. J. Lalezari, *N Engl J Med.*, 2003, **348**, 2175-2185.
30. A. Lazzarin, *N Engl J Med.*, 2003, **348**, 2186-2195.
31. M. Delmedico, Presented in 16th International AIDS Conference, Toronto, 2006.
32. D.K. Davidson, Sixteenth International AIDS Conference, Toronto, 2006.
33. Mechanism of action of Integrase inhibitor, [https://en.wikipedia.org/wiki/Discovery\\_and\\_development\\_of\\_integrase\\_inhibitors](https://en.wikipedia.org/wiki/Discovery_and_development_of_integrase_inhibitors), (accessed May 2015).
34. US Department of Health and Human Services, <http://www.cdc.gov/nchs/data/hus/hus14.pdf>, (accessed June 2015).
35. J. Henkel, Food and Drug Administration, US Dept. of Health and Human Services, <http://www.cdc.gov/nchs/data/hus/hus14.pdf>, (accessed June 2015)
36. N.E.C.G Davies, *Southern African Journal of HIV Medicine.*, 2013, **14**.
37. S. Staszewski, *N Engl J Med.*, 1999, **341**, 1865-1873.
38. K. Tashima, 15th International AIDS Conference, Bangkok, 2004.
39. J.R. Arribas, *AIDS.*, 2009, **16**, 1554-1556.
40. R. Schafer, 14th International AIDS Conference, Barcelona, 2012.
41. G. Robbins, 14th International Conference on AIDS, Barcelona, 2012.
42. S. Matthews, *AIDS 2000*, **14**, 33.
43. A.C. Friedl, *The Swiss HIV Cohort Study/AIDS.*, 2001, **15**, 1793-1800.

44. S.Y. Chen, 15th International AIDS Conference, Bangkok, 2004.
45. J.A. Bartlett, 14th International AIDS Conference, Barcelona, 2002.
46. UNAIDS Fact Sheet 2016, <http://www.unaids.org/en/resources/fact-sheet>, (accessed June, 2016).
47. V. Leth, *Lancet.*, 2004, **363**, 1253-1263.
48. V. Leth, *Antivir Ther.*, 2004, **9**, 721-728.
49. M.Nunez, 40th Inter science Conference on Antimicrobial Agents and Chemotherapy, Toronto, 2000.
50. A.N. Phillips, *AIDS.*, 2004, **18**, 1795-1804.
51. P.G. Yeni, *International AIDS Society-USA panel.*, 2004, **292**, 251-265.
52. S. Becker 18th Conference on Retroviruses and Opportunistic Infections, Chicago, 2011.
53. B. Hirsche, *AIDS.*, 2002, **16**, 381-385.
54. H. Knobel, 15th International AIDS Conference, Bangkok, 2004.
55. S.A. Riddler, *N Engl J Med.*, 2008, **358**, 2095-2106.
56. K. Tashima, *J Infect Dis.*, 1999, **180**, 862-864.
57. M. Dybul, 39th Inter science Conference on Antimicrobial Agents and Chemotherapy, San Francisco, 1999.
58. D. Burger, *Br J Clin Pharmacol*, 2006, **61**, 148-154.
59. J. Wang, A. Sönnernborg, A. Rane, F. Josephson, S. Lundgren, L. Ståhle and M. Ingelman-Sundberg, *Pharmacogenet Genomics*, 2006, **16**, 191-198.
60. S. Sadiq, Tariqa, Fredericks, Salimb, Khoo, H.C. Saye, Rice, Phillipd and Holt, *AIDS.*, 2005, **19**, 1716-1717.

61. T. Andrew, C. Edward, J.J.G. Edward and Y. Nouoshi, US Pat., WO 1996037457, 1996.
62. The benefits of flow chemistry, [syrris.com/applications/flow-chemistry](http://syrris.com/applications/flow-chemistry), (accessed September 2016)
63. Flow chemistry, [https://en.wikipedia.org/wiki/Flow\\_chemistry](https://en.wikipedia.org/wiki/Flow_chemistry), (accessed September 2016)
64. a) K. F.Jensen, B. J. Reizman and S. G. Newman, *Lab Chip.*, 2014, **14**, 3206. b) W. Reschetilowski, *Micoreactors in Preparative Chemistry*; Wiley-VCH, Weinheim, 2013.
65. Vaportech LTD [www.vapourtec.com](http://www.vapourtec.com), <https://www.vapourtec.com/products/flow-reactors/temperature-controlled-mixing-tube-features>, (accessed October 2016).
66. J. C. Pastre and D. L. Browne, S. V. Ley, *Chem. Soc. Rev.*, 2013, **42**, 8849.
67. a) P. Poechlauer, J. Manley, R. Broxterman, B. Gregertsen and M. Ridemark, *Org. Process Res. Dev.*, 2012, **16**, 1586–1590. b) J. Evans, *J.Chem. Eng.*, 2013, 32–34.
68. a) A. Gorsek and P.Glavic, *Chem. Eng. Res. Des.*, 1997, **75**, 709–717. b) H. Lowe, W. Ehrfeld, *Electro. Acta.*, 1999, **44**, 3679–3689.
69. Kent and Reigel's Handbook of Industrial Chemistry and Biotechnology, 11th ed, Springer, Verlag, 2007.
70. P. Watts and C. Wiles, *Chem Commun.*, 2007, 443–467.
71. V. Hessel, H.Lowe, A.Muller and G. Kolb, *Chemical Micro Process Engineering*, Weinheim, Wiley VCH, 2005.



- 72.** N. Kockmann, O.Brand, G.K. Fedder, C. Hierold, J.G. Korvink and O. Tabata. Micro Process Engineering. Fundamentals, Devices, Fabrication, and Applications, Weinheim, Wiley VCH, 2006.
- 73.** S. Braune, P. Poechlauer, R. Reintjens, S. Steinhof, M. Winter, L.Olivier, R. Guidat, P. Woehl and C. Guermur, *Chim Oggi.*, 2009, **27**, 26–29.
- 74.** B. Buisson, S. Donegan, D. Wray, A. Parracho, J. Gamble, P. Caze, J. Jorda and C. Guermur, *Chim Oggi.*, 2009, **27**, 12–16.
- 75.** U. Rodemerck, P. Ignaszewski, M. Lucas, P. Claus and M. Baerns, *Catal.*, 2000, **13**, 249–252.
- 76.** a) P. Plouffe and A .Macchi, *Org. Process Res. Dev.*, 2014, **18**, 1286. b) S. G. Newman and K. F. Jensen, *Green Chem.*, 2013, **15**, 1456.
- 77.** P.B. Cranwell, M. O’Brien, D.L. Browne, P. Koos, A. Polyzos, M. Peña-López and S.V. Ley, *Org. Biomol. Chem.*, 2012, **10**, 5574–5579.
- 78.** M. Baumann, I.R. Baxendale, L.J. Martin and S.V. Ley, *Tetrahedron.*, 2009, **65**, 6611–6625.
- 79.** C.B. McPake and G. Sandford, *Org. Process Res. Dev.*, 2012, **16**, 844–851.
- 80.** M. Baumann, I.R. Baxendale, S.V. Ley, N. Nikbin, C.D. Smith and J.P. Tierney *Org. Biomol. Chem.*, 2008, **6**, 1577–1586.
- 81.** E. Rossi, P.Woehl and M. Maggini, *Org. Process Res. Dev.*, 2012, **16**, 1146–1149.
- 82.** D. M. Roberge, C.Noti, E.Irle, M. Eyholzer, B. Rittiner,; G. Penn, G. Sedelmeier and B. Schenkel, *J. Flow Chem.*, 2014, **4**, 26–34.
- 83.** H. Wu, M. A. Khan and A.S. Hussain, *Chem. Eng. Commun.*, 2007,**194**, 760.

84. a) D. M. Roberge, B. Zimmermann, F. Rainone, M. Gottsponer, M. Eyholzer and N. Kockmann, *Org. Process Res. Dev.*, 2008, **12**, 905–910. b) F. Benaskar, A. Ben-Abdelmoumen, N. Patil, E. Rebrov, J. Meuldijk, L. Hulshof, V. Hessel, U. Krtischil and J. Schouten, *J. Flow.Chem.*, 2011, **1**, 74–89.
85. L. Ducry and D.M. Roberge, *Angew. Chem. Int. Ed.*, 2005, **44**, 7972.
86. N. G. Anderson, *Org. Process Res. Dev.*, 2012, **16**, 852–869.
87. B. Gutmann, D. Cantillo and C. O. Kappe, *Angew. Chem. Int. Ed*, 2015, **54**, 6688.
88. T. Tsubogo, H. Oyamada and S. Kobayashi, *Nature.*, 2015, **520**, 329.
89. Elenariva, Doctorate School of Chemical Sciences and Technologies, 2009-2010.
90. S. Okusu, K. Hirano, Y. Yasuda, E. Tokunagaa and N. Shibata, *RSC advances.*, DOI: 10.1039/C6RA19790F
91. A. R. Longstreet, S. M. Opalka, B. S. Campbell, B. F. Gupton and D.T. McQuade, *Beilstein J. Org. Chem.* 2013, **9**, 2570–2578.
92. C. Battilocchio, B. J. Deadman, N. Nikbin, M. O Kitching, I. C. Baxendale and S. V. Ley, *Chem. Eur. J.* 2013, **19**, 7917.
93. A. L. Radesca, S. Y. Lo, R. J. Moore and E. M. Pierce, *Synth. Commun.*, 1997, **27**, 4373-4384.
94. E. M. Pierce, L. R. Parsons, A. Lilian, Radesca, A. Y. Lo, S. Silverman, R. J. Moore, Q. Islam, A. Choudhury, M. D. Joseph, Fortnak, D. Nguyen, C. Luo, J. Morgan, P. W. Davis and N. P. Confalone, *J. Org. Chem.*, 1998, **63**, 8536-8543.
95. M. K. Gurjar, A. A. Deshmuch, S. S. Deshmukh and S. R. Mehta, US Pat., 8604189 B2, 2009.

96. B. Jiang, Q. F. Wang, C. G. Yang and M. Xu, *Tetrahedron Lett.*, 2001, **42**, 4083-4085.
97. K. C. Nicolaou, A. Krasovskiy, U. Majumder, E.V. Trepanier and Y.K. Chen, *J.Am.Chem. Soc.*, 2009, **131**, 3690-3699.
98. N. Shibata, H. Kawai, T. Kitayama and E.Tokunaga, *Eur. J. Org. Chem.*, 2011, **30**, 5959-5961.
99. B. Chen, Z.X. Wang, Y. Xue, L. Liu, and H. Chen, US Pat., 0015189A1, 2011.
100. R. Bollu, N. R.Ketavarapu, V. S. K. Indukuri, S. R. Gorantla and S. Chava, US Pat., 0264933A1, 2012.
101. M.E. Carreira, N. Chinkov, and A. Warm, *Angew. Chem. Int. Ed*, 2011, **50**, 2957-2961.
102. A. Leganza and M. Galvagni, US Pat., 0165650A1, 2013.
103. S.G. Pal, M. Praveen, S. Ganesh and K. Dabeer, Eur Pat., 2454244 B1, 2013.
104. H. Moffzal, L. Saswata, T. shilpi, S.P. Virindher and D. Debashish, *Indian journal of chemistry.*, 2009, **46**, 1174-1177.
105. M. Erick, C. Nicka, W. Aleksander and M. Carreira , *angewandte chemie.*, 2011, **50**, 2957–2961.
106. E.G. Corley, A.S. Thompson, M.F. Huntington, and E.J.J. Grabowski, *Tetrahedron Lett.*, 1995, **36**, 8937-40
107. A. Camille, Correia, K. Gilmore, D. T. McQuade, and P. H. Seeberger *Angew. Chem. Int. Ed.*, 2015, **54**, 4945 –4948.
108. S. Okusu, K. Hirano, Y. Yasuda, E. Tokunagaa and N. Shibata, *RSC advances.*, DOI: 10.1039/C6RA19790F

- 109.** K. Soai, S. Yokoyama and T. Hayasaka, *J. Org. Chem.*, 1991, **56**, 4264.
- 110.** Z. Dalian, C. Cheng, F. Xu, L. Tan, R. Tillyer, M.E. Pierce, and J.R. Moore, *Organic Syntheses.*, 2004, **10**, 556.
- 111.** G. E. Corley, A.S. Thompson, and M. Huntingtonm *Org. Synth.*, 2000, **77**, 231
- 112.** L.A. Radesca, Y.S. Lo, J.R. Moore and M.E. Pierce *synthetic communications.*, 2006, **27**, 4373-4384.
- 113.** Y. Zeng, R. Cao, T. Zhang, S. Li and W. Zhong, *European Journal of Medicinal Chemistry.*, 2015, **97**, 19-31
- 114.** D. Bradley, G. Williams and M. Lawton *J. Org. Chem.*, 2010, **75**, 8351–8354.
- 115.** J. M. Muchowski, M.C. Venuti, *J. Org. Chem.*, 1980, **45**, 4798-801.
- 116.** L. A. Radesca, Y.S. Lo, J.R. Moore and M.E. Pierce, *synthetic communications.*, 2006, **27**, 4373-4384.
- 117.** a) P. Stanetty, H. Koller and M. Mi-hovilovic, *J. Org. Chem.*, 1992, **57**, 6833–6837.  
b) J. N Reed and V.S. Snieckus, *Tetrahedron Lett.*1984, **25**, 5505–5508. c) K. Takagishi, G. Katsoulos and M. Schlosser, *Synlett.*, 1992, 360–362.
- 118.** V. Siddaiah, G. Mahaboob Basha, R. Srinuvasa rao and V. Yessayya, *Green Chemistry Letters and Reviews.*, 2012, **5**, 337-342.
- 119.** J.M. Mallan and R.L. Bebb, *Chem. Rev.*, 1969, **69**, 693.
- 120.** a) J.F. Biellmann and J.B. Ducep, *Org. React.*, 1982, **27**, 1. b) M. Desponds, O. Lehmann, R. Moret and E. Rauchschalbe, *Tetrahedron.*, 1993, **49**, 10175.
- 121.** a) H. W. Gschwend and H. R. Rodriguez, *Org. React.*, 1979, **26**, 1. b) R. D. Clark, A. Jahangir, *Org. React.*, 1995, **47**, 311-314.
- 122.** S.V. Kessar and P.Singh, *Chem. Rev.*, 1997, **97**, 721-738.

- 123.** P. Beak, *Chem. Rev.*, 1978, **78**, 275.
- 124.** a) P. Beak and V. Snieckus *Acc. Chem. Res.*, 1982, **15**, 306. b) N. S. Narasimhan and R. S. Mali *Top. Curr. Chem.*, 1987, **63**, 138.
- 125.** G. Queguiner, F. Marsais, V. Snieckus and L. Epsztajn, *Adv. Heterocycl. Chem.*, 1991, **52**, 187.
- 126.** a) K. Undheim, T. Benneche, *Act. Chem. Scand.*, 1993, **47**, 102. b) N.S. Narasimhan, R.S. Mali, *Synthesis.*, 1983, **32**, 950-957.
- 127.** F. Mongin and G. Queguiner, *Tetrahedron.*, 2001, **57**, 4059-4090.
- 128.** a) P. Beak, W. J. Zadjel and D. B. Reitz *Chem. Rev.*, 1984, **84**, 471. b) A.R. Katritzky, Z. Yang and D.J. Cundy, *Aldrichimica Acta.*, 1994, **27**, 31-38.
- 129.** P. Beak and A. I. Meyers *Accounts Chem. Res.*, 1986, **12**, 356-358.
- 130.** D.B. Collum, *Acc. Chem. Res.*, 1992, **25**, 442-448.
- 131.** a) A.J. Walker, *Tetrahedron Asymmetry* 1992, **3**, 952-961. b) R. Freeman, R. K. Haynes, W. A. Loughlin, C. Mitchell and J. V. Stokes, *Pure Appl. Chem.*, 1993, **65**, 647-54.
- 132.** W. E. Parham and C. K. Bradsher, *Acc. Chem. Res.*, 1982, **15**, 289-300.
- 133.** Krief, *Tetrahedron.*, 1980, **36**, 2531.
- 134.** W.F. Bailey and J.J. Patricia, *J. Organomet. Chem.*, 1988, **1**, 352,.
- 135.** a) H. J. Reich, *Organoselenium Chemistry*, D. Liotta, Ed. Wiley, 1987. b) S. Ponthieux, C. Paulmier, *Top. Curr. Chem.*, 2000, **208**, 113-42.
- 136.** P. L. Coe, *J. Fluor. Chem.*, 1999, **100**, 45-52.
- 137.** T. Satoh, *Chem. Rev.*, 1996, **96**, 3303-3325.
- 138.** H.U. Reissig, S. Hormuth, W. Schade, M.O. Amombo, T. Watanabe, R. Pulz,

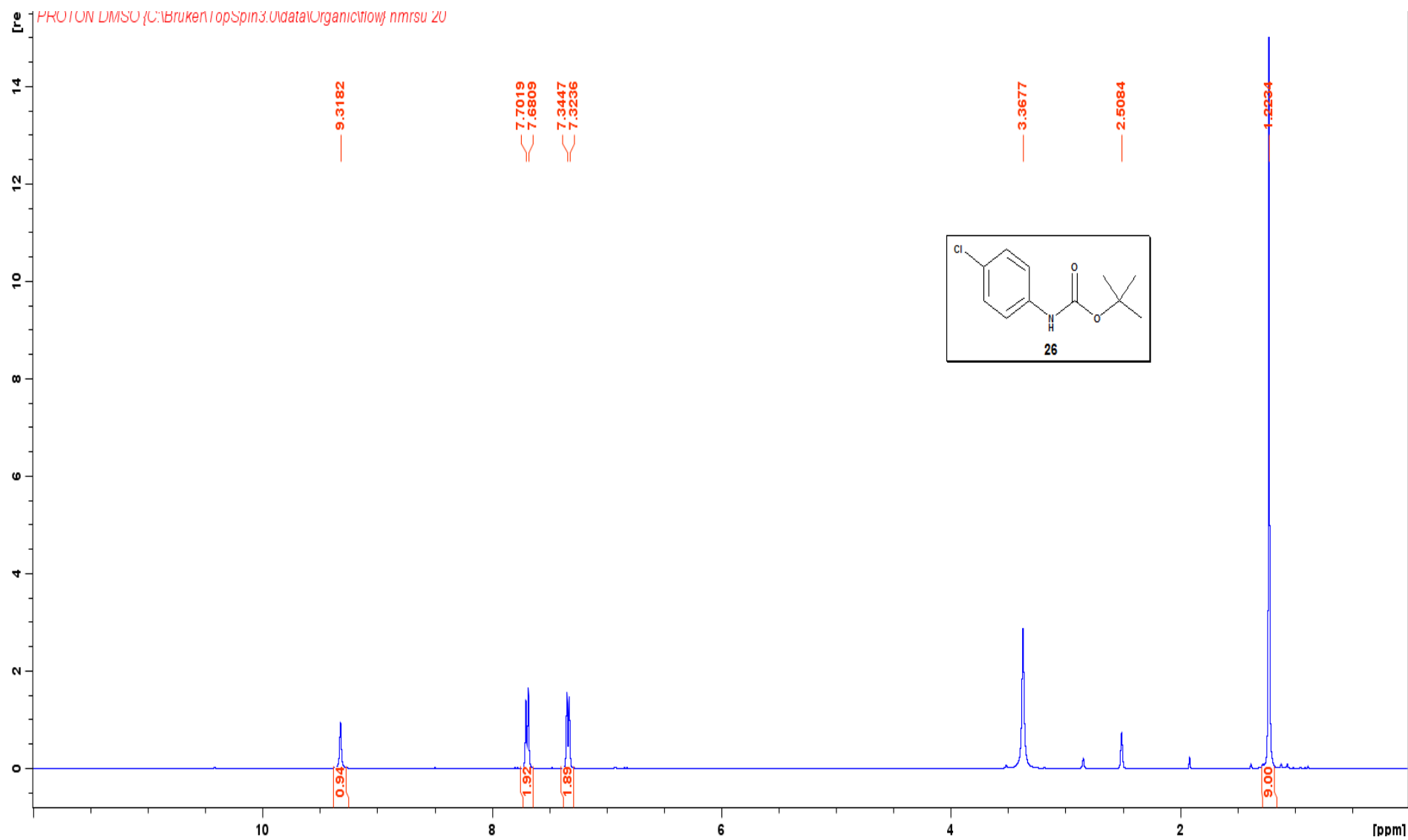
- A. Hausherr, and R. Zimmer, *J. Heterocycl. Chem.* 2000., **37**, 597-606.
- 139.** E.G. Corley, A.S. Thompson, and M. Huntington, *Org. Synth.*, 2000, **77**, 231
- 140.** M.E. Pierce, R.L. Parsons, L. A. Radesca, Y.S. Lo, S. Silverman, J.R. Moore, Q. Islam, C. Anusuya, M. D.Joseph, Fortunak, D. Nguyen, C. Luo, S.J. Morgan, W.P.Davis, P.N. Confalone, C.Chen, R.D. Tillyer, L. Frey, L. Tan, F. Xu, D. Zhao, A.S. Thompson, E.G. Corley, E.J. Grabowski, R. Reamer, and P.J. Reider *J.Org.Chem.*, 1998, **63**, 8536-8543.
- 141.** D. Zhao, C. Chen, F. Lushi T. Richard Tillyer, M.E. Pierce and J.R. Moore *Organic Syntheses.*, 2004, **10**, 556.
- 142.** D. Bradley, G. Williams and Michelle Lawton, *j.org.chem.*, 2010, **75**, 8351-8354.
- 143.** G. M. Keseru, T. soos and C.O. Kappe, *Chem.soc rev.*, 2014, **43**, 5387-5399.
- 144.** D.T McQuade and P.H. Seeberger, *J.org.chem.*, 2013, **78**, 6384-6389.
- 145.** J. Yoshida, A. Nagaki and D. Yamada, *Drug discovery today.*, 2013, **10**, 53-59
- 146.** D. Kirschneck, *Chem eng tech.*, 2013, **36**, 1061-1066.
- 147.** T.Schwalbe, V.autze, Wille and G. Chimia, *Microreactor Technology for Organic Synthesis*, Willy-VCH, 2002, **56**, 636-646.
- 148.** V.N. Telvekar, H.M. Bachhav and V.K. Bairawa, *synlet.*, 2012, **23**, 2219-2222.
- 149.** L. Le Bozec and C.moody, *J Aust j chem.*, 2009,**62**, 639-647.
- 150.** P.I. Abramenko, V.G. Zhiryakov and T.K. ponomareva, *chem heterocycl compd.*, 1975,**11**,1361-1364.
- 151.** G. S. Calabrese and S.Pissavini, *AIChE J.*, 2011, **57**,828.
- 152.** R. Snead and T. F. Jamison, *Chem. Sci.*, 2013, **4**,2822.
- 153.** L. Kupracz and A. Kirschning, *Adv.Synth.Catal.*, 2013, **355**,3375.

- 154.** M.D .Hopkin, I. R. Baxendale and S. V. Ley, *Org. Biomol. Chem.*, 2013, **11**,1822.
- 155.** T. Gustafsson, H. Sørensen and F. Pontin, *Org.Process Res.Dev.*, 2012,**16**,925.
- 156.** J.C. Pastre, D.L. Browne and S.V .Ley ,*Chem.Soc.Rev.*, 2013, **42**,8849.
- 157.** A. Camille, Correia, K. Gilmore, D. T. McQuade, and P. H. Seeberger *Angew. Chem. Int. Ed.*, 2015, **54**, 4945 –4948.
- 158.** P. H. Morgenstern and P.H. Seeberger, *Chem.Commun.*, 2014, **50**,12652.
- 159.** D.Ghislieri, K.Gilmore and P .H. Seeberger, *Angew.Chem. Int. Ed.*, 2015, **54**, 678 -688.

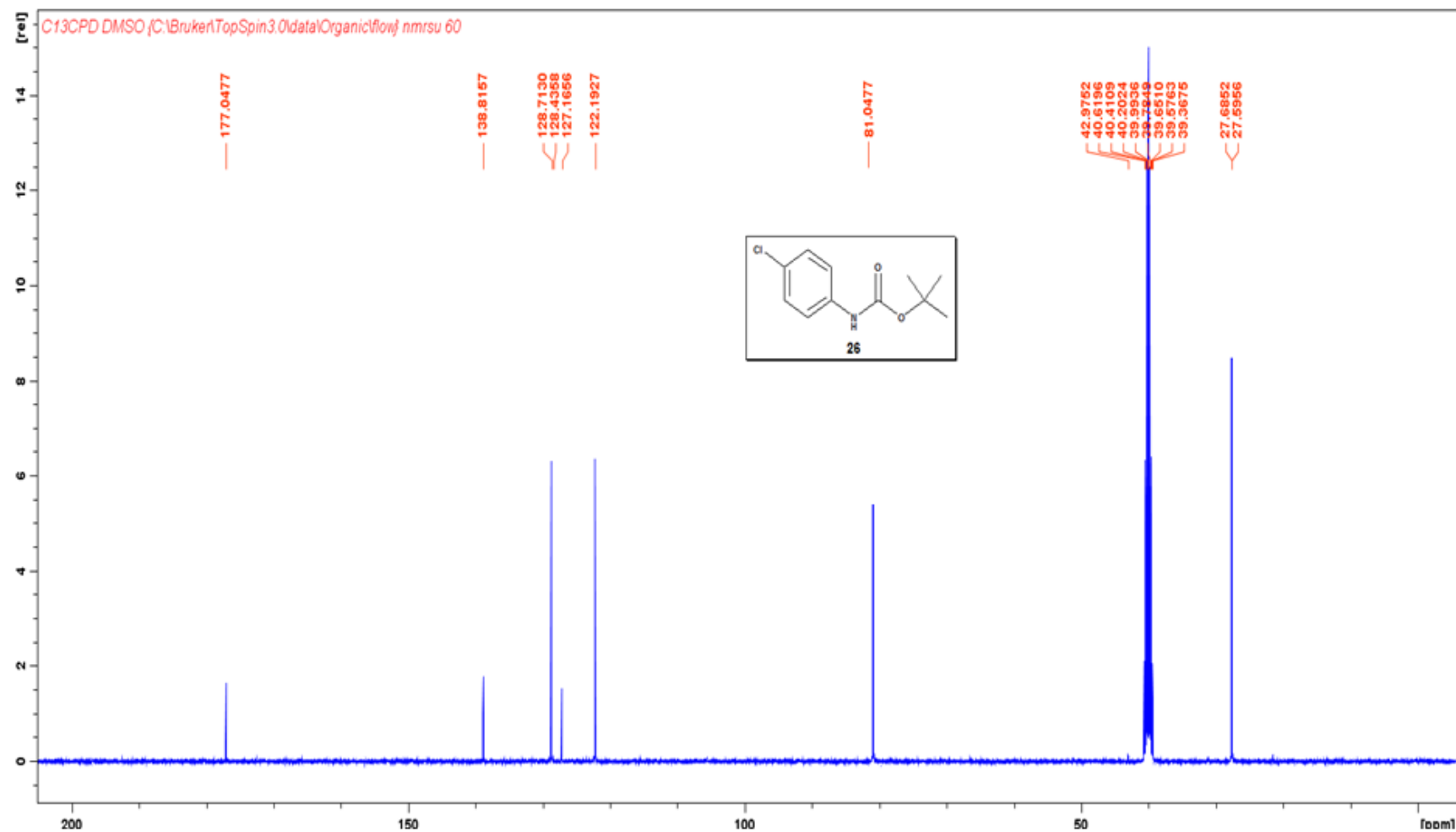
# CHAPTER 7

# APPENDIX

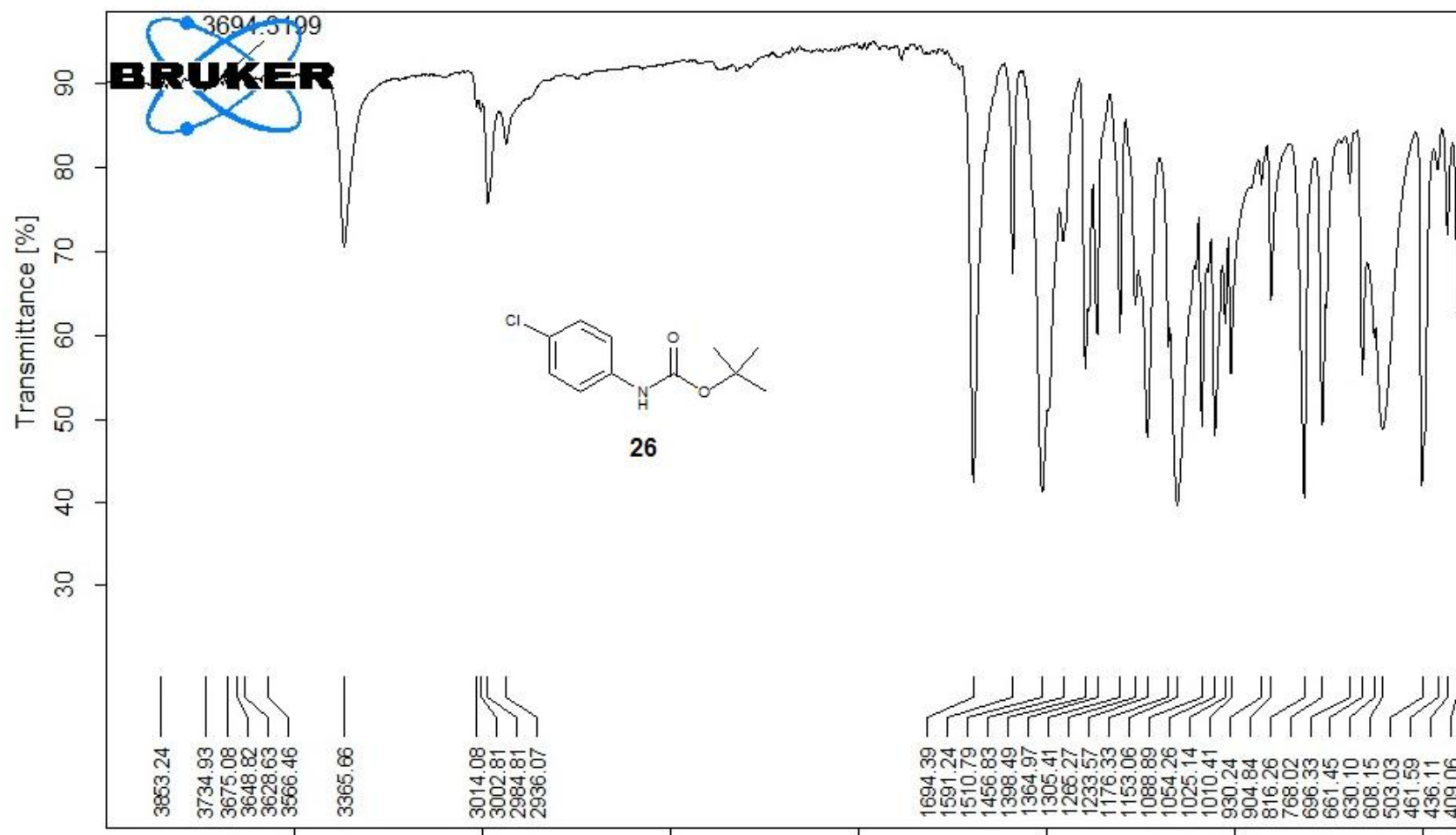




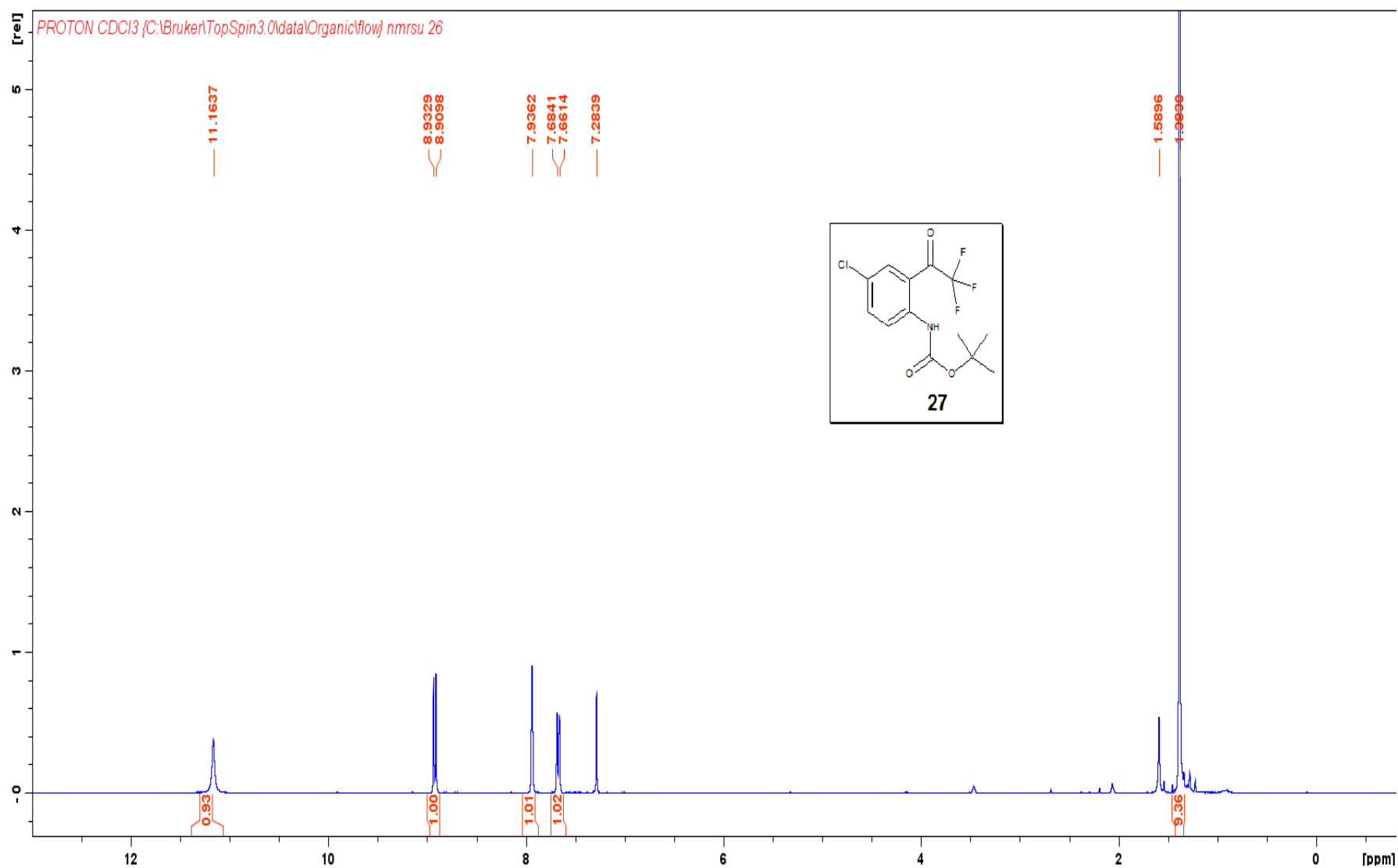
**<sup>1</sup>H NMR Spectrum (400 MHz) of tert-butyl 4-chloro phenyl carbamate 26 in DMSO-d<sub>6</sub>**



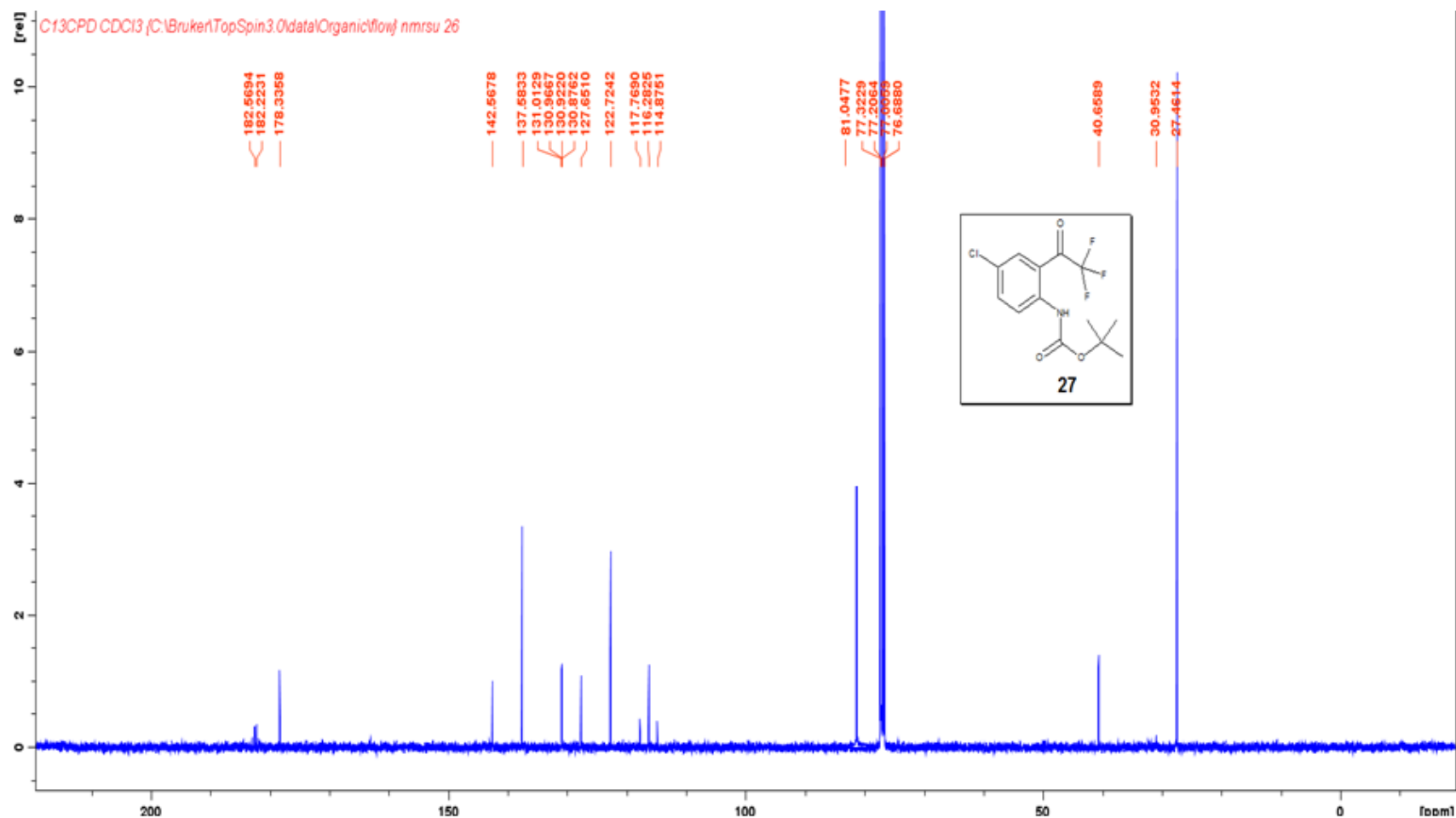
**<sup>13</sup>CNMR Spectrum (100 MHz) of *tert*-butyl 4-chloro phenyl carbamate 26 in DMSO-d<sub>6</sub>**



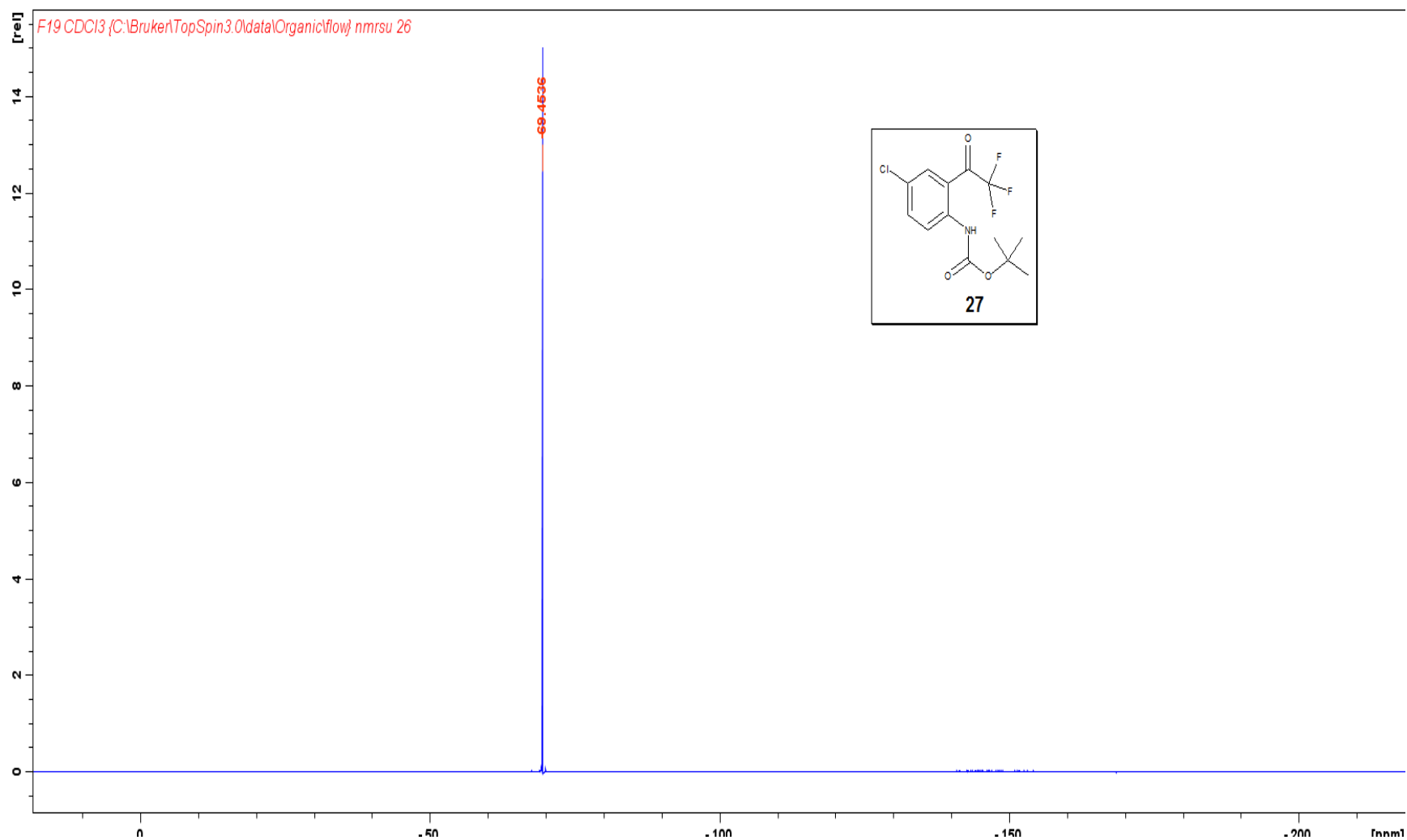
IR Spectrum of *tert*-butyl 4-chloro phenyl carbamate 26



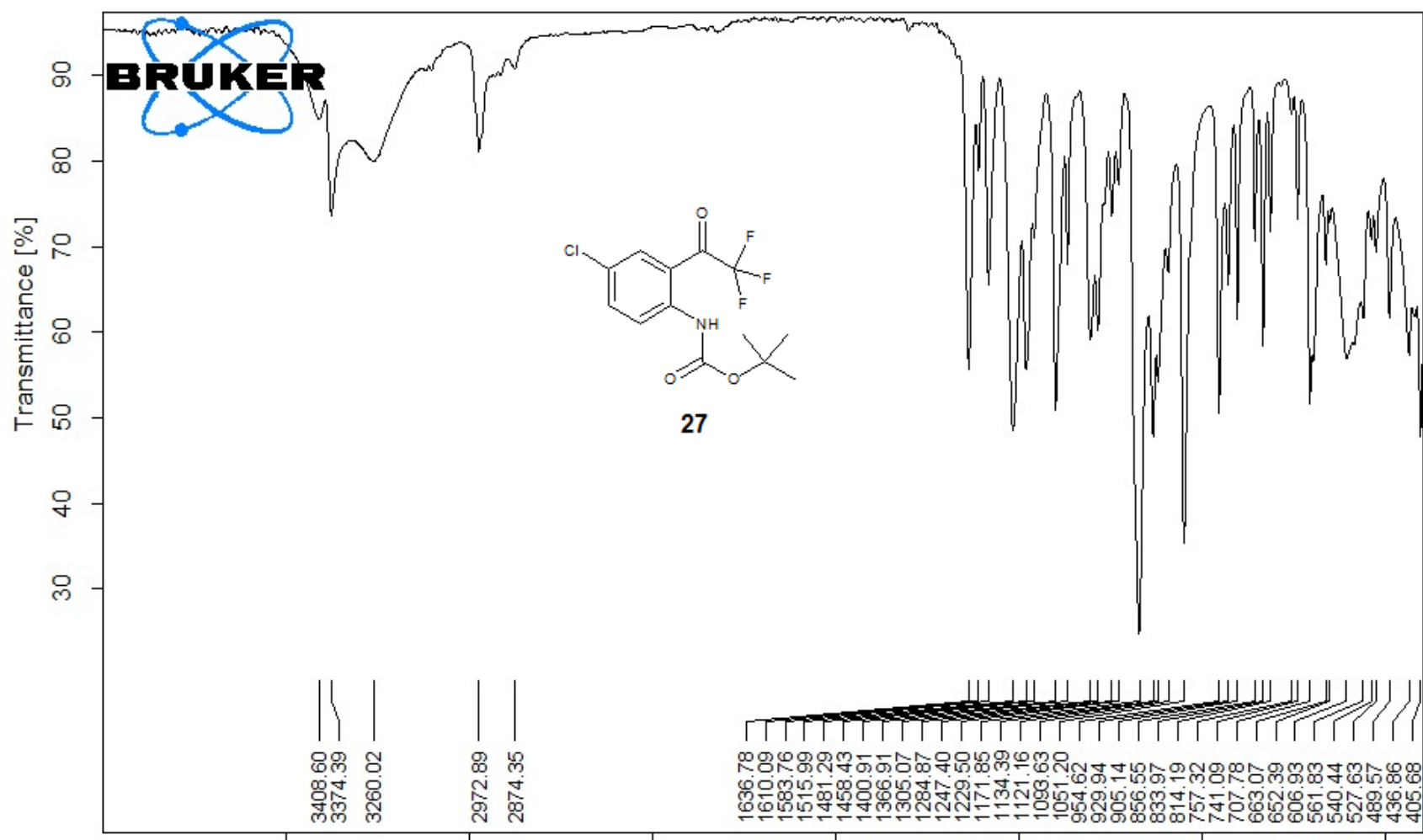
<sup>1</sup>H NMR spectrum (400 MHz) of *tert*-butyl 4-chloro-2-(2,2,2-trifluoroacetyl) phenylcarbamate **27** in CDCl<sub>3</sub>

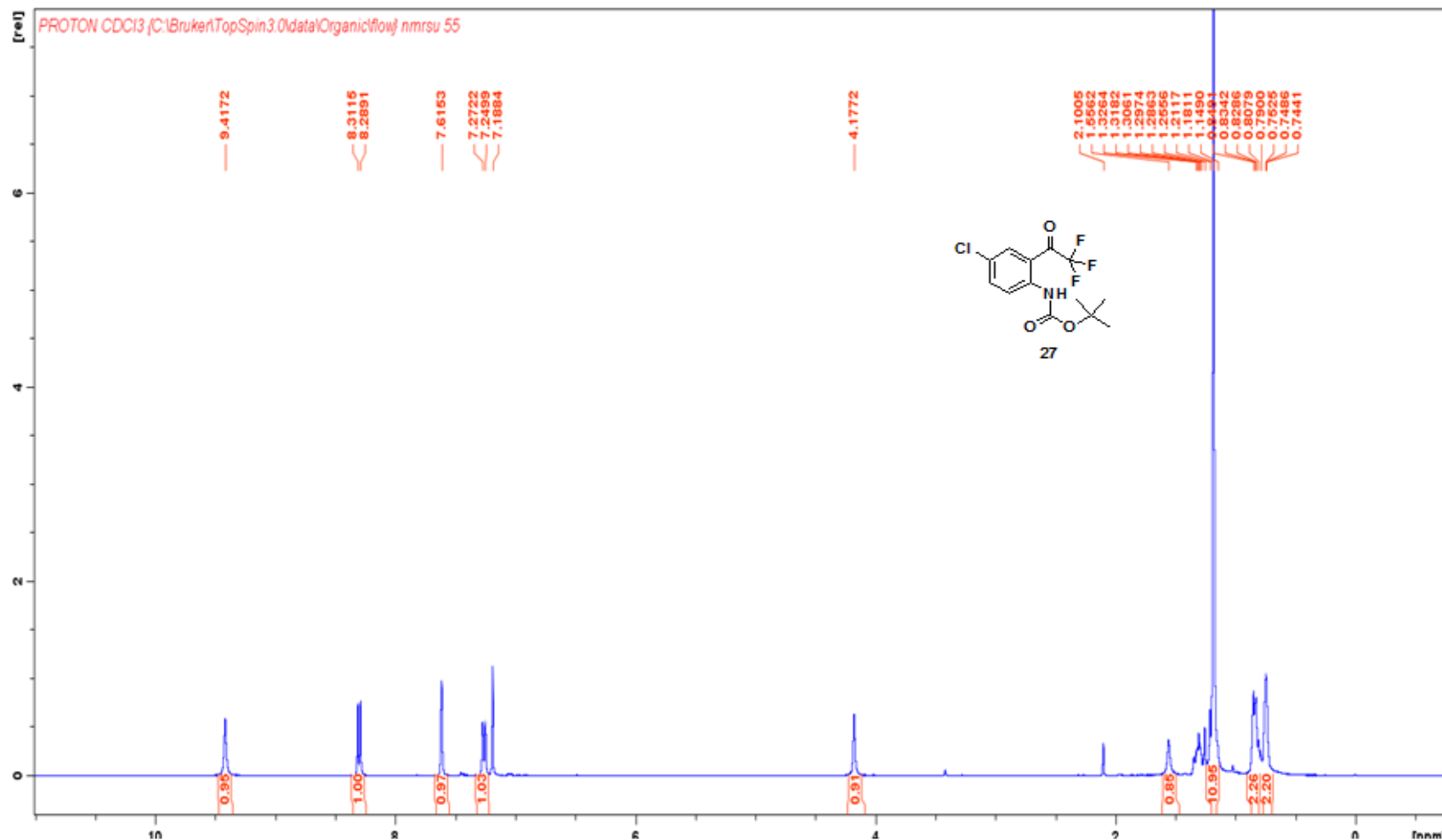


<sup>13</sup>CNMR spectrum (100 MHz) of *tert*-butyl 4-chloro-2-(2,2,2-trifluoroacetyl) phenylcarbamate **27** in CDCl<sub>3</sub>



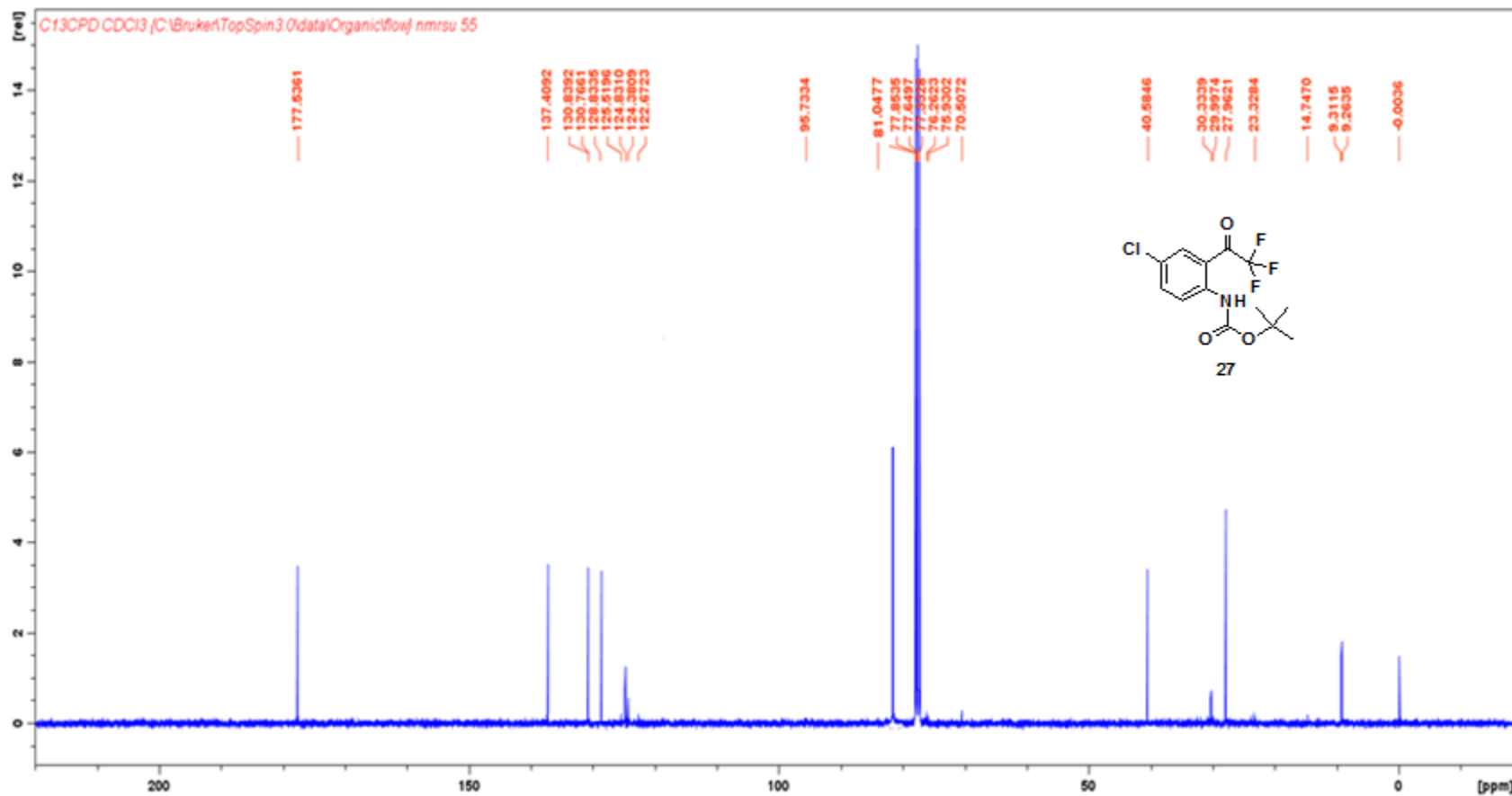
**<sup>19</sup>F** spectrum of *tert*-butyl 4-chloro-2-(2,2,2-trifluoroacetyl) phenylcarbamate **27** in CDCl<sub>3</sub>

IR spectrum of *tert*-butyl 4-chloro-2-(2,2,2-trifluoroacetyl) phenylcarbamate **27**

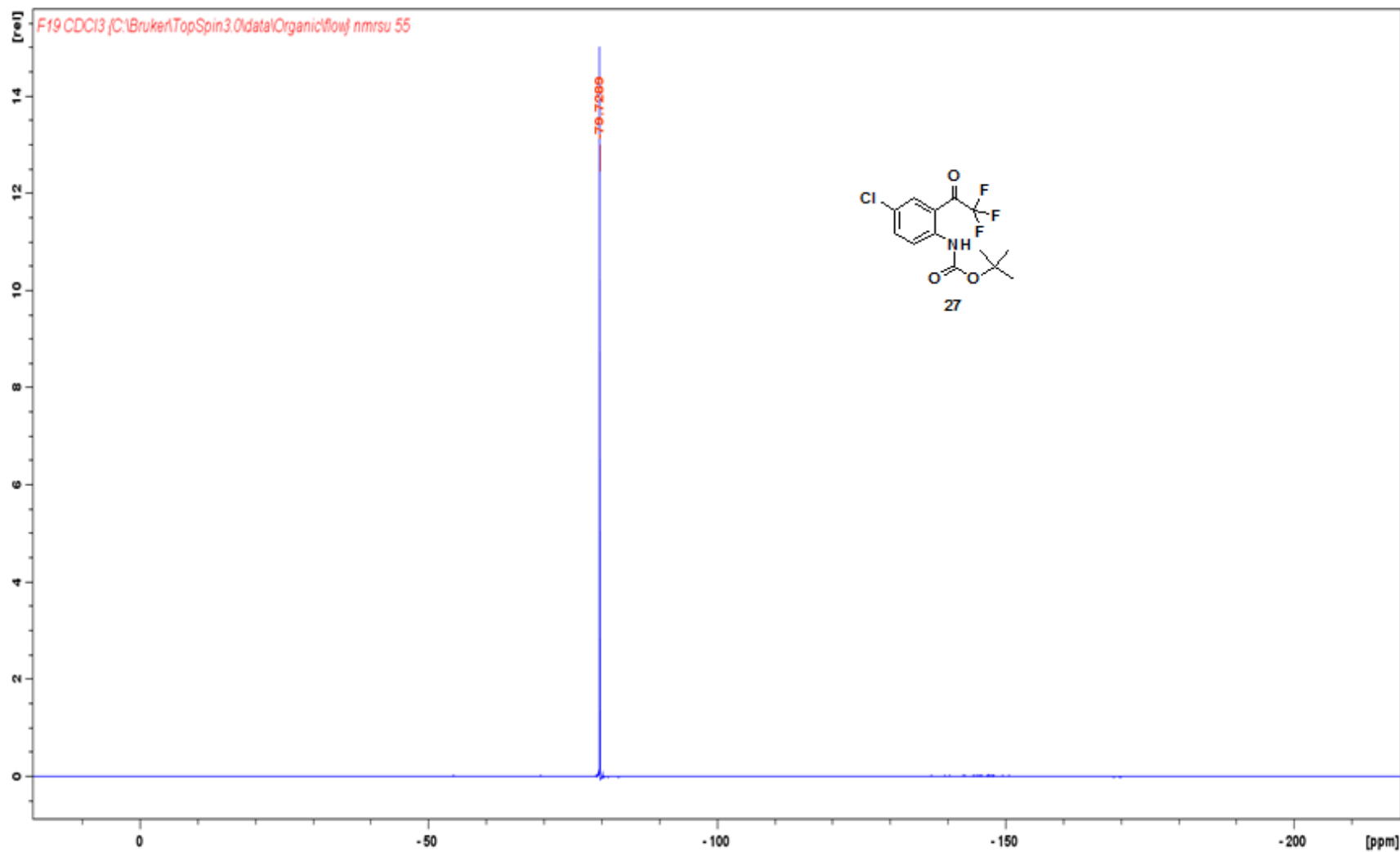


<sup>1</sup>H NMR Spectrum (400 MHz) of *tert*-butyl-4-chloro-2-(4-cyclo propyl-1,1-trifluoro-2-hydroxybut-3-yn-2-yl) phenyl carbamate 27 in CDCl<sub>3</sub>

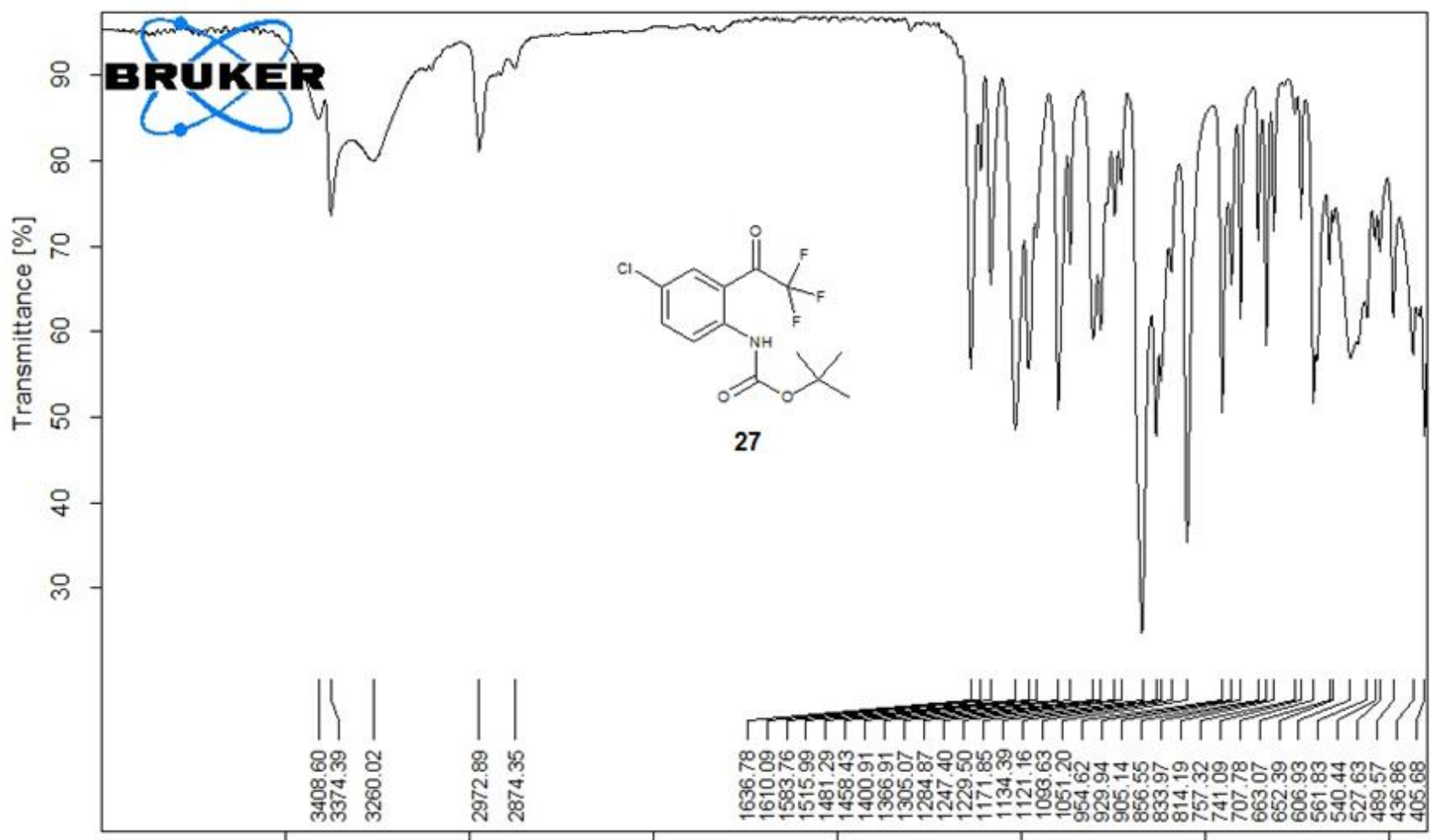




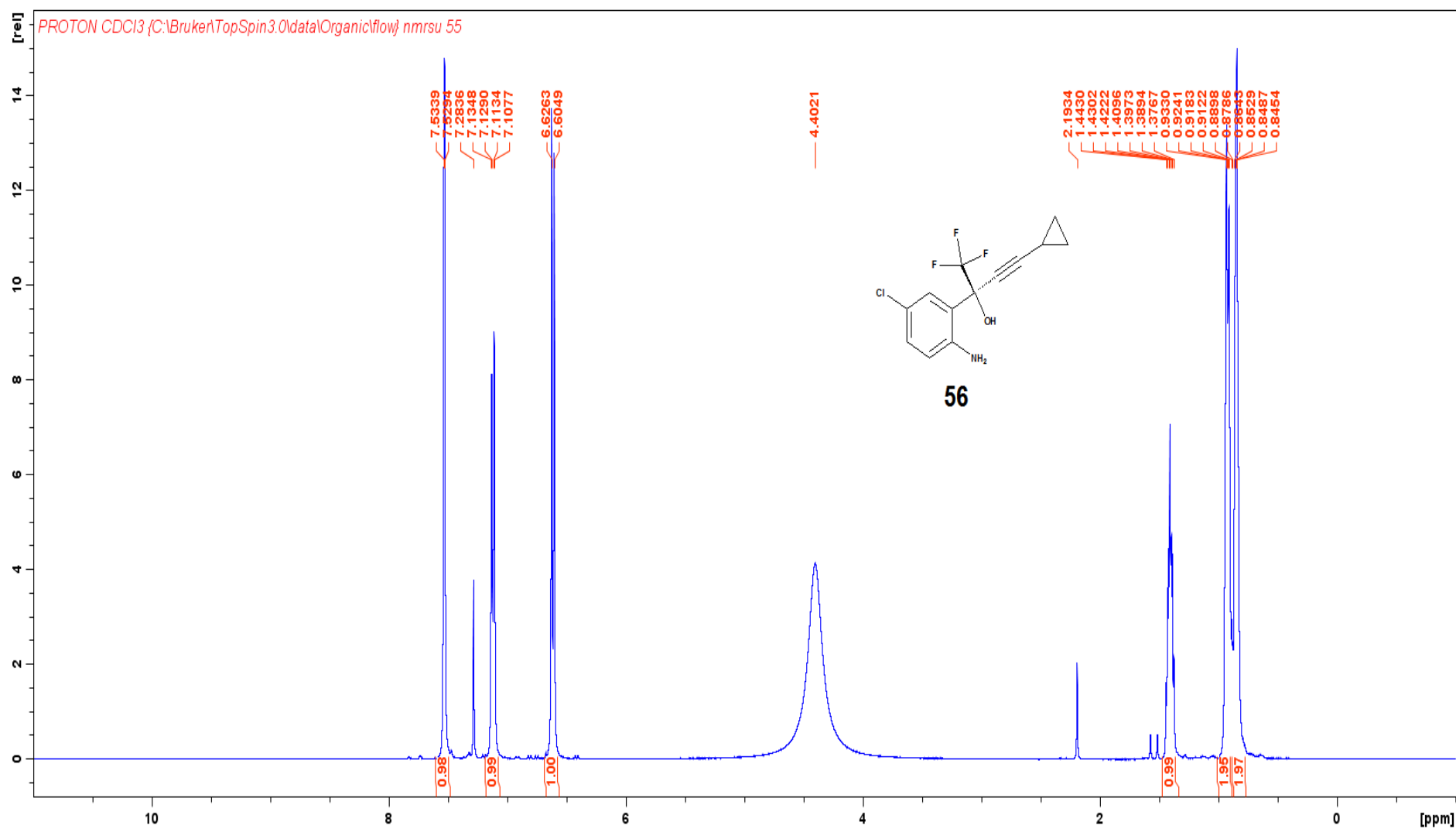
<sup>13</sup>C NMR spectrum (100 MHz) of *tert*-butyl-4-chloro-2-(4-cyclopropyl-1,1-trifluoro-2-hydroxybut-3-yn-2-yl) phenyl carbamate **27** in CDCl<sub>3</sub>



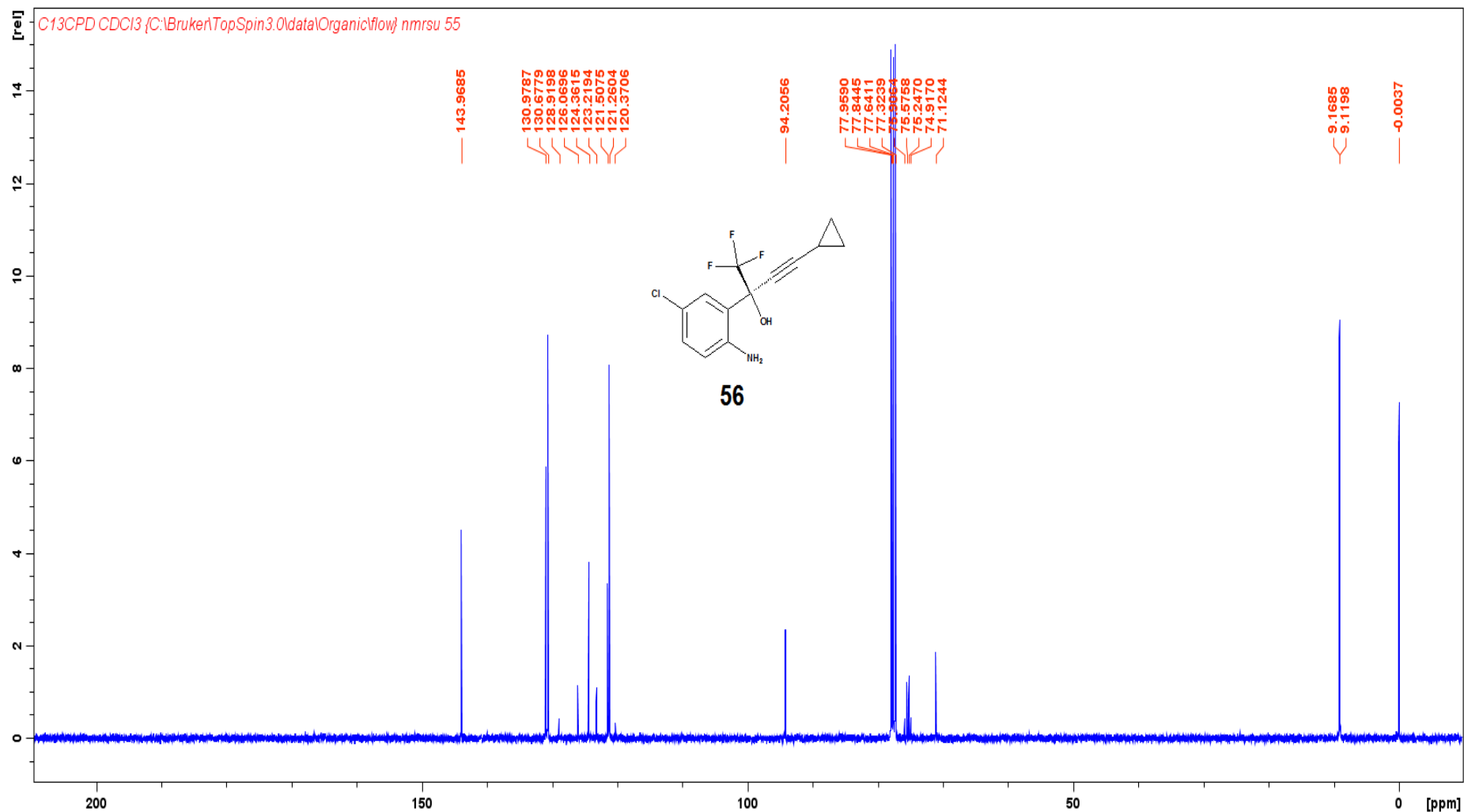
**<sup>19</sup>F Spectrum (100 MHz) of *tert*-butyl-4-chloro-2-(4-cyclo propyl-1, 1-trifluoro-2-hydroxybut-3-yn-2-yl) phenyl carbamate 27 in CDCl<sub>3</sub>**



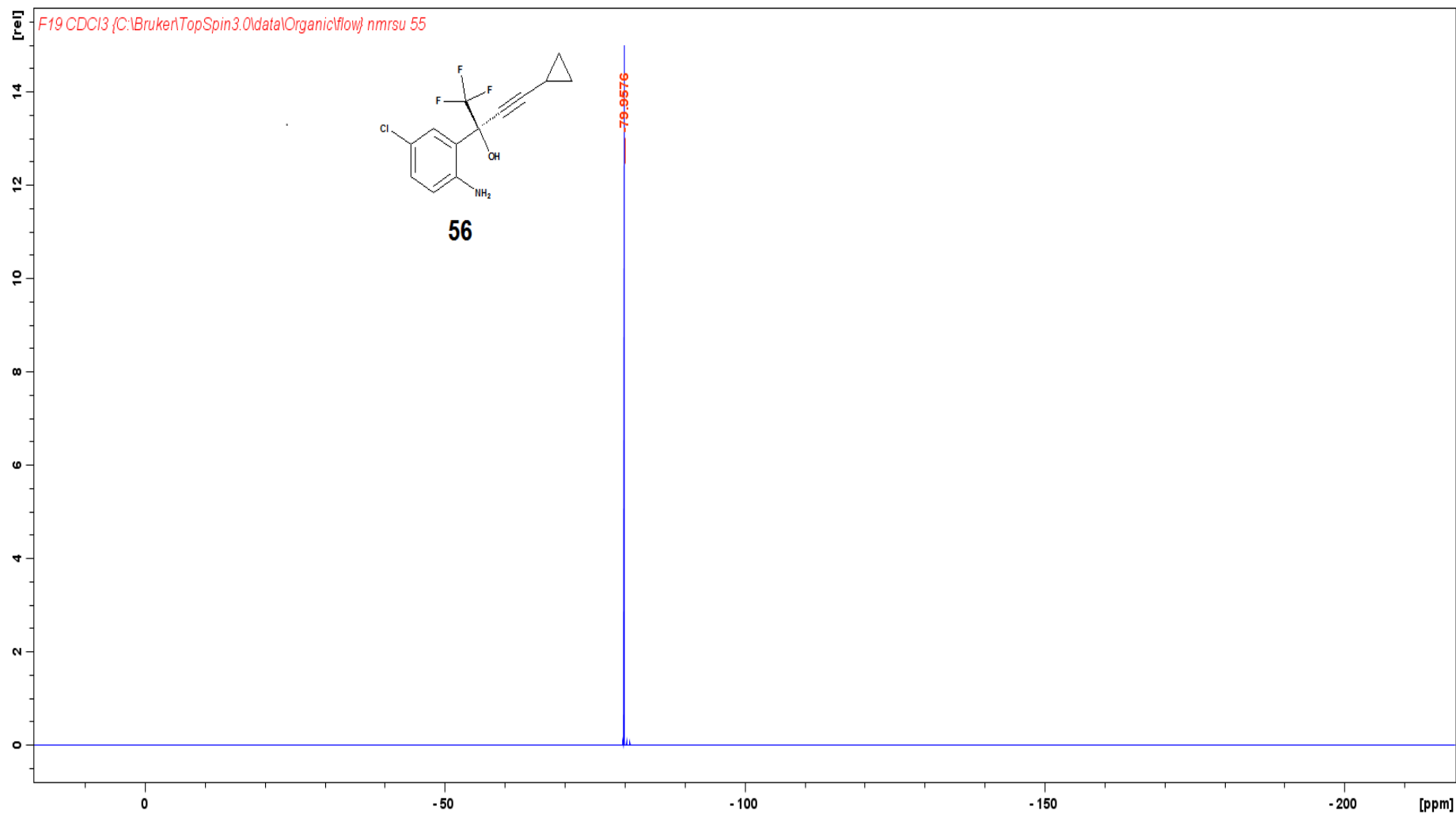
IR Spectrum of *tert*-butyl-4-chloro-2-(4-cyclo propyl-1, 1-trifluoro-2-hydroxybut-3-yn-2-yl) phenyl carbamate 27



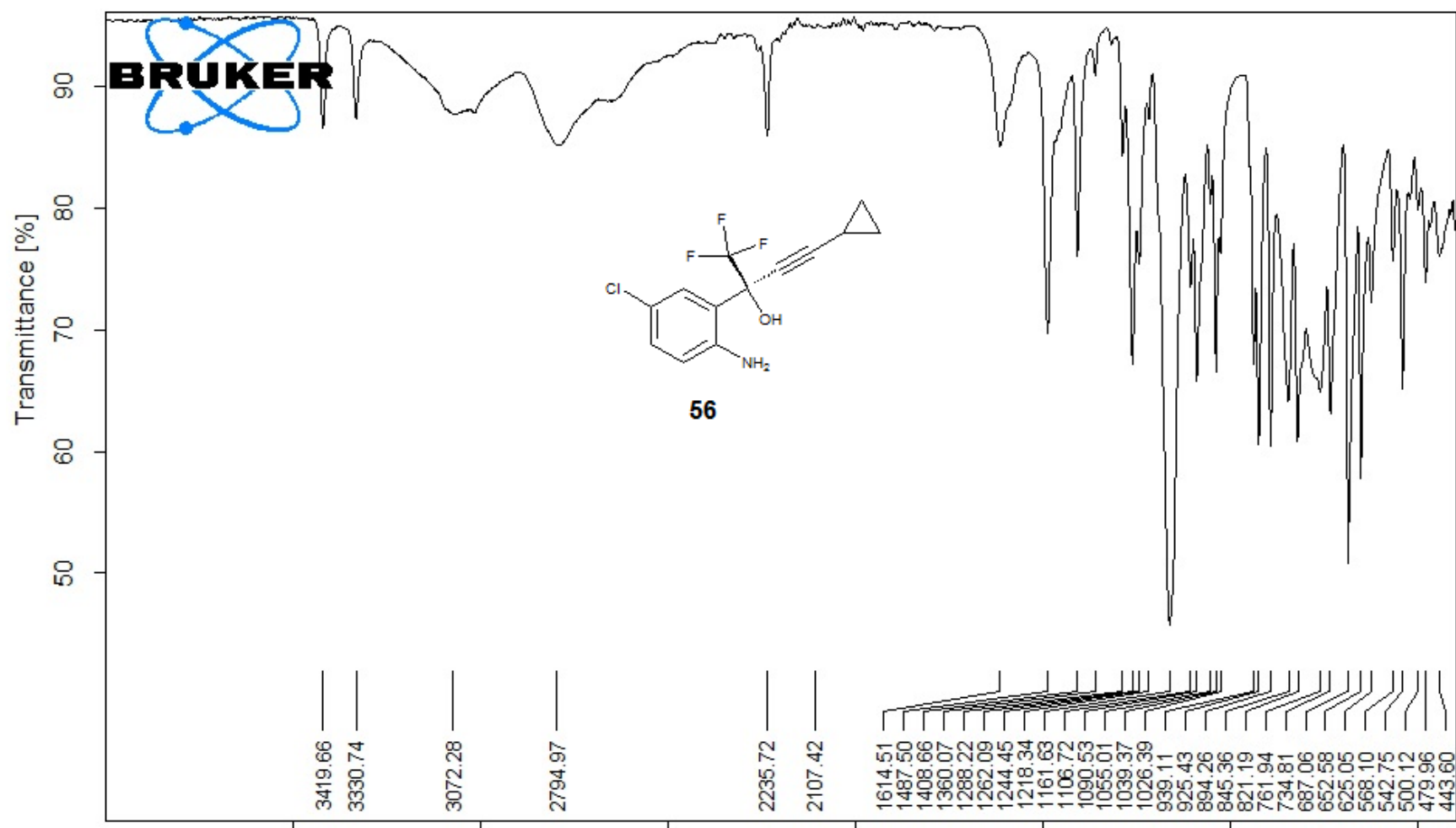
**<sup>1</sup>H NMR Spectrum (400 MHz) of 2-(2-amino-5-chlorophenyl)-4-cyclopropyl-1,1,1-trifluorobut-3-yn-2-ol 56 in CDCl<sub>3</sub>**



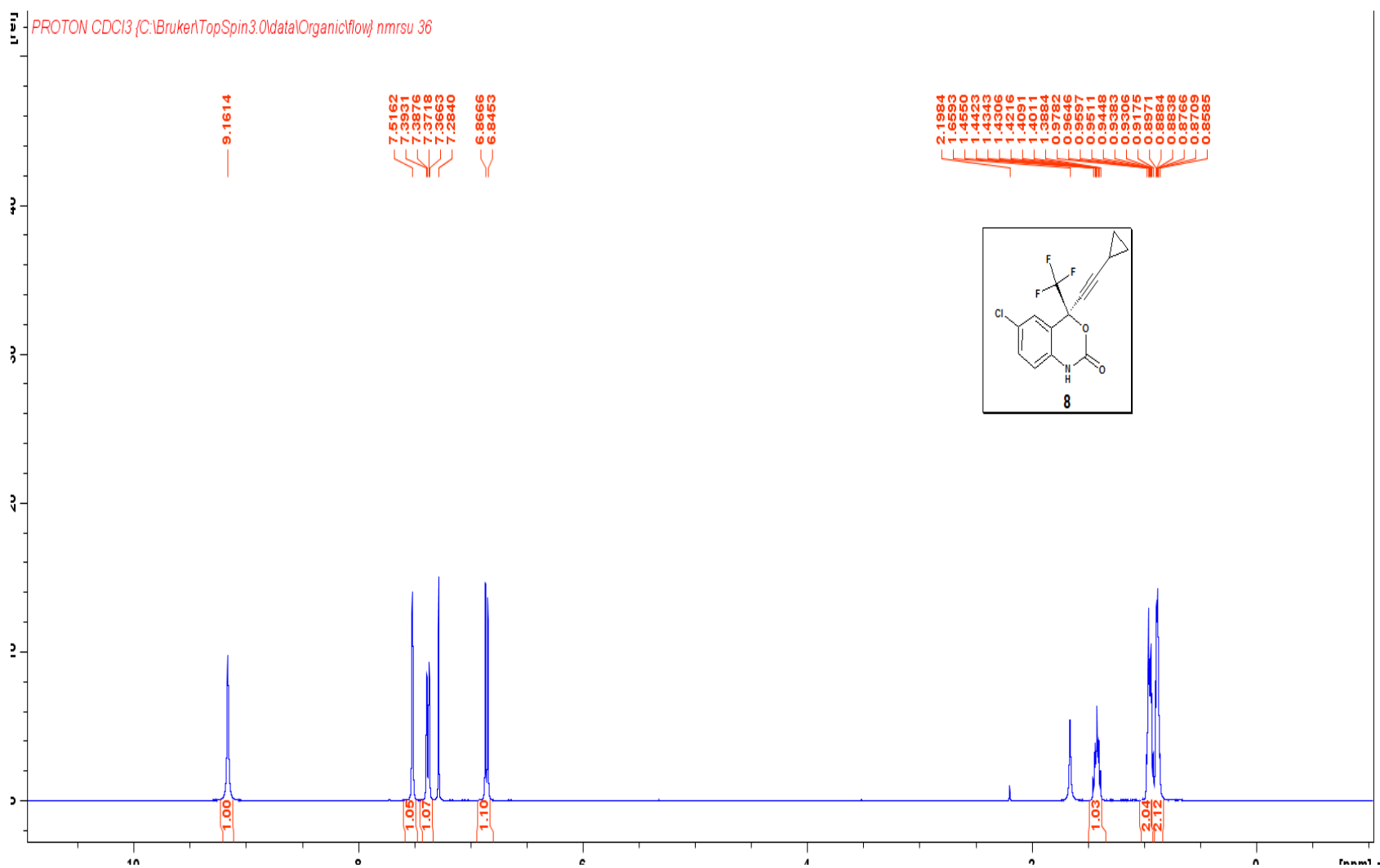
**<sup>13</sup>CNMR spectrum (100 MHz) of 2-(2-amino-5-chlorophenyl)-4-cyclopropyl-1,1,1-trifluorobut-3-yn-2-ol **56** in CDCl<sub>3</sub>**



**19F Spectrum (100 MHz) of 2-(2-amino-5-chlorophenyl)-4-cyclopropyl-1,1,1-trifluorobut-3-yn-2-ol 56 in CDCl<sub>3</sub>**

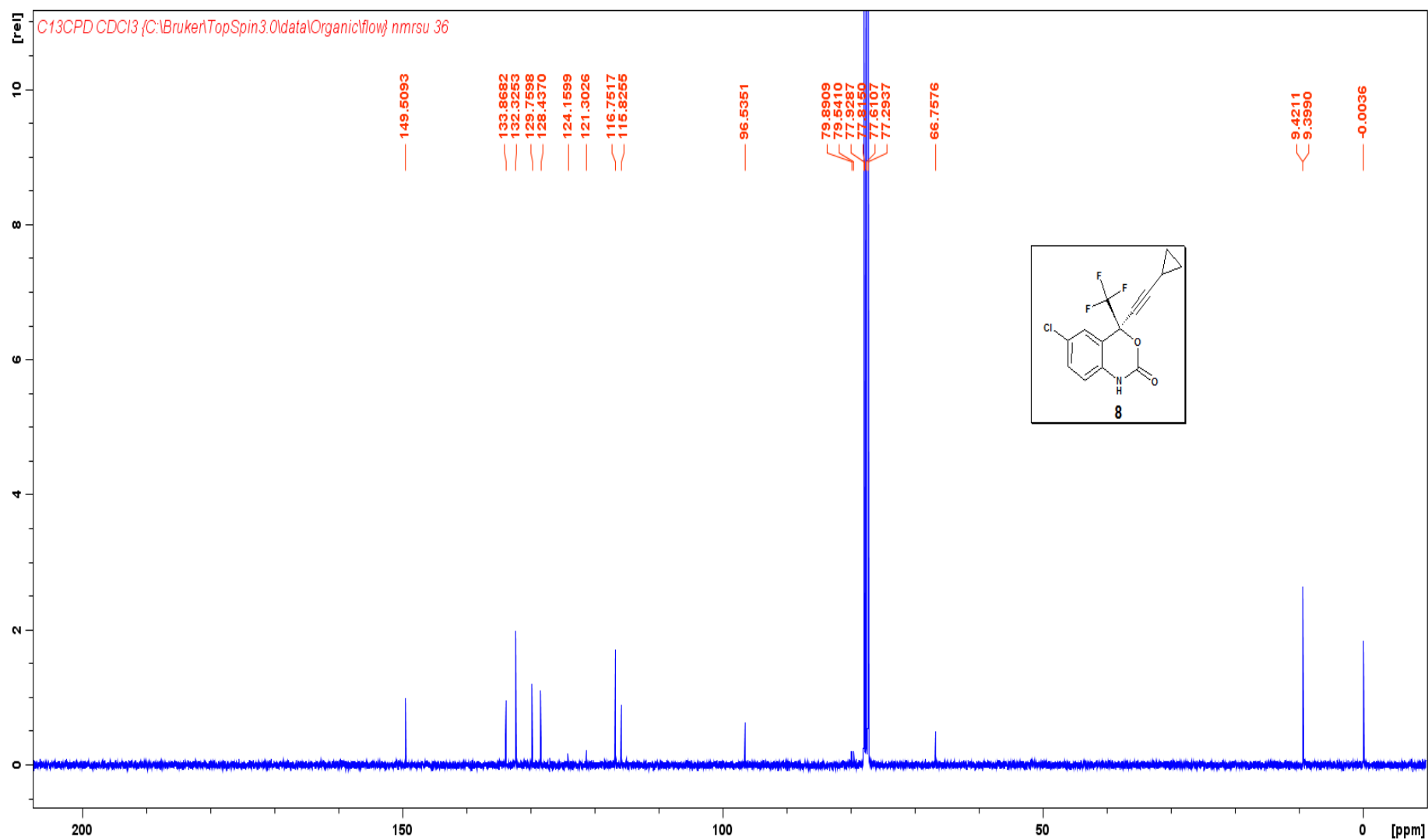


IR spectrum of 2-(2-amino-5-chlorophenyl)-4-cyclopropyl-1,1,1-trifluorobut-3-yn-2-ol 56

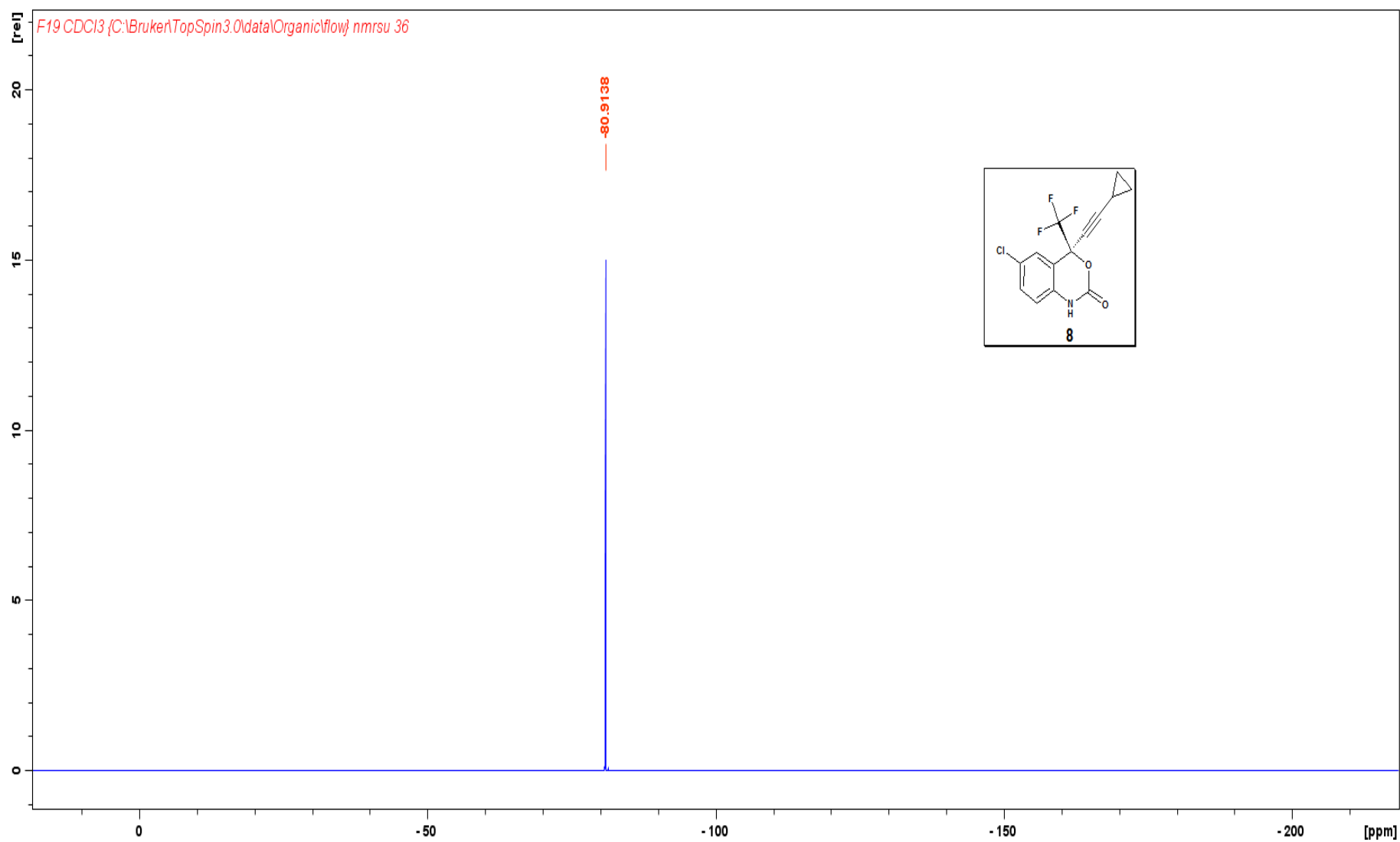


**<sup>1</sup>H NMR Spectrum (400 MHz) of 6-chloro-2-(4-cyclopropylethynyl)-4-(trifluoromethyl)-1H-benzo[d][1,3] oxazin-2-(4H)-one in CDCl<sub>3</sub>**



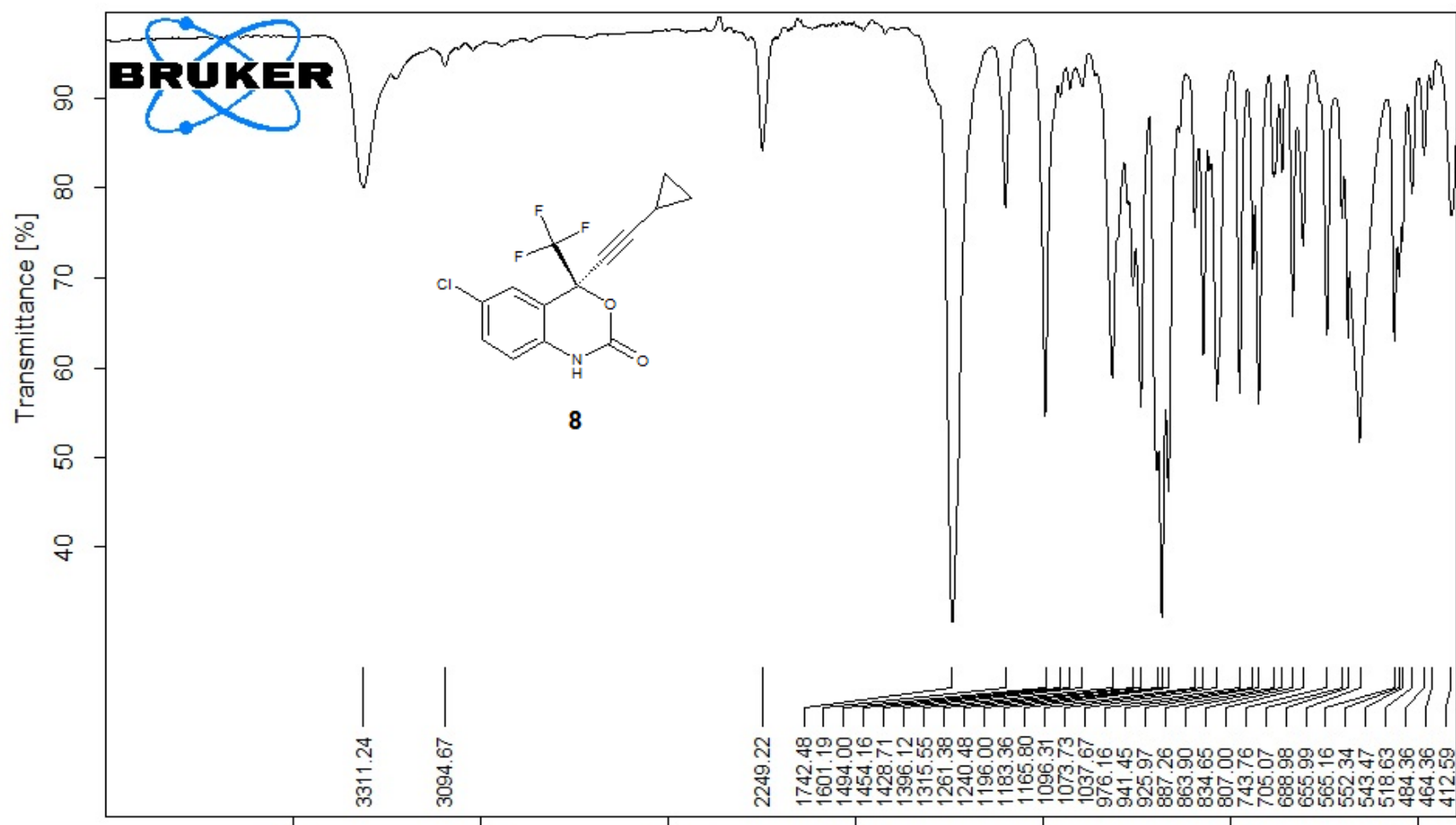


**$^{13}$  CNMR Spectrum (100 MHz) of 6-chloro-2-(4-cyclopropylethynyl)-4-(trifluoromethyl)-1*H*-benzo[*d*][1,3] oxazin-2-(4*H*)-one **8** in  $\text{CDCl}_3$**

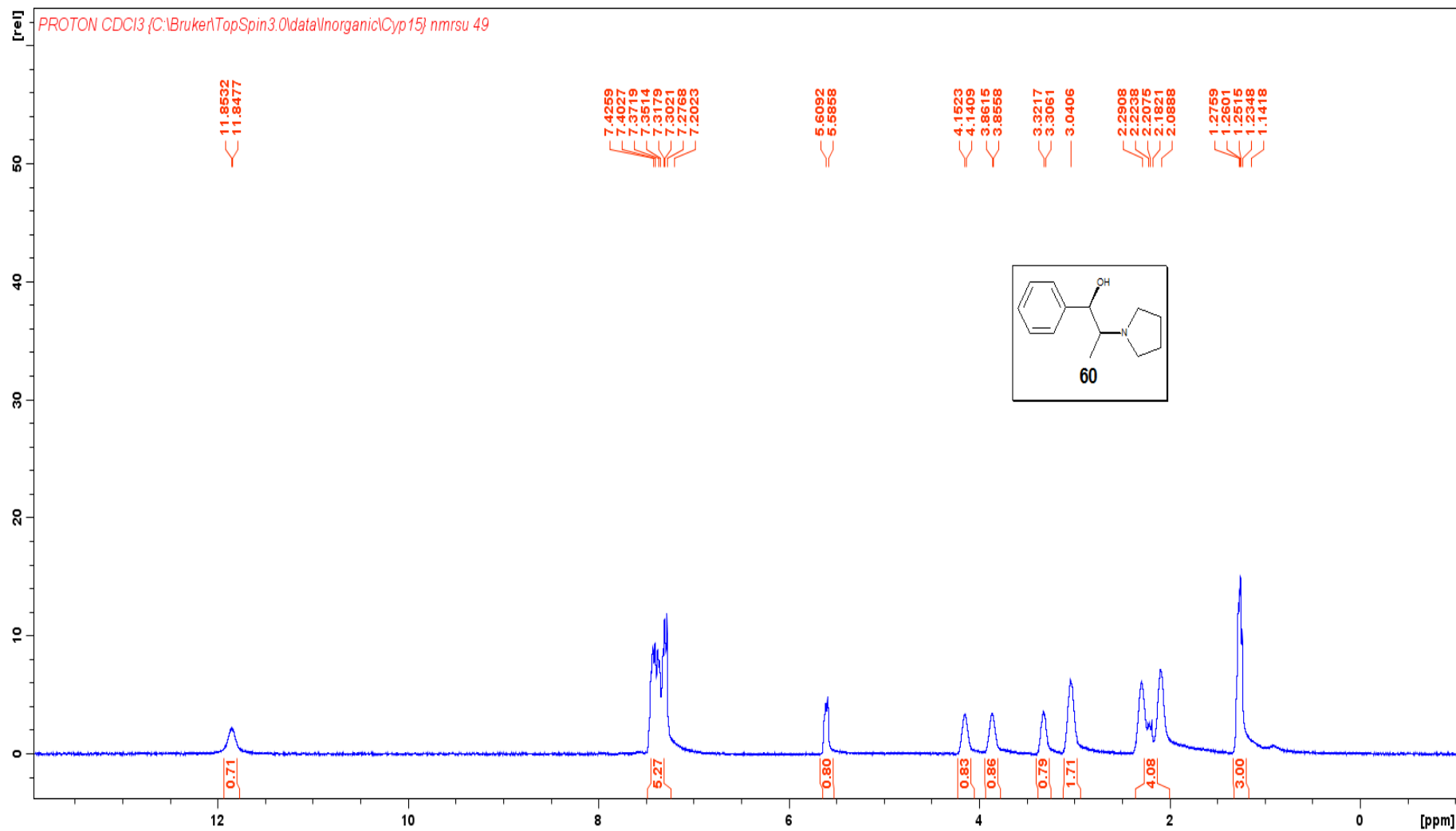


**19F Spectrum of 6-chloro-2-(4-cyclopropylethynyl)-4-(trifluoromethyl)-1H-benzo[d][1,3] oxazin-2-(4H)-one **8** in**

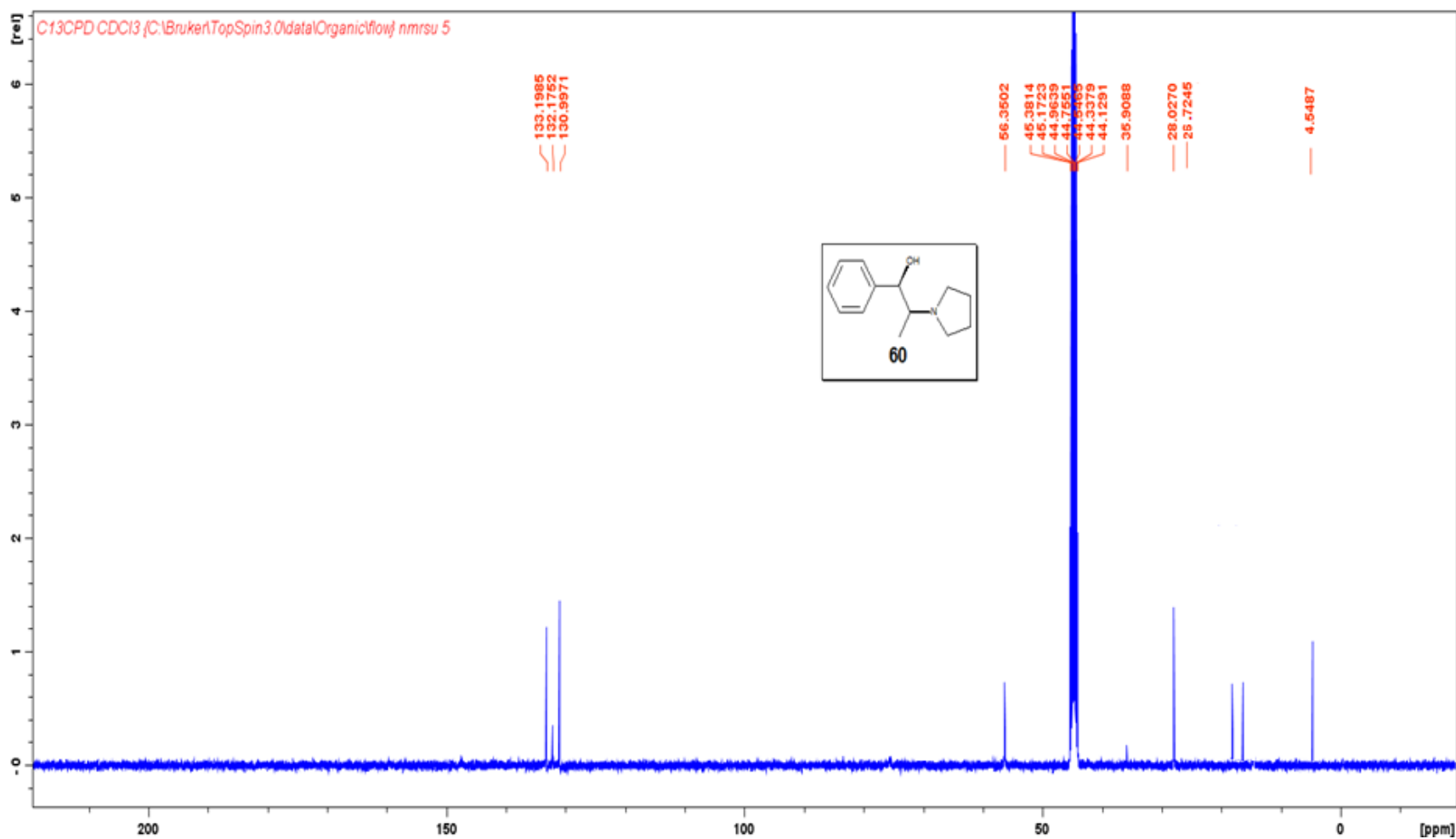
**CDCl<sub>3</sub>**



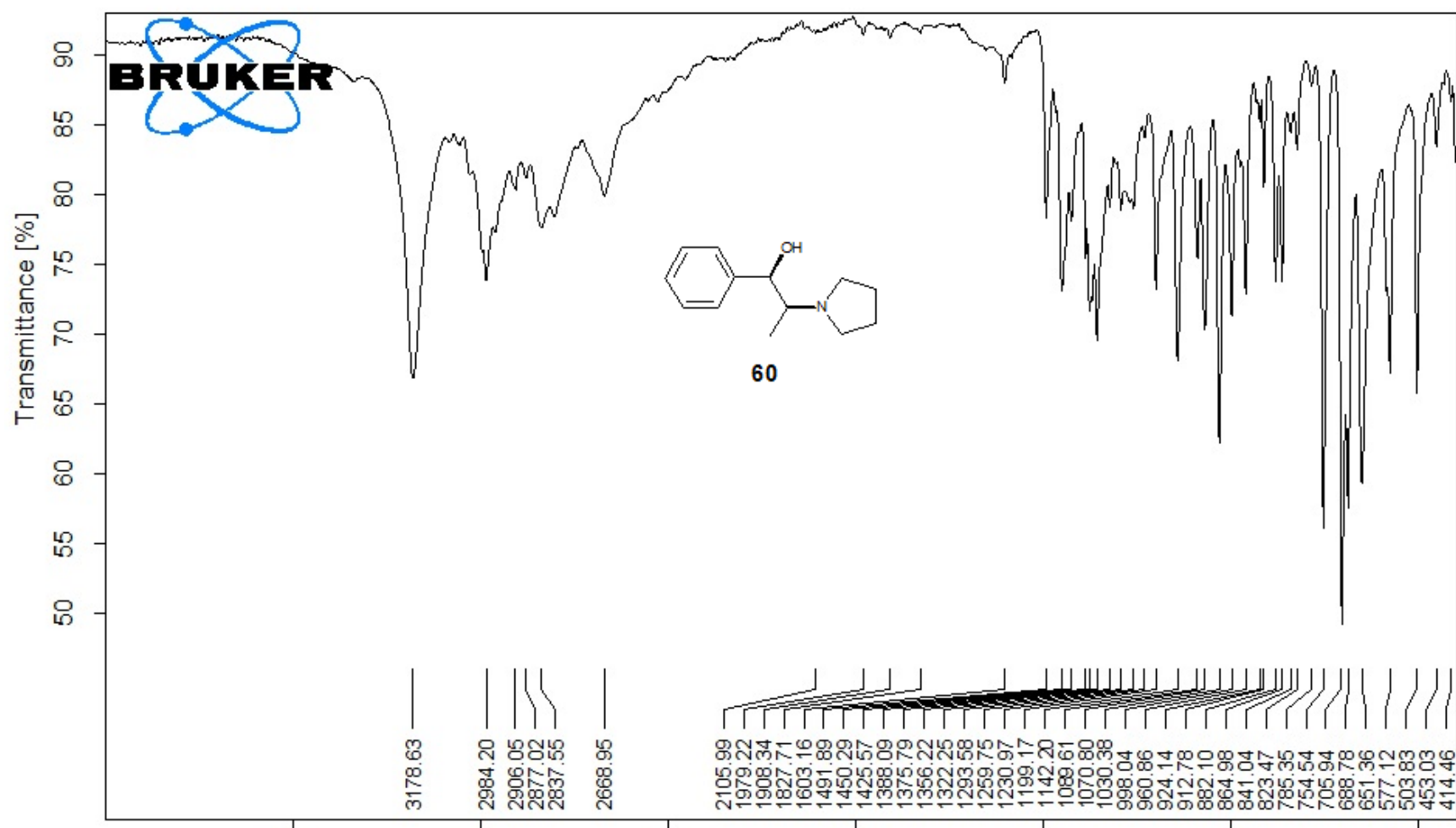
IR Spectrum of 6-chloro-2-(4-cyclopropylethynyl)-4-(trifluoromethyl)-1*H*-benzo[*d*][1,3] oxazin-2-(4*H*)-one 8

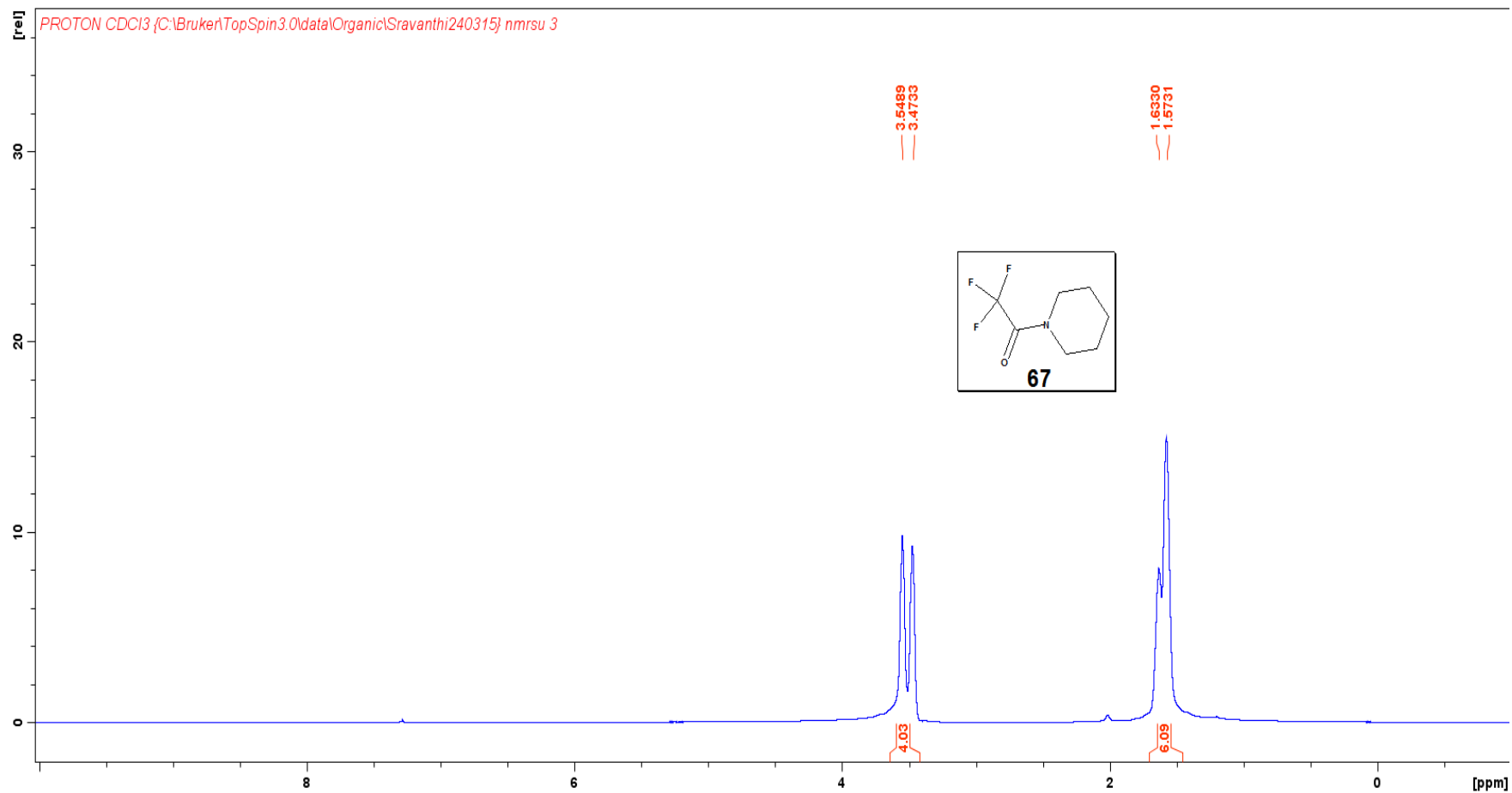


**<sup>1</sup>H NMR Spectrum (400 MHz) of *N*-pyrrolidinyl nor ephedrine 60**

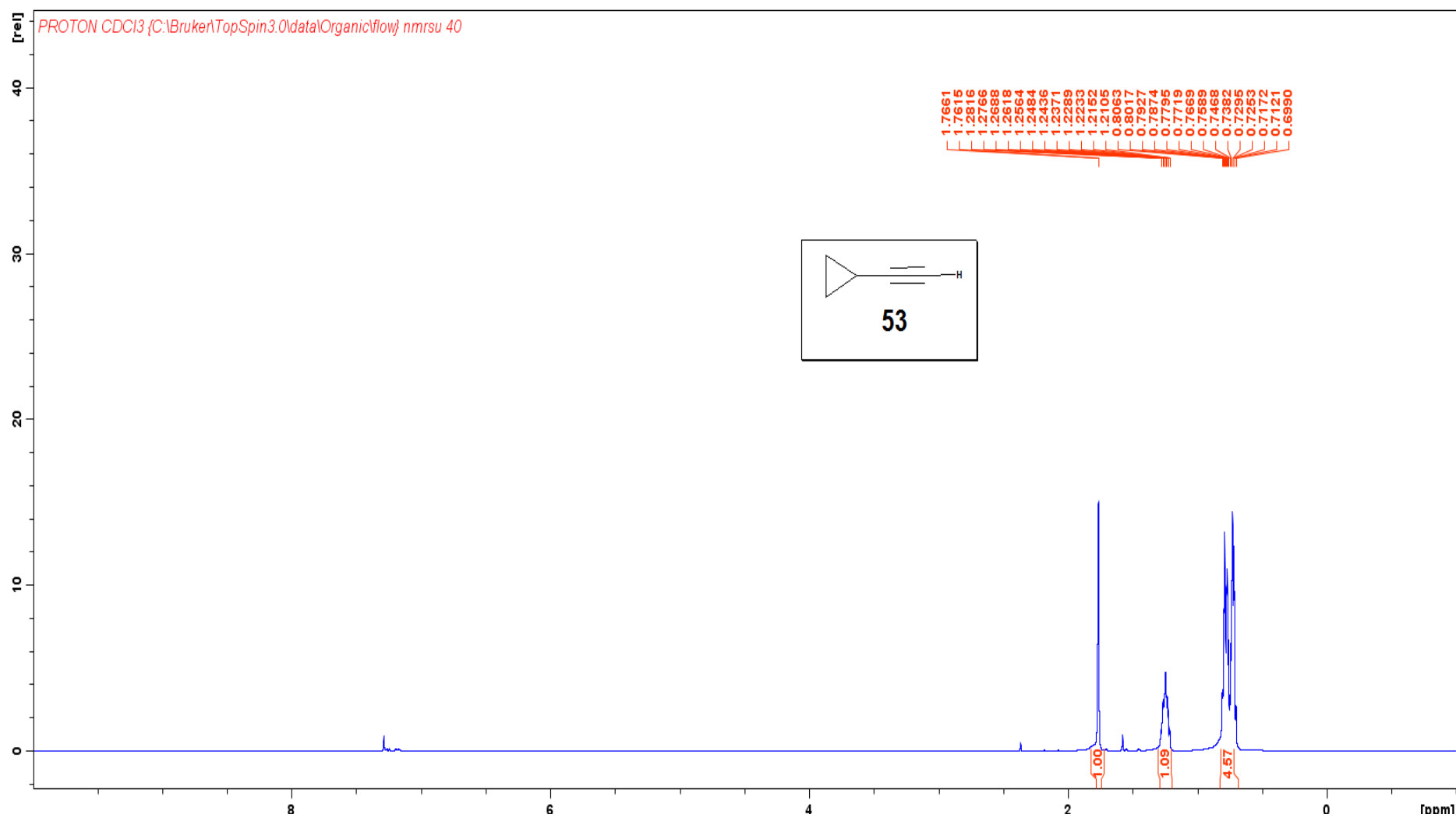


<sup>13</sup>CNMR Spectrum (100 MHz) of *N*-pyrrolidinylnor ephedrine 60

IR Spectrum of *N*-pyrrolidinyl nor ephedrine 60

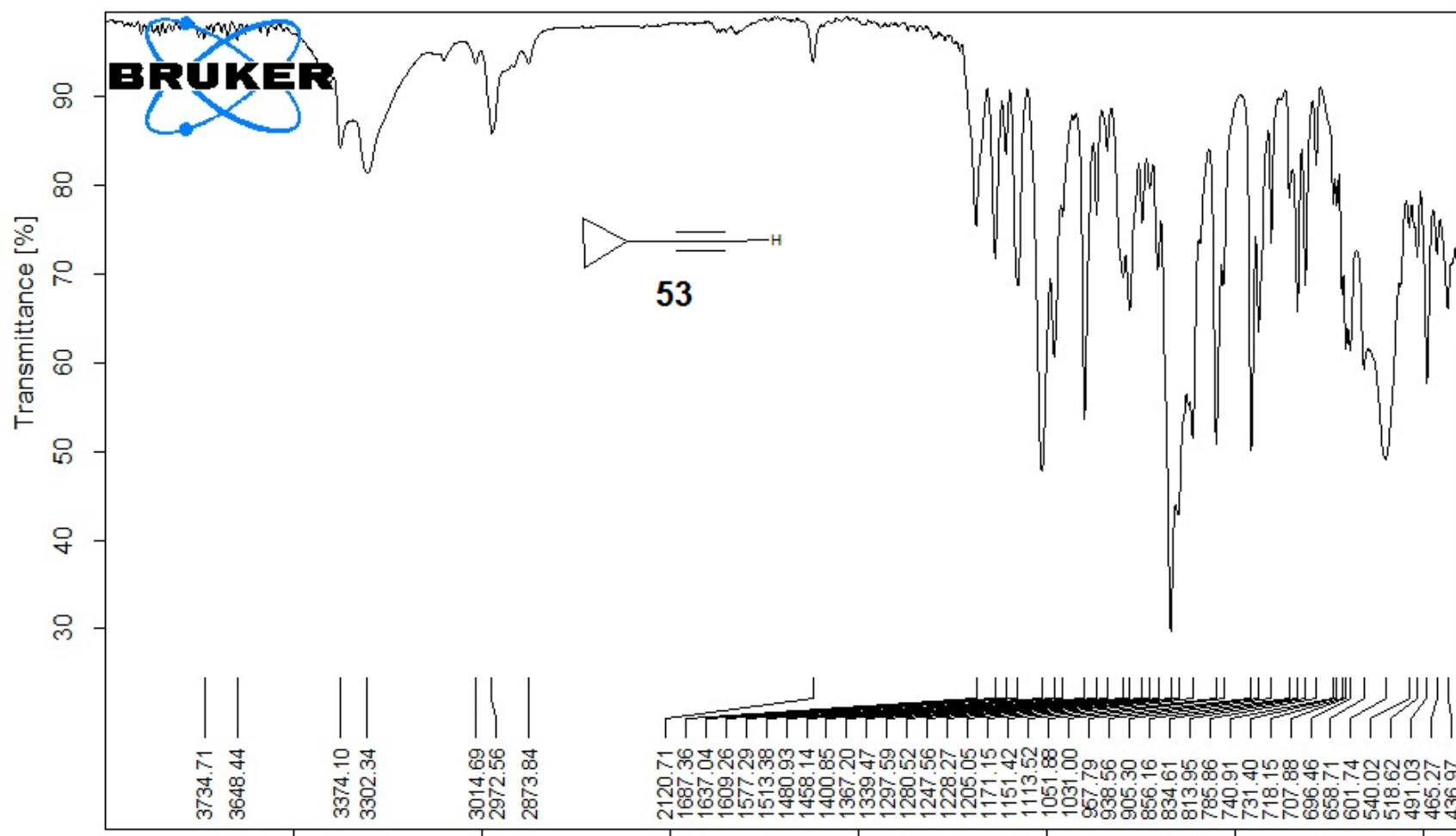


**<sup>1</sup>H NMR Spectrum (400 MHz) of piperidine trifluoro acetic acid 67 in CDCl<sub>3</sub>**

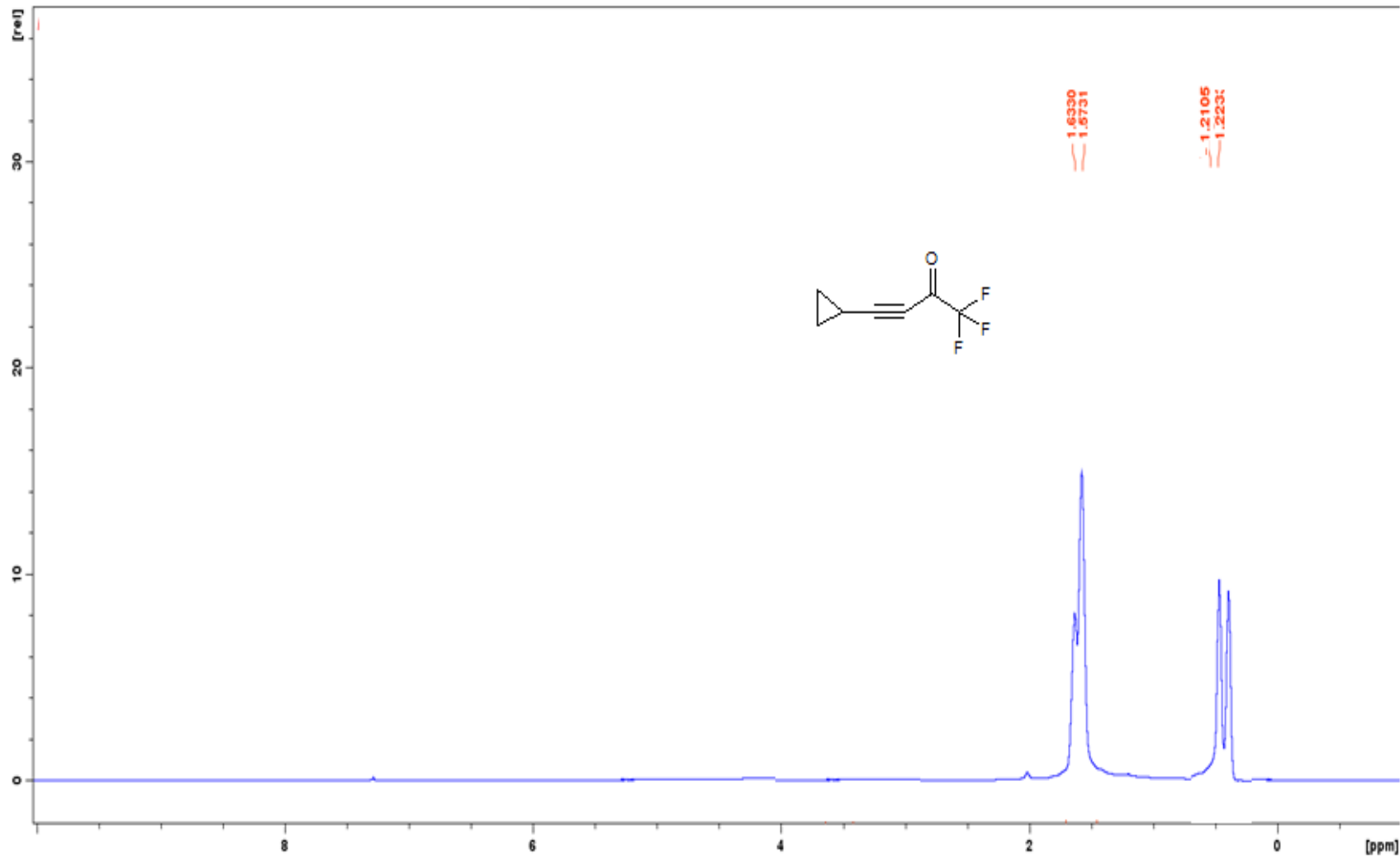


<sup>1</sup>H NMR Spectrum (400 MHz) of cyclopropyl acetylene 53 in CDCl<sub>3</sub>

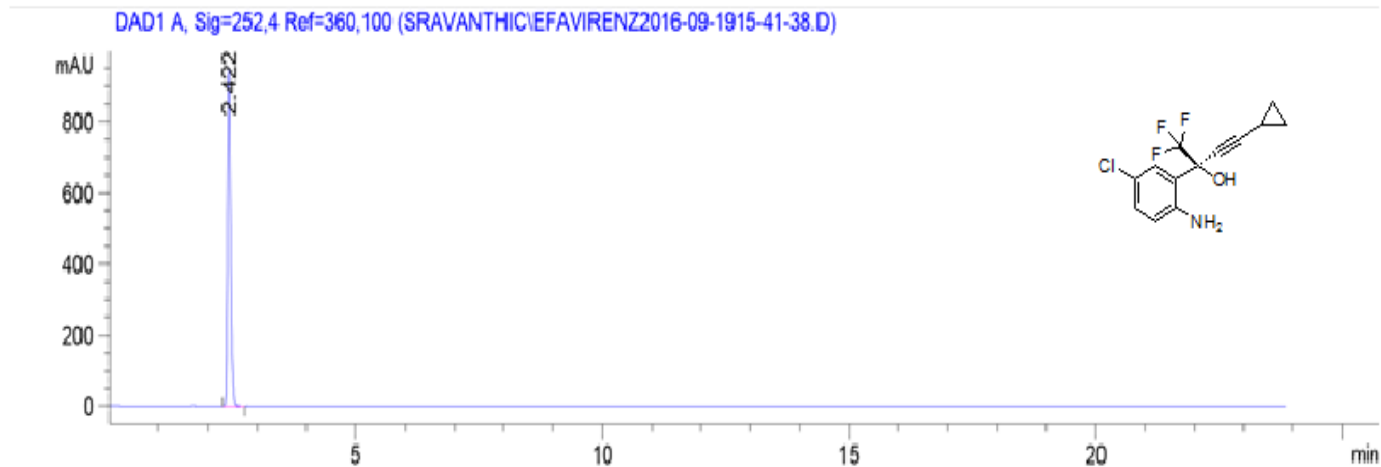




IR Spectrum of cyclopropyl acetylene 53



$^1\text{H}$ NMR Spectrum (400 MHz) of 4-cyclopropyl-1,1,1-trifluorobut-3-yn-2-one



Chiral HPLC chromatogram of 2-(2-amino-5-chlorophenyl)-4-cyclopropyl-1,1,1-trifluorobut-3-yn-2-ol



Chiral HPLC chromatogram of 6-chloro-2-(4-cyclopropylethynyl)-4-(trifluoromethyl)-1*H*-benzo[*d*][1,3] oxazin-2-(4*H*)-one 8



